5-2007

Quaternary Evolution of the Colorado River at Lees Ferry, Arizona

William Scott Cragun
Utah State University

QUATERNARY EVOLUTION OF THE COLORADO RIVER AT LEES FERRY, ARIZONA

by

William Scott Cragun

A thesis submitted in partial fulfillment
of the requirements for the degree

of

MASTER OF SCIENCE

in

Geology

Approved:

UTAH STATE UNIVERSITY
Logan, Utah

2007

ABSTRACT

Quaternary Evolution of the Colorado River at Lees Ferry, Arizona

by

William Scott Cragun, Master of Science

Utah State University, 2007

Major Professor: Dr. Joel L. Pederson
Department: Geology

A well-exposed suite of Colorado River fill terraces preserved at Lees Ferry records the oscillating history of this major river superimposed on its overall downcutting of the Colorado Plateau. Detailed mapping, sedimentology, cross-sectional surveys, and the use of two geochronometers have been used in order to establish a detailed chronostratigraphy for the area. Eight distinct deposits have been identified along the Colorado River (M1-M7, and S3), and four deposits have been identified along the Paria River (P1-P4).

Geochronology of six of these deposits using optically stimulated luminescence and cosmogenic ^{10}Be exposure techniques indicates a long-term average bedrock incision rate of 290 to 470 m/my. These incision rates are approximately two to three times higher than others reported in Grand Canyon and the upper Colorado River basin, but are similar to the recently reported high incision rates near Glen Canyon and along the Fremont River. These results suggest that there is a region of faster incision along the Colorado River in the central Colorado Plateau in the vicinity of Lees Ferry and Glen

Canyon. This apparent increase in central plateau Pleistocene incision rates may be caused by either epeirogenic uplift due to tectonics and erosional isostatic rebound, or transient waves of incision in response to original drainage integration.

In addition to recording the incision history of the Colorado River, the well-preserved Pleistocene fluvial terraces provide evidence regarding the timing and processes of terrace formation at Lees Ferry. Chronostratigraphic analysis indicates that aggradation was occurring at ~20 ka (M2), ~70 to 40 ka (M3), ~115 to 90 ka (M4), and ~130 ka (M5). Aggradation and incision along the Paria River appears to be occurring at the same time as that on the Colorado River. Deposits at Lees Ferry are generally younger than correlative deposits in headwater catchments and in eastern Grand Canyon. In addition, the most prominent deposit in the Lees Ferry area (M4) correlates to MIS stage 5b-c, a time in which no glaciations have been reported in headwater drainages. Data from this study indicate that fluvial responses at Lees Ferry are a complicated integration of signals from climate change in headwater catchments and sediment production from local hillslopes and tributaries.

(192 pages)

ACKNOWLEDGMENTS

First of all, I would like to thank my advisor, Joel Pederson, for his constant encouragement, support, and mentoring advice throughout the duration of this project. I am also grateful to my committee members, Jack Schmidt and Tammy Rittenour, whose thoughtful comments and suggestions have helped to improve the content of this thesis. John Gosse and Alan Hidy, at Dalhousie University, provided TCN analysis and ages for this research. Tammy Rittenour provided invaluable advice and excellent training on how to process and calculate OSL ages. Ron Goble and Paul Hansen, at University of Nebraska – Lincoln, also provided important OSL data for this research project.

I am indebted to the Glen Canyon National Recreational Area for permission to access the study area and to Richard Hereford for his detailed explanations of continuing research efforts along the Colorado and Paria rivers. I would also like to thank my field assistants, Ben DeJong, Rob Mackley, Kevin Hadder, Alan Hidy, Kelly Mitchell, Gary O'Brien, and my little brother Ben, for sharing the quiet magic of the Lees Ferry landscape. This project could not have been completed without financial support from the NSF grant EAR-0346054 awarded to Joel Pederson, the Four Corners Geological Society, the Rocky Mountain Section of the Society for Sedimentary Geology, and the Utah State University Geology department. Finally, I would like to thank my wife, Yvette, and my five little boys, Jonah, Enoch, Asher, Samuel, and Hiram, for their love and support through my endless educational endeavors. Thank you for standing patiently by my side and giving me the motivation that I need to always be better.

W. Scott Cragun

PREFACE

This research explores the geochronology and sedimentology of the well-preserved Colorado and Paria River terraces at Lees Ferry, Arizona. This thesis is organized into four chapters. Chapter 1 introduces the research problems and outlines the methods used to address these questions. Chapter 2 is a short manuscript written for journal submission, which discusses incision rates calculated at Lees Ferry and the differential incision of the central Colorado Plateau. Chapter 3 is a longer manuscript written for journal submission. This chapter addresses the timing of aggradation and degradation episodes at Lees Ferry in relation to local and distant climatic forcing. Chapter 4 reviews the results and conclusions discussed in Chapters 2 and 3. The appendices contain the complete data collected throughout the course of this research endeavor.

CONTENTS

LIST OF TABLES

LIST OF FIGURES

CHAPTER 1

INTRODUCTION

The timing and cause for incision of the Colorado Plateau by the Colorado River and its tributaries have been debated since the late 1800's when geologists first began to explore the deep canyons and excellent exposures of the region. Research through the past century has continued to shed light on the complex history of the Colorado River through the Colorado Plateau. Incision is generally thought to have begun ~6 Ma (Lucchitta, 1966) and been nearly complete by ~0.4 to 1.2 Ma (Hamblin, 1994; Fenton et al., 2004). However, new stratigraphic and chronologic research on Pleistocene river deposits throughout the Colorado Plateau indicates that significant incision has continued through the Quaternary (e.g. Lucchitta et al., 2000; Pederson et al., 2002).

The few river gravels and terraces that record the incision history of the Colorado River are generally preserved in locations where erosion of softer strata or structural controls have created wide valleys along the river corridor. Recent studies from sites along the Colorado River in western Grand Canyon, eastern Grand Canyon, Glen Canyon, Westwater Canyon, Glenwood Canyon, and along the tributary San Juan and Fremont Rivers have reported variable bedrock incision rates that indicate differential incision along the Colorado River drainage through the Quaternary. Lees Ferry also contains a well-exposed suite of Colorado River terraces that lie in the center of this region, and while the Holocene history has been explored in depth by Hereford et al. (2000), the Pleistocene terraces have remained relatively unstudied.

This study presents an analysis of the fluvial terraces at Lees Ferry in order to provide insight into two important questions: 1) are incision rates at Lees Ferry consistent with others in the region; and 2) is the timing of aggradation and incision at this central location consistent with climate changes in glaciated headwaters, or rather with changes in the non-glaciated landscapes of the immediate area? These questions have been addressed through various field observations, including detailed sedimentologic descriptions, clast counts, sand petrology, geologic mapping of Quaternary deposits, and topographic cross-sectional surveys of terrace heights and valley profiles. In addition, two dating methods have been employed in order to quantify the timing of aggradation and subsequent terrace abandonment: optically stimulated luminescence (OSL) and ^{10}Be terrestrial cosmogenic nuclide (TCN) dating. Results of this study have refined the regional picture of varying incision rates along the length of the Colorado and contributed to the debate on the timing of aggradation-degradation cycles in relation to local and distant climate forcing.

REFERENCES CITED

Fenton, C.R., Poreda, R.J., Nash, B.P., Webb, R.H., and Cerling, T.E., 2004, Geochemical discrimination of five Pleistocene lava-dam outburst-flood deposits, western Grand Canyon, Arizona: Journal of Geology, v. 112, p. 91-110.

Hamblin, W.K., 1994, Late Cenozoic lava dams in the western Grand Canyon: Geological Society of America Memoir 183, 139 p.

Hereford, R., Burke, K.J., and Thompson, K.S., 2000, Map showing Quaternary geology and geomorphology of the Lees Ferry area, Glen Canyon, Arizona: U.S. Geological Survey Geologic Investigations Series Map I-2663, scale 1:2000.

Lucchitta, I., 1966, Cenozoic geology of the Lake Mead area adjacent to the Grand Wash Cliffs, Arizona [Ph.D. dissertation]: Pennsylvania State University, 218 p.

Lucchitta, I., Garniss, H.C., and Turrin, B., 2000, Cyclic aggradation and downcutting, fluvial response to volcanic activity, and calibration of soil-carbonate stages in the western Grand Canyon, Arizona: Quaternary Research, v. 53, p. 23-33.

Pederson, J.L., Karlstrom, K., Sharp, W., and McIntosh, W., 2002, Differential incision of Grand Canyon related to Quaternary faulting—constraints from U-series and Ar/Ar dating: Geology, v. 30, no. 8, p. 739-742.

CHAPTER 2

PLEISTOCENE GEOCHRONOLOGY AND INCISION RATES OF THE COLORADO RIVER AT LEES FERRY: TOWARDS SOLVING THE MYSTERY OF DIFFERENTIAL INCISION ON THE COLORADO PLATEAU[1]

ABSTRACT

Chronostratigraphic analysis of the well-preserved Pleistocene fluvial terraces along the Colorado River at Lees Ferry indicate a long-term average bedrock incision rate of 290 to 470 m/my. These incision rates are approximately two to three times higher than others reported downstream in Grand Canyon and upstream in the upper Colorado River basin. In contrast, our incision rates at Lees Ferry are similar to the recently reported high incision rates near Glen Canyon and along the Fremont River. Our results suggest that there is a region of faster incision along the Colorado River in the central Colorado Plateau in the vicinity of Lees Ferry and Glen Canyon. We propose two possible mechanisms for this increase in central plateau incision rates: 1) epeirogenic uplift due to tectonics and erosional isostatic rebound; or 2) transient waves of incision in response to original drainage integration.

INTRODUCTION

The Colorado River flows through the heart of the Colorado Plateau and has carved a landscape of steep canyons that are commonly several hundred meters deep. Debate about the timing and causes of this large-scale incision has existed since the late

---

[1] Coauthored by W. Scott Cragun, Joel L. Pederson, and Tammy M. Rittenour

1800's when early geologists such as John Wesley Powell (1875), Clarence Dutton (1882), and William Morris Davis (1901) first explored the deep canyons and excellent rock exposures of the region. Additional research during the past century has continued to shed light on the complex history of the Colorado River through the Colorado Plateau (e.g. Hunt, 1969; McKee and McKee, 1972); however, the timing and driving forces of late-Cenozoic incision are still debated.

Incision of the Colorado Plateau region by the Colorado River and its drainages is thought to have occurred as the result of a large-scale reversal in drainage direction that occurred over the late-Cenozoic (Lucchitta, 1972; Pederson et al., 2002a). Paleo-drainage networks flowed approximately northwest off the Laramide highlands of central Arizona and were disrupted by Basin and Range extension and the opening of the Gulf of Mexico in Miocene time (e.g. Lucchitta, 1972; Young and McKee, 1978). The ancestral Colorado River was captured as developing drainages became integrated throughout the lower Colorado River region (Lucchitta, 1972), ultimately disrupting flow direction and driving incision throughout the plateau by lowering baselevel. Analysis of sediments deposited in the Grand Wash Trough, where the Colorado River exits the Grand Canyon, indicates that the Colorado River had established its present-day course and begun to incise the Grand Canyon ~5.6 Ma (Lucchitta, 1966; Faulds et al., 2001). Newer stratigraphic and chronologic research on Quaternary river deposits throughout the Colorado Plateau indicates that significant incision has continued through the Quaternary (e.g. Lucchitta et al., 2000; Pederson et al., 2002b).

In general, incision is driven by baselevel change through tectonics, eustacy, or drainage integration and may result in the formation of fluvial terraces within a river valley (e.g. Merritts et al., 1994). Glacial-interglacial climate cycles also influence the formation of terraces; however, climatic controls generally occur over shorter time scales and are generally superimposed on the long-term downcutting of a region (e.g. Hancock and Anderson, 2002). Analysis of fluvial terrace geometries and sedimentology of associated deposits, coupled with a geochronologic framework, provides valuable information for reconstructing the timing and causes of incision through the past. Here we present new geochronologic data and rigorous incision rates from the well-preserved fluvial terrace record of the Colorado River at Lees Ferry in order to explore the patterns and causes of late-Cenozoic incision of the Colorado Plateau.

BACKGROUND

With the advent of new geochronologic tools, recent research has focused on quantifying Quaternary incision rates at several localities along the length of the Colorado River and its tributaries (Figures 2.1 and 2.2). Although these studies have provided valuable results in specific locations along the profile of the Colorado River, a complete picture of regional incision throughout the Colorado Plateau has yet to be established. We review several of these studies in order to place our new results from Lees Ferry in the context of incision reported throughout the Colorado Plateau and provide a framework for interpreting the potential causes of differential incision throughout the region.

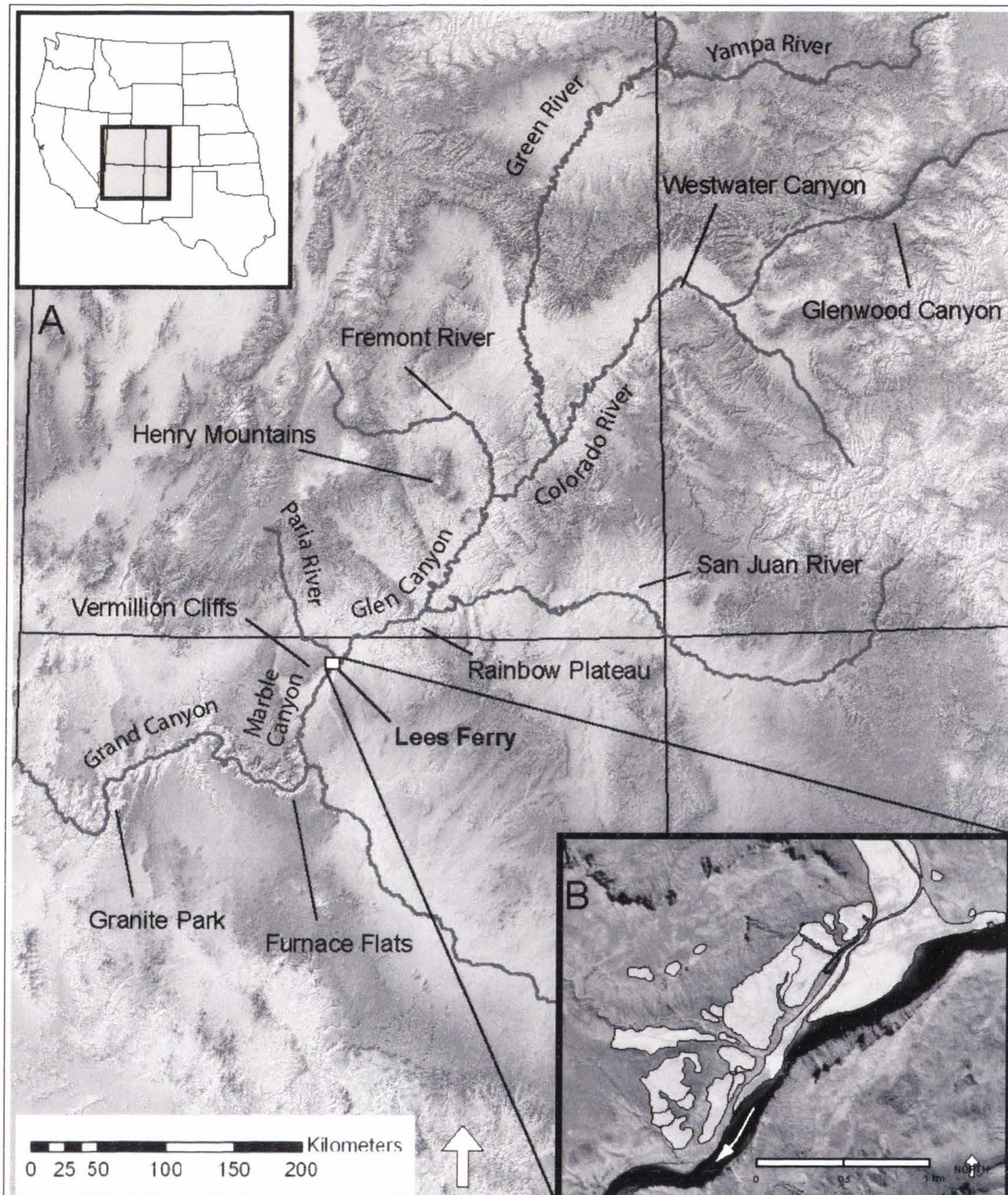

Figure 2.1 (A) Map of the central Colorado River and its drainages, showing locations of studies that have reported incision rates throughout the Colorado Plateau. (B) Map showing the distribution of Quaternary deposits at Lees Ferry.

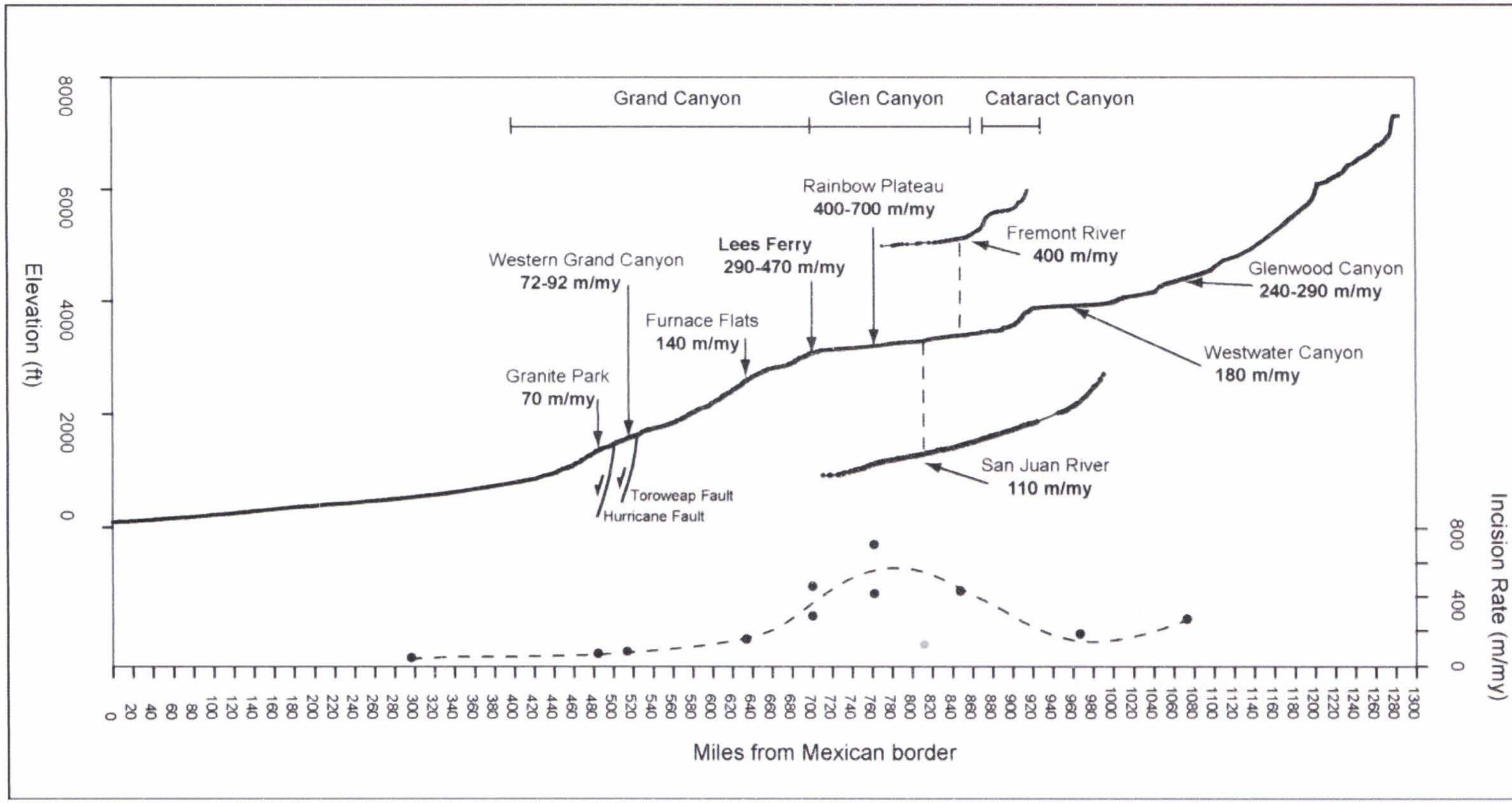

Figure 2.2. Longitudinal profile of the Colorado River from Kremling, CO to the Mexican border, including profiles of the San Juan and Fremont Rivers. Vertical exaggeration ~300. Incision rates from studies throughout the Colorado Plateau are plotted along the profiles and along the bottom of the figure in order to highlight the relatively high incision rates in the Lees Ferry and Glen Canyon reach. The San Juan incision rate shown with grey dot in order to highlight its relatively far distance from the trunk Colorado River and to indicate that it is a minimum rate.

Incision rates reported in the Granite Park area in western Grand Canyon over the past 300 to 600 ky are ~70 to 90 m/my (Lucchitta et al., 2000; Pederson et al., 2002b). In contrast, incision rates in the Furnace Flats area in eastern Grand Canyon, upstream of the Hurricane-Toroweap fault zone, are consistently ~140 m/my during approximately the same time period (Pederson et al., 2002b; Pederson et al., 2006).

Incision rates reported upstream in the tributary Fremont River over the past ~200 ky are 430 m/my (Marchetti and Cerling, 2005). Similar, yet slightly higher, incision rates of 400 to 700 m/my have been reported in the Glen Canyon region over the past ~500 ky (Garvin et al., 2005). In contrast to these relatively high rates within the greater Glen Canyon reach, Wolkowinsky and Granger (2004) report an incision rate along the tributary San Juan River of 110 m/my over the past 1.36 My. The different timescale used in this last calculation may be important in the interpretation of these data (Gardner et al., 1987). Adjustment using the scaling methods of Gardner et al. (1987) to the significantly longer-term San Juan River record (by an order of magnitude) yields an incision rate of ~170 m/my, which is more comparable to those reported downstream in Grand Canyon and in the upper Colorado River basin than to those in the Glen Canyon area.

Incision rates calculated in the upper Colorado River basin in Westwater Canyon using the Lava Creek B tephra (~600 ky) are ~180 m/my (Willis and Biek, 2001), significantly lower than rates reported from the Glen Canyon region. Similar incision rates (~150 m/my) have been reported from the upper Colorado River basin along the Green River and its major tributaries also using the Lava Creek B tephra (e.g. Reheis et al., 1991). Additional incision rates reported near the headwaters of the Colorado River in Glenwood Canyon over the past ~1.5 My are significantly higher (~240 m/my) than others in the upper Colorado River basin (Bryant et al., 2002).

The incision rates reported throughout the Colorado Plateau indicate differential incision along the Colorado River and its drainages through the Quaternary, especially in the Glen Canyon region (see bottom curve in Figure 2.2). Lees Ferry lies in the heart of this region at an inflection in long-profile gradient and contains a well-exposed suite of Pleistocene deposits and terraces (Hereford et al., 2000). Analysis of this fluvial record at Lees Ferry provides an independent datum between Glen and Grand canyons wherein the regionally variable incision rates from these sites can be investigated.

Lees Ferry is situated in a wide valley that marks the end of Glen Canyon and the start of Marble Canyon (Figure 2.1). Paleozoic and Mesozoic sedimentary rocks dominate the bedrock geology of the area and are well-exposed from river level to the surrounding escarpment of the Vermillion Cliffs (Phoenix, 1963). Differential erosion of the easily eroded Moenkopi Formation at river level has created a particularly wide valley wherein the preservation potential of fluvial deposits has been increased. The Paria River, a major tributary to the Colorado River, enters at this relatively open spot in the landscape. The Lees Ferry area is generally semiarid, although climate varies from the arid low-lying areas including terrace surfaces, to the subhumid higher elevations of surrounding high plateaus.

METHODS

We mapped Quaternary deposits in the Lees Ferry area in order to identify the sedimentary characteristics of fluvial deposits and correlate terrace levels. In addition, cross-sectional valley profiles have been surveyed using total station equipment in order to measure terrace heights. These field observations and measurements have been combined with two geochronologic tools, optically stimulated luminescence (OSL) and terrestrial cosmogenic nuclide ^{10}Be exposure (TCN) dating, in order to reconstruct the aggradation/incision history of the Colorado River and calculate incision rates at Lees Ferry. Although both dating methods have been used on fluvial deposits, ages calculated from OSL and TCN require different interpretations; OSL ages indicate the timing of aggradation, whereas TCN ages represent the timing of renewed incision.

Ten OSL sand samples were collected in aluminum tubes (5 cm x 20 cm) from recently exposed road or stream cuts. OSL sample preparation and analysis was performed at the University of Nebraska Luminescence Laboratory using the single-aliquot regenerative method on a RISO TL/OSL-DA-15B/C reader with blue-green light stimulation (470 nm, Hoya U340 filter). Additionally, four TCN surface samples were collected from terrace treads that exhibited long-term stability in the form of well-established desert pavements. Surface samples composed of ~100-200 quartzite pebbles (1-2 cm in diameter) were crushed and analyzed in a single amalgamated sample after the methods of Repka et al. (1997). A 220 cm depth-profile consisting of six quartz-rich sand samples (collected every 30 to 40 cm) was used to account for pre-depositional inheritance. This single good profile from the most prominent deposit in the area was used for all surface ages, with the assumption that the Colorado River has deposited sediment with a consistent amount of inheritance during each episode of aggradation in its cyclic history. TCN samples were prepared at Dalhousie University and accelerated mass spectrometer analysis was performed at Lawrence Livermore National Laboratory.

RESULTS

Seven distinct deposits (M1-M7) and ten terrace levels (M4y, M5m, and M5y are erosional fill-cut terraces) have been identified along the Colorado River in the Lees Ferry area (Figure 2.3). Deposits generally range from 10 to 30 m in thickness, and the most prominent of these deposits (M4) exhibits an irregular basal contact wherein a "false" strath is significantly higher than the true basal strath. Terrace levels range in height from 5.4 m (M1) to ~180 m (M7) above the reference river stage (380 m^3/s), and the treads of the M2-M5 terraces exhibit moderately- to well-developed desert pavements. Pavement surfaces have not formed on the M1 terrace due to recent or active deposition, whereas the M6 and M7 terraces are exhumed remnants and do not have preserved planar surfaces or well developed pavements. The deposits at Lees Ferry display three distinct sedimentary facies interpreted as: 1) a mixture of far-traveled (quartzite, volcanic porphyry) and local clasts (sandstone, chert, limestone) deposited in mainstem fluvial environments; 2) more massive debris flow beds dominated by local clast lithologies; and 3) overbank Colorado River sand.

Integrating the positions and ages of geochronologic samples (Table 2.1; Appendix D), we are able to reconstruct the fluvial history of the Colorado River at Lees Ferry and calculate a long-term bedrock incision rate. Maximum and minimum incision rates are reported due to the complex nature of aggradation and incision episodes represented by the fill terraces at Lees Ferry (Pederson et al., 2006). The minimum rate was calculated using elevation data and geochronology results from samples collected near the middle of the deposit (4-10 m above respective straths). The maximum rate was calculated using elevation data and geochronology results from samples near the terrace treads. Incision rates were calculated through linear regression of height vs. age plots of samples collected at similar positions within fluvial cycles (Figure 2.4). These are long-term average incision rates (>100 ky) that integrate pulses of incision, periods of stability, and aggradation episodes and should be comparable to other carefully calculated long-term rates reported throughout the Colorado Plateau.

DISCUSSION

Middle-late Pleistocene incision rates of 290 to 470 m/my at Lees Ferry are approximately two to three times higher than rates reported downstream along the Colorado River in eastern and western Grand Canyon (Pederson et al., 2002b; Lucchitta et al., 2000) (Figure 2.2). Similarly, incision rates at Lees Ferry are significantly higher than rates reported upstream in Westwater Canyon (~180 m/my; Willis and Biek, 2001), in the greater Green River basin (~150 m/my; Reheis et al., 1991), and along the San Juan River (~110 m/my; Wolkowinsky and Granger, 2005). In contrast, our range is similar to, yet slightly lower, than those reported just upstream in the greater Glen Canyon reach (Garvin et al., 2005), including the tributary Fremont River (Marchetti and Cerling, 2005). Incision rates of ~240 m/my near the headwaters in Glenwood Canyon reported by Bryant et al. (2002) are also slightly lower than those that we report from Lees Ferry.

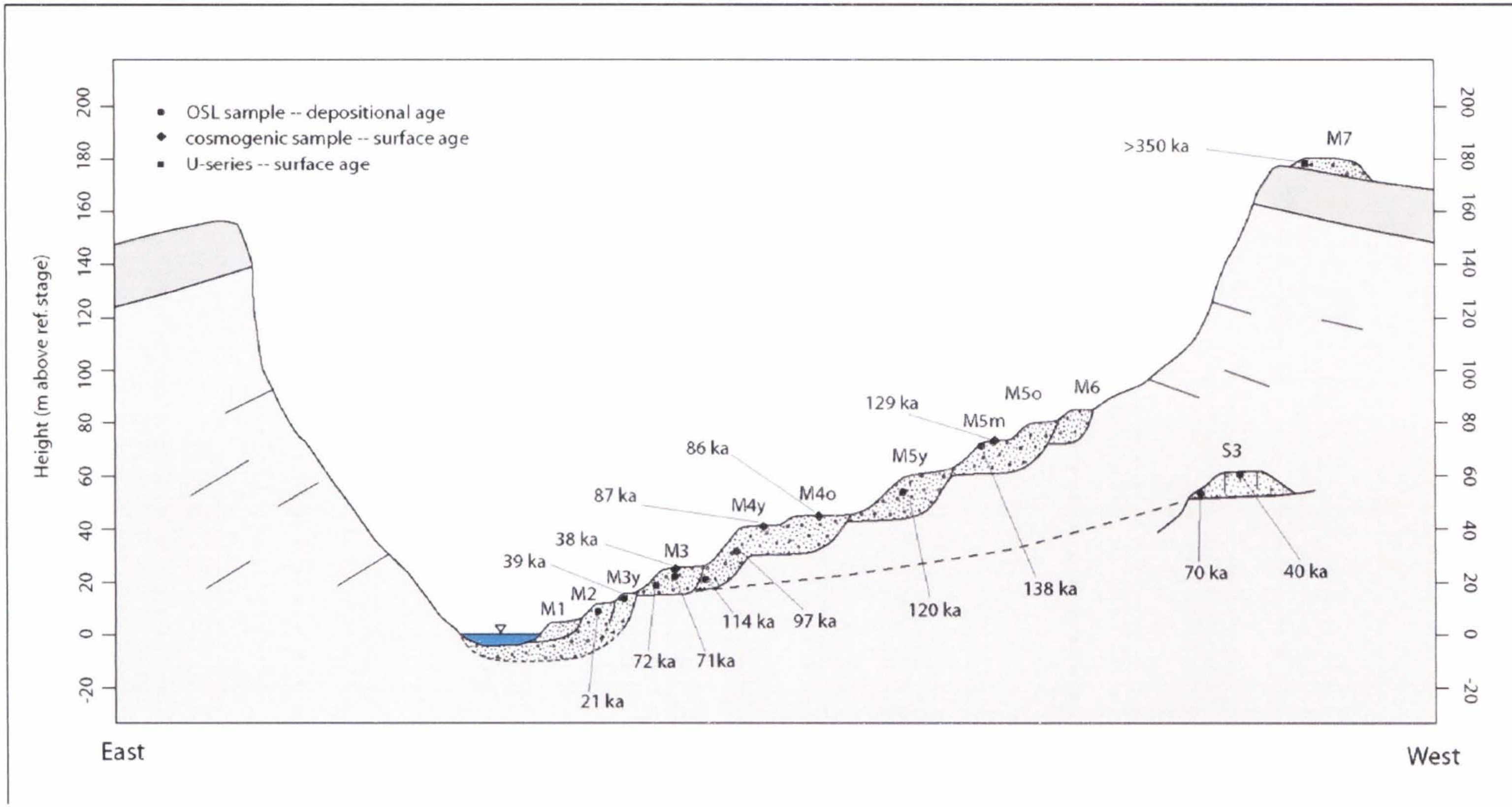

Figure 2.3. Schematic cross-sectional valley profile of the fill terraces at Lees Ferry, showing heights, geometries, and ages of deposits. See Table 2.1 for error calculations on individual ages.

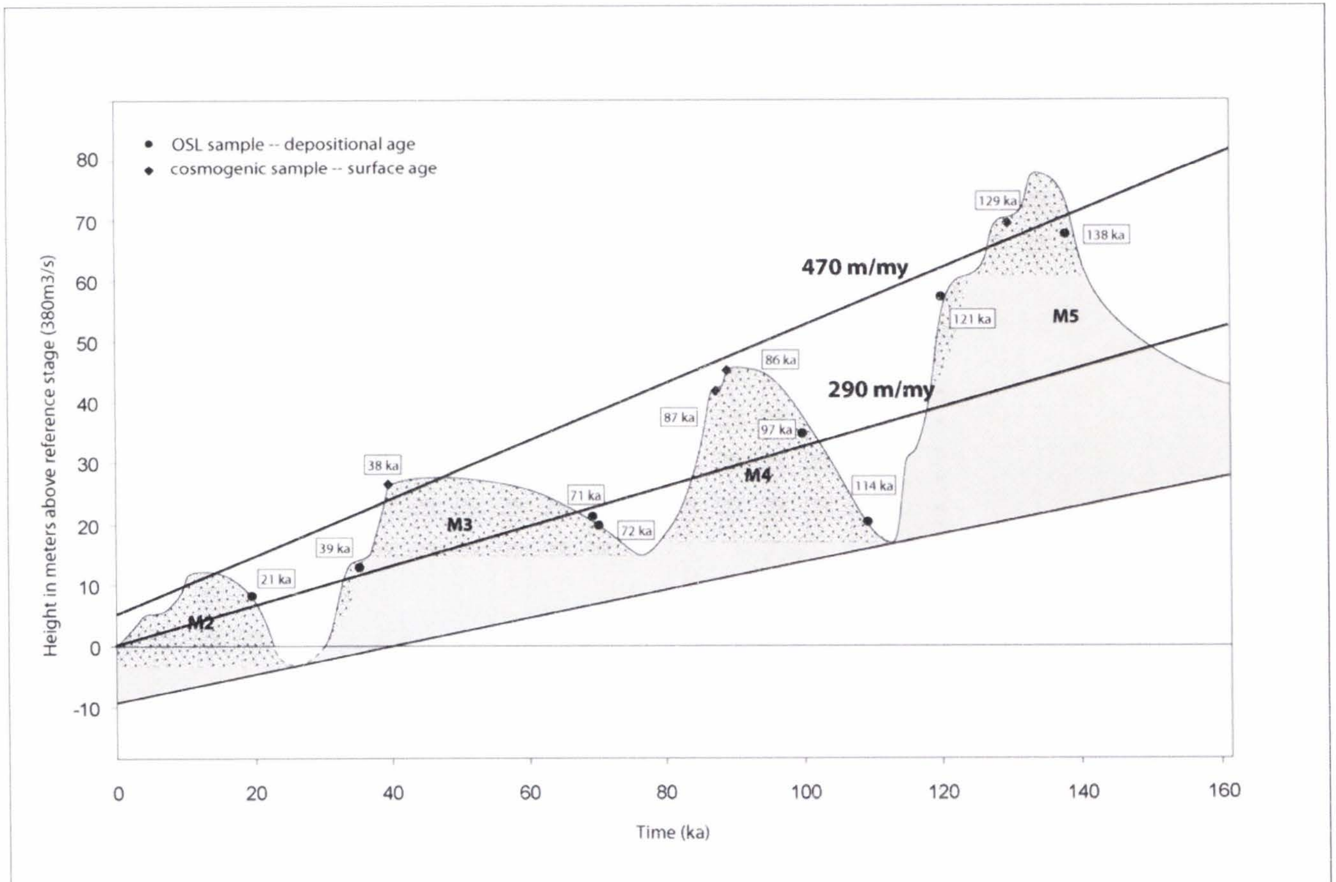

Figure 2.4. Curve representing the height of the Colorado River channel bed through time. Stippled pattern represents fill deposits, whereas the gray represents bedrock. Alluvial aggradation cycles are superimposed on overall downcutting at Lees Ferry. Solid bold lines are regressions approximating minimum and maximum incision rates at Lees Ferry. See Table 2.1 for error calculations on individual ages.

Table 2.1. Survey and geochronologic data for Colorado River deposits.

Data Point Description	Height (m)[1]	Age (ka)[2]	Dating Method
Colorado River			
Holocene flood deposits (M1)	0-6		Various
Surveyed M2 terrace tread	14.4	--	--
M2 sand lens in fill	10.7	21 ± 1	OSL[5]
M3y sand lens in fill	12.8	39 ± 3	OSL[5]
Surveyed M3 strath	15.3	--	--
Surveyed M3 terrace tread	25.6	--	--
M3 desert pavement	25.6	38 ± 3	TCN[4]
M3 sand lens in fill	19.2	72 ± 5	OSL[5]
M3 sand lens in fill	22.2	71 ± 5	OSL[5]
S3 sandy unit in fill	51.9	70 ± 6	OSL[5]
S3 sandy unit in fill	60.2	40 ± 3	OSL[5]
Surveyed M4 strath (lower)	15.8	--	--
Surveyed M4 strath (upper)	30.8	--	--
Surveyed M4y terrace tread	41.8	--	--
M4y desert pavement	41.8	87 ± 7	TCN[4]
Surveyed M4o terrace tread	45.8	--	--
M4o desert pavement	45.8	86 ± 7	TCN[4]
M4 sand lens in fill	34.9	97 ± 8	OSL[5]
M4 sand lens in fill	18.3	114 ± 8	OSL[5]
Surveyed M5 strath (lower)	42.5	--	--
Surveyed M5 strath (upper)	60.5	--	--
M5y sand lens in fill (lower)	45.0	121 ± 12	OSL[5]
M5 sand lens in fill (upper)	62.5	138 ± 10	OSL[5]
Surveyed M5y terrace tread	64.3	--	--
Surveyed M5m terrace tread	66.7	--	--
M5m desert pavement	66.7	129 ± 10	TCN[4]
Surveyed M5o terrace tread	78.7	--	--

[1] Referenced to a local river stage of 380 m^3/s (13,000 cfs)
[2] 2δ errors reported for all ages
[3] Fine-grained Holocene overbank sediment of the Colorado River (Hereford et al., 2000)
[4] Terrestrial cosmogenic-nuclide date of surface sample corrected for inheritance with depth-profile, minimum surface age (see Appendix E for complete data)
[5] OSL samples represent ages of deposition (see Appendix F for complete data)

Our data confirm that Quaternary incision of the central Colorado Plateau is relatively fast and indicate that a reach of faster incision may exist in the greater Lees Ferry and Glen Canyon region (Figure 2.2). Variable incision rates downstream of Lees Ferry in eastern and western Grand Canyon have been well explained by localized movement along active Quaternary faults (Pederson et al., 2002b); however, the cause of differential incision in the upper Colorado River and its drainages remains unresolved. We propose that differential incision of the Colorado Plateau, especially in the Lees Ferry and Glen Canyon region, may be caused by: 1) epeirogenic uplift enhanced by erosion exhumation of the central plateau; or 2) waves of incision (knickzones) passing through the region.

Data from the southern edges of the Colorado Plateau suggest that epeirogenic uplift rates of the region since ~5 Ma are ~220 m/my (Sahagian et al., 2002). Although these rates are broadly consistent with incision rates reported throughout the Colorado Plateau, epeirogenic uplift could only result in the regional pattern we report if a localized portion of the central plateau were uplifting faster than surrounding areas. This study will be the first to test this hypothesis in the greater Glen Canyon region.

One established positive feedback of epeirogenic rock uplift reported on the Colorado Plateau is isostatic rebound driven by erosional exhumation (Pederson et al., 2002a). Although epeirogenic uplift of a central portion of the Colorado Plateau remains untested, higher erosional exhumation in the Henry Mountain and Glen Canyon region could produce a localized isostatic response at a wavelength of ~400 km (Roy et al., 2005). Significantly higher incision rates within the potentially affected region would be expected, particularly in the Lees Ferry and Glen Canyon areas. In contrast, the apparently low incision rates reported near this region from Westwater Canyon (~180 m/my) and the San Juan River (~110 m/my) argue against this hypothesis. However, these latter incision rates have been calculated from areas that are located on the flanks of this region of high total exhumation (Pederson et al., 2002a) and would be expected to have slightly lower incision rates.

Alternatively, the higher incision rates along the Lees Ferry and Glen Canyon reach may indicate that a transient knickzone has passed through the region. In terms of faulting that might drive such a knickpoint, the Hurricane and Toroweap faults in western Grand Canyon are the only active faults downstream of Lees Ferry. However, the down-to-the-west motion on these normal faults primarily results in hangingwall subsidence, not footwall uplift, and can only be geometrically responsible for dampening some downstream incision rather than driving upstream downcutting (Pederson et al., 2002b).

Another possible source of baselevel fall that would result in a transient knickzone is the drainage integration of the Colorado River off the Colorado Plateau. This resulted in a geologically instantaneous >1000 m baselevel drop at ~6 Ma that must have been transferred upstream through the Grand Canyon and into the upper Colorado River basin (Pederson et al., 2002b). The question remains: would this ancient drainage capture event still have a transient signal in the central plateau region today? Bryant et al. (2002) report incision rates that increase from the late Miocene and early Pliocene (24 m/my) to the Pleistocene (241 m/my) in Glenwood Canyon (see also Larson et al., 1975). This may indicate the upper portion of the Colorado River basin had already felt at least a portion of this baselevel fall by ~1.5 Ma. However, the Colorado River and its tributaries could reasonably still be responding to the original drainage integration today and a partial signal of that initial event may still have a transient signal in the region. In particular, hard bedrock may act to delay or hold up a knickzone as it passes through a system and diffuses (Gardner, 1983; Crosby and Whipple, in press), slowing incision and creating locally steep reaches. In contrast, weak bedrock may locally enable incision and result in low gradient reaches (e.g. Stock et al., 2005; Mackley, 2005). The steeper gradient but relatively low incision rates in Grand Canyon may indicate that part of the signal from the original drainage capture is held up by the harder bedrock of the area. In contrast, the lower gradient, soft bedrock, and higher incision rates reported from Lees Ferry up through Glen Canyon is consistent with a signal that may have passed through the area quickly.

In conclusion, as our knowledge of the evolution of the Colorado River system improves, a complex picture of river incision is beginning to emerge. On the scale of the entire drainage basin, incision of the Colorado Plateau is driven by the baselevel fall that occurred at the onset of drainage integration 5-6 Ma. However, a zone of higher incision rates in the greater Lees Ferry and Glen Canyon reach has become evident with the addition of this research. These faster mid-late Pleistocene incision rates of the central Colorado Plateau may be caused by: 1) localized epeirogenic uplift due to tectonics and isostatic rebound; or 2) transient knickzones resulting from drainage integration ~6 Ma, which are moderated by variations in bedrock resistance.

REFERENCES CITED

Bryant, B., Kunk, M.J., and Kirkham, R.M., 2002, Timing and rates of late-Cenozoic incision by the Colorado River in Glenwood Canyon, Colorado: GSA Abstracts with Programs, v. 34, p. 320.

Crosby, B.T., and Whipple, K.X., in press, Knickpoint initiation and distribution within fluvial networks: 236 waterfalls in the Waipaoa River, North Island, New Zealand: submitted to Geomorphology.

Davis, W.M., 1901, An excursion to the Grand Canyon of the Colorado: Harvard College, Bulletin of the Museum of Comparative Zoology, v. 38, p. 120-126.

Dutton, C.E., 1882, The Tertiary history of the Grand Canyon district: U.S. Geological Survey Monograph 2, 264 p.

Faulds, J.E., Wallace, M.A., Gonzalez, L.A., and Heizler, M.T., 2001, Depositional environment and paleogeographic implications of the late Miocene Hualapai Limestone, northwestern Arizona and southern Nevada: *in* Young, R.A. and Spamer, E.E., eds., Colorado River—Origin and Evolution: Grand Canyon, AZ, Grand Canyon Association, p.81-87.

Gardner, T.W., 1983, Experimental study of knickpoint and longitudinal profile evolution in cohesive, homogeneous material: Geological Society of America Bulletin, v. 94, p. 664-672.

Gardner, T.W., Jorgensen, D.W., Shuman, C., and Lemieux, C.R., 1987, Geomorphic and tectonic process rates: effects of measured time interval: Geology, v. 15, p. 1035-1038.

Garvin, C., Hanks, T, Finkel, R.C., and Heimsath, A.M., 2005, Episodic incision of the Colorado River in Glen Canyon, Utah: Earth Surface Processes and Landforms, v. 30, issue 8, p. 973-984.

Hancock, G.S., and Anderson, R.S., 2002, Numerical modeling of fluvial strath terrace formation in response to oscillating climate: Geological Society of America Bulletin, v. 114, p. 1131-1142.

Hereford, R., Burke, K.J., and Thompson, K.S., 2000, Map showing Quaternary geology and geomorphology of the Lees Ferry area, Glen Canyon, Arizona: U.S. Geological Survey Geologic Investigations Series Map I-2663, scale 1:2000.

Hunt, C.B., 1969, Geologic history of the Colorado River: *in* The Colorado River Region and John Wesley Powell: U.S. Geological Survey Professional Paper 669, p. 59-130.

Larson, E.E., Ozima, M., and Bradley, W.C., 1975, Late Cenozoic basic volcanism in northwestern Colorado and its implications concerning tectonism and the origin of the Colorado River system: *in* Curtis, B.F., ed., Cenozoic history of the southern Rocky Mountains: Geological Society of America Memoir 144, p. 155-178.

Lucchitta, I., 1966, Cenozoic geology of the Lake Mead area adjacent to the Grand Wash Cliffs, Arizona [Ph.D. dissertation]: Pennsylvania State University, 218 p.

Lucchitta, I., 1972, Early history of the Colorado River in the Basin and Range province: Geological Society of America Bulletin, v. 83, p. 1933-1948.

Lucchitta, I., Garniss, H.C., and Turrin, B., 2000, Cyclic aggradation and downcutting, fluvial response to volcanic activity, and calibration of soil-carbonate stages in the western Grand Canyon, Arizona: Quaternary Research, v. 53, p. 23-33.

Mackley, R.D., 2005, Relating bedrock strength to hydraulic driving forces along the large-scale profile of the Colorado River in Glen and Grand Canyons [M.S. thesis]: Utah State University, 165 p.

Marchetti, D.W., and Cerling, T.E., 2005, Cosmogenic 3He ages of Pleistocene debris flows and desert pavements in Capital Reef National Park, Utah: Geomorphology, v. 67, p. 423-435.

McKee, E.D., and McKee, E.H., 1972, Pliocene uplift of the Grand Canyon region: time of drainage adjustment: Geological Society of America Bulletin, v. 83, no. 7, p. 1923-1932.

Merritts, D.J., Vincent, K.R., and Wohl, E.E., 1994, Long river profiles, tectonism, and eustacy: a guide to interpreting fluvial terraces: Journal of Geophysical Research, v. 29, no., B7, p. 14,031-14,050.

Pederson, J.L, Mackley, R.D., and Eddleman, J.L., 2002a, Colorado Plateau uplift and erosion evaluated using GIS: GSA Today, v. 12, no. 8, p. 4-10.

Pederson, J.L., Karlstrom, K., Sharp, W., and McIntosh, W., 2002b, Differential incision of Grand Canyon related to Quaternary faulting—constraints from U-series and Ar/Ar dating: Geology, v. 30, no. 8, p. 739-742.

Pederson, J.L, Anders, M.D., Rittenour, T.M., Sharp, W.D., Gosse, J.C., Karlstrom, K.E., Crossey, L.J., Goble, R.J., and Finkel, R.C., 2006, Using fill terraces to understand incision rates and evolution of the Colorado River in eastern Grand Canyon, Arizona: Journal of Geophysical Reseach-Earth Surface, v. 111, F02003.

Phoenix, D.A., 1963, Geology of the Lees Ferry area, Coconino County, Arizona: U.S. Geological Survey Bulletin 1137, 86 p.

Powell, J.W., 1875, Exploration of the Colorado River of the West and its tributaries, 1869-1872: Washington D.C., U.S. Government Printing Office, Smithsonian Institute Publication, 291 p.

Reheis, M.C., Palmquist, R.C., Agard, S.S., Jaworowski, C., Mears, B., Jr., Madole, R.F., Nelson, A.R., and Osborn, G.D., 1991, Quaternary history of some southern and central

Rocky Mountain basins: Bighorn basin, Green Mountain – Sweetwater River area, Laramie basin, Yampa River basin, northwestern Uinta basin: *in* Morrison, R.B., ed., Quaternary nonglacial geology: Conterminous U.S.: Boulder, Colorado, Geological Society of America, Geology of North America, v. K-2, p. 427-431.

Repka, J.L., Anderson, R.S., and Finkel, R.C., 1997, Cosmogenic dating of fluvial terrace, Fremont River, Utah: Earth and Planetary Science Letters, v. 152, p. 59-73.

Roy, M., MacCarthy, J.K., and J. Selverstone, 2005, Upper mantle structure beneath the eastern Colorado Plateau and Rio Grande rift revealed by Bouguer gravity, seismic velocities, and xenolith data: *Geochemistry Geophysics Geosystems*, v. 6.

Sahagian, D.A., Proussevitch, A., and Carlson, W., 2002, Timing of Colorado Plateau uplift: initial constraints from vesicular basalt-derived paleoelevations: Geology, v. 31 (2), p. 191-191.

Stock, J. D., Montgomery, D. R., Collins, B. D., Dietrich, W. E., and Sklar, L., 2005, Field rates of incision following bedrock exposure: Implications for process controls on the long-profiles of valleys cut by rivers and debris flows, Geological Society of America Bulletin, v. 117, p. 174-194.

Willis, G.C., and Biek, R.F., 2001, Quaternary incision rates of the Colorado River and major tributaries in the Colorado Plateau, Utah: *in* Young, R.A. and Spamer, E.E., eds., Colorado River—Origin and Evolution: Grand Canyon, AZ, Grand Canyon Association, p. 119-124.

Wolkowinsky, A. J., and Granger, D. E., 2004, Early Pleistocene incision of the San Juan River, Utah, dated with 26-Al and 10-Be: Geology, v. 32 , p. 749-752.

Young, R.A., and McKee, E.D., 1978, Early and middle Cenozoic drainage and erosion in west-central Arizona: Geological Society of America Bulletin, v. 89, p. 1745-1750.

CHAPTER 3

PATTERNS OF FLUVIAL AGGRADATION AND DEGRADATION RELATED TO CLIMATE CHANGE ALONG THE COLORADO RIVER AT LEES FERRY, ARIZONA[2]

ABSTRACT

A well-exposed suite of Colorado River fill terraces preserved at Lees Ferry records the oscillating history of this major river superimposed on its overall downcutting of the Colorado Plateau. Detailed mapping, sedimentology, and the use of two geochronometers has been undertaken in order to establish a detailed chronostratigraphy for the area. Seven distinct deposits have been identified along the Colorado River, and four deposits have been identified along the Paria River. Geochronology of six of these deposits using optically stimulated luminescence and cosmogenic ^{10}Be exposure dating techniques indicates that river aggradation occurred at ~20 ka (M2), ~70 to 40 ka (M3), ~115 to 90 ka (M4), and ~130 ka (M5). Aggradation and incision along the Paria River appears to have occurred in concert with that on the Colorado River, at least at its mouth where baselevel affects may be a strong control. Sedimentologic and stratigraphic examination of the deposits suggests that far-traveled sediment has been mixed with locally derived fluvial and debris-flow facies, with the proportion of these not detectably changing through time. Deposits at Lees Ferry are generally younger than correlative deposits in headwater catchments and in eastern Grand Canyon. In addition, deposition of the M4 occurred ~115 to 90 ka during a time in which no glaciations have been

[2] Coauthored by W. Scott Cragun, Joel L. Pederson, and Tammy M. Rittenour

reported in headwater drainages. Our data indicate that fluvial responses at Lees Ferry are a complicated integration of signals from climate change in headwater catchments and sediment production from local hillslopes and tributaries.

INTRODUCTION

The influence of climate change on fluvial processes and the evolution of river systems has been debated since the early 1900's when Penck and Brückner (1909) recognized the connection between glacial moraines in the Alps and fluvial deposits in the Alpine foreland. Research on this subject has been revitalized in the past several decades with the advent of innovative dating techniques such as cosmogenic exposure and optically stimulated luminescence (e.g. Repka et al., 1997; Aitken, 1998; Forman et al., 2000; Zreda and Phillips, 2000). Detailed fluvial chronologies have been reported from headwater rivers within or near glaciated terrain that suggest the timing of aggradation and degradation cycles closely matches glacial-interglacial oscillations observed throughout the Quaternary (e.g. Chadwick et al., 1997; Pan et al., 2003). Deposition and incision along large continental rivers also occurs in response to glacial-interglacial scale climate change (e.g. Blum and Törnqvist, 2000; Straffin et al., 2000; Törnqvist et al., 2000; Anders et al., 2005); however, our understanding of how regional rivers integrate climate signals from the diverse bio-climatic and geomorphic terrains within their drainage basins remains incomplete.

In general, local patterns of aggradation and degradation along the length of large fluvial systems are determined by climate change, sea-level fluctuation, and baselevel change in response to drainage integration or tectonic movement (e.g. Blum and

Törnqvist, 2000; Wallinga et al., 2004). Climate change resulting in the advance and retreat of glaciers creates signals that migrate downstream from headwater sources, whereas baselevel change in response to fluctuating sea-level generally affects only the lower portion of fluvial systems (Blum and Törnqvist, 2000). Drainage integration and tectonic movement may also affect the responses of large fluvial systems within specific reaches where these processes are active. In addition, changes in hillslope sediment production and hydrology as a result of local climate change may create unique responses within specific reaches and will become integrated with both upstream and downstream-sourced signals. Sorting out the interplay between these spatially and temporally variable factors is not simple. However, analysis of terrace geometries and sedimentology, coupled with a geochronologic framework, provides a valuable first step in deciphering the various controls on fluvial responses within these complex systems.

The Colorado River has a drainage area of ~640,000 km^2 and passes through seven U.S. states before reaching the Pacific Ocean in the Gulf of Mexico. The ~2300 km course of this continental-scale river begins in the alpine headwaters of the Rocky Mountains and traverses the semiarid and arid regions of the Colorado Plateau and Great Basin. Lees Ferry lies in the center of the Colorado River drainage in an open valley between the generally steep landscapes of Glen and Grand canyons (Figure 3.1). The Lees Ferry area features a well-exposed suite of fill terraces that record an integrated signal of changes occurring within its large and varied catchment.

In this paper, we present a robust chronostratigraphy of the fill terraces along the Colorado and Paria rivers at Lees Ferry using optically stimulated luminescence (OSL) and terrestrial cosmogenic nuclide ^{10}Be exposure (TCN) dating techniques in conjunction with stratigraphic and sedimentologic analyses. The chronostratigraphy of these deposits is presented elsewhere in order to derive long-term incision rates (Chapter 2). Here we focus on the relation between sedimentology, stratigraphy, and geochronology of deposits in the greater Lees Ferry area in order to document the timing and patterns of aggradation and incision of this large river and begin to interpret its relation to distant and local climatic forcing.

BACKGROUND

Factors controlling the aggradation and degradation of fluvial systems have been debated for many years and continue to be explored by geomorphologists. Long-term regional erosion typically occurs as a result of baselevel fall through large-scale tectonic events. In contrast, shorter-term aggradation and degradation cycles, which are the subject of this paper, may be superimposed on overall downcutting of a region and occur in response to three major forcing factors: 1) climate change; 2) sea level fluctuation; and 3) baselevel controls such as tectonic activity or drainage integration.

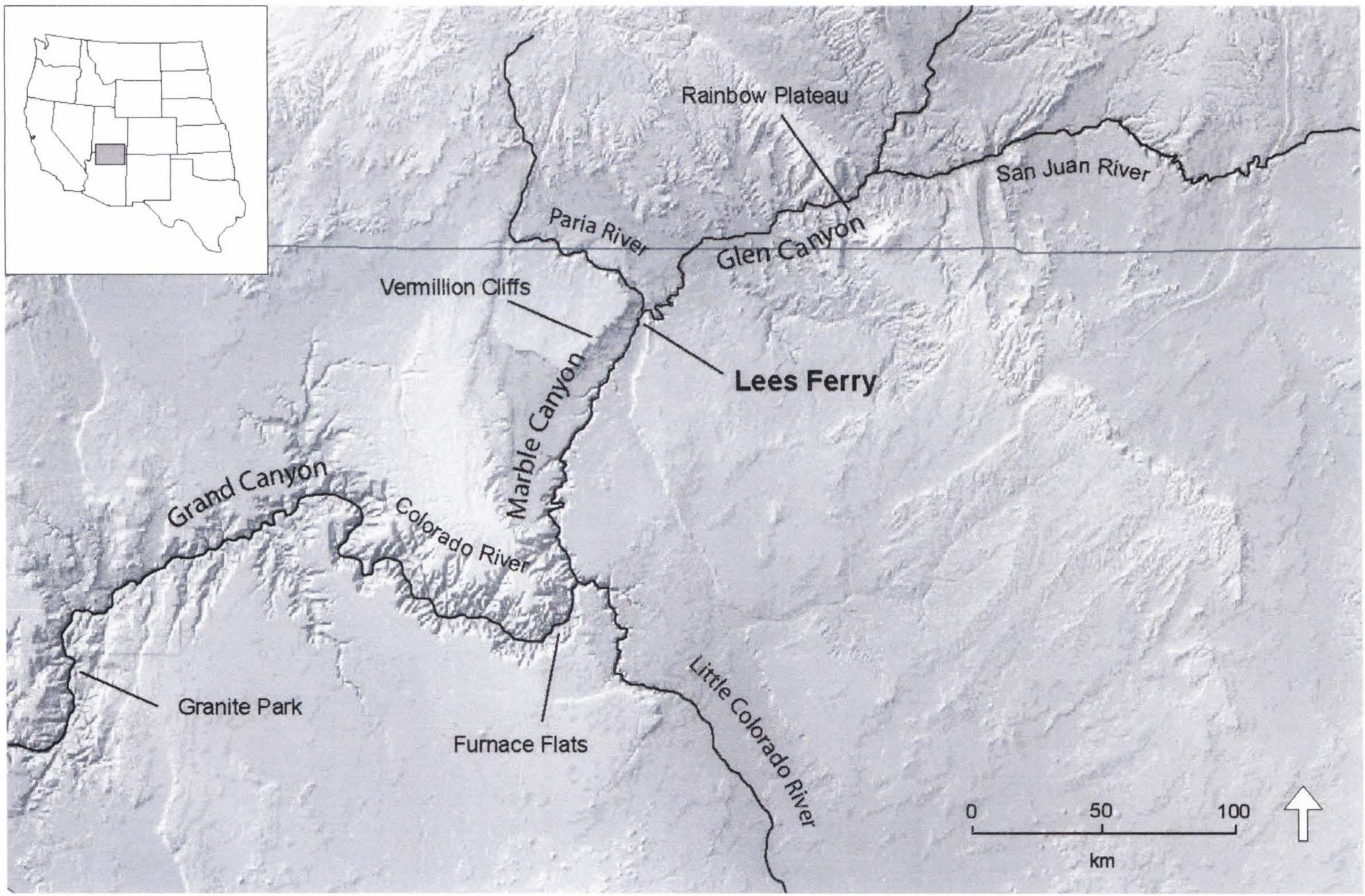

Figure 3.1. Shaded relief map of the central Colorado Plateau, showing the Colorado River and its major tributaries.

In general, climate change influences the balance between hydrology and sediment supply within a fluvial system. The extent of alpine and continental glaciers, weathering rates, topography, and vegetation cover within headwater catchments ultimately govern the amount of water and sediment delivered to a system through time. The ratio between the size and quantity of sediment and the ability of a stream to transport that sediment determines whether a stream will aggrade, incise, or remain in equilibrium (Lane, 1955; Bull, 1991). Aggradation occurs as flow competence within a fluvial system decreases, either as a result of decreasing discharge or increasing quantity of sediment delivered to the system. Greater sediment production in drainage basins during times of particularly intense physical or chemical weathering (i.e. glacial environments or changes in vegetation cover) can overwhelm a fluvial system with more sediment than can be carried. Decreases in effective discharge will also reduce the ability of a river to move sediment and may occur in response to lower precipitation or greater infiltration within a basin (e.g. Bull, 1991; Tucker and Slingerland, 1997). In contrast, incision happens as discharge increases or sediment supply from hillslopes decreases. Greater effective discharge may occur as a result of increased quantity or intensity of precipitation, increased effective runoff from catchments, or from glacial meltwater. Decreased sediment supply may be a result of increased storage in catchments or lower sediment production on hillslopes. These climatically controlled variations in discharge and sediment supply in response to glacial-interglacial oscillations are transferred downstream and become integrated throughout the entire length of large fluvial systems (e.g. Hancock and Anderson, 2002).

Sea-level fluctuations resulting from varying volumes of global ice introduce the potential for aggradation and degradation through the lower reaches of fluvial systems that reach the sea (Blum and Törnqvist, 2000). Rising sea-level results in decreased gradients that cause localized aggradation or increased sinuosity as lower reaches are flooded (Leopold and Bull, 1979; Schumm, 1993; Merritts et al., 1994). In contrast, lowered sea-level results in steeper gradients that effectively increase stream power and allow rivers to re-establish graded profiles through vertical incision (Mackin, 1948). A rapid sea-level fall can result in the formation of a knickpoint that can migrate tens of kilometers upstream creating a transient pulse of incision through the system (e.g. Crosby and Whipple, in press).

Baselevel changes in response to tectonic movement or drainage integration further influence the pattern of aggradation and degradation occurring throughout large fluvial systems, particularly in localized areas where these forces are active (e.g. Pederson et al., 2002). Tectonic movement due to faulting or epeirogeny has the potential to create or reduce accommodation space for deposition and influences the baselevel for specific reaches along the length of a river. Drainage integration has been a significant factor in the evolution of rivers in the interior western U.S (e.g. Longwell, 1946; Hunt, 1969). Stream capture occurs as river systems evolve and become integrated through headward erosion and stream piracy or by basin-spillover (Pederson, 2001).

Oscillating fluvial processes in response to the complex interaction between climate change, sea-level fluctuation, and tectonic/drainage integration controls often result in the formation of terrace sequences along fluvial valleys. Several studies from around the world have reported detailed fluvial chronostratigraphic records in order to help refine our understanding of how fluvial processes respond to upstream and downstream controls. The following is an overview of the literature surrounding this debate and is organized in two sections. The first section reviews the response of major continental rivers to climate change, sea-level fluctuation, and tectonic controls. The second section examines sub-catchments within the Colorado River drainage and studies relating their response to Quaternary climate change.

Responses of continental-scale rivers

Observations and studies from several large fluvial systems throughout Europe and the United States illustrate the complex and varied responses of fluvial systems to upstream, downstream, and local controls (e.g. Straffin et al., 2000; Lewis et al., 2001; Rittenour et al., 2003; Anders et al., 2005). However, given the different climatic settings and varying thresholds that may exist within these systems, it is reasonable to expect that the fluvial responses of large rivers to global climate change will have varying lag-times and will not always be in phase (Blum and Törnqvist, 2000). For example, episodic deposition of two major braided channel belt systems along the lower Mississippi River valley occurred during marine isotope stage (MIS) 6 and 2 in response to high discharge conditions from melting glaciers (Blum and Törnqvist, 2000; Rittenour et al., 2003). In contrast, deposition of fluvial gravels along the River Loire in France occurred during marine isotope stages (MIS) 5e, 5b, 4-3, and 2, contemporaneously through both warm and cold periods (Straffin et al., 2000; Colls et al., 2001).

Not only are disparities in the timing of deposition apparent when comparing the large rivers of the world, but the mechanisms responsible for aggradation-degradation episodes can be spatially variable along the length of a single system. The River Seine in France is of particular interest relative to the Colorado River since it contains a well-developed sequence of Pleistocene fluvial terraces that record the variable influence of climate and sea-level change along the distinct middle and lower portions of the system (Antoine et al., 2000). The dominant control on river evolution and incision along the lower Seine is interpreted to be the lowering of sea-level, particularly during the coldest periods observed in the record (MIS 2, 6, 12, 16, and 22). In contrast, the middle Seine is beyond the influence of sea-level fall and has responded to climatically controlled variations in discharge and sediment supplied to the system during glacial-interglacial variations (Antoine et al., 2000).

Further complexities have been documented in the Rhine-Meuse system in west-central Netherlands, wherein fluvial responses at a single location within the system have been interpreted to be controlled by different forcing mechanisms through time (Törnqvist et al., 2000; Wallinga et al., 2004). Sedimentologic and geochronologic analysis of a ~20 m thick sequence of inset fluvial sediments near the river's mouth reveals two significant episodes of degradation and subsequent aggradation over the last two glacial cycles. The older phase of incision occurred at the MIS 5/4 transition in response to a significant sea-level fall, whereas the younger phase of incision occurred at the MIS 3/2 transition and is interpreted as the result of crustal updoming along a glacial forebulge. In addition, the older depositional episode occurred during MIS 4-3 and was interpreted to be controlled by cold and dry climatic conditions wherein relative sediment supplies were increased. The younger episode of aggradation occurred after the last glacial maximum (MIS 2) in response to collapse of the glacial forebulge.

Similar temporal variations in climate responses have been reported from the River Thames in England (Maddy et al., 2001; Lewis et al., 2001). Abrupt climate changes during the transition to glacial conditions at ~70 ka and the rapid climate fluctuations during deglaciation from 13 to 11 ka resulted in an increase in overall sediment grain size and a change from single-channel to a braided system. Aggradation of the River Thames is constrained through luminescence and radiocarbon geochronology and is bracketed during the latter part of MIS 5 between ~110 and 70 ka and during the last glacial maximum (LGM) between ~18 and 10 ka (Lewis et al., 2001).

In summary, patterns of aggradation and degradation along large continental rivers vary depending upon position within the system and generally occur in response to the interplay between upstream, downstream, and local controls. Variations in the timing of deposition and incision throughout the large fluvial systems of the world are evident, especially when comparing fluvial responses within a particular glacial period. In addition, temporal and spatial variations in response to forcing mechanisms within a single drainage have been documented throughout the world, making it difficult to correlate records. Our study focuses on the aggradation-incision responses recorded along the Colorado River at Lees Ferry where variations in local sediment supply have likely become incorporated with distant hydrologic signals from headwater sources through the Quaternary (Anders et al., 2005).

Responses of Colorado River sub-catchments

The connection between glacial-interglacial scale climate change and fluvial aggradation-incision can be readily observed in the headwater drainages of the Colorado

River. Fluvial terraces have been traced in several alpine tributaries within the Rocky Mountains directly upstream to outwash plains and moraines emplaced during the last glacial advance (e.g. Reheis et al., 1991; Chadwick et al., 1997; Counts and Pederson, 2005). Detailed mapping of fluvial deposits and correlation to locally dated glacial moraines along the Henry's Fork (Counts and Pederson, 2005), Yampa River (Madole, 1991), and within the Uinta Basin (Nelson and Osborn, 1991) indicate that the two most prominent terrace levels within these tributaries appear to have developed synchronously with the MIS 6 Bull Lake (~140 ka) and MIS 2 Pinedale (~20 ka) glacial advances. The early Wisconsin MIS 4 glacial advance is typically missing in the Rocky Mountain glacial record and often very minor in the pro-glacial fluvial record.

Although observed field relations within headwater drainages provide a reasonable correlation between glacial advances and aggradation-incision episodes, geochronologic data from several drainages within the region and further downstream along the Colorado River provide a more precise, yet incomplete, characterization as to the timing of these fluvial responses. Adjacent to the Colorado River headwaters, well-constrained studies from the upper Wind River have recognized several well-preserved terrace levels near the heavily glaciated Wind River Mountains (Gosse et al., 1995; Chadwick et al., 1997; Phillips et al., 1997). Minimum ages of terrace treads have been calculated using cosmogenic and U-series methods for terrace levels WR-3 (125 ka or 150 ka – MIS 6), WR-2 (55 ka – MIS 4), and WR-1 (21 ka – MIS 2). These ages indicate that the timing of fluvial incision (terrace abandonment) generally corresponds to reported peak glaciations or subsequent deglacial transitions of the region (Hancock et al., 1999; Sharp et al., 2003).

Fluvial incision recorded by cosmogenic surface ages of the well preserved Fremont River terraces in southern Utah at 151 ka (MIS 6) and 60 ka (MIS 4) similarly correlate well with the timing of glacial peaks or deglaciation in the region (Marchetti and Cerling, 2005). However, an additional incision event observed at ~100 ka does not correlate with any reported glaciation in the region and may reflect other sediment or hydrologic controls. In addition, no deposit of MIS 2 age has been reported from the Fremont drainage.

Portions of the Colorado River system located well downstream of glaciated catchments also respond to glacial-interglacial scale climate change. Geochronology of the fill terraces along the Colorado River in eastern Grand Canyon indicates that aggradation occurred from 385 to 322 ka (M5), about 130 to 90 ka (M4), and from about 75 to 60 ka (M3), with significant river incision following each event (Anders et al., 2005; unpublished data). Comparison to global and regional paleoclimate records suggests that aggradation in eastern Grand Canyon began during the latter part of glacial periods and into early interglacial periods, followed by incision that begins at some point within subsequent interglacial periods (Anders et al., 2005). Notably, the authors recognize that deposition in local catchments of the Grand Canyon does not match the timing and stratigraphy along the Colorado River and hypothesize that distinct local sediment production and hydrologic processes control the aggradation and incision of side drainages.

As noted in the studies above, new geochronologic data from deposits throughout the Colorado River drainage system are providing an emerging picture as to the timing of aggradation and incision in response to upstream climatic forcing factors. However, discrepancies between various drainages are apparent. Deposits from the MIS 2 last-glacial episode that are readily observed in headwater drainages have not been identified in either the Fremont River or along the Colorado River through the Grand Canyon. In addition, the detailed yet complex record from the mainstem Colorado River and its small tributaries demonstrates the complex interaction between upstream glacial and local climatic control. Our results from Lees Ferry provide a robust chronostratigraphy that contributes to an emerging picture of the responses of this large river to climatic forcing.

SETTING

The preservation of deposits and landforms that record the fluvial history of the Colorado River in the erosional landscape of the Colorado Plateau are understandably rare. The few river gravels and terraces that remain along the river corridor generally exist in locations where erosion of softer strata or bedrock structural controls have created wide valleys. Lees Ferry is situated in a short but relatively wide valley that marks the end of Glen Canyon and the start of Marble Canyon (Figure 3.1). The Paria River, a major tributary to the Colorado River, enters at this relatively open spot in the landscape. Lees Ferry is one of the only places in the Grand Canyon region to have been used historically as a river crossing due to the ease of river access. Native Americans used the crossing for centuries before the arrival of early western settlers (Andrews, 1990). John D. Lee, for whom the area is named, established a ferry in 1874 that was used until Marble Canyon Bridge was completed in 1929. Today, Lees Ferry serves as the launching point for all Grand Canyon river trips.

Late-Paleozoic and Mesozoic sedimentary rocks dominate the bedrock geology of the area and are well-exposed from river level to the surrounding escarpment of the Vermillion Cliffs. These deposits have remained relatively undeformed through uplift of the Colorado Plateau, except for the formation of the Echo Monocline during the early Cenozoic Laramide orogeny. This structural feature has a north-south trend through the study area and brings the easily eroded Moenkopi Formation to river level (Phoenix, 1963). Differential erosion of softer strata throughout the Lees Ferry area has created a beautiful desert landscape of alternating massive cliffs and colorful slopes rising to the surrounding high plateaus.

The climate in the region surrounding Lees Ferry varies from arid low-lying river valleys to semiarid high elevations of the Vermillion Cliffs and Paria Plateau. Vegetation patterns similarly follow an elevational gradient, ranging from upland vegetation in the higher elevations to desert shrub communities in the lower areas (Patton and Morrison, 1991). The terraces at Lees Ferry lie in lower elevational zones and are populated by sparse desert shrubs, whereas the banks of the Colorado River are lined with riparian vegetation such as willow and exotic tamarisk.

METHODS

Surficial deposits were mapped in the Lees Ferry area in order to record their stratigraphic characteristics and correlate terrace levels. Existing surficial geologic maps focusing on Holocene deposits along the Colorado and Paria rivers have been published by Richard Hereford and others at the USGS (Hereford et al. 2000; Hereford 2004) and were used where possible. Seven cross-sectional valley profiles were surveyed using a total station. Ten measured sections of parts of terrace fills have been described in detail in order to interpret depositional processes during aggradation episodes. Terrace gravels at Lees Ferry exhibit complex compositional variations that result from the mixing of sediment delivered from the Colorado and Paria rivers. Nine clast counts (>100 clasts) and eight sand petrographic point counts of grain-mount thin sections stained for the identification of feldspars (>300 counts) were performed in order to distinguish sediment from local hillslope, tributary, or mainstem Colorado River provenance.

In addition to mapping and sedimentologic observations and measurements, two dating methods have been employed to constrain the timing of aggradation and subsequent terrace abandonment at Lees Ferry: optically stimulated luminescence (OSL) and terrestrial cosmogenic nuclide ^{10}Be exposure (TCN). Although both dating methods have been used on fluvial deposits, ages that are calculated from OSL and TCN require different interpretations. TCN ages represent the duration of surficial exposure since the onset of incision, whereas OSL ages indicate the timing of sediment deposition and burial. A vertical sequence of precise OSL ages taken from a single deposit should record the timing and duration of aggradation within a fluvial system, whereas a single TCN age from a terrace surface indicates the timing of floodplain abandonment and subsequent incision.

OSL sand samples were collected in 5 x 20 cm aluminum tubes from recently exposed road or stream cuts. Ten OSL samples were collected from Colorado River deposits and four samples were collected from Paria River deposits. OSL sample preparation and analysis of the 90 to 150 μm fraction was performed at the University of

Nebraska Luminescence Laboratory using the single-aliquot regenerative method on a RISO TL/OSL-DA-15B/C reader with blue-green light stimulation (470 nm, Hoya U340 filter). OSL results reported up to this point in the research are preliminary, with 6 to 15 disks reported for each sample. This is only about half of the expected number of disks that will be used to calculate final ages (20 total for each sample).

Four TCN surface samples were collected from only those Colorado River terrace treads that exhibited long-term stability in the form of well-developed desert pavements. Surface samples composed of ~100-200 quartzite pebbles (1-2 cm in diameter) were crushed and analyzed in a single amalgamated sample after the methods of Repka et al. (1997). A 220 cm depth-profile consisting of six sand samples was used to account for pre-depositional inheritance. This profile from the most prominent deposit in the area was used for all surface ages with the assumption that the Colorado River has transported well-mixed sediment with a comparable amount of inheritance during each aggradation episode. TCN samples composed of ~250 kg of medium sand-sized grains (355-500 μm) were prepared at Dalhousie University and accelerator mass spectrometer analysis was performed at Lawrence Livermore National Laboratory.

RESULTS

Deposits from the Colorado River, Paria River, and small tributary washes have been identified in the Lees Ferry area. Description of each of these deposits is presented below, including geometry and landscape position, sedimentology, provenance, and age.

Colorado River deposits

Seven distinct deposits (M1-M7) and ten terrace levels (M4y, M5y, and M5m are erosional fill-cut terraces) have been identified along the Colorado and Paria rivers in the Lees Ferry area (Figure 3.2). Deposits generally range in thickness from 10 to 30 m and have basal straths that can be irregular, often exhibiting false straths that are significantly higher than the true basal strath. Terrace treads range in height from 5 m (M1) to ~180 m (M7) above the reference river stage of 380 m^3/s (~13,000 cfs) and generally exhibit moderately to well-developed desert pavements (Figure 3.3). Colorado River deposits are characterized by the interfingering of five distinct facies described in Table 3.1: clast-supported gravel, cross-stratified sand, immature pebble-gravel, cobble-pebble diamicton, and boulder diamicton. Sand petrogaphic analysis indicates that mainstem Colorado River sands are ~75% quartz and may be slightly more feldspathic than sand from Paria River deposits (Appendix B).

The M1 deposit is well-exposed along the Colorado River in the Lees Ferry area and occurs up to ~5 meters above the modern river. This deposit represents middle Holocene to modern deposition of the fluvial system. The M1 has been mapped and described in detail by Hereford et al. (2000), who subdivided these Holocene deposits on the basis of dated archeological remains, tree-ring dates, content of driftwood, and comparison to similar terrace sequences from established records elsewhere within the region (Hereford et al., 1986; 1998). Mapping of these Holocene deposits and studies of historic sand bars and the sediment budget along the Colorado River have been performed in an attempt to understand how Glen Canyon Dam is affecting aquatic habitat and the sediment and water budgets of the Colorado River (e.g. Schmidt and Graf, 1990).

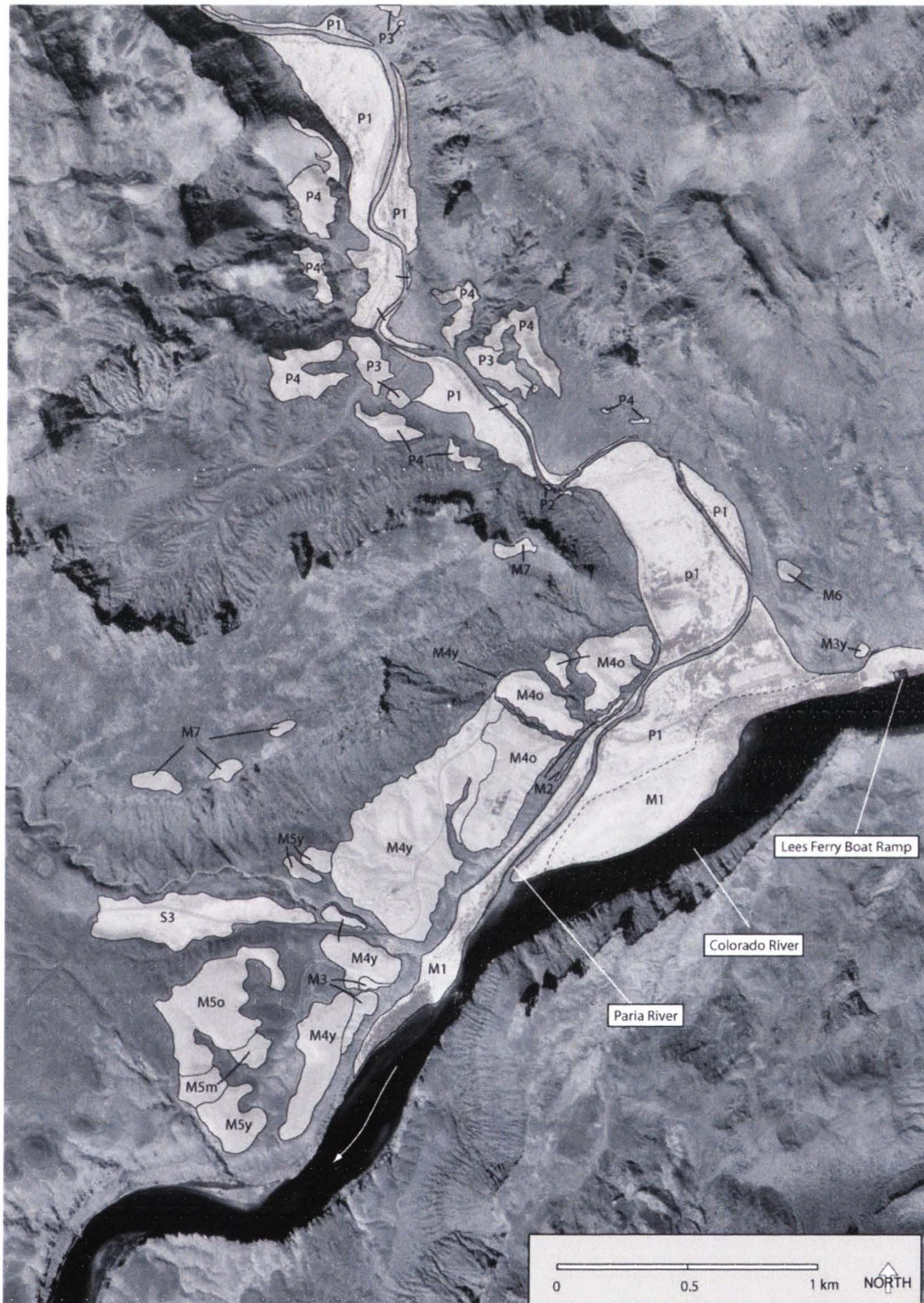

Figure 3.2. Map of Quaternary alluvium in the Lees Ferry area, including the Colorado (M1-M7) and Paria (P1-P4) river deposits, as well as the Johnson Wash deposit (S3).

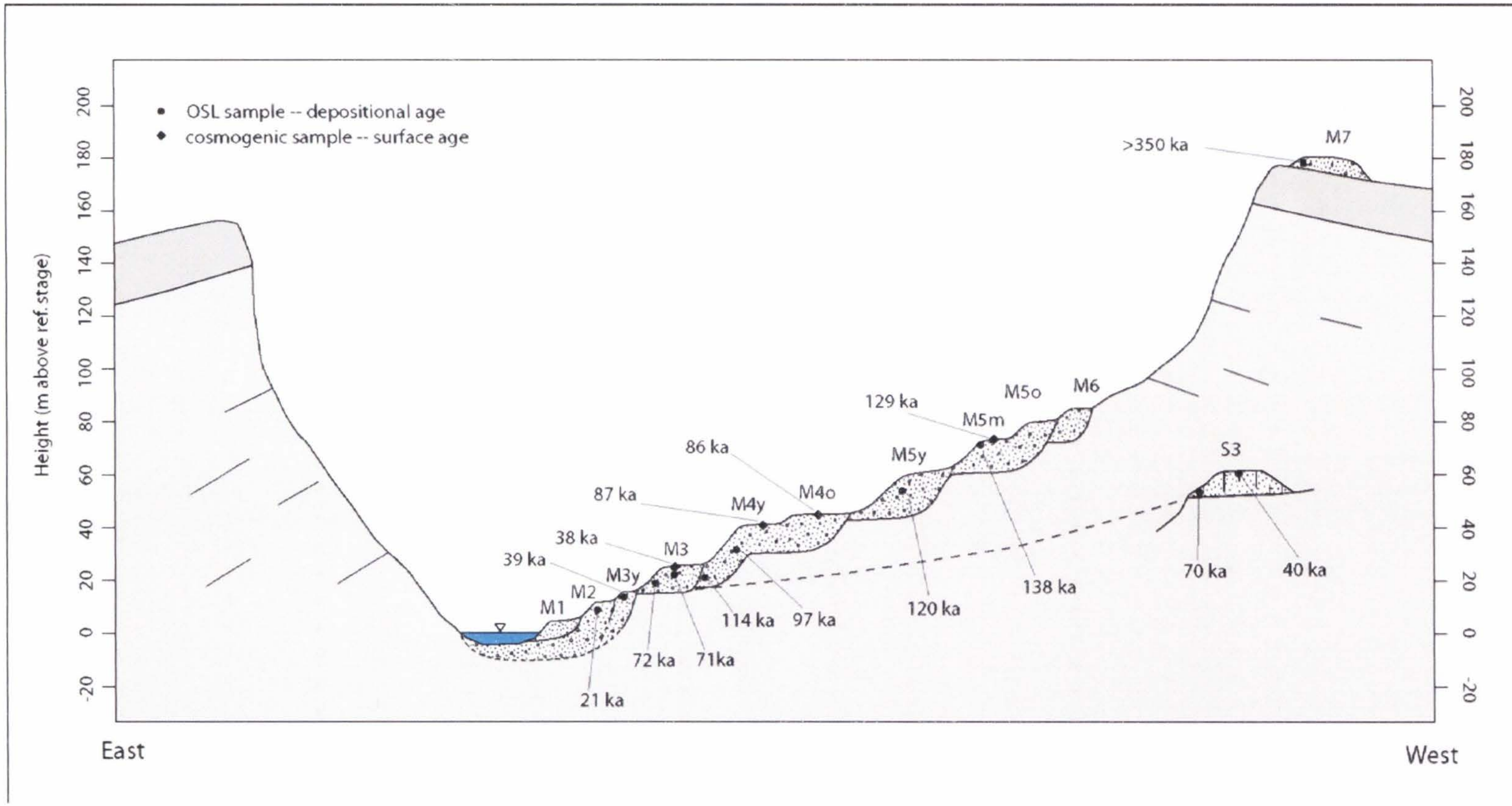

Figure 3.3. Schematic cross-sectional valley profile of the Colorado River fill terraces at Lees Ferry, showing heights, geometries, and ages of deposits. See Table 3.2 for error calculations on individual ages.

Table 3.1. Sedimentary facies, descriptions, and interpretations for deposits at Lees Ferry, Arizona.

Facies	Description	Interpretation
Clast-supported gravel	Light brown to pink, clast-supported, cobble-pebble gravel; rounded to sub-angular; medium to thick lenticular and tabular bedding; well-imbricated, predominantly far-traveled clasts; matrix is medium to coarse grained sand.	Mainstem or Paria channel
Cross-stratified sand	Light reddish brown to light-brownish gray, fine to coarse sand; rounded to sub-angular; medium lenticular and tabular bedding; planar, low-angle, and ripple cross-stratification; predominantly quatz sand, with few pebbles.	Mainstem or Paria overbank
Immature-pebble gravel	Light-gray to very pale brown, clast-supported to matrix-supported pebble-gravel; sub-rounded to angular; medium lenticular bedding; crudely imbricatated; predominantly locally-derived clasts; matrix is very fine to medium grained sand.	Hillslope overland flow
Cobble-pebble diamicton	Reddish-brown, clast-supported to matrix-supported, pebble-cobble gravel; sub-rounded to angular; medium lenticular to tabular bedding; crudely imbricatated, predominantly locally-derived clasts; matrix is fine to medium grained sand.	Side canyon fluvial
Boulder diamicton	Reddish-brown, boulder to pebble gravel; sub-rounded to angular massive, thick tabular bedding; matrix-supported, predominantly locally-derived clasts; matrix is very fine to coarse grained sand.	Debris flow

Table 3.2. Survey and geochronologic data for Lees Ferry deposits

Data Point Description	Height (m)[1]	Age (ka)[2]	Dating Method
Colorado River			
Holocene flood deposits (M1)	0-6		Various
Surveyed M2 terrace tread	14.4	--	--
M2 sand lens in fill	10.7	21 ± 1	OSL[5]
M3y sand lens in fill	12.8	39 ± 3	OSL[5]
Surveyed M3 strath	15.3	--	--
Surveyed M3 terrace tread	25.6	--	--
M3 desert pavement	25.6	38 ± 3	TCN[4]
M3 sand lens in fill	19.2	72 ± 5	OSL[5]
M3 sand lens in fill	22.2	71 ± 5	OSL[5]
S3 sandy unit in fill	51.9	70 ± 6	OSL[5]
S3 sandy unit in fill	60.2	40 ± 3	OSL[5]
Surveyed M4 strath (lower)	15.8	--	--
Surveyed M4 strath (upper)	30.8	--	--
Surveyed M4y terrace tread	41.8	--	--
M4y desert pavement	41.8	87 ± 7	TCN[4]
Surveyed M4o terrace tread	45.8	--	--
M4o desert pavement	45.8	86 ± 7	TCN[4]
M4 sand lens in fill	34.9	97 ± 8	OSL[5]
M4 sand lens in fill	18.3	114 ± 8	OSL[5]
Surveyed M5 strath (lower)	42.5	--	--
Surveyed M5 strath (upper)	60.5	--	--
M5y sand lens in fill (lower)	45.0	121 ± 12	OSL[5]
M5 sand lens in fill (upper)	62.5	138 ± 10	OSL[5]
Surveyed M5y terrace tread	64.3	--	--
Surveyed M5m terrace tread	66.7	--	--
M5m desert pavement	66.7	129 ± 10	TCN[4]
Surveyed M5o terrace tread	78.7	--	--
Paria River			
Holocene flood deposits (P1)	0-5		Various
Surveyed P2 terrace tread	14.6	--	--
Surveyed P3 strath	8.7	--	--
Surveyed P3 terrace tread	23.1	--	--
P3 sand lens in fill	12.2	74 ± 7	OSL[5]
Surveyed P4 strath (lower)	15.8	--	--
Surveyed P4 strath (upper)	33.5	--	--
Surveyed P4y terrace tread	38.6	--	--
Surveyed P40 terrace tread	46.5	--	--
P4 sand lens in fill	17.6	214 ± 23	OSL[5]
P4 sand lens in fill	23.6	96 ± 11	OSL[5]
P4 sand lens in fill	33.3	102 ± 9	OSL[5]

[1] Referenced to a local river stage of 380 m^3/s (13,000 cfs)
[2] 2δ errors reported for all ages
[3] Fine-grained Holocene overbank sediment of the Colorado River (Hereford et al., 2000)
[4] Terrestrial cosmogenic-nuclide date of surface sample corrected for inheritance with depth-profile, minimum surface age (see Appendix E for complete data)
[5] OSL samples represent ages of deposition (see Appendix F for complete data)

The M2 at Lees Ferry is preserved in only two places just upstream of the confluence with the Paria River (Figure 3.2). It has a minimum thickness of 14 m and the base lies below the modern Colorado River. Sedimentology of the lower portion of the deposit (at the southern-most outcrop) is dominated by local debris flow and interfingered side canyon fluvial facies. The upper 1.5 to 5 m of the M2 is characterized by very fine to medium sand with ripple-cross stratification interpreted to have been deposited in mainstem overbank environments. This is typically interfingered with hillslope deposits. OSL geochronology from sandy units indicates that aggradation of the M2 began prior to 21 ± 1 ka and continued until sometime after this (Table 3.2). A deposit first interpreted as an M2 near the Lees Ferry boat ramp may turn out instead to be a mainstem channel facies remnant from a time between the major M3 and M2 fill depositions, based on results of an OSL sample. An age of 39 ± 3 ka from this deposit indicates that a pause in the overall incision may have occurred after the M3 episode and before the onset of M2 aggradation ~20 ka. Sedimentology of this unit indicates deposition of predominantly far-traveled cobbles (~83% of clasts) in the mainstem Colorado River channel (Table 3.1; Figure 3.7; Appendix A). Far-traveled clasts include rocks identified as quartzites and volcanic porphyries.

The M3 deposit is preserved in only one location in the Lees Ferry area. The total preserved thickness of the local M3 is at least 11 m and its base is 14 m above the reference river stage. This deposit exhibits complex interfingering of mainstem gravels, fluvial side-canyon gravels from Johnson Wash, and mainstem overbank deposits. A clast count from the middle of the deposit indicates that 68% of the clasts are of local lithologies (sandstones, limestone, and rocks of the Claron formation), whereas 32% are far-traveled quartzites and volcanic porphyries (Figure 3.7; Appendix A). Aggradation of the M3 began by ~70 ka, based on two OSL ages of 72 ± 5 ka and 71 ± 5 ka obtained from the middle portion of the deposit, respectively (Table 3.2; Figure 3.4). A TCN date obtained from the well-preserved desert pavement on the terrace tread suggests that incision occurred prior to 38 ± 3 ka. Based on the thickness, extent of preservation, and timing of degradation of the M3 deposit in eastern Grand Canyon (Anders et al., 2005), it is likely that the full thickness of the M3 is not preserved at Lees Ferry.

The M4 is by far the most extensively preserved deposit in the Lees Ferry area. The thickness of the M4 ranges from 10 to 30 m due to topography of the basal strath. A prominent higher false strath lies 31 m above the reference river stage, whereas the lower planar bedrock contact lies 15 m above the reference river stage (Figure 3.3). The lower half of the M4 deposit has interfingering mainstem gravel and overbank sand facies. In contrast, mainstem gravel and sandy facies in the upper half of the deposit are interrupted by ~3 m thick debris flow units dominated by locally derived clasts (Figure 3.6). Clast counts within three units (units 2, 5, and 10) indicate that far-traveled lithologies (~50%) are sub-equally mixed with local clast types (~50%) (Figure 3.7; Appendix A). The M4 aggradation episode began prior to 114 ± 8 ka, and continued until at least 97 ± 8 ka, based on OSL dates obtained near the base and from the upper portion of the deposit (Table 3.2; Figure 3.5). Degradation of the M4 was accomplished in two phases. Initial incision occurred by 86 ± 7 ka and resulted in the abandonment of the M4o surface. Incision halted for a brief time (less than the resolution of TCN methods) prior to ultimate abandonment and formation of the M4y surface by 87 ± 7 ka (Table 3.2).

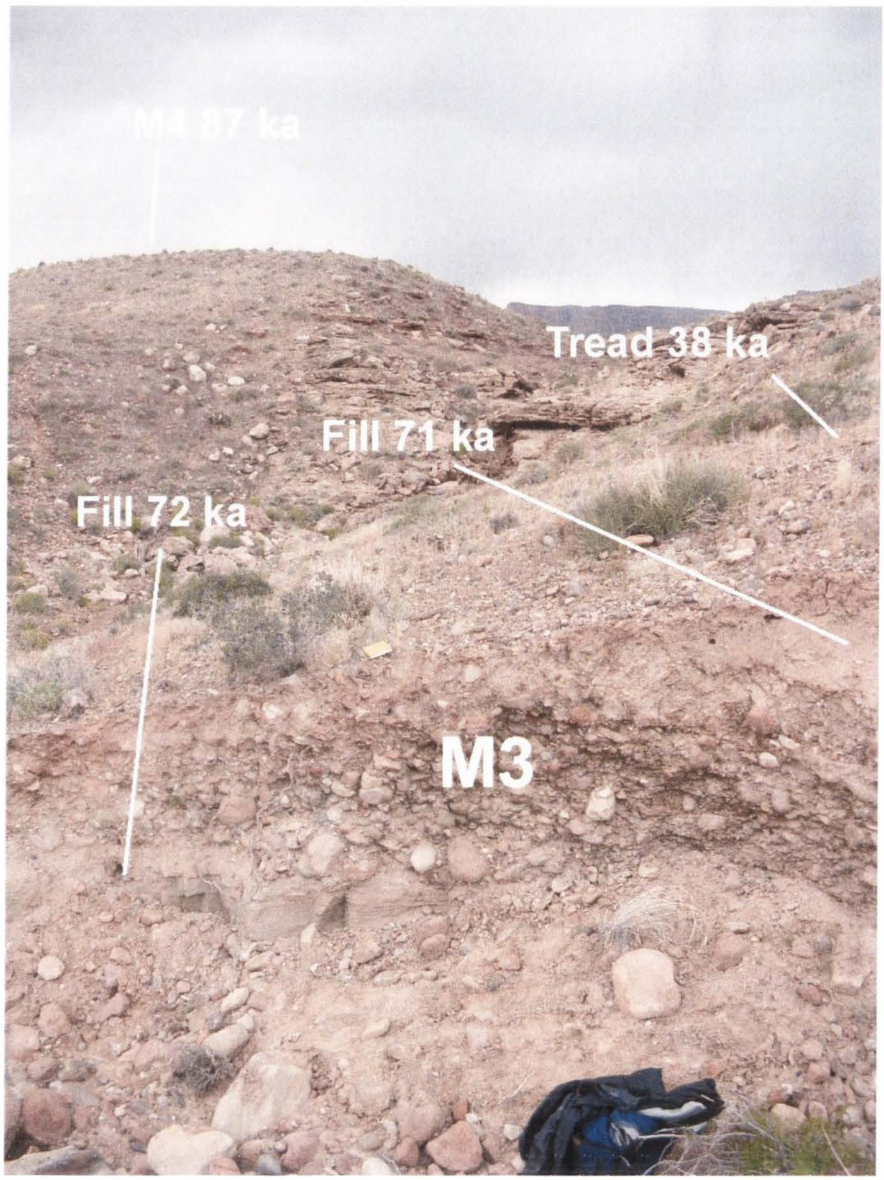

Figure 3.4. Photo of the M3 deposit showing location and ages of OSL (fill) and TCN (tread) samples. The M4 deposit is in background, including the M4y TCN age obtained from the terrace tread. For uncertainty of dates and other geochronologic information, see Table 3.2 and Appendix E and F.

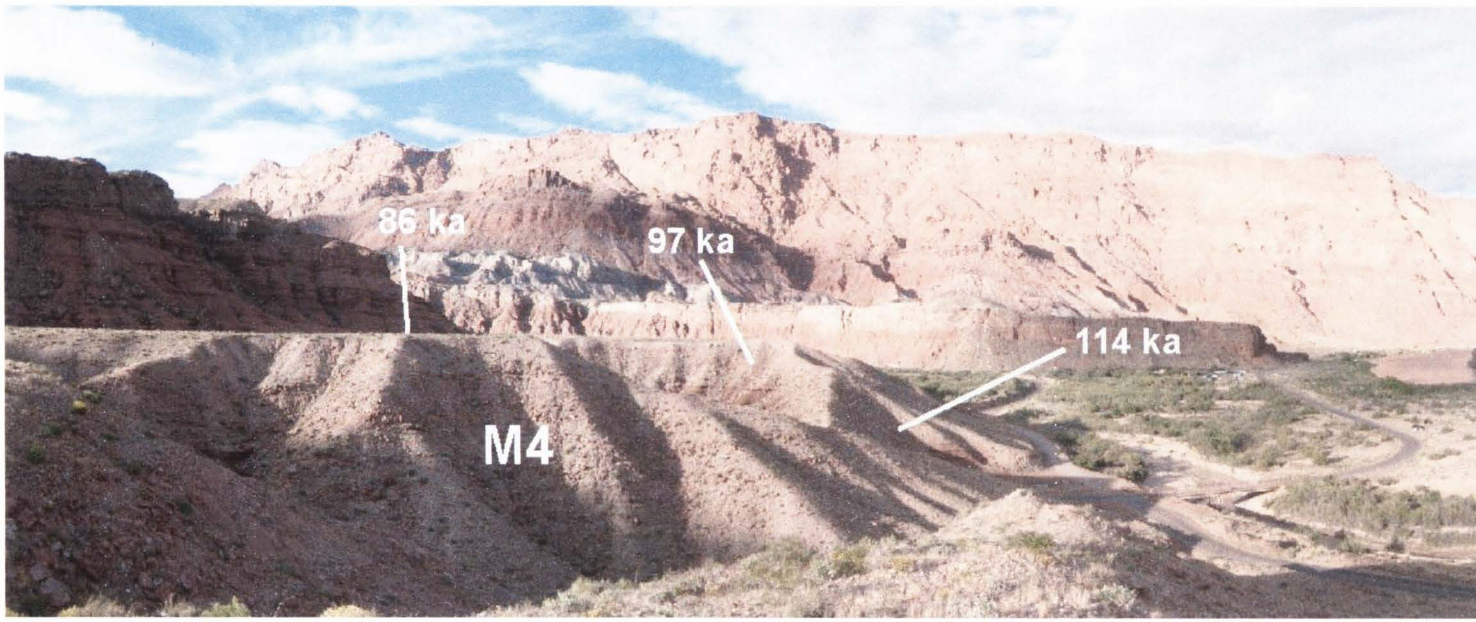

Figure 3.5. Part of the M4 deposit showing location and age of OSL samples collected near the base and middle of the deposit, as well as TCN age collected from the M4o terrace tread. Photo taken looking upstream (north) at confluence. For geochronologic data and uncertainties, see Table 3.2 and Appendix E and F.

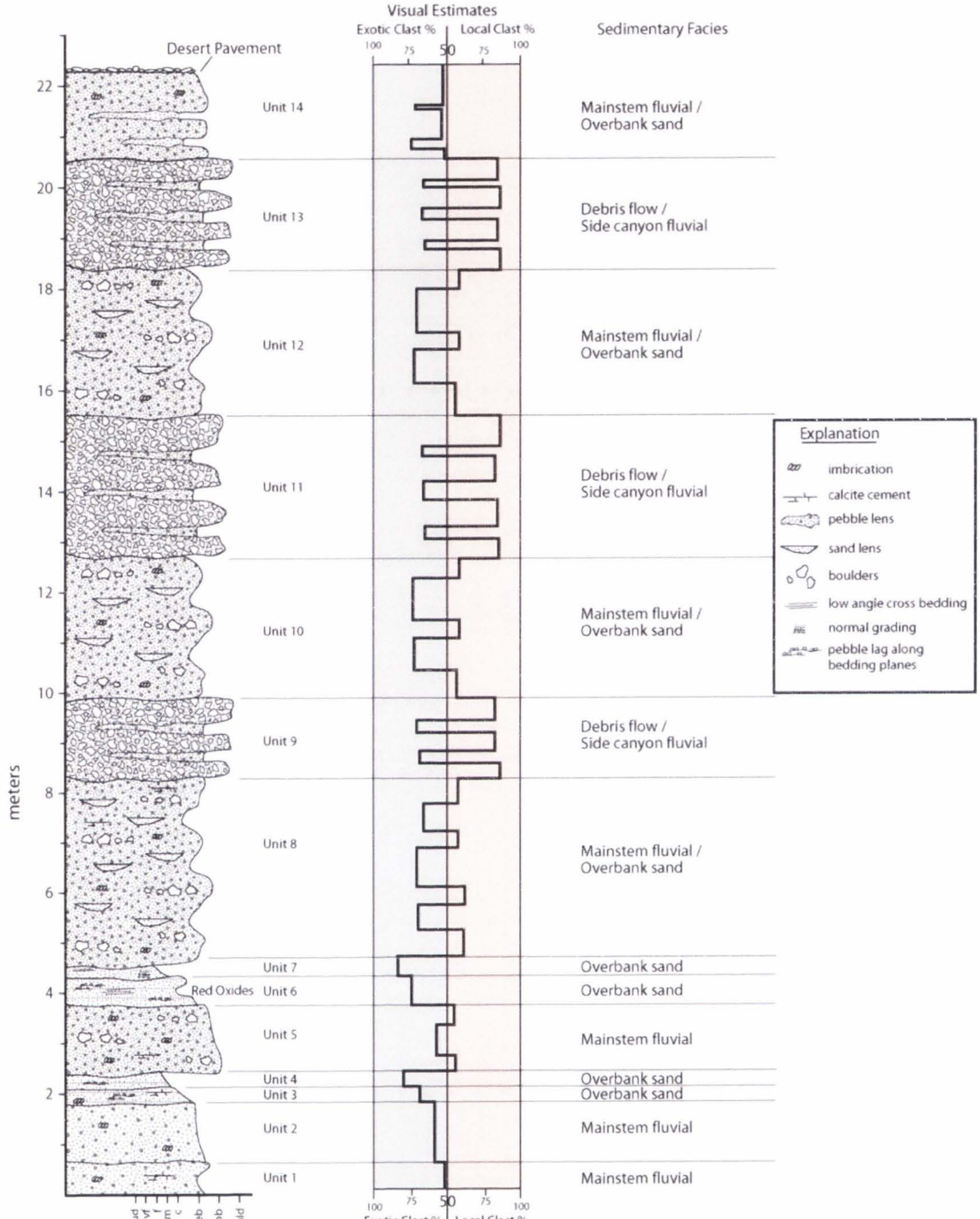

Figure 3.6. Type sedimentary section of the M4 deposit. Visual proportions of exotic and local clasts were made in order to estimate the dominant source throughout deposition. Sedimentary facies interpretations are also included. Sedimentary descriptions can be found in Appendix C.

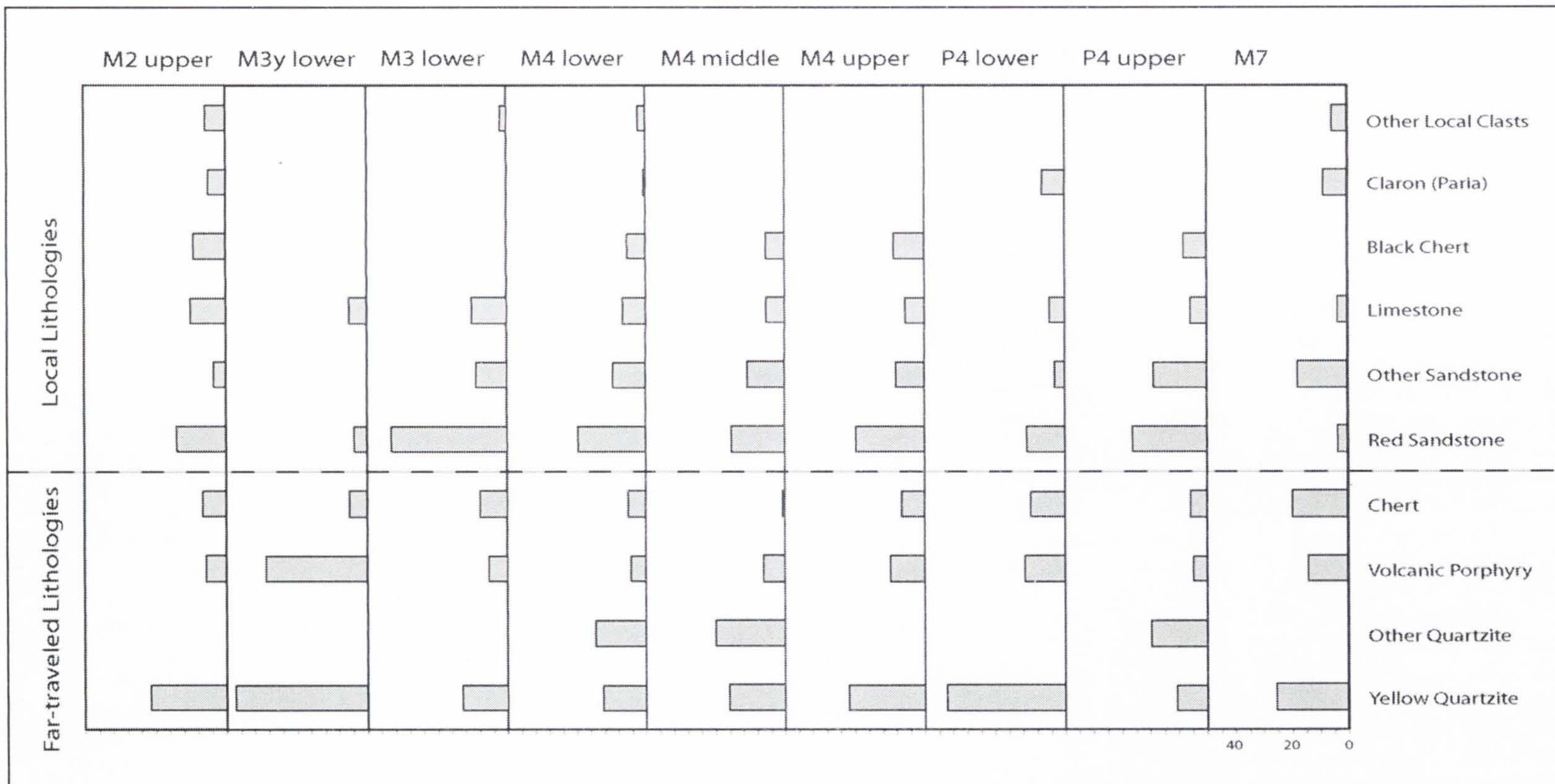

Figure 3.7. Histograms of clast-count data collected from Colorado and Paria river deposits. Total counts were of 100 or more clasts. Raw data are found in Appendix A.

The M5 deposit is preserved in three locations in the southwestern part of the Lees Ferry area. Local thickness of the M5 ranges from 10 to 30 m due to topography of the basal strath. A significant higher strath lies 61 m above the reference river stage, whereas the lower bedrock contact lies 43 m above the reference river stage (Figure 3.3). The sedimentology of the M5 is obscured due to poor exposure; however, tributary debris flow units dominate the top of the deposit and appear to be interfingered with mainstem sand and gravel facies near the middle and base. Preliminary OSL analysis from a sand lens in the middle of the deposit suggests that aggradation was ongoing at 138 ± 10. Subsequent degradation occurred in at least two phases, the first resulting in the formation of the M5o surface. A new floodplain (M5m) was established ~4 m below this level some time before 129 ± 10 ka, as indicated by a TCN date. In addition, a subsequent pause in overall incision may have occurred after the M5 episode and before the onset of M4 aggradation, as indicated by an OSL age of 121 ± 12 ka from a slightly lower landform.

The M6 and M7 deposits are erosional remnants perched high above the modern Colorado River. The top of the M6 lies 72 m above the reference river stage and is called Lees Lookout on USGS topographic maps. Remnants of this deposit are also likely preserved downstream on the high benches of Marble Canyon. The M6 has not been dated due to lack of exposure of datable material.

The M7 lies ~180 m above the present day Colorado River on Johnson Mesa in three isolated patches. The M7 has stage V soil carbonate development, and was estimated to have an age of ~500 ka by Lucchitta et al. (2000). U-series methods were used to date the well-developed carbonate rinds of the M7 (data provided by Warren

Sharp and Richard Phillips at Berkeley Geochronology), and initial results indicate that deposition occurred >350 ka (secular equilibrium). However, a younger stage of carbonate growth occurred ~60 ka based on U-series analyses of carbonate coatings that envelope older rinds (Warren Sharp and Richard Phillips, personal communication). This suggests that a climate episode at ~60 ka (during M3 deposition) resulted in renewed soil-carbonate formation in this high, old soil profile.

Paria River deposits

Four distinct deposits (P1-P4) and five terrace levels (P4y is an erosional fill-cut terrace) have been identified near the mouth of the Paria River (Figure 3.2). Deposits range in thickness from 9 to 30 m and have irregular basal straths similar to those observed in the Colorado River terraces. Terrace treads have moderately-developed desert pavements and range in height from 4 m (P1) to 46 m (P4o) above the modern Paria River (Figure 3.8). Paria River deposits are sedimentologically similar to Colorado River deposits, displaying interfingering of the five facies described in Table 3.1. Results from sand petrology indicate that sands from the Paria River near the confluence are ~80% quartz, perhaps slightly more quartz rich than sand of the mainstem Colorado River (Appendix B).

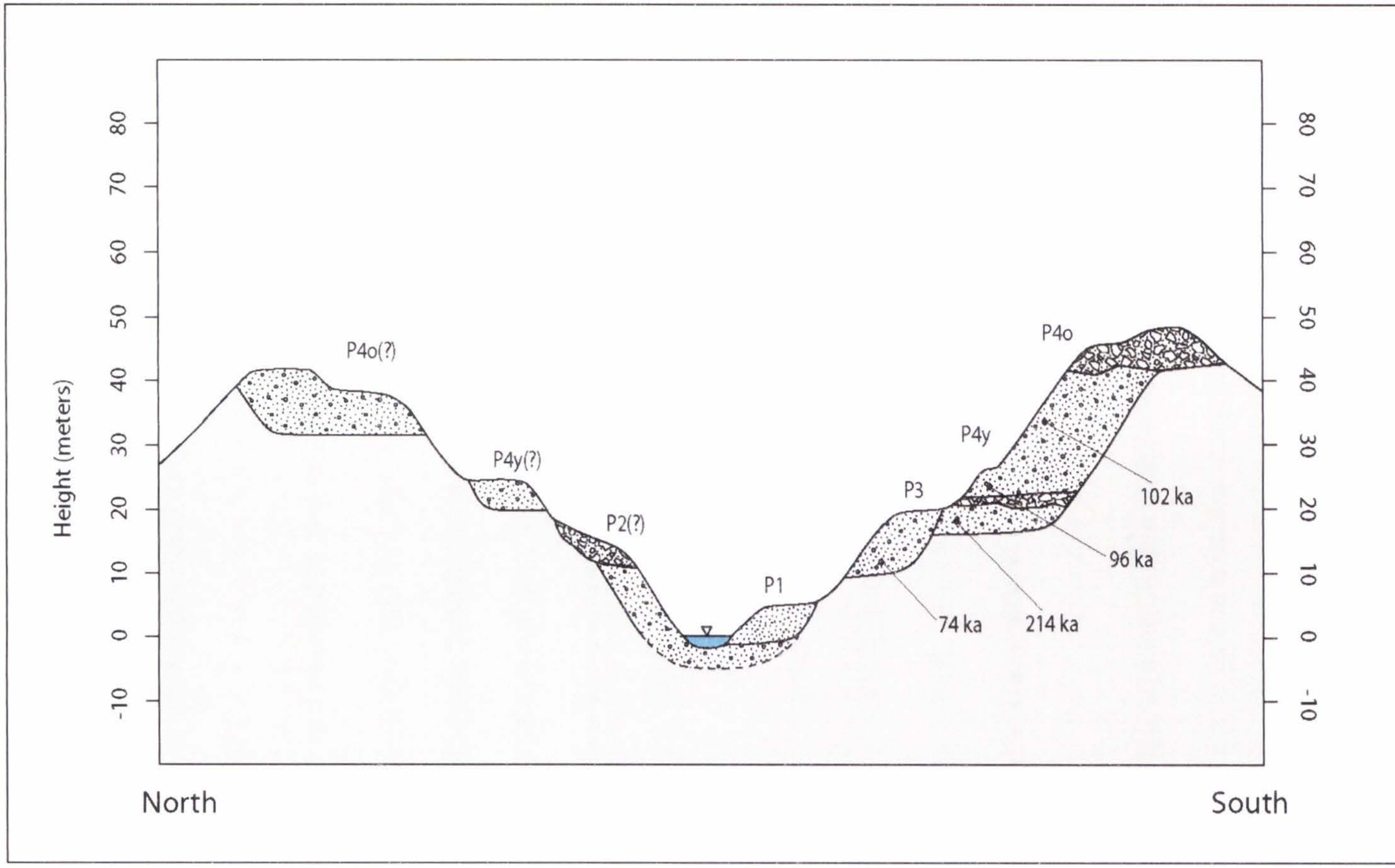

Figure 3.8. Schematic cross-sectional profile of the Paria River fill terraces near Lees Ferry, showing heights, geometries, and ages of the deposits. Details of geochronology can be found in Table 3.2 and Appendix F.

The P1 is composed of several inset Holocene sandy deposits that have been the subject of several studies over the past 20 years (e.g. Hereford, 1986; Graf et al., 1991; Hereford, 2002). The P1 has an exposed thickness of 4 m and the base lies below the modern Paria River (Figure 3.8). The suite of P1 deposits have been correlated with incision due to frequent large floods during episodes of frequent positive El Nino-Southern Oscillations, and aggradation during times of low flood magnitudes (Hereford, 1986; Graf et al., 1991).

The P2 deposit is preserved along the lower Paria River valley near the confluence with the Colorado River (Figure 3.2). It has a maximum thickness of ~14 m, and its base lies below the modern Paria River (Figure 3.8). The P2 is characterized by the interfingering of overbank sand and hillslope overland flow facies (Table 3.1). OSL dating of this deposit has not yet been completed; however, physical correlation to the M2 just downstream suggests aggradation was ongoing ~20 ka.

The P3 deposit is found in three locations along the lower Paria River valley. This deposit is 9 m thick and its base lies 12 m above the modern Paria River (Figure 3.8). Although the P3 deposit is not well-exposed, fluvial gravels appear to be interfingered with overbank sand facies. An OSL date from a laterally extensive sand lens in the middle of the P3 indicates that aggradation was occurring at 74 ± 7 ka (Table 3.2).

The P4 is the most extensively preserved deposit in the Paria River valley. It has a thickness of 24 m and its base exhibits two distinct planar levels. The upper strath lies 31 m above the modern Paria River, whereas the lowest strath is 16 m above the Paria River. The P4 has two distinct depositional units, each overlain by a bouldery debris flow package that followed pulses of Paria aggradation. Paria River deposits are characterized by fluvial gravels derived from the Paria catchment (including ~5% of the distinctive limestone clasts of the Claron Formation) interfingered with significant overbank sand lenses (Figure 3.7; Table 3.1; Appendix A). OSL geochronology from the P4 suggests that the lower depositional unit may be a buried older deposit (214 ± 23 ka), but results show a good deal of uncertainty. Aggradation of the upper depositional unit occurred at ~110 to 90 ka, based on two OSL ages of 96 ± 11 ka and 102 ± 9 ka from the upper 20 m of the deposit, which are the same age within error (Figure 3.8; Table 3.2). Although the timing of terrace abandonment has not been numerically constrained, initial degradation resulted in the formation of the P4o surface and the establishment of a new floodplain ~20 m below this surface (P4y surface).

Tributary side canyon deposit

Previous research at Lees Ferry performed by Kaufman et al. (2002) described a fossiliferous deposit of interfingered silty-sand, carbonate-mud, and coarse-grained sediment located within Johnson Wash (S3 in Figure 3.2). Hamblin (1994) speculated that this deposit was lacustrine in origin, having formed in an extensive lava-dam lake more than 1 Ma. However, Kaufman et al. (2002) cite sedimentologic, fossil assemblage, and stratigraphic evidence to interpret it as spring-fed carbonate deposition occurring contemporaneously with side canyon debris flows. The authors report an age of ~40 ka based on amino-acid dating of snails found within the deposit.

Detailed sedimentologic and geochronologic data from our study expands on the findings of Kaufman et al. (2002). The S3 is generally ~10 m thick, although the irregular basal strath may increase or decrease local thicknesses. Landscape position of the S3 indicates that it is graded to and can be correlated to the M3. The lower portion of the deposit is characterized by carbonate-rich silt to medium sand deposited in a paludal environment. In contrast, carbonate-rich sands in the upper deposit are interfingered with medium beds of debris flow diamictons (Table 3.1; Appendix C), indicating significant influx of tributary sediment near the end of deposition. Two new OSL dates from the S3 indicate deposition began prior to 70 ± 6 ka and was nearly complete by 40 ± 3 ka (Table 3.2), correlating well to the M3 on the Colorado River.

DISCUSSION

Climatically induced changes in sediment supply and hydrology have resulted in the formation of thick fill terraces at Lees Ferry that are superimposed on overall incision of the region. The observed spatial extent and thickness of these deposits gives us some idea about the magnitude of climate responses during different aggradation events in middle-late Pleistocene time, although this is also influenced by valley geometry (Figure 3.2). The M4 is of particular interest since it is the most extensive deposit in the Lees Ferry area, and it is tempting to interpret the M4 as responding to a very large climate event. However, significant vertical and lateral erosion by the Colorado River at Lees Ferry just prior to deposition of the M4 was potentially facilitated by the erosional bench created by the recessive Moenkopi Formation and underlying resistant Kaibab Limestone. This contact is brought to river level right where the M4 is largest, immediately downstream of the Paria River confluence. Aggradation of the M4 occurred along this wide valley bottom and the deposit may have been protected from subsequent erosion because of its position above the resistant Kaibab Limestone ledge. It is interesting to note that correlative deposits ~130 km downstream in eastern Grand Canyon are only partially preserved in isolated locations (Anders, 2003). The M3 is not well preserved at Lees Ferry, perhaps because it lies confined riverward and below the resistant Kaibab Limestone. In contrast, the M3 dominates the stratigraphy in eastern Grand Canyon since it is the youngest major aggradation event preserved within the relatively narrow canyon (Anders, 2003).

Some broad patterns can be observed in the provenance data of the Lees Ferry deposits. First, clast counts generally indicate that local sandstones are sub-equally mixed with far-traveled quartzites and volcanic porphyries in the mainstem channel facies (Figure 3.7). Second, some pink limestone clasts from the Claron Formation of the upper Paria River catchment are observed in several Colorado River clast counts below its confluence with the Paria River. This indicates that sediment from the Colorado and Paria Rivers are mixed, although accurate proportions of mixing cannot be deciphered from clast count data due to the similar clast types in each catchment. Third, debris flow deposits are typically observed in the upper portions of depositional packages, perhaps indicating that local hillslope and tributary activity is greatest near the end of aggradational episodes. In addition, sedimentologic and stratigraphic evidence indicates that the relative abundance of channel and overbank facies in the Colorado and Paria river deposits has not significantly changed through the preserved record. In particular, the presence of imbricated cobble channel facies and overbank sands with lower preservation potential throughout each deposit suggests that the depositional style of the paleo-Colorado and Paria Rivers have been relatively similar during each aggradation episode. It is difficult, however, to directly compare plan-form proportions of modern river depositional facies to those preserved in vertical outcrops of fill terraces emplaced during aggradational modes of the river.

Regional comparison of fluvial records

Regional comparison between the chronostratigraphy at Lees Ferry and fluvial records throughout the middle-upper Colorado River catchment highlight both similarities and differences. The M2 deposit at Lees Ferry area has an OSL depositional age of 21 ± 1 ka, equivalent to the 21 ± 5 ka surface age reported from a terrace along the Wind River (Sharp et al., 2003). These deposits appear to be associated with the last glacial maximum episode reported from the headwater drainages of the Colorado River. A deposit of this age has not yet been reported from the Colorado River on the Colorado Plateau, but was hypothesized to exist under the modern river in eastern Grand Canyon (Anders et al., 2005). The presence of the M2 deposit in the Lees Ferry area suggests that the Colorado River responded to climate change that occurred during the last glacial maximum by aggrading; however, the total thickness and full timing of deposition remains unknown.

Aggradation of the M3 is generally consistent with regional fluvial records. In particular, the onset of deposition at Lees Ferry at 72 ± 5 ka is synchronous with the timing of aggradation reported downstream in eastern Grand Canyon (Anders et al., 2005). However, degradation of the M3 and S3 at Lees Ferry at ~40 ka appears to be later than the onset of incision (~50-60 ka) reported from eastern Grand Canyon (Anders et al., 2005), the Wind River (Hancock et al., 1999; Sharp et al., 2003), and the Fremont

River (Repka et al., 1997). There are two possible explanations for this discrepancy. First, the M3 TCN date may be on a lower erosional terrace level rather than the true top of the original deposit, which may not be preserved at Lees Ferry. Second, incision of the M3 at Lees Ferry may have been delayed due to high influxes of sediment from local hillslope and tributary systems. Comparison to the nearby fluvial record reported from eastern Grand Canyon wherein significant side canyon aggradation was occurring from 50-30 ka supports this second explanation.

Aggradation of the M4 deposit at Lees Ferry beginning prior to 114 ± 8 ka is broadly consistent with or slightly younger than deposition reported in eastern Grand Canyon starting by 124 ± 1 ka and continuing after 118 ± 3 ka. However, subsequent degradation of the M4 at Lees Ferry at 87 ± 4 ka significantly post-dates the timing of incision reported for the stratigraphically equivalent WR-3 in the Wind River (150 ± 8 or 125 ± 37 ka). There are at least two possible reasons for this discrepancy. First, geochronologic comparison between the M4 deposit at Lees Ferry and the WR-3 in the Wind River may indicate a potential depositional lag time of ~20 to 40 ka associated with the downstream transfer of sedimentary signals from glaciated headwaters. Second, the influence of local climatic events in the central Colorado Plateau region may have overshadowed any distant climatic control in the headwaters. Although the M4 is the most extensive deposit in the Lees Ferry area, the timing of aggradation and degradation appear to be consistent with ages reported from the tributary S4 in eastern Grand Canyon of ~110 to 90 ka (Anders et al., 2005; unpublished data). Further, the incision of the Fremont River recorded by a cosmogenic surface age at 102 ± 16 ka (Repka et al., 1997) lies within this time frame.

Aggradation of the M5 before 138 ± 10 ka does not appear to correlate to any preserved deposit in eastern Grand Canyon, although deposits of this age may have subsequently been eroded in the steep canyon landscape. Abandonment of the M5 at ~130 ka at Lees Ferry appears to significantly post-date incision reported along the Fremont River (151 ± 24 ka) and near the headwaters along the Wind River (WR4 = 167 ± 6 ka). Considerable scatter and a lack of data from deposits of these ages preclude any definitive correlations between the timing of incision in these regional records; however, it appears that events at Lees Ferry are somewhat younger than those occurring upstream in headwater catchments.

Although a robust dataset from the Paria River is not yet available, comparison between the fluvial records obtained from the Paria River, Johnson Wash, and the Colorado River at Lees Ferry are generally consistent. The P3 and M3 have equivalent depositional ages of ~70 ka, and the P4 and M4 were both aggrading ~100 ka. Similarly, aggradation of the Johnson Wash paludal deposit has comparable ages with the Colorado River M3 deposit (70 ± 6 to 40 ± 3 ka). These similarities suggest that deposition along Colorado River, tributary Paria River, and side canyon environments at Lees Ferry occurred at or nearly in-step with each other despite issuing from catchments of varying size and climatic setting. At this close proximity to their confluences, local aggradation and incision of the tributary systems may have ultimately been controlled by the baselevel of the Colorado River. Additional detailed geochronologic analysis of deposits located farther up the Paria drainage would allow testing of this observation.

Response of the Colorado River to climate change

Geochronology of the Colorado River deposits at Lees Ferry indicates that aggradation and degradation of this continental-scale river generally occur in response to upstream climatic controls from headwater drainages and are not affected by sea-level controls occurring ~1,200 km downstream at the mouth. However, the timing of fluvial responses of the Colorado River at Lees Ferry is not always perfectly consistent with fluvial records reported within the region or with independent climate records. Comparison between the chronostratigraphy at Lees Ferry and the regional Devils Hole and global SPECMAP climate records indicates that aggradation at Lees Ferry occurred during regionally cold and wet periods, whereas incision occurred during relatively warm and dry periods (Figure 3.9). However, no simple or direct relation between aggradation-degradation events at Lees Ferry and Marine Isotope Stages (MIS) is observed. Aggradation of the M2, M3, and M6 appears to have consistently begun during the full glacial conditions of MIS 2, 4, and 6, respectively. In contrast, incision of the Lees Ferry deposits does not appear to have occurred at an equivalent point within marine isotope stages. Incision of the M6 and incision of the M2 appears to have begun during interglacial conditions after glaciers in headwater drainages melted. In contrast, degradation of the M3 occurred well into the colder MIS 3.

Interestingly, the most prominent and best dated deposit in the Lees Ferry area (M4) was deposited during MIS 5d-b, a time in which no glaciations have been reported in the headwater drainages or in global climate records. Although the M4 does not appear to be associated with a specific glacial episode, the regional Devils Hole and global SPECMAP climate records indicate that aggradation occurred when regional temperatures were relatively low and global ice volume was relatively high ~115 to 90 ka (Figure 3.9). In addition, these climate records indicate that incision of the M4 occurred during an apparent warming period in MIS 5b-a ~90 to 80 ka. Emplacement and abandonment of the M4 during relatively small global climate fluctuations within MIS 5 may indicate that fluvial responses at Lees Ferry are sensitive to relatively small changes. Local sediment production and hydrology may be significantly affected by apparently minor shifts in temperature and ice volume, ultimately resulting in the formation of terraces at Lees Ferry during times in which fluvial responses were not pronounced in other areas throughout the region or world.

CONCLUSIONS

The data from this study suggest that deposits at Lees Ferry are younger than those in equivalent landscape positions in headwater catchments and perhaps somewhat younger than correlative deposits in eastern Grand Canyon. In addition, the presence of a predominant ~115 to 90 ka M4 deposit at a time without known glaciation in headwater catchments supports the conclusion that local sediment production and hydrologic factors have significantly influenced the timing and nature of aggradation and incision during certain times within the Quaternary record.

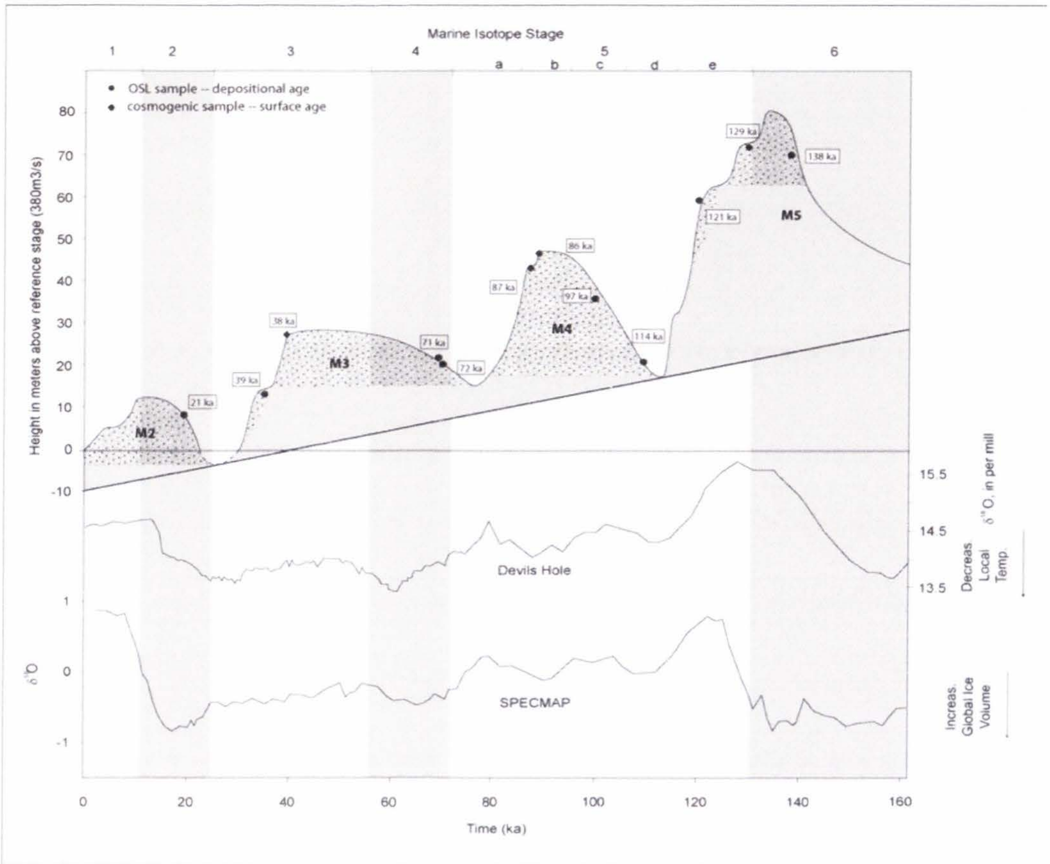

Figure 3.9. Curve representing the height of the Colorado River channel bed through time. Stippled pattern represents fill deposits, whereas the gray represents bedrock. Alluvial aggradation cycles are superimposed on overall downcutting at Lees Ferry. Solid bold lines are regressions approximating minimum and maximum incision rates at Lees Ferry. The regional Devils Hole record (modified from Winograd et al., 1992) and global SPECMAP record (modified from Martinson et al., 1987) are shown below. Shaded bars represent glacial periods. See Table 3.2 for error calculations on individual ages.

The timing of aggradation and degradation reported from the deposits at Lees Ferry illustrates the complex nature of large fluvial systems and their potential responses to local and distant climatic forcing. Anders et al. (2005) propose a revised conceptual model for dryland environments in which increased sediment production on local hillslopes in the Grand Canyon region during glacial conditions is initially stored in thick colluvial mantles. A subsequent change to warmer and wetter climate regimes initiates the transport of that stored material through incremental events down tributary channels, ultimately reaching the mainstem river. Climatically controlled aggradation-degradation cycles at Lees Ferry may be integrated with localized controls on sediment supply such as those envisioned by Anders et al. (2005). Far-traveled clasts were deposited simultaneously with local hillslope and Paria River sediment in fluvial environments, suggesting that aggradation episodes were not simply controlled by variations in discharge and sediment supply from distant headwaters. Rather, the influx of sediment from tributaries and local hillslopes has likely influenced the timing and magnitude of aggradation and degradation at Lees Ferry.

In summary, aggradation and degradation episodes at Lees Ferry are influenced by hydrologic driving forces that are likely tied to climate conditions and the advance and retreat of glaciers in headwaters. However, changes in sediment supply are likely driven mostly by local sediment production from hillslopes and tributaries. Large drainages, such as the Colorado River, may exhibit patterns of deposition and incision that are controlled by this complex mixture of upstream-driven hydrology and local sediment production.

REFERENCES CITED

Aitken, M.J., 1998, Introduction to optical dating: Oxford, Oxford University Press.

Anders, M.D., 2003, Quaternary geology and landscape evolution of eastern Grand Canyon [M.S. thesis]: Utah State University, 141 p.

Anders, M.D., Pederson, J.L., Rittenour, T.M., Sharp, W.D., Gosse, J.C., Karlstrom, K.E., Crossey, L.J., Finkel, R.C., Goble, R.J., Stockli, L., and Yang, G., 2005, Middle-Late Pleistocene geomorphology of eastern Grand Canyon: linkages of dryland landscape components during climate change: submitted to Quaternary Science Reviews.

Andrews, E.D., 1990, The Colorado River: a perspective from Lees Ferry, Arizona: *in* Wolman, M.G., and Riggs, H.C., eds., Surface water hydrology: The geology of North America, v. O-1, p. 304-310.

Antoine, P., Lautridou, J.P., and Laurent, M., 2000, Long-term fluvial archives in NW France: response of the Seine and Somme rivers to tectonic movements, climatic variations and sea-level changes: Geomorphology, v. 33, p. 183-207.

Blum M.D., and Törnqvist, T.E., 2000, Fluvial responses to climate change and sea-level change: a review and look forward: Sedimentology, v. 47, p. 2-48.

Bull, W.L., 1991, Geomorphic responses to climatic change: New York, Oxford University Press, 326 p.

Chadwick, O.A., Hall, R.D., and Phillips, F.M., 1997, Chronology of Pleistocene glacial advances in the central Rocky Mountains: Geological Society of America Bulletin, v. 109, p. 1443-1452.

Colls, A.E., Stokes, S., Blum, M.D., and Straffin, E., 2001, Age limits on the late Quaternary evolution of the upper Loire River: Quaternary Science Reviews, v. 20, p. 743-750.

Counts, R., and Pederson, J.L., 2005, The nonglacial surficial geology of the Henrys Fork, Uinta Mountains, Utah and Wyoming: *in* Dehler, C.M., Pederson, J.L., Sprinkel, D.A., and Kowallis, B.J., ed, Uinta Mountain Geology, Salt Lake City, Utah Geological Association Publication 33, p. 155-169.

Crosby, B.T., and Whipple, K.X., *in press*, Knickpoint initiation and distribution within fluvial networks: 236 waterfalls in the Waipaoa River, North Island, New Zealand: submitted to Geomorphology: The Bedrock Channels Special Issue.

Forman, S.L., Pierson, J., and Lepper, K., 2000, Luminescence geochronology: *in* Noller, J.S., Sowers, J.M., and Lettis, W.R., ed., Quaternary Geochronology: Methods and Applications, Washington DC, American Geophysical Union, p. 157-176.

Graf, J.B., Webb, R.H., and Hereford, R., 1991, Relation of sediment load and floodplain formation to climatic variability, Paria River drainage basin, Utah and Arizona: Geological Society of America Bulletin, v. 103, p. 1405-1415.

Gosse, J.C., Klein, J., Lawn, B., Middleton, R., and Evenson, E.B., 1995, Beryllium-10 Dating of the Duration and Retreat of the Last Pinedale Glacial Sequence: Science, v. 268, no. 5215, p. 1329-1333.

Hamblin, W.K., 1994, Late Cenozoic lava dams in the western Grand Canyon: Geological Society of America Memoir 183, 139 p.

Hancock, G.S., Anderson, R.S., Chadwick, O.A., and Finkel, R.C., 1999, Dating fluvial terraces with ^{10}Be and ^{26}Al profiles: application to the Wind River, Wyoming: Geomorphology, v. 27, p. 41-60.

Hancock, G.S., and Anderson, R.S., 2002, Numerical modeling of fluvial strath terrace formation in response to oscillating climate: Geological Society of America Bulletin, v. 114, p. 1131-1142.

Hereford, R., 1986, Modern alluvial history of the Paria River drainage basin, southern Utah: Quaternary Research, v. 25, p. 293-311.

Hereford, R., 2002, Valley-fill alluviation during the Little Ice Age (ca. A.D. 1400-1880), Paria River basin and southern Colorado Plateau, United States: Geological Society of America Bulletin, v. 114, no. 12, p. 1550-1563.

Hereford, R., 2004, Map showing Quaternary geology and geomorphology of the Lonely Dell reach of the Paria River, Lees Ferry, Arizona: U.S. Geological Survey Investigations Series Map I-2772, scale 1:5000.

Hereford, R., Burke, K.J., and Thompson, K.S., 1998, Map showing Quaternary geology and geomorphology of the Nankoweap Rapids area, Marble Canyon, Arizona, U.S.: Geological Survey Investigations Series Map I-2608, scale 1:2000.

Hereford, R., Burke, K.J., and Thompson, K.S., 2000, Map showing Quaternary geology and geomorphology of the Lees Ferry area, Glen Canyon, Arizona: U.S. Geological Survey Geologic Investigations Series Map I-2663, scale 1:2000.

Hunt, C.B., 1969, Geologic history of the Colorado River: *in* The Colorado River Region and John Wesley Powell: U.S. Geological Survey Professional Paper 669, p. 59-130.

Kaufman, D.S., O'Brien, G., Mead, J.I., Bright, J., and Umhoefer, P., 2002, Late Quaternary spring-fed deposits of the Grand Canyon and their implication for deep lava-dammed lakes: Quaternary Research, v. 58, p. 329-340.

Lane, E.W., 1955, The importance of fluvial morphology in river hydraulic engineering: American Society of Civil Engineers Proceedings, v. 81, p. 1-17.

Leopold, L.B., and Bull, W.B., 1979, Base level, aggradation, and grade: American Philosophical Society Proceedings, v. 123, p. 168-202.

Lewis, S.G., Maddy, S., and Scaife, R.G., 2001, The fluvial system response to abrupt climate change during the last cold stage: the upper Pleistocene River Thames fluvial succession at Ashton Keynes, UK: Global and Planetary Change, v. 28, p. 341-359.

Longwell, C.R., 1946, How old is the Colorado River?: American Journal of Science, v. 244, p. 817-835.

Lucchitta, I., Garniss, H.C., and Turrin, B., 2000, Cyclic aggradation and downcutting, fluvial response to volcanic activity, and calibration of soil-carbonate stages in the western Grand Canyon, Arizona: Quaternary Research, v. 53, p. 23-33.

Mackin, J.H., 1948, Concept of the graded stream: Geological Society of America Bulletin, v. 59, p. 463-512.

Maddy, D., Bridglend, D., and Westaway, R., 2001, Uplift-driven valley incision and climate-controlled river terrace development in the Thames Valley, UK: Quaternary International, v. 79, p. 23-26.

Madole, R.F., 1991, Quaternary history of some southern and central Rocky Mountain basins – Yampa River basin: *in* Morrison, R.B., ed., The Geology of North America Volume K-2, Quaternary Nonglacial Geology: Conterminous U.S.: Denver, Geological Society of America, p. 427-432

Marchetti, D.W., and Cerling, T.E., 2005, Cosmogenic 3He ages of Pleistocene debris flows and desert pavements in Capital Reef National Park, Utah: Geomorphology, v. 67, p. 423-435.

Martinson, D.G., Pisias, N.G., Hays, J.D., Imbrie, J., Moore, Jr., T.C., and Shackleton, N.J., 1987, Age dating and the orbital theory of the Ice Ages: development of a high-resolution 0 to 300,000-year chronostratigraphy: Quaternary Research, v. 27, p. 1-29.

Merritts, D.J., Vincent, K.R., and Wohl, E.E., 1994, Long river profiles, tectonism, and eustacy: a guide to interpreting fluvial terraces: Journal of Geophysical Research, v. 29, no., B7, p. 14,031-14,050.

Nelson and Osborne, 1991, Quaternary history of some southern and central Rocky Mountain basins – Northwestern Uinta Basin: *in* Morrison, R.B., ed., The Geology of North America Volume K-2, Quaternary Nonglacial Geology: Conterminous U.S.: Denver, Geological Society of America, p. 432-437.

Pan, B., Burbank, D., Wang, Y., Wu, G., Li, J., and Guan, Q., 2003, A 900 k.y. record of strath terrace formation during glacial-interglacial transitions in northwest China: Geology, v. 31, no. 11, p. 957-960.

Patton, P.C., and Morrison, R.B., 1991, Quaternary geology of the Colorado Plateau: Introduction: *in* Morrison, R.B., ed., The Geology of North America Volume K-2, Quaternary Nonglacial Geology: Conterminous U.S.: Denver, Geological Society of America, p. 373-378.

Pederson, D.T., 2001, Stream piracy revisited: a groundwater sapping solution: Geological Society of America Today, September, p. 4-10.

Pederson, J.L., Karlstrom, K., Sharp, W., and McIntosh, W., 2002, Differential incision of Grand Canyon related to Quaternary faulting—constraints from U-series and Ar/Ar dating: Geology, v. 30, no. 8, p. 739-742.

Penck, A., and Bruckner, E., 1909, Die Alpen im Eiszeitalter: Leipzig, Tachnitz: *in* Pan, B., Burbank, D., Wang, Y., Wu, G., Li, J., and Guan, Q., 2003, A 900 k.y. record of strath terrace formation during glacial-interglacial transitions in northwest China: Geology, v. 31, no. 11, p. 957-960.

Phillips, F.M., Zreda, M.G., Gosse, J.C., Klein, J., Evenson, E.B., Hall, R.D., Chadwick, O.A., and Sharma, P., 1997, Cosmogenic 36Cl and 10Be ages of Quaternary glacial and fluvial deposits of the Wind River Range, Wyoming: Geological Society of America Bulletin, v. 109, no. 11, p. 1453-1463.

Phoenix, D.A., 1963, Geology of the Lees Ferry area, Coconino County, Arizona: U.S. Geological Survey Bulletin 1137, 86 p.

Reheis, M.C., Palmquist, R.C., Agard, S.S., Jaworowski, C., Mears, B., Jr., Madole, R.F., Nelson, A.R., and Osborn, G.D., 1991, Quaternary history of some southern and central Rocky Mountain basins: Bighorn basin, Green Mountain – Sweetwater River area, Laramie basin, Yampa River basin, northwestern Uinta basin: *in* Morrison, R.B., ed., Quaternary nonglacial geology: Conterminous U.S.: Boulder, Colorado, Geological Society of America, Geology of North America, v. K-2, p. 427-431.

Repka, J.L., Anderson, R.S., and Finkel, R.C., 1997, Cosmogenic dating of fluvial terrace, Fremont River, Utah: Earth and Planetary Science Letters, v. 152, p. 59-73.

Rittenour, T.M., Goble, R.J., and Blum, M.D., 2003, An optical age chronology of late Pleistocene fluvial deposits in the northern lower Mississippi Valley: Quaternary Science Reviews, v. 22, p. 1105-1110.

Schmidt, J.C., and Graf, J.B., 1990, Aggradation and degradation of alluvial sand deposits, 1965 to 1986, Colorado River, Grand Canyon National Park, Arizona: U.S. Geological Survey Professional Paper 1493, 74 p.

Schumm, S.A., 1993, River response to baselevel change: implications for sequence stratigraphy: Journal of Geology, v. 101, p. 279-294.

Sharp, W.D., Ludwig, K.R., Chadwick, O.A., Amundson, R., and Glaser, L.L., 2003, Dating fluvial terraces by 230^{Th}/U on pedogenic carbonate, Wind River basin, Wyoming: Quaternary Research, v. 59, p. 139-150.

Straffin, E.C., Blum, M.D., and Stokes, S., 2000, 140 Ka record of fluvial response to climate change in the middle Loire basin, France: Quaternaire, v. 10, p. 271-282.

Törnqvist, T.E., Wallinga, J., Murray, A.S., Wolf, H., Cleveringa, P., and Gans, W., 2000, Response of the Rhine-Meuse system (west-central Netherlands) to the last Quaternary glacio-eustatic cycles: a first assessment: Global and Planetary Change, v. 27, p. 89-111.

Tucker, G.E., and Slingerland, R., 1997, Drainage basin responses to climate change: Water Resources Research, v. 33, no. 8, p. 2031-2047.

Wallinga, J., Tonqvist, T.E., Busschers, F.S., and Weerts, H.J.T., 2004, Allogenic forcing on the late Quaternary Rhine-Meuse fluvial record: the interplay of sea-level change, climate change and crustal movements:

Winograd, I.J., Coplen, T.B., Landwehr, J.M., Riggs, A.C., Ludwig, K.R., Szabo, B.J., Kolesar, P.T., and Revesz, K.M., 1992, Continuous 500,000-year climate records from vein calcite in Devils Hole, Nevada: Science, v. 258, p. 255-260.

Zreda, M.G., and Phillips, F.M., 2000, Cosmogenic nuclide buildup in surficial materials: *in* Noller, J.S., Sowers, J.M., and Lettis, W.R., ed., Quaternary Geochronology: Methods and Applications, Washington D.C., American Geophysical Union, p. 61-76.

CHAPTER 4

CONCLUSIONS

As our knowledge of the evolution of the Colorado River system improves, a complex picture of overall river incision and fluvial responses is beginning to emerge. Chronostratigraphic analysis of the well-preserved Pleistocene fluvial terraces along the Colorado River at Lees Ferry indicate a middle-late Pleistocene bedrock incision rate of 290 to 470 m/my. These incision rates are approximately two to three times higher than others reported downstream in Grand Canyon and upstream in the upper Colorado River basin. In contrast, our incision rates at Lees Ferry are similar to the recently reported high incision rates near Glen Canyon and along the Fremont River, suggesting there is a reach of faster incision along the Colorado River in the vicinity of Lees Ferry and Glen Canyon. These faster mid-late Pleistocene incision rates of the central Colorado Plateau region may be caused by: 1) localized epeirogenic uplift due to tectonics and potentially enhanced by isostatic rebound; or 2) transient knickzones resulting from drainage integration ~6 Ma, moderated by variations in bedrock resistance.

Superimposed on this long-term regional incision are several aggradation and degradation episodes that illustrate the potentially complex nature of a large river's responses to local and distant climatic forcing. Comparison between the chronostratigraphy at Lees Ferry to both fluvial records within the region and independent climate records indicates that the timing and magnitude of fluvial responses may be spatially and temporally variable. Although aggradation appears to occur during relatively cold and wet periods and incision during relatively warm and dry periods, no simple relation between the magnitude of fluvial responses at Lees Ferry and marine isotope stages is observed. Specifically, the timing of aggradation and incision within the Lees Ferry record potentially occurs somewhat later than that which has been reported in the glaciated headwaters, as well as downstream in the Grand Canyon. In contrast, the timing of aggradation and incision often matches the timing of Grand Canyon tributaries studied in other research. In conclusion, the results from Lees Ferry should support and encourage further study into how large drainages, such as the Colorado River, may exhibit patterns of deposition and incision controlled by the interaction between upstream hydrologic forcing factors and local sediment production.

APPENDICES

Appendix A. CLAST COUNT DATA

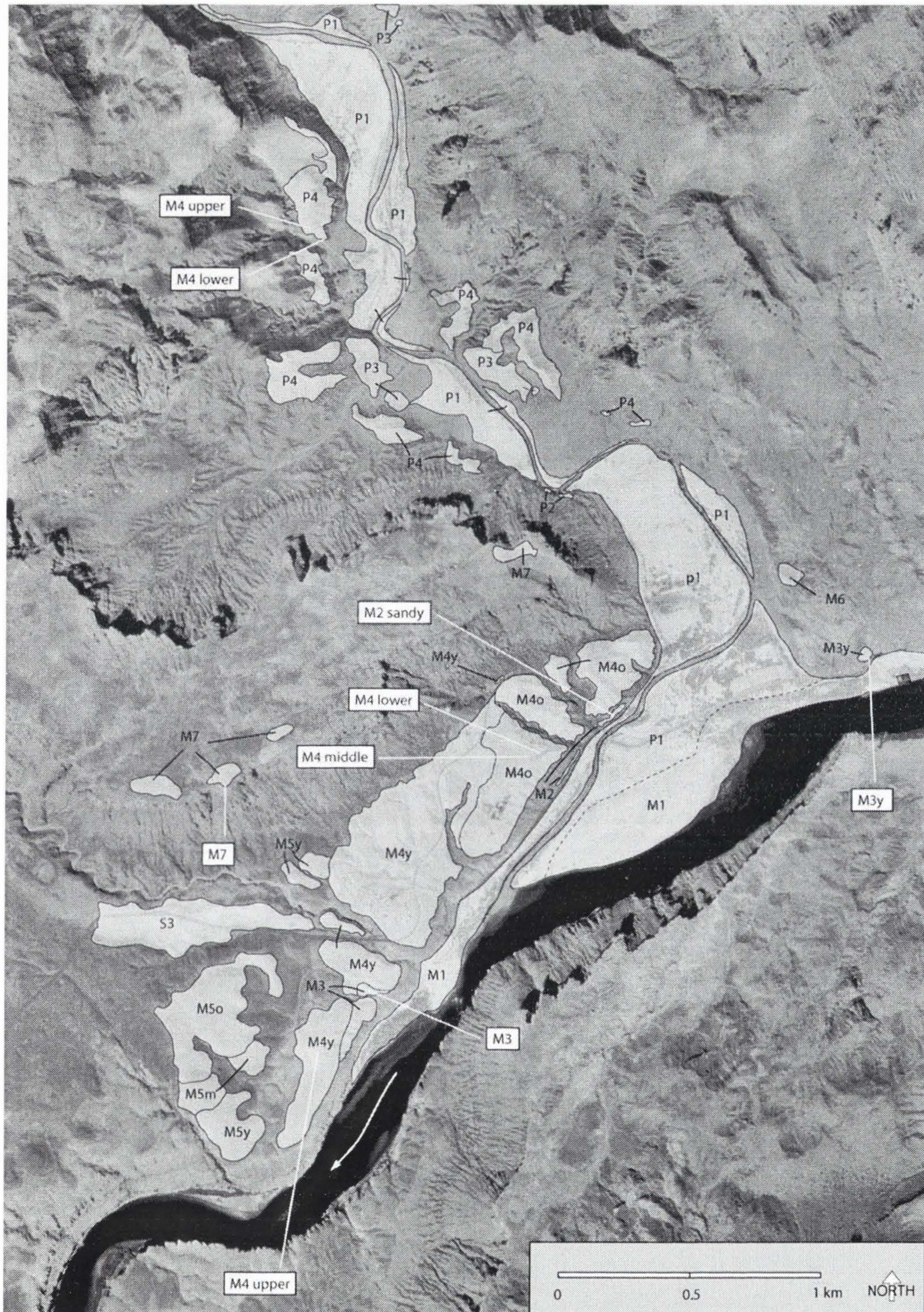

Figure A.1. Map of Quaternary deposits in the Lees Ferry area, showing approximate locations where clast counts were performed.

Table A.1. Clast count data for the M2 deposit.

Unit:	M2 (sandy flood deposit)
Location:	446827 E, 4079927 N
Notes:	Count performed in unit 1 of M2 sandy sed description

	Red SS	W/Y Qtz	Ylw Qtz	V Porph	Bl Chert	Lt Chert	Rd Chrt	Limestne	Claron	Rd Silt
	1.5	1.5	9	5	2	1	1.5	0.5	2.5	2
	3.5	3	0.5	9.5	1	1	0.5	4	1.5	3.5
	1	2.5	2.5	2	2	0.5		0.5	1	0.5
	1.5	2	1.5	3	2	1.5		2	2	1
	1.5		3.5	4	1	0.5		4	0.5	2.5
	3.5		3	2.5	4	3		1.5	1.5	2
	10		1	1.5	2.5			1		1
	0.5		8		2.5			0.5		
	3		2		1.5			1		
	2		0.5		1			2		
	1.5		3.5		1			1		
	1.5		3.5					1.5		
	1.5		2.5							
	1		2.5							
	1		2.5							
	0.5		6							
	1		3							
			1.5							
			3							
			2							
			1.5							
			2							
			0.5							
			0.5							
			5							
			2							
Avg Size - cm	2.1	2.3	2.8	3.9	1.9	1.3	1.0	1.6	1.5	1.8
Percent Total	17.5	4.1	26.8	7.2	11.3	6.2	2.1	12.4	6.2	7.2

Table A.2. Clast count data for the M3y deposit.

Unit:	M3y
Location:	447685 E, 4080059 N
Notes:	Clasts counted in bottom of drainage/channel…behind LF ramp bathroom.

	Red SS	W/Y SS	Qrtzite	V Porph	Bl Chert	Chert	Limestone	Granite
	21		3	11		2	18	5
	9		2	1		2.5	18	
	2		12	3		1	3	
	11		4	4		1.5	6	
	1.5		11	14		1	1	
			13	6		1.5	15	
			3	4			1	
			8	4				
			6	7				
			6	4.5				
			10	6.5				
			3	5.5				
			1	10				
			1.5	2				
			6	8				
			12	8				
			7	3				
			6	5				
			5.5	10				
			2.5	2				
			4	2.5				
			2	5				
			1.5	18				
			8	3				
			7	2				
			14	6				
			4	5				
			4	4.5				
			5	3				
			2	1				
			4	4				
			14	2.5				
			11	3				
			1	5				
			8	3.5				
			4	7				
			7.5	7.5				
			3	4				
			1	8				
			2	5				
			3					
			7					
			2					
			2					
			6					
			1					
			2					
			3					
			4.5					
			11					
			16					
			7					
Average Size - cm	8.9	0.0	5.7	5.5	0.0	1.6	8.9	5.0
Percent Total	4.5	0.0	46.9	36.0	0.0	5.4	6.3	0.9

Table A.3. Clast count data for the M3 deposit.

Unit: M3
Location: 446036 E, 4078918 N
Notes: M3 deposit in culvert near Paria beach… cobble unit above M3 OSL.

	Red SS	W/Y SS	Qrtzite	V Porph	Bl Chert	Chert	Limestone	Shinarump
	4	21	5	6		2	6	2
	11	4	1.5	2		2	3	3
	6	7	3.5	11		0.5	6	8
	1.5	7	2	6		1	5	
	3	3	2	2		1	1	
	0.5	9	2.5	4		2	14	
	2	3	1	4		4	5	
	7	13	1.5	3		1.5	3	
	2	4	1	3		3	0.5	
	11	4	2			2.5	1	
	12	0.5	2.5			2	5	
	10	1.5	2			1.5	7	
	5	5	1.5			4	3.5	
	3	1	1				2	
	1.5	8	1				2	
	8		1				5	
	3		0.5				7	
	6		1					
	9		4.5					
	1.5		2					
	1.5		3					
	11		2					
	6							
	6							
	11							
	2							
	11							
	1							
	2							
	3							
	5							
	0.5							
	1.5							
	6							
	2							
	5							
	3.5							
	2							
	7							
	2.5							
	6							
	1							
	2.5							
	2.5							
	1							
	4							
	9							
	4							
12	3							
0.5	3							
0.5	5							
2.5	14							
Average Size - cm	4.8	6.1	2.0	4.6	0.0	2.1	4.5	4.3
Percent Total	41.5	11.1	16.3	6.7	0.0	9.6	12.6	2.2

Table A.4. Clast count data for the M4 lower deposit.

Unit: M4 (lower)
Location:
Notes: M4 in gully cut north of housing terrace… unite 5 of sed description.

	Red SS	W/Y SS	Yllw Qtz	Wht Qtz	Dark Qtz	P/Gy Qtz	Moen SS	V Prph	Bl Chert	Chrt	Red Chrt	Lime-stne	Clarn	Drk SS	Shin rump
	2.5	0.5	3	3	3.5	7	7	2	2	3	1	5	3	1	2
	3	0.5	3	1	7		8	0.5	2	1	2.5	1.5		5.5	
	3.5	1.5	7	1	1			2	1.5	4	0.5	1.5		1.5	
	8	1	4	11	5			2	0.5		1	2.5			
	48	1.5	1.5	7	1			5.5	1			1			
	10	1.5	2	2.5	7			4.5	1.5			1			
	2	3.5	2.5	7.5	4.5				2			2.5			
	5	4.5	3		4.5							4			
	7.5	1	4		1							1			
	2.5	1.5	1.5		0.5										
	2		6		2										
	3.5		3.5		2										
	13		3												
	2.5		0.5												
	8		1.5												
	4		4												
	0.5		3												
	6														
	7														
	2.5														
	2.5														
	9														
	2.5														
	8														
	5														
	4.5														
	17														
Avg. Size - cm	7.0	1.7	3.1	4.7	3.3	7.0	7.5	2.8	1.5	2.7	1.3	2.2	3.0	2.7	2.0
Percent Total	24.6	9.1	15.5	6.4	10.9	0.9	1.8	5.5	6.4	2.7	3.6	8.2	0.9	2.7	0.9

Table A.5. Clast count data for the M4 middle deposit.

Unit: M4 (middle)
Location:
Notes: M4 in gully cut north of housing terrace…

	Red SS	W/Y SS	Yllw Qtz	Wht Qtz	Dark Qtz	P/Gy Qtz	Red Qtz	V Porph	Blk Chert	Red Chert	Lime-stone	Drk SS
	2	1.5	1.5	2.5	5	10	6	3.5	3.5	1	3.5	4.5
	2.5	0.5	0.5	1.5	4	1.5	2	2.5	1.5		2.5	
	4	2	4	5.5	4	9	3.5	7	2		2	
	15	2	2	3.5	3.5	22	4	5	2.5		5	
	13	1.5	9	3.5	1	8		5	4.5		1.5	
	6.5	4.5	9.5		1.5			3	2		2	
	4	7.5	1		8			3	3		3	
	4.5	4.5	3		4			2				
	5	1.5	4		1.5							
	8	1.5	4		2.5							
	3.5	3.5	1		3.5							
	15	3.5	2.5		4							
	5	8	1.5									
	4		0.5									
	2.5		3.5									
	7		3.5									
	4		1									
	4		3									
	2.5		8									
	9		2									
			5									
Avg. Size - cm	6.1	3.2	3.3	3.3	3.5	10.1	3.9	3.9	2.7	1.0	2.8	4.5
Percent Total	19.2	12.5	20.2	4.8	11.5	4.8	3.9	7.7	6.7	1.0	6.7	1.0

Table A.6. Clast count data for the M4 upper deposit.

Unit: M4 (upper)

Location:

Notes: M4 in gully cut north of housing terrace…

	Red SS	W/Y SS	Quartzite	V Porph	Blk Chert	Chert	Limestone
	5	1	3	9	5.5	1	10
	29	6	4	4	7	1	13
	12	3	4	3	2	3	13
	2.5	12	3	4	1	2.5	5
	14	7	9	2	3	2	3
	4	5	3	9	3	2	8
	6	2	2	5	7	7	31
	5	8	7	4	2	2	6
	4	4	3.5	8	3	4	12
	15	3	2	1	4	2	4
	28	1	5	3	4	2	
	12.5	3	4	4	1	2	
	12	3	6	3.5	2		
	21	3	1	3	2.5		
	3	5	7	2.5	1.5		
	3		6	4	5		
	11		3	12			
	20		3	3			
	9		2				
	4		1.5				
	14		11				
	20		6				
	25		3				
	5		2.5				
	6		2				
	6		2.5				
	3.5		4				
	12		0.5				
	11		5				
	39		3				
	3		3				
	2		2				
	2		2				
	2		1				
	4		1				
	6		2				
			3				
			3				
			3.5				
			7				
Avg. Size – cm	10.6	4.4	3.7	4.7	3.3	2.5	10.5
Percent Total	24.3	10.2	27.2	12.2	10.9	8.2	6.8

Table A.7. Clast count data for the S4 lower deposit.

Unit:	S4 (lower)
Location:	445846 E, 4081455 N
Notes:	Lowest unit of deposit (see sed description), calcite cemented…

	Quartzite	Red SS	W/Y SS	V Porph	Blk Chert	Chert	Limestone	Claron
	15	36	6	3		1	5	1.5
	9	18	5	4.5		1.5	10	1.5
	12	16	3	11		1	10	4.5
	2.5	6	6.5	11		0.5	12.5	3.5
	5	9.5	4	4		1	1	1
	6	2.5	3	3.5		1	0.5	3
	8	2		6		1.5	9.5	1.5
	8	13		1.5		2	1.5	1
	5.5	0.5		2.2		2	2	2.5
	3	5		4.5		0.5		3.5
	1	8		5		1		3
	9	5		3		3.5		3
	3	5.5		4		1		2
	3	14		16		1.5		
	1	3		1.5		1		
	1	16		3		2.5		
	16	16		3		0.5		
	13	3		4		1		
	6	2.5		7		1		
	2.5	5		3		2		
	4	15		7.5				
	5	33		3.5				
	2			5				
	16							
	7.5							
2.5	3							
1	0.5							
1.5	5.5							
4	0.5							
3.5	13							
1	10							
12	0.5							
2	4							
2.5	1.5							
5.5	13.5							
2	2.5							
2.5	1							
1.5	2.5							
6	2.5							
4	1							
1.5	2.5							
9	4.5							
0.5	5							
6	3							
9	9							
5	4							
2.5	1							
Avg. Size - cm	5.5	10.7	4.6	5.1	0.0	1.4	5.8	2.4
Percent Total	28.6	13.7	3.7	14.3	0.0	12.4	5.6	8.1

Table A.8. Clast count data for the S4 upper deposit.

Unit:	S4 (upper)
Location:	445842 E, 4081450 N
Notes:	Big Momma S4 deposit, second-most upper cemented gravel bed.

	Red SS	W/Y SS	Yllw Qtz	Drk Qtz	P/Gy Qtz	Wht Qtz	V Porph	Blk Chert	Wht Chert	Red Chert	Lime-stone
	1.5	2	1	4	5	4.5	6.5	2	5.5	1	8
	2	1	3	7	1.5	4	3	1.5	0.5		22
	4.5	1.5	6	1	12.5	6	11	1.5	1.5		1
	15	0.5	7	2.5	13	3	2	0.5	1.5		3.5
	7.5	2.5	2	3	3	3	4.5	3	3.5		1
	7.5	2.5	1	3.5	4	1.5	2.5	2.5	2		14.5
	1	3	1	4		8		3			2.5
	1.5	1	1.5	4.5				1			
	10.5	1.5	1.5	6.5				2.5			
	4.5	2	4.5	2				1			
	1	1	2.5	1.5							
	12	6	1.5								
	1	2.5	12								
	4	1.5									
	9	1									
	9	8									
	3	4.5									
	8.5	3.5									
	7	1									
	5	2									
	4	6									
	3.5	4									
	3	2.5									
	14										
	4										
	6.5										
	24										
	6										
	3.5										
	11										
	3.5										
	3										
Avg. Size – cm	6.3	2.7	3.4	3.6	6.5	4.3	4.9	1.9	2.4	1.0	7.5
Percent Total	26.2	18.9	10.7	9.0	4.9	5.7	4.9	8.2	4.9	0.8	5.7

Table A.9. Clast count data for the M7 deposit.

Unit: M7 (Johnson Mesa)
Location:
Notes: Johnson Mesa gravels, cleared/exposed pit face, looking down on LF…

	Red SS	W/Y SS	Quartzite	V Porph	Blk Chert	Chert	Lime-stone	Shina-rump	Claron	Tan Silt Stone
	1	1.5	1	1.5		1	3	8	3	2
	4	1.5	1.5	4		1	1	2	1.5	
	1	2	2.5	2.5		3	1	1	1.5	
	1.5	2.5	5	2		1.5	2.5	2	1.5	
	2	1.5	3	1.5		1.5	2	2.5	1.5	
	1.5	1	1	3		1.5	2.5	3	2	
		6	1.5	2		1.5		1	1.5	
		1.5	0.5	4		0.5		3	3	
		2	1	3		0.5			1	
		1	3.5	2		1			0.5	
		2	6	2		0.5			2	
		1.5	3	1.5		0.5			1	
		5	2	2		0.5			1	
		1	3	1		1			2.5	
		1	1	0.5		1				
		3	1.5	3		1				
		1	1	2		2				
		2	1.5	6.5		0.5				
		2	2	3		1				
		0.5	2	1.5		2				
		3	1.5	2		1				
		2.5	1	3		0.5				
		2.5	0.5	1		2				
		3	1.5			0.5				
		1.5	2			2				
		3.5	2.5			1				
		3	1.5			0.5				
		2	0.5			1.5				
		1	1			3.5				
			1.5			2				
			2.5			3				
			1.5			2.5				
			1							
			2							
			1.5							
			3							
			5							
			1							
			2							
			2							
			3							
Avg. Size – cm	1.8	2.1	2.0	2.4	0.0	1.3	2.0	2.8	1.7	2.0
Percent Total	3.8	18.1	25.6	14.4	0.0	20.0	3.8	5.0	8.8	0.6

Table A.10. Summary clast count data for deposits at Lees Ferry, showing percent of clast type at each site. Clast count data was grouped into the most commonly observed clast types.

	Yellow Qrtzite	Other Qrtzite	V Porph	Other Chert	Red SS	Other SS	Lime-stone	Black Chert	Claron	Other Local Clasts
M2 upper site 1	27	0	7	8	18	4	12	11	6	7
M3y Site2	47	0	36	6	5	0	6	0	0	0
M3 Site 2	16	0	7	10	41	11	13	0	0	2
M4 Lower Site 4	15	18	5	6	25	12	8	6	1	3
M4 Middle Site 5	20	25	8	1	19	13	7	7	0	0
M4 Upper Site 6	27	0	12	8	24	10	7	11	0	0
P4 Lower Site 7	42	0	14	12	14	4	6	0	8	0
P4 Upper Site 8	11	20	5	6	26	19	6	8	0	0
M7 Site 9	26	0	14	20	4	18	4	0	9	6

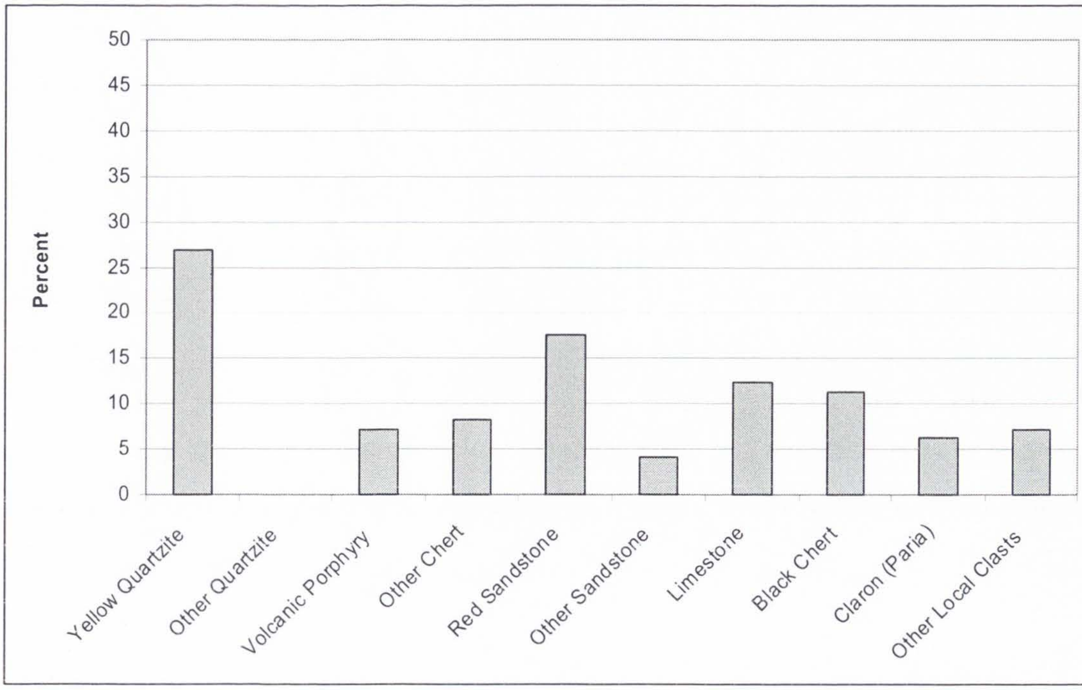

Figure A.2. Histogram of clast-count data collected from the M2 sandy deposit. Total counts were of 97 clasts.

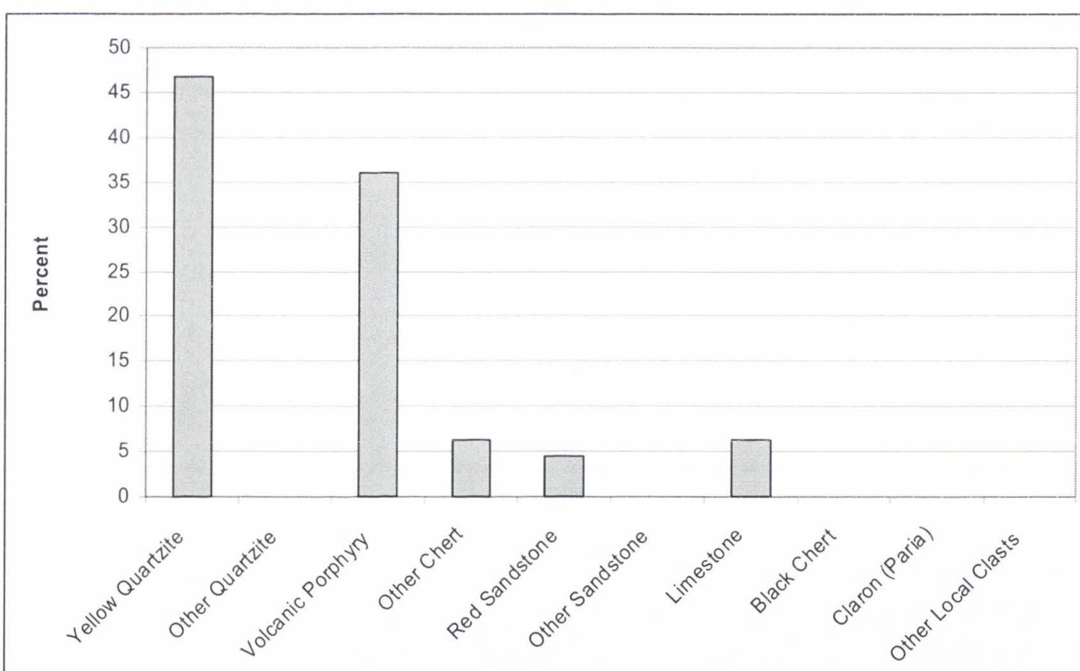

Figure A.3. Histogram of clast-count data collected from the M3y deposit. Total counts were of 111 clasts.

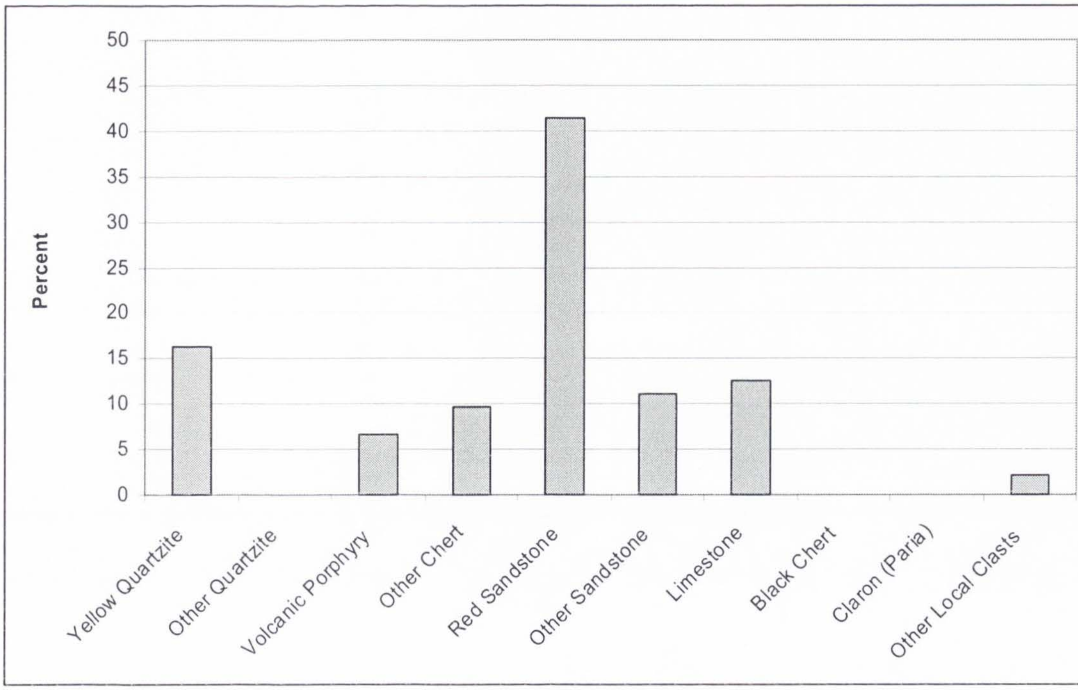

Figure A.4. Histogram of clast-count data collected from the M3 lower deposit. Total counts were of 135 clasts.

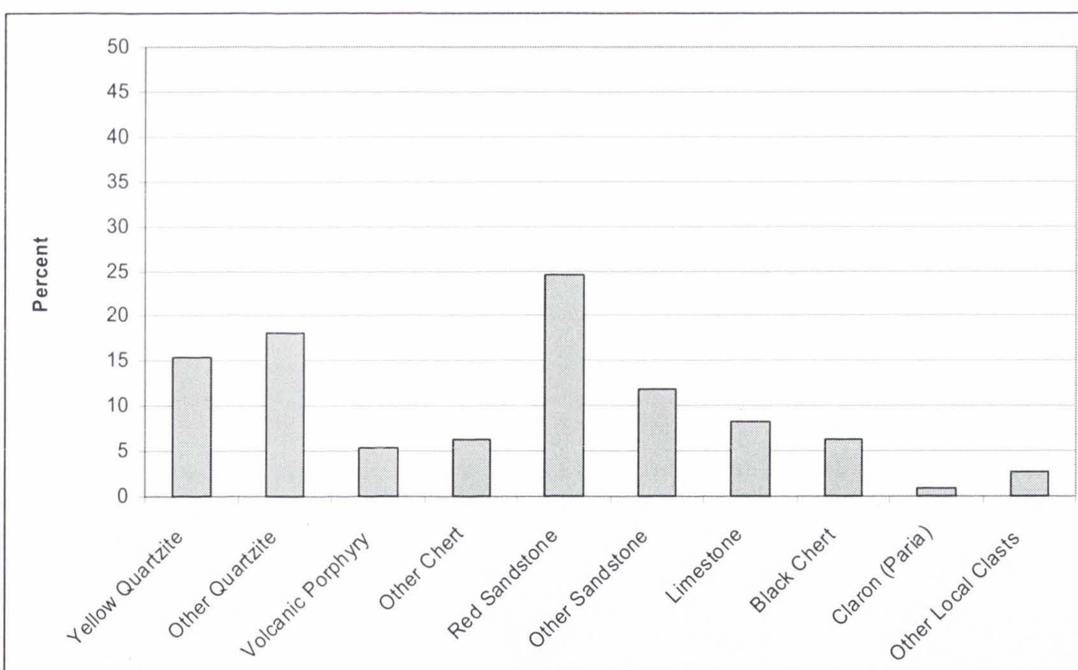

Figure A.5. Histogram of clast-count data collected from the M4 lower deposit. Total counts were of 110 clasts.

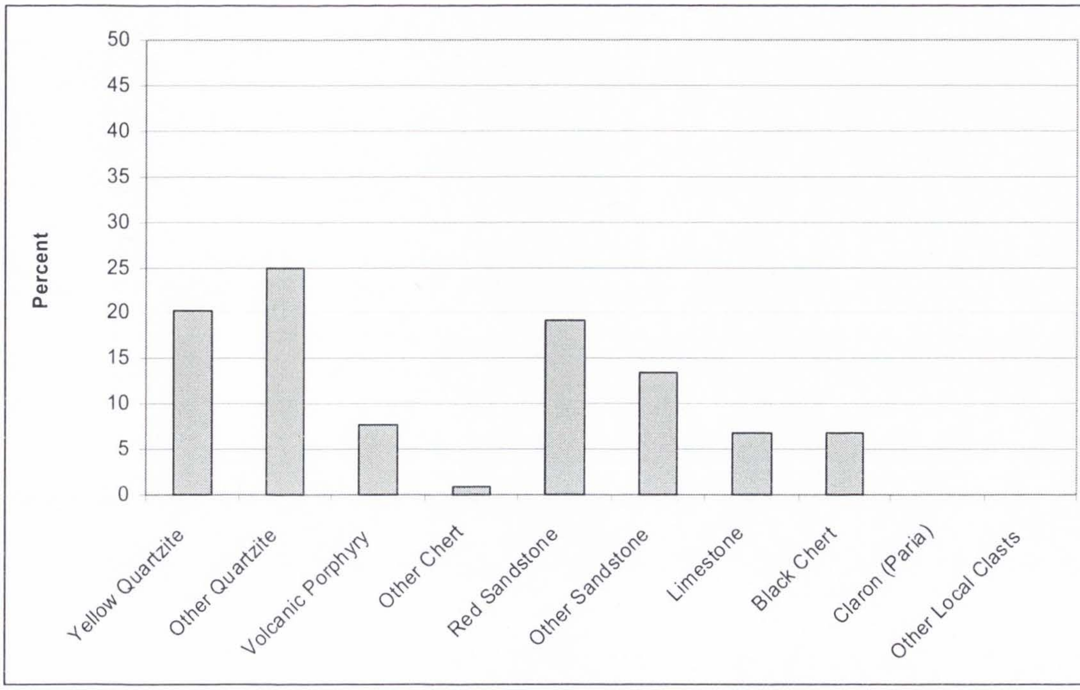

Figure A.6. Histogram of clast-count data collected from the M4 middle deposit. Total counts were of 104 clasts.

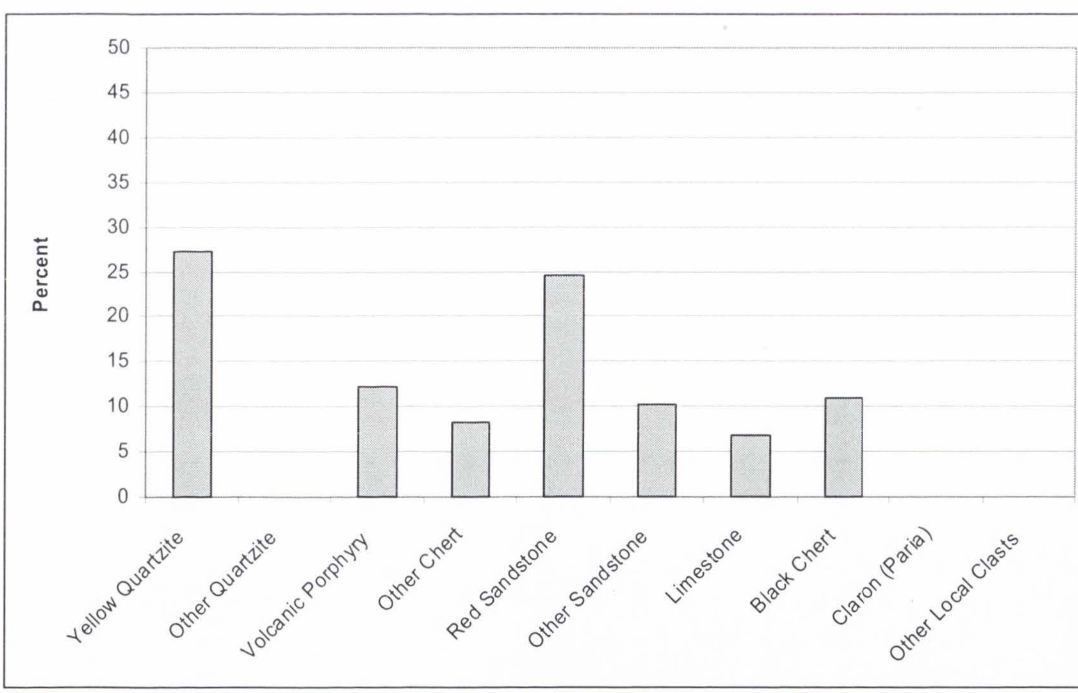

Figure A.7. Histogram of clast-count data collected from the M4 upper deposit. Total counts were of 147 clasts.

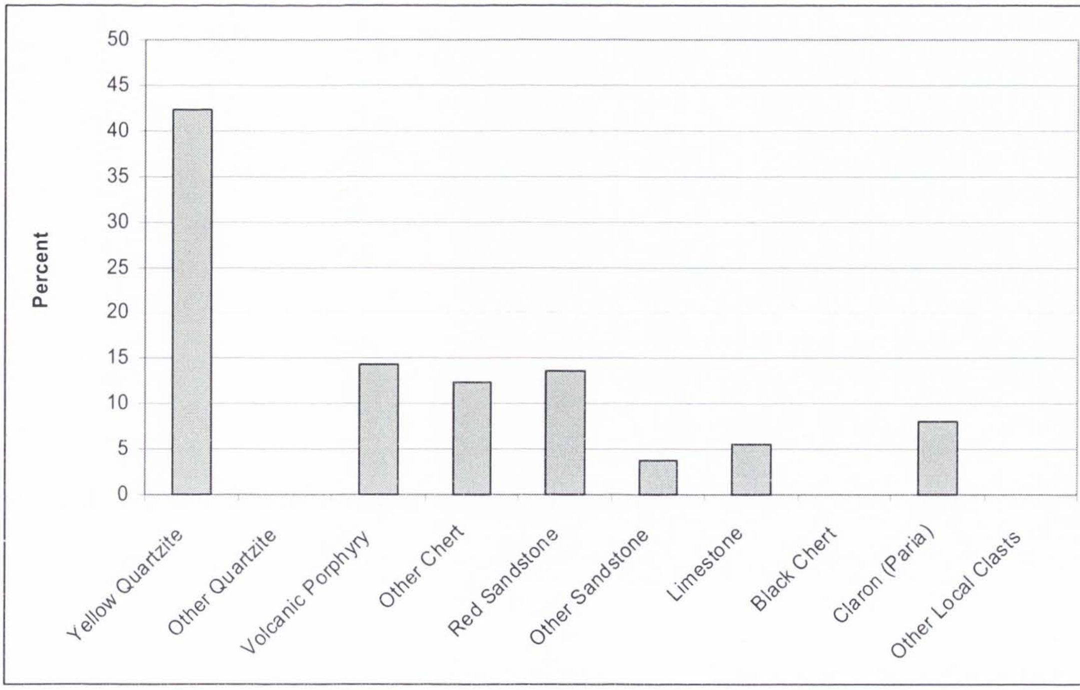

Figure A.8. Histogram of clast-count data collected from the P4 lower deposit. Total counts were of 161 clasts.

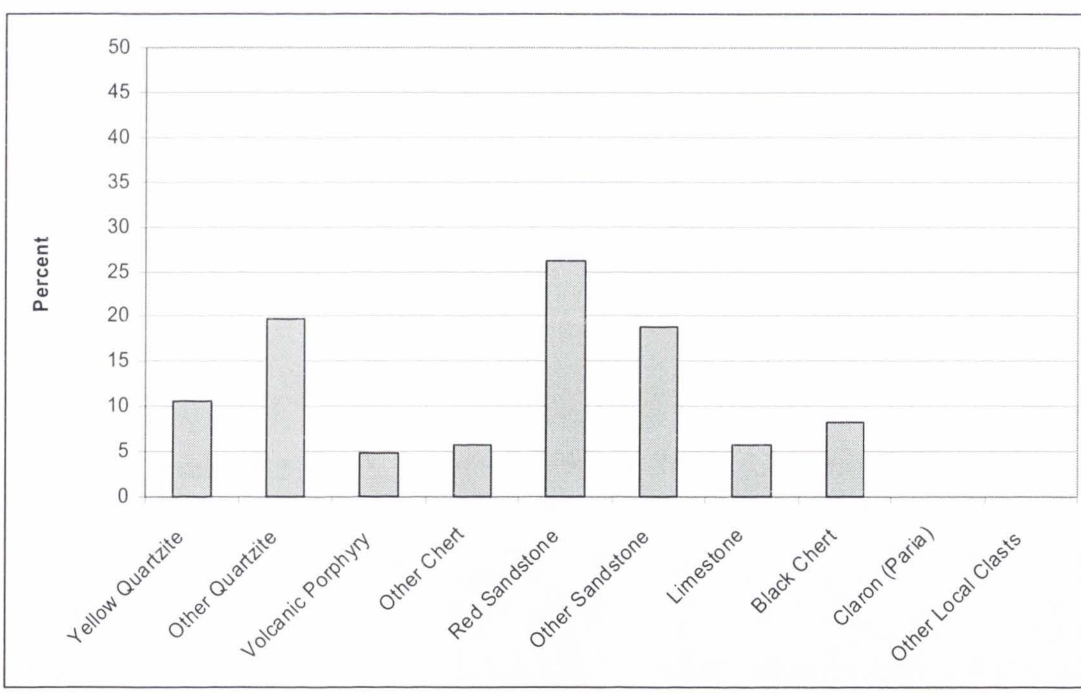

Figure A.9. Histogram of clast-count data collected from the P4 upper deposit. Total counts were of 122 clasts.

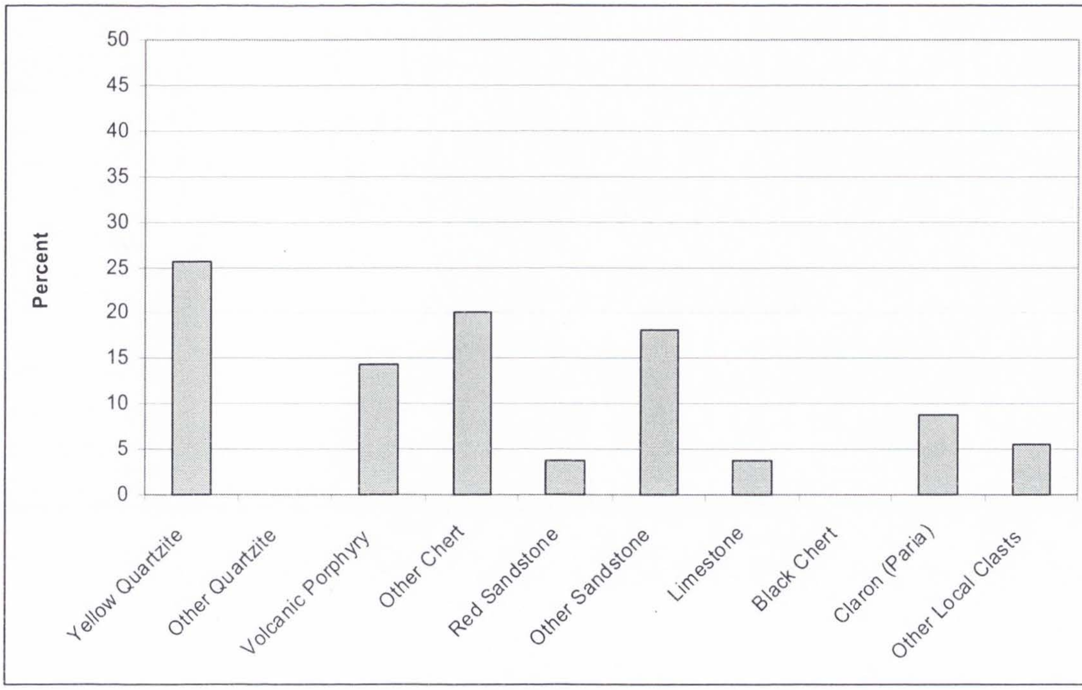

Figure A.10. Histogram of clast-count data collected from the M7 deposit. Total counts were of 160 clasts.

Appendix B. SAND PETROLOGY DATA

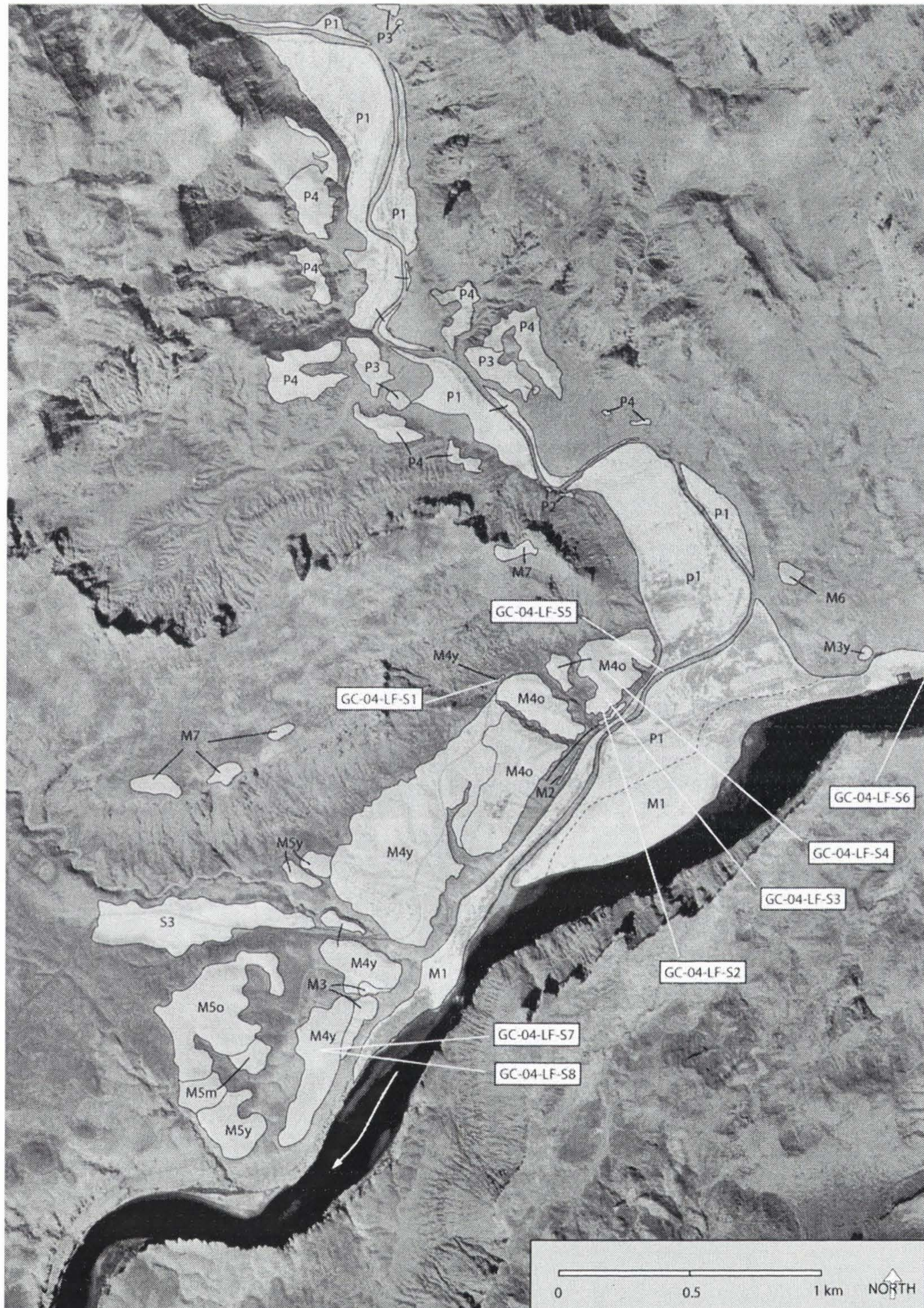

Figure B.1. Map of Quaternary deposits in the Lees Ferry area, showing approximate locations where sand petrology samples were collected.

Table B.1. Description of sample location and predicted sediment source.

	Location Description	Notes
GC-04-LF-S1	Sample location and depth at GC-04-LF-OSL1. Sample taken from depth of ~138 cm from surface.	Interpreted as mainstream sediment
GC-04-LF-S2	~1 m above basal contact of M4 deposit; same location as sed description #1, north of stop sign. .	Interpreted as mainstem sediment. Well-cemented unit.
GC-04-LF-S3	~6 m above basal contact of M4 deposit; same location as sed description #1, north of stop sign.	Interpreted as a combination of mainstream and Paria sediment.
GC-04-LF-S4	~1 m from surface of M4 deposit; same location as sed description #1, north of stop sign.	Interpreted as a combination of mainstream and Paria sediment.
GC-04-LF-S5	Just east of Paria trailhead parking area; sample taken from modern flood deposits of Paria River.	Sampled during high monsoon flows of Paria.
GC-04-LF-S6	~100 m N of Lees Ferry boat launch; sample taken from modern flood deposits of the Colorado River.	Sampled from '83 Sands.
GC-04-LF-S7	Soil pit, ~0.5 m depth, taken from soil horizon #4. M4 deposit, younger surface.	Interpreted as a combination of mainstream and Paria sediment.
GC-04-LF-S8	Soil pit, ~1.5 m depth, taken from soil horizon #6. M4 deposit, younger surface.	Interpreted as a combination of mainstream and Paria sediment.

Table B.2. Raw sand petrographic data collected from deposits in the Lees Ferry area.

	n	Qrtz	Kspar	Plag	Bio	Musc	Lith	Ply Xst	Carb	Grnt Hvy	Amph	Vol	Mud	Othr Obscd
GC-04-LF-S1	336	267	28	1	5	3	11	2	4	5	4	0	0	6
GC-04-LF-S2	356	256	23	2	13	0	11	9	21	3	1	0	0	17
GC-04-LF-S3	355	257	23	0	11	1	20	9	7	7	9	2	0	9
GC-04-LF-S4	363	280	29	2	14	0	5	7	8	8	6	0	3	1
GC-04-LF-S5	396	333	14	3	9	1	8	5	13	4	5	0	0	1
GC-04-LF-S6	383	287	46	6	7	4	4	5	14	7	3	0	0	0
GC-04-LF-S7	366	283	30	2	14	0	13	4	8	5	5	0	1	1
GC-04-LF-S8	342	263	30	6	11	2	9	1	7	9	3	0	1	0

Table B.3. Percent composition calculated from sand petrographic data for deposits in the Lees Ferry area.

	n	Qrtz	Kspar	Plag	Bio	Musc	Lith	Ply Xst	Carb	Grnt Hvy	Amph	Vol	Mud	Othr Obscd
GC-04-LF-S1	336	79.5	8.3	0.3	1.5	0.9	3.3	0.6	1.2	1.5	1.2	0.0	0.0	1.8
GC-04-LF-S2	356	71.9	6.5	0.6	3.7	0.0	3.1	2.5	5.9	0.8	0.3	0.0	0.0	4.8
GC-04-LF-S3	355	72.4	6.5	0.0	3.1	0.3	5.6	2.5	2.0	2.0	2.5	0.6	0.0	2.5
GC-04-LF-S4	363	77.1	8.0	0.6	3.9	0.0	1.4	1.9	2.2	2.2	1.7	0.0	0.8	0.3
GC-04-LF-S5	396	84.1	3.5	0.8	2.3	0.3	2.0	1.3	3.3	1.0	1.3	0.0	0.0	0.3
GC-04-LF-S6	383	74.9	12.0	1.6	1.8	1.0	1.0	1.3	3.7	1.8	0.8	0.0	0.0	0.0
GC-04-LF-S7	366	77.3	8.2	0.6	3.8	0.0	3.6	1.1	2.2	1.4	1.4	0.0	0.3	0.3
GC-04-LF-S8	342	76.9	8.8	1.8	3.2	0.6	2.6	0.3	2.0	2.6	0.9	0.0	0.3	0.0

Appendix C. SEDIMENTARY COLUMNS AND DESCRIPTIONS

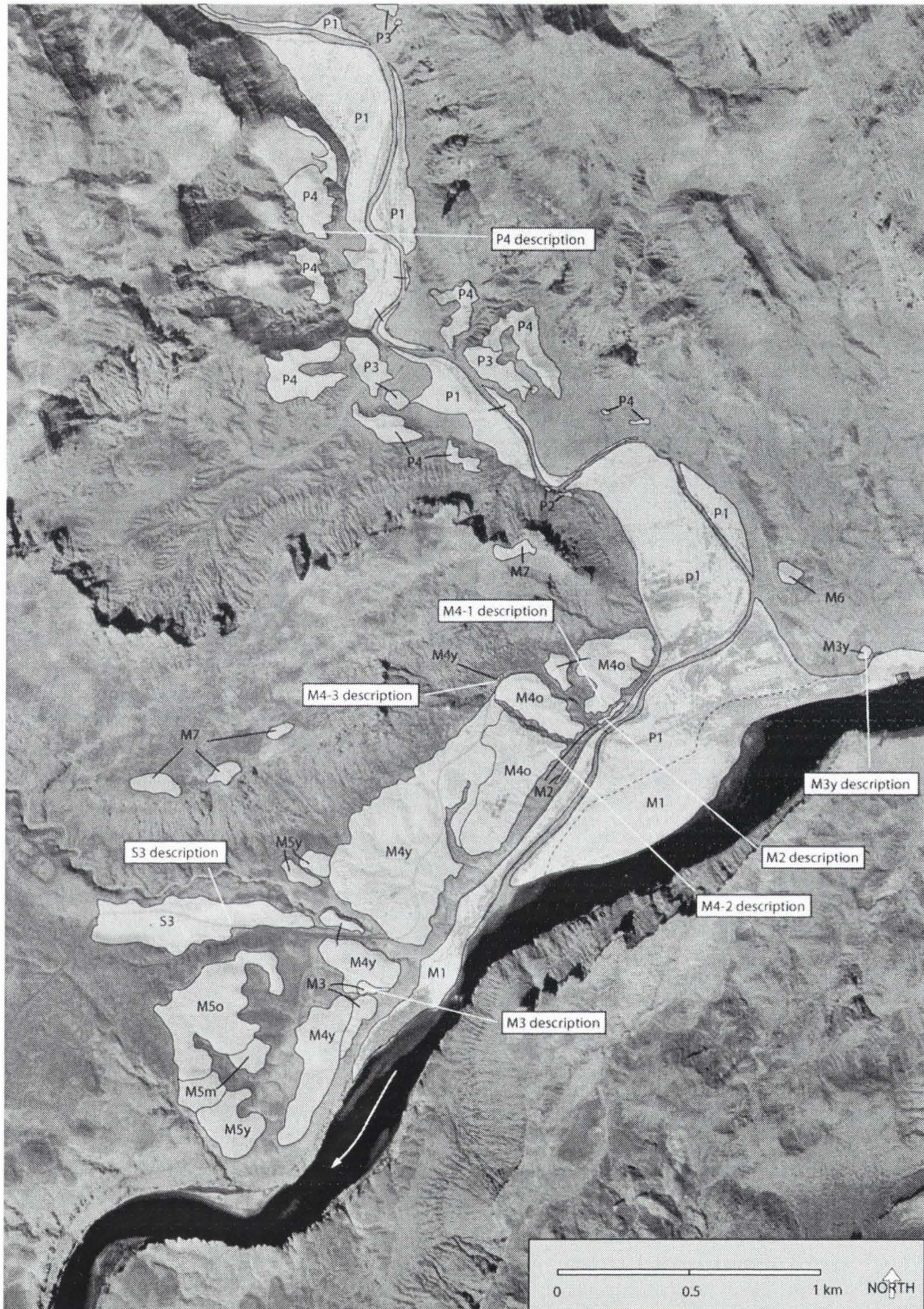

Figure C.1. Map of Quaternary deposits in the Lees Ferry area, showing approximate locations where sedimentary descriptions were made.

Table C.1. Sedimentary description of the M2 deposit.

Geographic location (UTM): 4079927 N, 446830 E
Stop sign, Paria bridge, sandy outcrop
Outcrop description:
Road cut, exposure includes a strath, but is likely not the lowest part, catching side channel…
Total outcrop thickness ~4.5 m
Bedding ranges from 10 cm to 50 cm
Bedding is not generally tabular or continuous; rather it is lenticular, irregular, with notable "pockets" of coarser gravel
Outcrop is likely capped (upper unit) by slopewash originating in terraces above (M4)

Unit 1:
Thickness: 23 cm
Contact: abrupt, bedrock below
Extent: partially laterally extensive downstream – pinches off in lenses
Sedimentary structures: crude imbrication, rip-up clasts
Texture:
Matrix – Max: c. sand Min: silt Average: vf sand
Grain size – Max: 17 cm Min: 2 mm Average: 1-2 cm
Roundness – subrounded - angular
Sorting: poorly sorted
Color: tan-reddish buff
Composition:
Matrix: mostly quartz
Clasts: quartzite, porphyry, sandstone, limestone – see clast count for proportions…
Cement: n/a
General rock name: clast to matrix supported cobble pebble gravel
Secondary features: n/a
Final notes: pockets of clast supported, even amount of matrix supported; lower contact is abrupt, but not smooth.

Unit 2:
Thickness: ~3 m
Contact: abrupt decrease in grain size, wavy
Extent: extensive, generally tabular top
Sedimentary structures: fine portion does not appear to have any; mostly massive; clast portion has crude imbrication
Texture:
Matrix – Max: vf. sand Min: silt Average: vf sand
Grain size – Max: -- Min: -- Average: --
Roundness – too small to see well
Sorting: sand is well sorted
Color: light tan grayish red
Composition:
Matrix: mostly quartz, very few dark minerals
Clasts: --
Cement: n/a
General rock name: very fine sand
Secondary features: n/a
Final notes: fine portion contains pockets/lenses of coarse grained material; represents multiple events instead of single flood.

Coarse texture:
Matrix – Max: c. sand Min: vf. snad Average: m. sand
Grain size – Max: 12 cm Min: 2 mm Average: 1-2 cm
Roundness – subrounded – subangular – clast supported
Sorting: poorly sorted
Color: light brownish red with speckles of other colors
Composition:

Matrix: mostly quartz
Clasts: black chert, red sandstone, quartzite, porphyry, mudstone (Moenkopi), limestone – similar proportions to clast count
Cement: n/a
General rock name: clast supported pebble gravel
Secondary features: n/a
Final notes: pockets/lenses range from 20 cm to 1 m long, from 7 cm to 20 cm thick; some are lenticular, come irregular shape.

Unit 3:
Thickness: 20 cm
Contact: abrupt, blankets unit 2
Extent: laterally extensive, tabular
Sedimentary structures: n/a
Texture:

Matrix	– Max: c. sand	Min: silt	Average: silt
Grain size	– Max: --	Min: --	Average: --

Roundness – c. sand is subangular to angular
Sorting: moderately well sorted
Color: light gray buff
Composition:
Matrix: mostly quartz
C. sand: red sandstone, mudstones
Cement: well cemented carbonate (?)
General rock name: silt
Secondary features: n/a
Final notes: sporadic floating pebbles and cobbles (largest is 24 cm long red sandstone flagstone)

Unit 4:
Thickness: 60 cm
Contact: abrupt, erosional
Extent: not laterally extensive – confined to paleo channel – channel fill
Sedimentary structures: crude imbrication
Texture:
Same as coarse pockets in unit 2, but redder
Final notes: more complex than initially thought; complex filling of paleo channel (?); third dimension may solve the problem.

Unit 5:
Thickness: 72 cm
Contact: relatively planar, clear, marked color difference
Extent: laterally extensive, interbedded fine beds and coarse lenses 15-20 cm thick
Sedimentary structures: coarse lag over unit ¾; local crude imbrication
Texture:
Similar to unit 2; coarser portion cobble dominated; ratio of coarse pockets to fine beds is greater and closer to 1:1; more equal dispersion; more red color
Final notes: cobbles range from subrounded to angular; majority of larger cobbles are red sandstones.

Outcrop cap: pseudo-pavement with cactus…

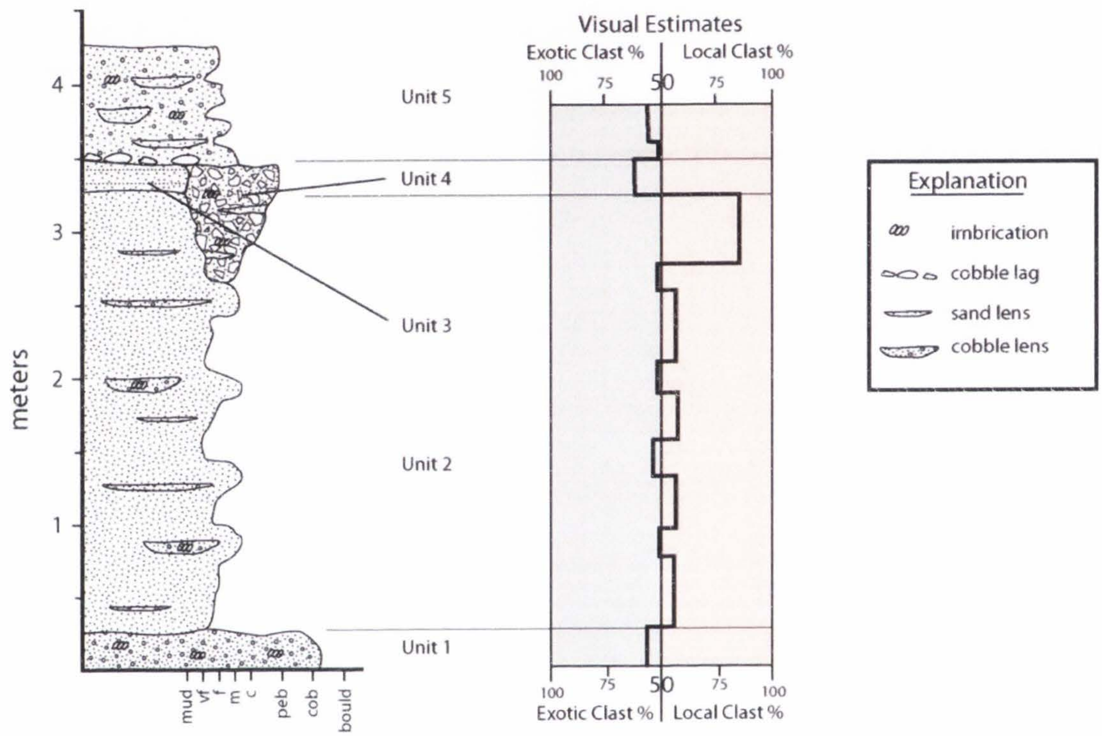

Figure C.2. Sedimentary units of the M2 deposit. Visual proportions of exotic and local clasts were made in order to estimate the dominant source throughout deposition.

Table C.2. Sedimentary description of the M3y deposit.

Geographic location (UTM):
Outcrop description:

- Stream cut exposes outcrop
- Outcrop ~7 m tall
- Lower portion – quartzite clasts >1 m thick
- Middle portion dominated by thick clast-supported angular side canyon red clasts
- Top is capped with quartzites in desert pavement
- Flat top, undulating (highly) erosive; irregular basal strath
- Cosmo surface sample GC-04-LF-408 collected from top

Unit 1:

Thickness: 0-110 cm
Contact: obscured, lowest contact dives underground on either side of terrace
Extent: laterally extensive where exposed
Sedimentary structures: crude imbrication
Texture:

Matrix	– Max: --	Min: --	Average: --
Grain size	– Max: 18 cm	Min: m. sand	Average: 2-4 cm

Roundness – subrounded - subangular

Sorting: poorly sorted
Color: multi-colored, many different colored clasts; overall light brown/gray reddish tan
Composition:

- Matrix: --
- Clasts: see clast count …

Cement: n/a
General rock name: clast supported pebble cobble gravel
Secondary features: calcite/gypsum ppt. under clasts
Final notes: pockets mainstem fluvial clasts.

Unit 2:

Thickness: 110-700 cm
Contact: abrupt contact; change in clast type and roundness; uneven wavy contact - sharp
Extent: laterally extensive, filling mainstem carved channel, overriding lower fluvial gravels and reworking some of them up into debris flow deposit
Sedimentary structures: n/a
Texture:

Matrix	– Max: --	Min: --	Average: --
Grain size	– Max: 30-50 cm	Min: f. sand	Average: 5-7 cm

Roundness – angular - subangular

Sorting: poorly sorted
Color: red sandstone / sand throughout
Composition:

- Matrix: red sand – quartz (local)
- Clasts: red ss 90%; quartzites 1 %; white ss/limestone ?%

Cement: n/a
General rock name: clast supported angular pebble cobble gravel
Secondary features: n/a
Final notes: appears to be debris flow from side canyon, one package filled in and overrode underlying fluvial sediments; additional flows followed and were separated by episodes of more regular (organized) side stream deposition.

Unit 3:

Thickness: interfingers throughout unit 2
Contact: not always clear/distinct, but grain size change marks separation
Extent: laterally extensive where exposed

Sedimentary structures: crude imbrication
Texture:

Matrix	– Max: --	Min: --	Average: --
Grain size	– Max: 12 cm	Min: f. sand	Average: 1 cm

Roundness – angular - subangular

Sorting: poorly sorted
Color: red
Composition:

Matrix: --
Clasts: sandstone – red – side drainage

Cement: n/a
General rock name: matrix supported angular pebble gravel (some cobbles)
Secondary features: n/a
Final notes: interfingers, separating possible episodic debris flow activity from side drainages; this unit and previous appear to fill channel cut by main river.

Unit 4:

Thickness: 700-800 (?) cm
Contact: can't see, we dug a hole in the surface of the terrace ~75 cm deep
Extent: --
Sedimentary structures: n/a
Texture:

Matrix	– Max: --	Min: --	Average: m. sand
Grain size	– Max: 5 cm	Min: f. sand	Average: 1-2 cm

Roundness – rounded - subangular

Sorting: poorly sorted
Color: red/tan sand
Composition:

Matrix: mostly quartz
Clasts: red ss 25%; quartzites 40 %; volcanics 10%

Cement: n/a
General rock name: matrix supported pebble gravel
Secondary features: n/a
Final notes: not very similar to unit 1; surface is littered with abundant quartzite clasts; quartzite clasts spill over terrace surface and appear to overlie debris flow unit; surface or upper layer of extensive quartzite clasts would have to have been present at one time.

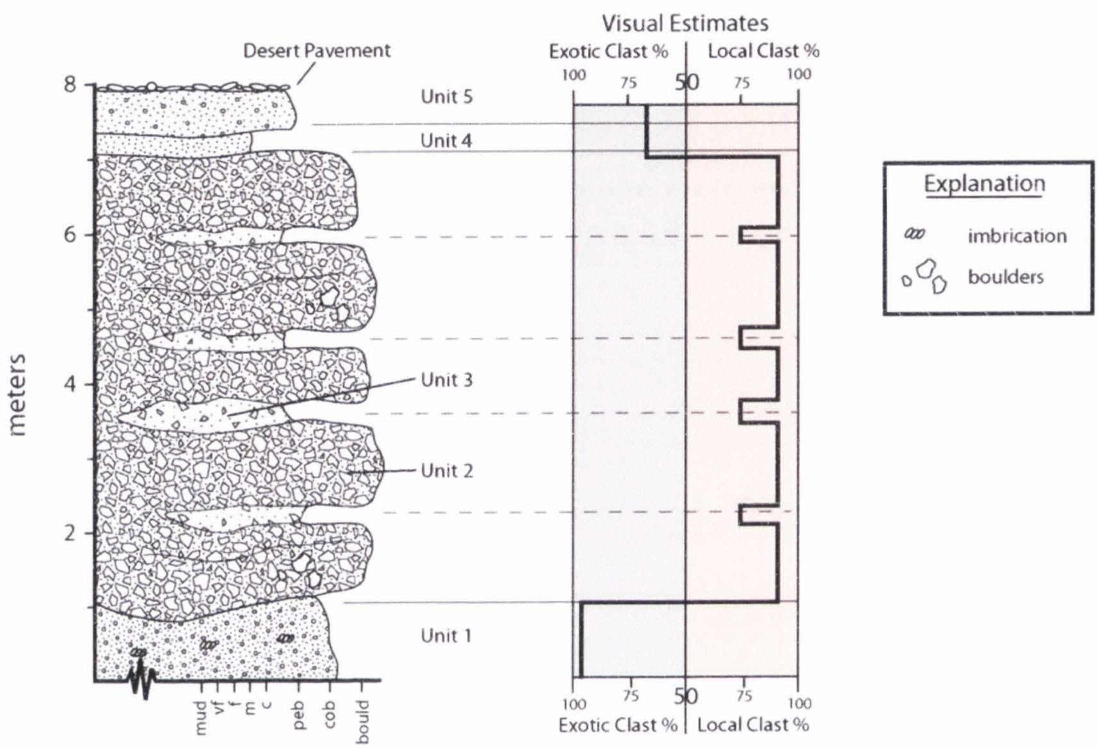

Figure C.3. Sedimentary units of the M3y deposit. Visual proportions of exotic and local clasts were made in order to estimate the dominant source throughout deposition.

Table C.3. Sedimentary description of the M3 deposit.

Geographic location (UTM): 4078918 N, 446036 E
M3 deposit – culvert cut and nearby hillslopes
Outcrop description:
Lower 2.38 m from basal strath to 1st identifiable undisturbed unit is obscured and will be described by hillslope digging
Middle portion of outcrop exposed nicely in stream/culvert cut
Upper portions begin to be disturbed by road and culvert cut and will be described across the drainage on main M3 deposit – cosmo surface sample
Total outcrop thickness ~9 m
Beds are typically 0.5 to 1 m thick
Hillslope deposits blanket unconformably over truncated terrace gravels
Although this is a culvert cut, middle portion is nicely exposed, allowing good characterization of the M3

Unit 1:
Thickness: 0-238 cm
Contact: obscured, covered by poor exposure
Extent: laterally extensive where exposed
Sedimentary structures: digging to find; cobbles unearthed, red sand, large red ss clasts, small quartzites; start to have better exposure at ~200 cm; crude imbrication of large red ss clasts; clast supported
Matrix – Max: -- Min: -- Average: --
Grain size – Max: 17 cm Min: f.-m. sand Average: 2.5 cm
Roundness – well rounded - subangular
Sorting: poorly sorted
Color: overall light brownish to red
Composition:
Matrix: quartz – likely locally sourced (red)
Clasts: ss 68%; quartzite 12%; others in small amounts
Cement: n/a
General rock name: clast supported pebble cobble gravel
Secondary features: calcite/gypsum ppt.
Final notes: lower contact obscured, visible thickness of unit ~0.5 m, dominated by red sand and red local clasts

Unit 2:
Thickness: 238-280 cm
Contact: distinct color contrast, although unit separated out due to apparent relative abundance of quartzite clasts
Extent: laterally extensive over 2 m of exposure
Sedimentary structures: crude imbrication
Texture:
Matrix – Max: -- Min: -- Average: --
Grain size – Max: 15 cm Min: f. sand Average: 2 cm
Roundness – subrounded - subangular
Sorting: poorly sorted
Color: lighter brown, tan, some red clast (but less than previous unit)
Composition:
Matrix: quartz
Clasts: red ss 20%; white ss 25%; quartzite 35&; carbonate 10%; few volcanics
Cement: n/a
General rock name: clast supported pebble cobble gravel
Secondary features: calcite ppt.
Final notes: unit is not as red as lower unit; noticeable amounts of quartzites present.

Unit 3:
Thickness: 280-340 cm
Contact: abrupt change to sand
Extent: laterally extensive, appears on both sides of gully wall

Sedimentary structures: plane beds, low angle cross strata, small scale laminations (less abundant)
Texture:
Matrix – Max: -- Min: -- Average: --
Grain size – Max: m. sand Min: silt Average: f. sand --Some 2 cm pebbles--
Roundness – subrounded - subangular
Sorting: well sorted
Color: tan buff
Composition:
Matrix: quartz sand, iron stained grains concentrated in plane beds
Clasts: --
Cement: n/a
General rock name: fine sand
Secondary features: iron staining
Final notes: No separate bedding features present; good sand, good sed structures: OSL sample GC-05-LF-OSL10 taken from this unit.

Unit 4:
Thickness: 340-630 cm
Complex unit…
Pocket of coarser cobbles observed on south end of unit – grades/interfingers with smaller pebble concentrated packages to the north
Distinct pockets of channelized sand observed sporadically up throughout the unit, starting ~1 m above lower contact

Coarse grained component:
Abrupt change in grain size compared to unit 3
Laterally extensive contact over planar sand unit
Sedimentary structures: moderate imbrication, subtle grading (getting finer) to the north (upstream) and up deposit
Texture:
Grain size – Max: 25 cm Min: f. sand Average: 2-3 cm
Roundness – rounded - subangular
Sorting: poorly sorted
Color: reddish tan
Composition:
Matrix: --
Clasts: see clast count … red ss may increase upward through deposit, although size may decrease
Cement: n/a
General rock name: clast supported pebble cobble gravel
Secondary features: calcite/gypsum ppt. under clasts
Final notes: local outsized clasts observed throughout; large clast clusters on south end – including increase in quartzite clasts.

Sand component:
Channelized pockets 1-2 m in length / 20-50 cm in height
Scattered throughout / interfingering with coarse grained component
Sedimentary structures: low angle cross strata, ripple cross laminations dominate
Texture:
Matrix – Max: m.-c. sand Min: silt Average: f. sand
Roundness – rounded - subangular
Sorting: well sorted
Color: tan buff
Composition:
Matrix: quartz
Cement: n/a
General rock name: fine sand
Secondary features: iron staining
Final notes: GC-05-LF-OSL11 taken from upper sand pocket
--IT'S RAINING HARD—

Unit 5:
Thickness: 630-950 cm
Covered slope – loose description made in gully along main M3 deposit where cosmo surface sample collected

1st Hole Dug:
At 640 cm - ~50 cm deep / with 30 cm exposed of undisturbed sediment
No contacts visible
Sed structures not apparent
Texture:

Matrix	– Max: --	Min: --	Average: --
Grain size	– Max: 6 cm	Min: m. sand	Average: c. sand – 2-5 mm
Roundness	– subrounded - subangular		

Sorting: poorly sorted, but not extremely
Color: tannish light brown, red/gray components
Composition:
Matrix: quartz sand
Clasts: red ss 60%; quartzites 10%
Cement: n/a
General rock name: matrix supported pebble gravel
Secondary features: n/a
Final notes: poorly exposed, but good enough…

2nd Hole Dug:
At 790 cm
Texture:

Matrix	– Max: --	Min: --	Average: --
Grain size	– Max: 12 cm	Min: f. sand	Average: 2 cm
Roundness	– subrounded - subangular		

Sorting: poorly sorted
Color: tan buff
Composition:
Matrix: quartz sand
Clasts: red ss 10%; quartzites 60%; volcanics 5%; chert 2%
Cement: n/a
General rock name: clast supported pebble cobble gravel
Secondary features: n/a
Final notes: has appearance of good mainstem sand, lots of quartzites

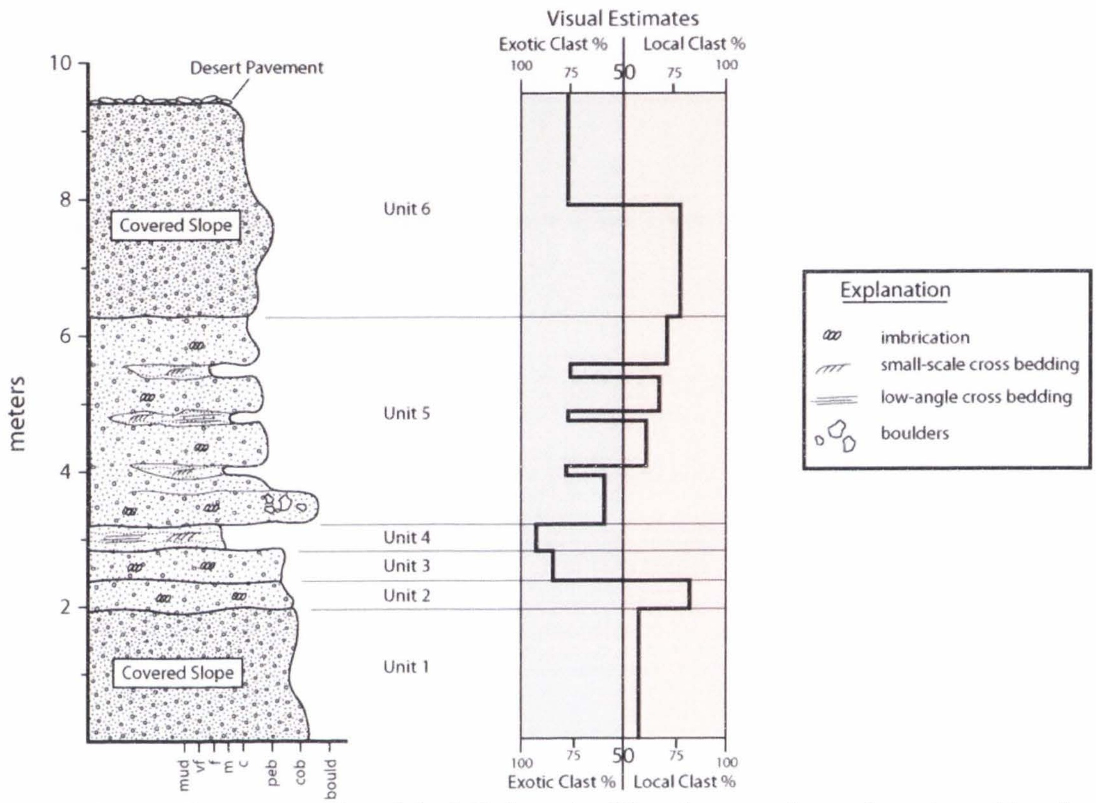

Figure C.4. Sedimentary units of the M3 deposit. Visual proportions of exotic and local clasts were made in order to estimate the dominant source throughout deposition.

Table C.4. Sedimentary description of the S3 paludal deposit.

Geographic location (UTM): 407097 N, 445507 E
S3 paludal deposit of Kaufman et al…
Outcrop description:
Stream/gully cut
Well exposed lower portion on south side of road
Can trace bedding near top of lower portion to bedding at lower portion of top section across road (north)
Deposit is ~10 m thick
Encompasses carbonate spring deposits and local debris flows
Bedding ranges from 20 to 1 m

Unit 1:
Thickness: 62 cm
Contact: sharp with bedrock
Extent: apparently continuous but obscured by large slump
Sedimentary structures: low angle cross strata
Texture:

Matrix	– Max: c. sand	Min: f. snad	Average: m. sand
Grain size	– Max: 13 cm	Min: 2 cm	Average: 5 cm

Roundness – subrounded - angular
Sorting: poorly sorted – matrix supported
Color: yellowish red/tan
Composition:
Matrix: grains fizz, some quartz
Clasts: --
Cement: n/a
General rock name: --
Secondary features: iron staining, gypsiferous nodules
Final notes: clasts floating in matrix

Unit 2:
Thickness: 25 cm
Contact: clear contact; color change; loss of clasts
Extent: extensive, relatively tabular/wavy
Sedimentary structures: planar bedding, accentuated by iron staining
Texture:

Matrix	– Max: m. sand	Min: silt	Average: vf. sand
Grain size	– Max: --	Min: --	Average: --

Roundness – --
Sorting: moderately well sorted
Color: yellowish buff
Composition:
Matrix: mostly quartz, some grains fizz
Clasts: --
Cement: n/a
General rock name: --
Secondary features: iron staining along bedding planes
Final notes: --

Unit 3:
Thickness: 52 cm
Contact: unclear contact; gradual color change
Extent: same as unit 2
Sedimentary structures: wavy bedding near top
Texture:

Matrix	– Max: c. sand	Min: silt	Average: vf. sand

Grain size – Max: -- Min: -- Average: --
Roundness – --
Sorting: fairly poorly sorted
Color: light grayish with light rust streaks
Composition:
Matrix: mostly quartz, some grains fizz
Clasts: --
Cement: n/a
General rock name: --
Secondary features: iron staining
Final notes: wavy beds, possible grain size reduction at bed contacts

Unit 4:
Thickness: 118 cm
Same as unit 3 – differences noted
Contact: abrupt; color change to yellow
Color: Dijon mustard
Texture: mostly fine sand with significant silt and finely disseminated (FDC) carbonate; few coarse grains
Secondary features: some vertical iron staining and gypsiferous crystals, iron staining more significant (similar wavy beds as unit 3).

Unit 5:
opposite side of gully for convenience
Thickness: 75 cm
Contact: abrupt and wavy
Extent: laterally extensive
Sedimentary structures: faint wavy bedding
Texture:
Matrix – Max: c. sand Min: silt Average: f. sand
Grain size – Max: 4 cm Min: 0.5 cm Average: 2.5 cm -- floating in matrix--
Roundness – well rounded to angular
Sorting: moderately: well sorted
Color: weathered color – reddish buff; fresh color – white grayish dijon mustard
Composition:
Matrix: mostly quartz, FDC
Clasts: quartzite, chert, sandstone, siltstone (all from local rocks)
Cement: n/a
General rock name: --
Secondary features: gypsum crystals, FDC
Final notes: --

Unit 6:
Thickness: ~300 cm
Contact: gradual, not well defined
Extent: laterally extensive
Sedimentary structures: same as unit 5
Texture:
Matrix – Max: m. sand Min: vf. sand Average: f. sand
Grain size – same as unit 5
Roundness – --
Sorting: moderately well sorted
Color: medium reddish brown
Composition:
Matrix: same as unit 5
Clasts: same as unit 5; clasts appear to cluster along pseudo-bedding planes
Cementy punky stuff: silt to fine sand; well sorted; carbonate cemented; distributed in discontinuous planes parallel to bedding
Cement: n/a

General rock name: --
Secondary features: carbonate cement in discontinuous layers; cemented layers seem to increase towards top – become more continuous
Final notes: jump across road…

Unit 7:
Thickness: 40 cm
Contact: obscured/covered – best guess across road
Extent: laterally extensive, but probably pinches out
Sedimentary structures: none, maybe some crude imbrication
Texture:

Matrix	– Max: vc. sand	Min: vf. snad	Average: f. sand
Grain size	– Max: 25 cm	Min: 2 cm	Average: 5 cm
Roundness	– angular to subangular		

Sorting: poorly sorted
Color: reddish brown
Composition:
Matrix: mostly quartz
Clasts: -- array of local clasts
Cement: compacted
General rock name: --
Secondary features: n/a
Final notes: likely debris flow

Unit 8:
Thickness: 45 cm
Contact: clear contact
Extent: laterally extensive, planar in an interfingering way
Sedimentary structures: faint bedding planes
Texture:

Matrix	– Max: vc. sand	Min: vf. Sand	Average: m. sand
Grain size	– Max: --	Min: --	Average: --
Roundness	– --		

Sorting: moderately well sorted
Color: medium reddish brown
Composition:
Matrix: mostly quartz, small grains of local siltstones
Clasts: --
Cement: compacted
General rock name: --
Secondary features: n/a
Final notes: occasional floating clasts 0.5 to 1 cm

Unit 9:
Thickness: 83 cm
Contact: clear contact; noted by grain size change
Extent: tabular, laterally extensive
Sedimentary structures: good imbrication in pebbles; crude imbrication in cobbles; coarsens upward at base
Texture:

Matrix	– same as unit 8		
Grain size	– Max: 17 cm	Min: 2 mm	Average: 5 cm
Roundness	– angular to subangular		

Sorting: poorly sorted – clast supported
Color: varies
Composition:
Matrix: same as unit 8
Clasts: array of local clasts, primarily red ss
Cement: n/a

General rock name: --
Secondary features: n/a
Final notes: good candidate for debris flow

Unit 10:
Thickness: 55 cm
Contact: change in grain size, semi-abrupt
Extent: laterally extensive, tabular
Sedimentary structures: moderate imbrication in pebbles; planar bedding at bottom
Texture:
Matrix – same as unit 8
Grain size – Max: 6 cm Min: 2 mm Average: 2 cm
Roundness – angular
Sorting: poorly sorted
Color: medium reddish brown
Composition:
Matrix: same as unit 8
Clasts: local clasts, especially siltstones (Moenkopi)
Cement: compacted (for all compacted units there may be minor carbonate cementing)
General rock name: --
Secondary features: n/a
Final notes: clasts concentrated along bedding planes, 1 to 3 cm thick beds with clasts; clast beds spaced 2 to 10 cm near bottom half, upper half mostly massive.

Unit 11:
Thickness: 74 cm
Contact: clear contact; change in grain size
Extent: lenticular, channel shaped - ~30 m in lateral extent
Sedimentary structures: crude imbrication in large boulders
Texture:
Matrix – same as unit 7
Grain size – Max: 80 cm Min: 0.5 cm Average: 18 cm
Roundness – angular
Sorting: very poorly sorted
Color: medium reddish brown
Composition:
Matrix: same as unit 7
Clasts: array of local clasts including Navajo Sandstone
Cement: compacted
General rock name: --
Secondary features: n/a
Final notes: big boulders clast supported with finer matrix in between; big boulders disappear down paleoslope.

Unit 12:
Thickness: 85 cm
Same as unit 10

Unit 13:
moved ~20 m to NW, 10 m E of GC-04-LF-OSL16 sampling site
Thickness: 92 cm
Contact: sharp, noted in OSL site description; based on color change
Extent: thickness varies laterally
Sedimentary structures: n/a
Texture:
Matrix – Max: f. sand Min: silt Average: vf. sand
Grain size – Max: -- Min: -- Average: --
Roundness – --

Sorting: fairly well sorted
Color: light yellowish buff
Composition:
Matrix: mostly quartz, some FDC
Clasts: --
Cement: n/a
General rock name: --
Secondary features: some iron staining in upper parts; irregular shaped carbonate pieces (cm scale); wavy shaped to jagged
Final notes: bedding appears draped in mound shape towards top.

Unit 14:
Thickness: 14 cm to only a few cm
Contact: sharp – wavy draping over underlying unit
Extent: wavy, capping several mounds in area
Sedimentary structures: n/a
Texture:

Matrix	– Max: f. sand	Min: silt	Average: f. sand
Grain size	– Max: --	Min: --	Average: --
Roundness	– --		

Sorting: moderately well sorted
Color: light reddish brown yellow
Composition:
Matrix: mostly carbonate with some quartz grains
Clasts: --
Cement: carbonate
General rock name: --
Secondary features: iron staining
Final notes: punky texture… from rain erosion (?)

Unit 15:
Thickness: 55 cm, may vary throughout deposit
Contact: obscured, not clear
Extent: only found on highest points – 3 or 4 mounds
Sedimentary structures: n/a
Texture:

Matrix	– Max: vf. sand	Min: silt	Average: silt
Grain size	– Max: --	Min: --	Average: --
Roundness	– --		

Sorting: fairly well sorted
Color: light whitish gray
Composition:
Matrix: quartz sand and FDC
Clasts: --
Cement: n/a
General rock name: --
Secondary features: maybe iron staining near top
Final notes: unit of Kaufman et al. snails; capped by unit similar to unit 14 in a draping manner…

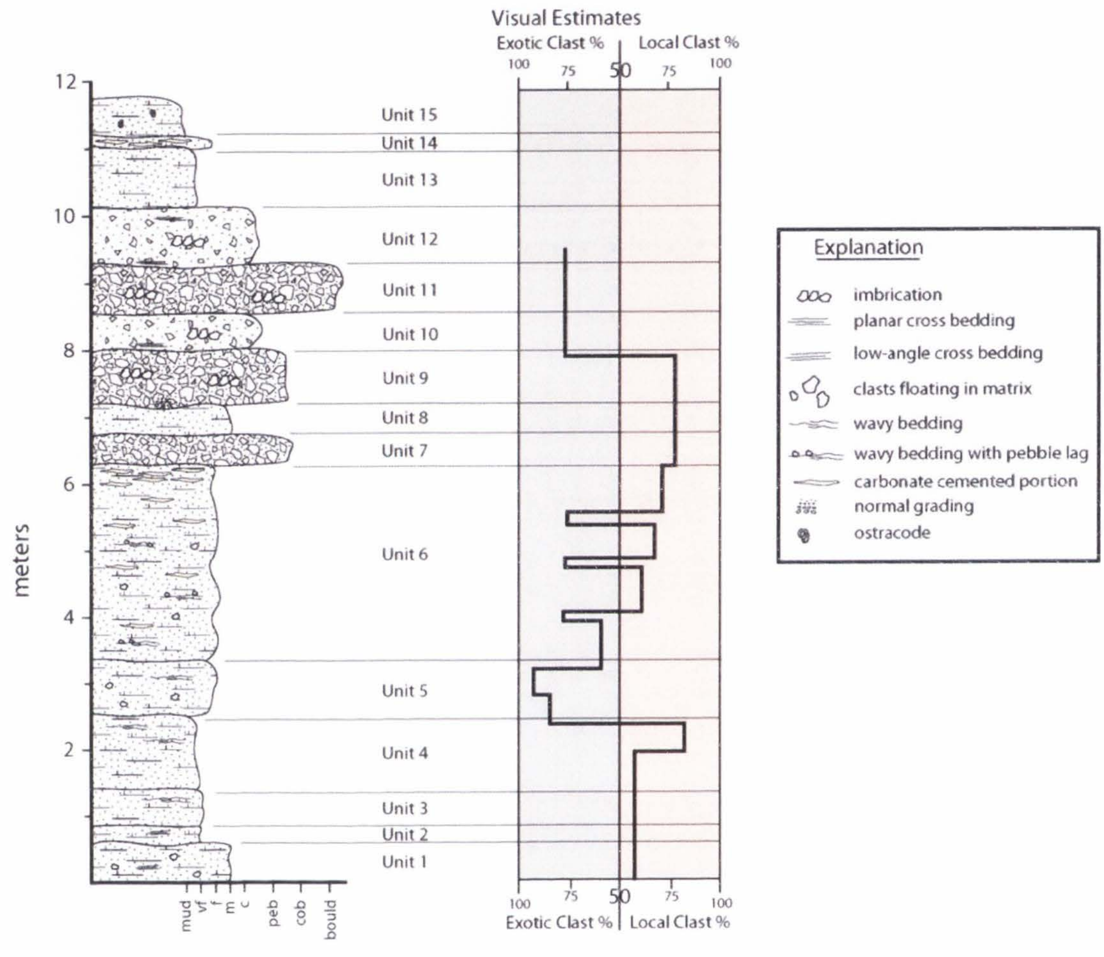

Figure C.5. Sedimentary units of the S3 deposit. Visual proportions of exotic and local clasts were made in order to estimate the dominant source throughout deposition.

Table C.5. Sedimentary description of the M4 deposit, M4-1 description.

Geographic location (UTM):
    Thick M4 deposit near the stop sign at Paria River bridge
Outcrop description:
    Bottom ~4 m forms cliff (well cemented); upper ~6 m is less consolidated and more recessive
    Bed thickness is ~0.5 to 1 m, with some apparently thicker beds (~2 m) towards top
    Bedding appears laterally extensive, with interspersed channel form (sandy) within tabular units

Unit 1:
Thickness: varies from 0.5 to 1.1 m
Contact: abrupt lower bedrock strath contact
Extent: laterally extensive, but varying thickness
Sedimentary structures: very slight imbrication, rip-up clasts (Moenkopi)
Texture:
    Grain size – Max: 90 cm   Min: m. sand   Average: 3-4 cm
    Roundness – subrounded to subangular
Sorting: poorly sorted
Color: 7.5 YR 7/4; varying clast colors
Composition:
    Matrix: quartz grains
    Clasts: quartzite 15%; red and white ss 55%; carbonate 10%; Moenkopi 5%
Cement: carbonate
General rock name: clast supported bouldery cobble gravel
Secondary features: carbonate cement, carbonate pendants on underside of clasts
Final notes: appears to be a mixture of local and far-traveled clasts; very large clasts (boulders are unique to this lower unit – compared to next few units).

Unit 2:
Thickness: 55 cm, although varies up to 75 cm on bottom
Contact: sharp – irregular
Extent: laterally extensive with varying thicknesses on bottom
Sedimentary structures: slight imbrication
Texture:
    Grain size – Max: 20 cm   Min: m. sand   Average: 0.5-1 cm
    Roundness – rounded to subangular
Sorting: --
Color: 5 YR 7/3; varying clast colors
Composition:
    Matrix: quartz grains
    Clasts: ss 35%; quartzite 30%; volcanics 5%; carbonate 13 %; Moenkopi 3% (more worked than unit 1)
Cement: carbonate
General rock name: clast supported cobble gravel
Secondary features: calcite cement
Final notes: larger clasts are sandstones; less matrix than unit 1; channel cut of sandy gravel with cross strata.

Unit 3:
Thickness: ~85 cm
Contact: abrupt and laterally planar
Extent: laterally extensive
Sedimentary structures: imbrication (especially in smaller clasts)
Texture:
    Grain size – Max: 10 cm   Min: m. sand   Average: 0.5 cm
    Roundness – rounded to subangular
Sorting: poorly sorted, but clasts are generally unimodal
Color: 7.5 YR 7/3; varying clast colors, but white seems to dominate
Composition:

Matrix: quartz grains

Clasts: ss 5%; quartzite 40%; volcanics 1%; carbonate/chert 42% (chert coming out of Kaibab ?)

Cement: carbonate

General rock name: clast supported pebble gravel

Secondary features: calcite cement (well developed)

Final notes: finer grained than previously defined units; dominantly white (chert/carbonates??); lighter colored matrix.

Unit 4:

Thickness: 90 cm

Contact: gradational

Extent: laterally extensive, tabular unit

Sedimentary structures: massive

Texture:

Grain size – Max: 40 cm   Min: m. sand   Average: 0.5-1 cm

Roundness – rounded to subangular

Sorting: --

Color: 5 YR 7/3

Composition:

Matrix: quartz grains

Clasts: ss 53%; quartzite 30%; volcanics 4%; Moenkopi and local clasts 8%

Cement: carbonate

General rock name: clast supported cobble gravel

Secondary features: calcite cement

Final notes: similar in appearance to unit 2, but sandstone clasts are larger.

Unit 5:

Thickness: 190 cm

Contact: gradational, but tabular and continuous

Extent: laterally extensive

Sedimentary structures: massive

Texture:

Grain size – Max: 15 cm   Min: m. sand   Average: 1 cm

Roundness – rounded to subangular

Sorting: poorly sorted

Color: matrix – 7.5 YR 6/4: clasts – look at unit 1

Composition:

Matrix: quartz grains

Clasts: ss 23%; quartzite 37%; volcanics 6%; chert 2%; weathered quartzite (?) 13%

Cement: carbonate

General rock name: clast supported pebble cobble gravel

Secondary features: calcite cement, not as well developed

Final notes: more recessive weathering profile; in between units 5 and 6 there appears to be a small, ~6 cm thick, channel fill, but will be included in next unit.

Unit 6:

Thickness: 40 cm

Contact: marked by the abrupt appearance of cobbles

Extent: laterally extensive, appears tabular except for channel form at the base

Sedimentary structures: slight imbrication, some channel forms at thé base

Texture:

Grain size – Max: 24 cm   Min: m. sand   Average: 0.25-1.5 cm

Roundness – subrounded to subangular

Sorting: poorly sorted, with zones of slightly better poorly sorted

Color: matrix – 10 YR 7/2; clasts – look at unit 1 (some yellow quartzites)

Composition:

Matrix: quartz grains

Clasts: ss 25%; quartzite 35%; volcanics 17%; chert 3%; weathered quartzite (?)%; limestone 10%

Cement: carbonate (not as well developed)

General rock name: clast supported cobble pebble gravel
Secondary features: slight calcite cement
Final notes: has channel forms and is cut by the upper unit.

Unit 7:
Thickness: 105 cm
Contact: abrupt appearance of boulders
Extent: laterally extensive
Sedimentary structures: n/a
Texture:
Grain size – Max: 83 cm Min: f. sand Average: 36 cm
Roundness – rounded to subangular
Sorting: extremely poorly sorted
Color: matrix – 5 YR 6/6; clasts – reddish sandstones
Composition:
Matrix: quartz grains
Clasts: red ss 61%; quartzite 27%
Cement: n/a
General rock name: clast supported cobble boulder gravel
Secondary features: n/a
Final notes: big boulders.

Unit 8:
Thickness: 165 cm
Contact: obscured
Extent: laterally extensive, appears tabular
Sedimentary structures: n/a
Texture:
Grain size – Max: 42 cm Min: f. sand Average: 1.5-2 cm
Roundness – subrounded to subangular
Sorting: poorly sorted, with lenses of coarser cobbles and boulders between more gravelly portions
Color: matrix – 2.5 YR 5/8; clasts – same, more red ss
Composition:
Matrix: quartz grains
Clasts: ss 56%; quartzite 28%; volcanics 10%
Cement: n/a
General rock name: clast supported boulder cobble gravel
Secondary features: n/a
Final notes: getting sandier, vegetation increasing, less carbonates, still steep slope.

Unit 9:
Thickness: 250 cm
Contact: gradual, marked by angular appearance
Extent: laterally extensive
Sedimentary structures: n/a
Texture:
Grain size – Max: 76 cm Min: f. sand Average: 13 cm
Roundness – subrounded to angular
Sorting: poorly sorted
Color: matrix – 2.5 YR 5/6; clasts – same as all
Composition:
Matrix: quartz grains
Clasts: ss 68%; quartzite 23%; volcanics 3%
Cement: n/a
General rock name: clast supported boulder cobble gravel
Secondary features: n/a
Final notes: angular appearance, appears to have colluvial component, but channels with locally rounded gravels are present and may be reworking locally delivered cobbles and boulders of sandstone.

Unit 10:
Thickness: 158 cm
Similar to units 6 and 8
But max grain size is 12 cm, min in fine sand, average is 0.5-1 cm
Color is redder, no vegetation, laterally extensive

Unit 11:
Thickness: 160 cm
Contact: planar, abrupt appearance of predominantly cobbles
Extent: laterally extensive, but slightly lenticular
Sedimentary structures: faint / slight imbrication
Texture:
    Grain size – Max: 42 cm   Min: f. sand   Average: 2 cm
    Roundness – subrounded to subangular
Sorting: poorly sorted
Color: matrix – red; clasts – same as all
Composition:
    Matrix: quartz grains
    Clasts: ss 52%; quartzite 35%; volcanics 5%
Cement: n/a
General rock name: clast supported cobble gravel
Secondary features: n/a
Final notes: still has red appearance, more sandstones, less quartzites than unit 10, smaller quartzites but sandstones are red and subangular to subrounded.

Unit 12:
Thickness: 124 cm
Contact: gradational with the marked appearance of more abundant gravel sized quartzites
Extent: laterally extensive, sitting on top of boulders
Sedimentary structures: slight imbrication, nothing definitive, hinted at in structure
Texture:
    Grain size – Max: 13 cm   Min: f. sand   Average: 0.5-1 cm
    Roundness – subrounded
Sorting: poorly sorted
Color: matrix – reddish, but lighter than units 8 through 10; clasts – same as all
Composition:
    Matrix: quartz grains
    Clasts: -- ss 68%; quartzite 23%; volcanics 3% -- (??)
Cement: n/a
General rock name: clast supported cobble gravel
Secondary features: n/a
Final notes: got dark, working too hard… time to sleep for the day.

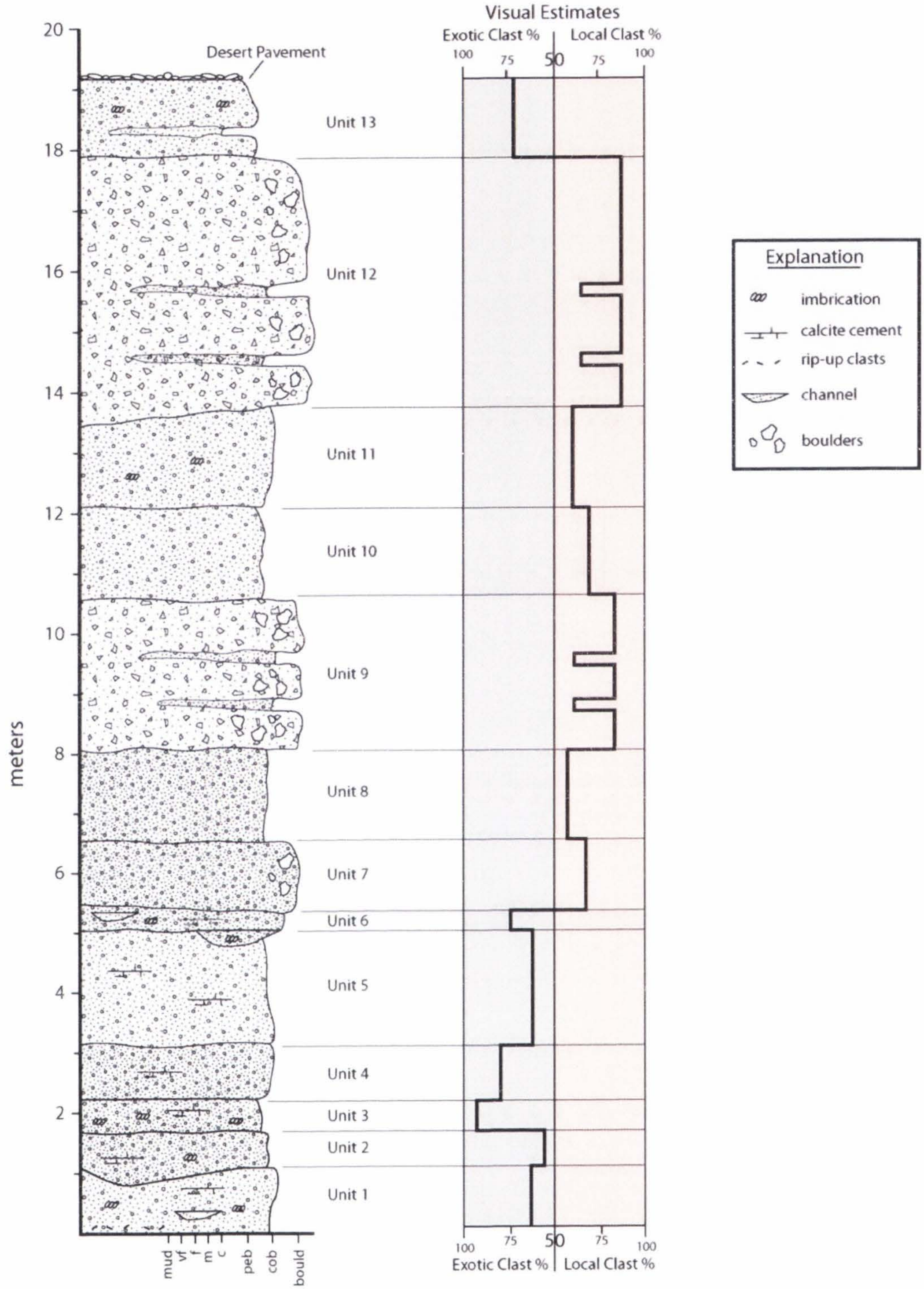

Figure C.6. Sedimentary units of the M4 deposit – M4-1 description. Visual proportions of exotic and local clasts were made in order to estimate the dominant source throughout deposition.

Table C.6. Sedimentary description of the M4 deposit, M4-2 description.

Geographic location (UTM):
Just south of stop sign, below housing terrace in south side of gully leading directly up to houses
M4 deposit, including the lowest portion of the deposit, near lowest surveyed strath
Outcrop description:
Fairly decent gully cut, exposing ~3/4 of the deposit very well
Total thickness is ~20 m
Bedding ranges from 10 cm to > 1 m
Bedding is not always tabular or continuous, several lenticular/channel shaped beds included

Unit 1:
Thickness: 70 cm
Contact: abrupt contact with bedrock strath
Extent: apparently extensive, although dives quickly underground
Sedimentary structures: crude imbrication
Texture:
Matrix – Max: vc. sand Min: vf. sand Average: m. sand
Grain size – Max: 19 cm Min: 2 mm Average: 1.5 cm
Roundness – subrounded to rounded
Sorting: moderately to fairly poorly sorted – generally clast supported
Color: matrix – light reddish brown gray; clasts – assorted
Composition:
Matrix: mostly quartz
Clasts: red ss 22%; quartzite 12%; porphyry 3%; black chert 7%; other ss 12%
Cement: carbonate in some places
General rock name: --
Secondary features: calcite cement
Final notes: unit is more obscured than most, although some limited good exposure exists; matrix is very sandy; has a colorful salt and pepper look; there are actually many < 0.5 cm clasts throughout matrix.

Unit 2:
Thickness: 110 cm
Contact: difficult to see, slight decrease in grain size, specifically a loss of large clasts
Extent: apparently extensive
Sedimentary structures: crude imbrication in larger clasts
Texture:
Matrix – Max: vc. sand Min: vf. sand Average: m. sand
Grain size – Max: 12 cm Min: 2 mm Average: 1-2 cm
Roundness – subrounded to rounded
Sorting: overall poorly sorted – clast and matrix supported areas throughout
Color: matrix – light grayish brown; clasts – colorful salt and pepper appearance
Composition:
Matrix: mostly quartz
Clasts: red ss 8%; quartzite 20%; porphyry 5%; black chert 8%; other ss 12%; limestone 6%
Cement: n/a
General rock name: --
Secondary features: n/a
Final notes: very sandy unit with pebbles throughout; quartzites are present but do not visibly dominate.

Unit 3:
Thickness: 28 cm
Contact: fairly abrupt, better cemented, sandy lens separating
Extent: not continuous, thickens down paleoslope
Sedimentary structures: planar cross strata, pebble lags on bedding planes, crude imbrication
Texture:
Matrix – Max: m. sand Min: vf. sand Average: f. sand

Grain size – Max: 7 cm Min: 2 mm Average: 1 cm
Roundness – subrounded to subrounded

Sorting: zones or beds of fairly well (sand) and fairly poorly (pebbles) sorted; matrix and clast supported zones
Color: matrix – light reddish brown; clasts – speckled appearance
Composition:
Matrix: mostly quartz
Clasts: red ss 9%; quartzite 18%; porphyry 3%; black chert 6%; other ss 19%; limestone 3%
Cement: carbonate
General rock name: --
Secondary features: calcite cement
Final notes: lowest ~10 cm is composed of well sorted sand lens that pinches out; upper portion contains pebbles that are generally sorted on bedding planes, or form planar bedding planes throughout.

Unit 4:
Thickness: 26 cm
Contact: fairly sharp
Extent: lenticular, not extensive, but observed in most of outcrop (~3m across)
Sedimentary structures: crude imbrication in larger clasts
Texture:
Matrix – Max: vc. sand Min: vf. sand Average: m. sand
Grain size – Max: 1.5 cm Min: 2 mm Average: 0.4 cm
Roundness – subrounded to subangular
Sorting: overall moderately sorted – matrix supported
Color: matrix – light grayish brown; clasts – --
Composition:
Matrix: mostly quartz
Clasts: red ss, quartzite, black chert, limestone – all less than 5% of deposit
Cement: n/a
General rock name: --
Secondary features: some gypsum coatings
Final notes: very sandy unit, almost no clasts.

Unit 5:
Thickness: 153 cm
Contact: fairly abrupt, appearance of large clasts
Extent: generally tabular, extensive
Sedimentary structures: good imbrication
Texture:
Matrix – Max: vc. sand Min: vf. sand Average: m. sand
Grain size – Max: 48 cm Min: 2 mm Average: 3-4 cm (red ss – 9 cm)
Roundness – subrounded to rounded
Sorting: overall poorly sorted – clast and matrix supported areas throughout
Color: matrix – light grayish brown; clasts – --
Composition:
Matrix: mostly quartz
Clasts: see clast count…
Cement: some carbonate
General rock name: --
Secondary features: calcite cement
Final notes: interfingering of definite mainstem river gravels with clusters of large red sandstone cobbles and boulders; few lenses of generally small pebbles and sand.

Note: continually moving semi-laterally up gully

Unit 6:
Thickness: 45 cm
Contact: fairly abrupt, marked by dark organic and iron staining beds
Extent: continuous in outcrop

Sedimentary structures: low angle beds, planar beds
Texture:

Matrix – Max: c. sand Min: f. sand Average: m. sand
Grain size – Max: 12 cm Min: 2 mm Average: bimodal – 1) subang. 0.5 cm; 2) subround. 4.5 cm
Roundness – subrounded to subangular

Sorting: overall fairly poorly sorted – clast supported (mostly small clasts)
Color: matrix –grayish buff with dark gray and rust
Composition:

Matrix: mostly quartz
Clasts: red ss 8%; quartzite 20%; porphyry 5%; black chert 8%; other ss 12%; limestone 6%

Cement: n/a
General rock name: --
Secondary features: paleosol (?)
Final notes: if paleosol, would have been part of previous unit.

Unit 7:
Thickness: 19 cm (variable due to lens shape)
Contact: faintish, marked by decrease in grain size
Extent: lenticular, pinches out
Sedimentary structures: fining upward, plane beds at top where sand dominates
Texture:

Matrix – Max: vc. sand Min: f. sand Average: m. sand
Grain size – Max: -- Min: -- Average: --
Roundness – subrounded to subangular

Sorting: fairly poorly sorted, becomes fairly well sorted at top where sand dominates (~7cm)
Color: matrix – light grayish buff
Composition:

Matrix: mostly quartz
Clasts: red ss 8%; quartzite 20%; porphyry 5%; black chert 8%; other ss 12%; limestone 6%

Cement: compacted
General rock name: --
Secondary features: n/a
Final notes: there are some few pebbles, less than 1 cm near bottom of unit.

Unit 8:
Thickness: 378 cm
Contact: abrupt change in grain size
Extent: apparently tabular and extensive
Sedimentary structures: imbrication, planar cross strata in sand lenses
Sand lens: vf. to c. sand, average: m. sand; subrounded, moderately well sorted; mostly quartz; occasional small pebbles <1 cm
Majority of deposit:
Texture:

Matrix – Max: vc. sand Min: vf. sand Average: m. sand
Grain size – Max: 36 cm Min: 2 mm Average: 2-3 cm (red sandstone – 13 cm)
Roundness – subrounded to rounded

Sorting: overall poorly sorted – clast supported
Color: matrix – light grayish buff; clasts – speckled with light gray buff reddish
Composition:

Matrix: mostly quartz
Clasts: see clast count…

Cement: carbonate in some places, especially near top
General rock name: --
Secondary features: calcite cement, some gypsum
Final notes: sand lenses throughout, although generally spaced every 1.2 m or so – some as close as 20 cm; there are some areas of slightly lower average grain size that are still clast supported, but much sandier; interfingered red ss boulders appear in a few places (spaced ~1.5 m) and are often clustered together on a single bed; some sand lenses are small, others are quite extensive.

Unit 9:
Thickness: 160 cm
Contact: fairly easy to see, appearances of red sandstone boulders
Extent: laterally extensive, obscured on other side of ravine to north
Sedimentary structures: crude imbrication, stacked boulders
Texture:
Matrix – Max: vc. sand Min: vf. sand Average: m. sand
Grain size – Max: 43 cm Min: 1 cm Average: 7-8 cm
Roundness – subrounded to subangular
Sorting: overall poorly sorted – clast supported – big boulders touching, filled with fines and pebbles
Color: sandstones give more reddish appearance
Composition:
Matrix: quartz and local clast chips
Clasts: red ss 50%; quartzite 13%; other ss 20%; others 10%
Cement: n/a
General rock name: --
Secondary features: n/a
Final notes: not likely one event; lenses of more organized clasts that are smaller; boulders generally stacked on single planar surface.

Unit 10:
Thickness: ~300 cm
Contact: good, clear, appearance of fluvial dominated gravels
Extent: extensive, tabular
Sedimentary structures: imbrication, planar cross strata in sand lenses
Sand lens: vf. to c. sand, average: m. sand; subrounded, moderately well sorted; mostly quartz; occasional small pebbles <1 cm
Majority of deposit:
Texture:
Matrix – Max: vc. sand Min: vf. sand Average: m. sand
Grain size – Max: 36 cm Min: 2 mm Average: 2-3 cm (red sandstone – 13 cm)
Roundness – subrounded to rounded
Sorting: overall poorly sorted – clast supported
Color: matrix – light grayish buff; clasts – speckled with light gray buff reddish
Composition:
Matrix: mostly quartz
Clasts: see clast count…
Cement: carbonate in some places, especially near top
General rock name: --
Secondary features: calcite cement, some gypsum
Final notes: sand lenses throughout, although generally spaced every 1.2 m or so – some as close as 20 cm; there are some areas of slightly lower average grain size that are still clast supported, but much sandier; interfingered red ss boulders appear in a few places (spaced ~1.5 m) and are often clustered together on a single bed; some sand lenses are small, others are quite extensive.

Unit 11:
Thickness: ~260 cm
Same as unit 8

Unit 12:
Thickness: ~350 cm
Same as unit 8 (approximately)
Covered slope, best estimate…

Unit 13:
Thickness: ~200 cm
Same as unit 9

Unit 14:
Thickness: ~130 cm
Same as unit 8

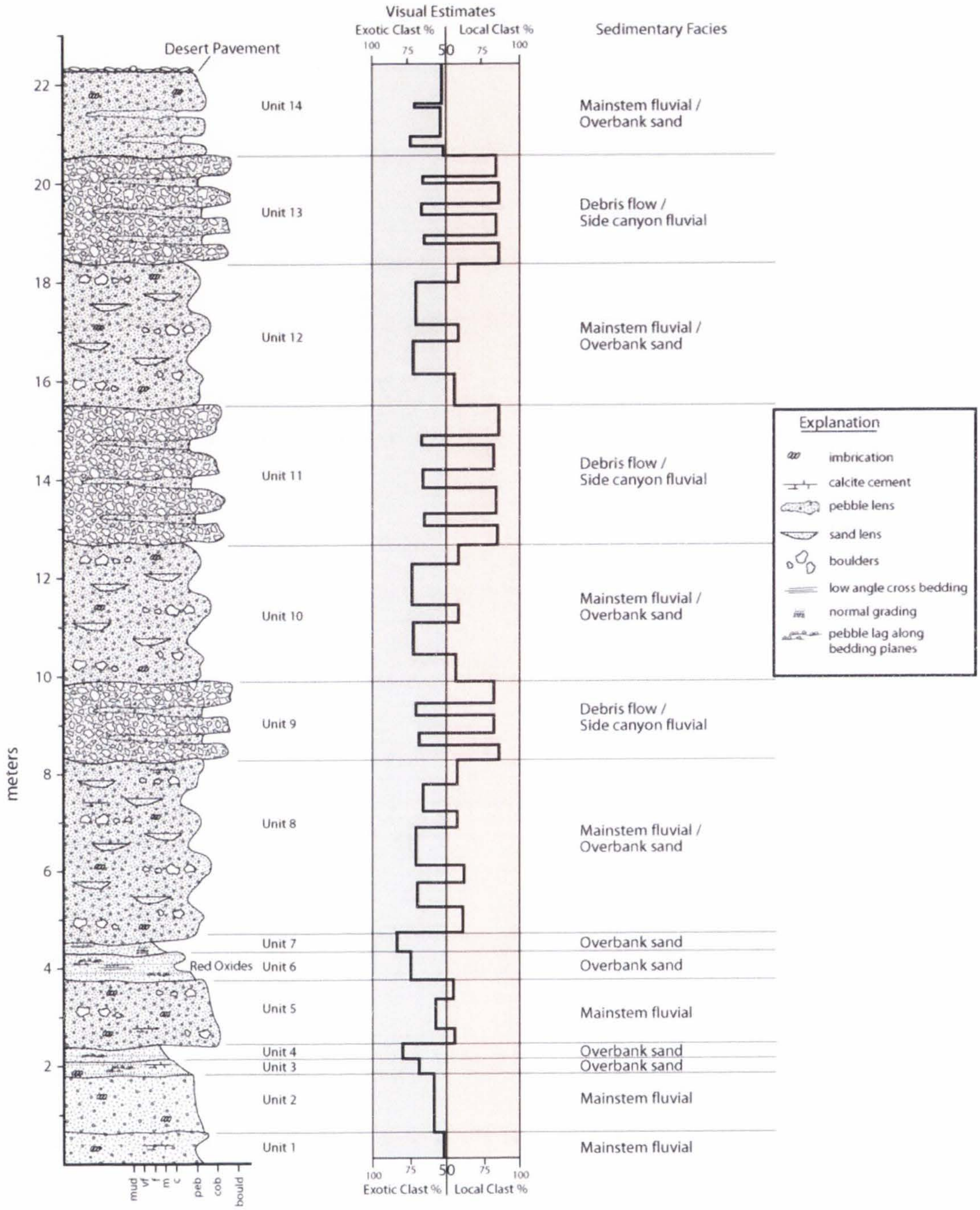

Figure C.7. Sedimentary units of the M4 deposit, M4-2 description. Visual proportions of exotic and local clasts were made in order to estimate the dominant source throughout deposition. Sedimentary facies interpretations are also included.

Table C.7. Sedimentary description of the M4 deposit, M4-3 description (upper).

Geographic location (UTM): 4079938 N, 446458 E
Approximately 300 m north of Ranger Station
Prominent sandy road cut on west side of road
Outcrop description:
Extremely large boulder truncates sand and gravel lenses
Unit is generally light tan/yellow with local reddish clasts throughout, especially in upper 0.5 m
Lenticular and tabular beds present

Unit 1:
Thickness: 75 cm
Contact: obscured
Extent: extensive, tabular
Sedimentary structures: n/a
Texture:
Grain size – Max: 26 cm Min: silt Average: 0.5-1 cm
Roundness – subrounded to angular
Sorting: moderately sorted
Color: tan/red/brown/gray – overall tannish red
Composition:
Matrix: mostly quartz
Clasts: red ss 50%; quartzite 15%; chert 15%; volcanics 2%; carbonate 5%
Cement: n/a
General rock name: clast supported pebble gravel with overlying cobble lag
Secondary features: n/a
Final notes: cobble lag on upper boundary – red sandstone.

Unit 2:
Thickness: 25 cm
Contact: undulates around boulder lag of unit 1 - sharp
Extent: not extensive, channel scour/lenticular
Sedimentary structures: low angle cross strata with some 1-2 mm clast lags on paleo-surfaces
Texture:
Grain size – Max: 5 cm Min: f. sand Average: 0.2 cm
Roundness – subrounded to angular
Sorting: moderately sorted – grading
Color: tan to reddish brown, lighter at top
Composition:
Matrix: mostly quartz
Clasts: red ss 30%; quartzite 15%; chert 30%
Cement: n/a
General rock name: coarse sand
Secondary features: n/a
Final notes: unit coarsens upward in three apparently distinct packages.

Unit 3:
Thickness: 40 cm
Contact: gradual, sharp in some places
Extent: fairly extensive, tabular
Sedimentary structures: n/a
Texture:
Grain size – Max: 21 cm Min: silt Average: 4 cm
Roundness – subrounded to subangular
Sorting: poorly sorted
Color: tannish red – more red than other units
Composition:

Matrix: mostly quartz
Clasts: red ss70%; quartzite 10%; chert 10%
Cement: n/a
General rock name: clast supported pebble cobble gravel
Secondary features: n/a
Final notes: no real imbrication, but apparent preferred orientation.

Unit 4:
Thickness: 50 cm
Contact: sharp
Extent: channel shaped, scour
Sedimentary structures: small scale pebble (1-2 mm) overlying finer grains (no cross bedding)
Texture:
Grain size – Max: 7 cm Min: silt Average: <1 cm
Roundness – subrounded to subangular
Sorting: somewhat poorly sorted
Color: light tannish red
Composition:
Same as unit 2…
Cement: n/a
General rock name: matrix supported pebble gravel
Secondary features: n/a
Final notes: generally harder than previous units; apparent channel form.

Unit 5:
Thickness: 80 cm
Contact: sharp/abrupt
Extent: tabular, extensive
Sedimentary structures: laminations apparent due to weathering; 20 cm scale cross strata
Texture:
Grain size – Max: f. sand Min: clay Average: silt
Roundness – subrounded to subangular
Sorting: fairly well sorted
Color: tan
Composition:
Matrix: quartz, clay
Cement: n/a
General rock name: matrix supported pebble gravel
Secondary features: clay formation (?)
Final notes: mud crack weathering pattern – external pattern.

Unit 6:
Thickness: 95 cm
Contact: abrupt change in grain size
Extent: not extensive, thins to the south
Sedimentary structures: n/a
Texture:
Grain size – Max: 30 cm Min: vf. sand Average: 4 cm
Roundness – subrounded to subangular
Sorting: poorly sorted
Color: light reddish tan
Composition:
Matrix: mostly quartz
Clasts: red ss70%; quartzite 10%; chert 10%; volcanics 2%
Cement: n/a
General rock name: clast supported pebble cobble gravel
Secondary features: n/a
Final notes: better rounded than previous units; local fine grained section void of bigger clasts.

Unit 7:
Thickness: 81 cm
Same as unit 5
But with a slightly coarser (0.5 cm) 20 cm thick package separating the two.

Unit 8:
Thickness: 105 cm
Interbedded unit of the description to follow with material similar to unit 5
Contact: abrupt at each boundary
Extent: laterally extensive
Sedimentary structures: crude imbrication
Texture:
Grain size – Max: 4 cm Min: f. sand Average: 0.5 cm
Roundness – subrounded to subangular
Sorting: fairly poorly sorted
Color: light red
Composition:
Matrix: mostly quartz
Clasts: same as unit 3
Cement: n/a
General rock name: clast supported pebble gravel
Secondary features: n/a
Final notes: --

Unit 9:
Thickness: 120 cm
Contact: gradual
Extent: laterally extensive
Sedimentary structures: crude imbrication
Texture:
Grain size – Max: 20 cm Min: f. sand Average: 3 cm
Roundness – subrounded to subangular
Sorting: poorly sorted
Color: multi colored (yellow, black, white, red, brown)
Composition:
Matrix: mostly quartz
Clasts: red ss 30%; quartzite 40%; chert 10%
Cement: n/a
General rock name: clast supported cobble pebble gravel
Secondary features: n/a
Final notes: better: more quartzite than observed in other units in this deposit.

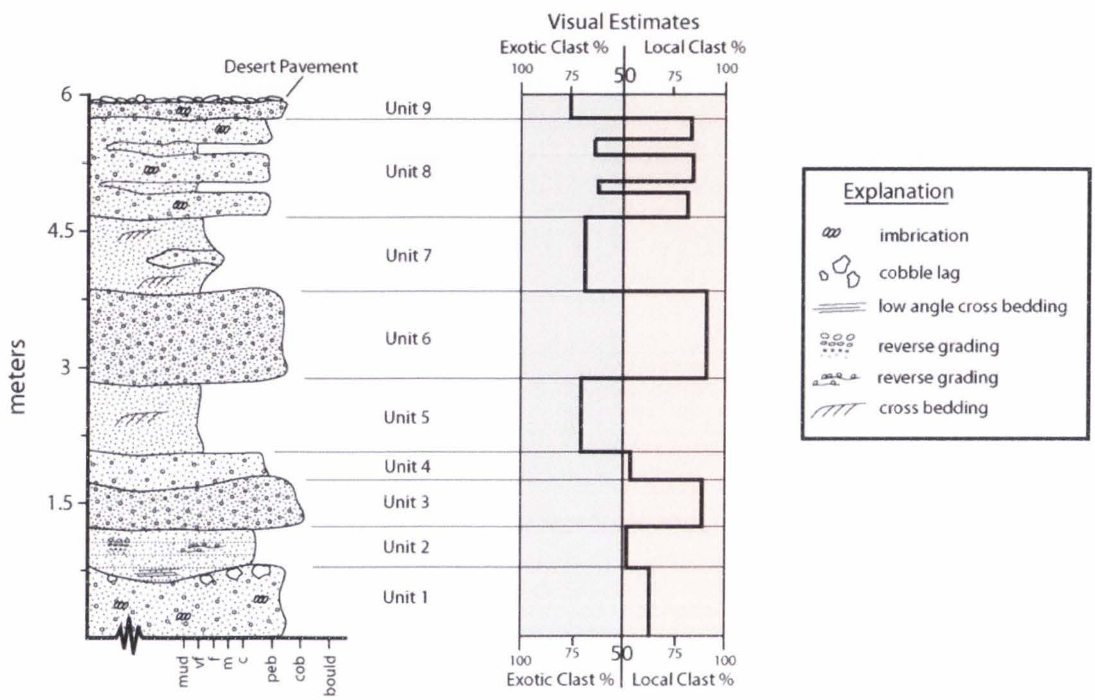

Figure C.8. Sedimentary units of the upper M4 deposit, M4-3 description. Visual proportions of exotic and local clasts were made in order to estimate the dominant source throughout deposition.

Table C.8. Sedimentary description of the P4 deposit.

Geographic location (UTM): 4081455N, 445846 E
Big P4 deposit upstream along the Paria River
Outcrop description:
Some good exposures throughout deposit, particularly where units are cemented
Sand units are present in either lenses or pockets (good for OSL samples throughout)
Total outcrop thickness ~20 m
Not sure whether this is a P3 and P4, or just a P4 with younger and older surfaces

Unit 1:
Thickness: 120 cm
Contact: abrupt and sharp of bedrock
Extent: laterally extensive
Sedimentary structures: excellent imbrication, plane beds, faint ripples
Texture:
Grain size – Max: 35 cm Min: f. sand Average: 2 cm
Roundness – rounded to subangular
Sorting: poorly sorted with pockets of well sorted sand
Color: light reddish tan
Composition:
Matrix: mostly quartz
Clasts: see clast count…
Cement: carbonate
General rock name: clast supported / matrix supported cobble pebble gravel
Secondary features: calcite cement
Final notes: large unit, extensive, well cemented, pockets of sand.

Unit 2:
Thickness: 275 cm
Contact: gradual, marked by a decrease in grain size
Extent: laterally extensive
Sedimentary structures: localized crude imbrication
Texture:
Grain size – Max: >1m Min: f. sand Average: pebbles – 1.5 cm; boulders – 15-30 cm
Roundness – subrounded to subangular
Sorting: poorly sorted
Color: tannish red, but huge variation between localized clasts
Composition:
Matrix: mostly quartz
Clasts: boulders – local lithologies; pebbles – same as unit 1
Cement: carbonate
General rock name: clast supported boulder cobble pebble gravel
Secondary features: calcite cement
Final notes: boulders come loose easily… smashed Ben's leg… scary; unit not as well exposed as unit 1.

Unit 3:
Thickness: 210 cm
Mixture of unit 1 and 2
With gradual increase in sand towards top.

Unit 4:
Thickness: 200 cm
Contact: obscured, but noted by significant increase in sand
Extent: not laterally extensive, but large pocket of sand
Sedimentary structures: small scale cross strata, few coarsening upward sequences, massive portions

Texture:

Grain size – Max: m. sand Min: f. sand Average: f. sand

Roundness – rounded to subangular

Sorting: well sorted

Color: light tannish gray

Composition:

Matrix: mostly quartz

Clasts: --

Cement: n/a

General rock name: fine sand

Secondary features: n/a

Final notes: large unit of Paria River sand, GC-05-LF-OSL3 collected from this unit; some few pebbles observed within massive matrix.

<u>Unit 5:</u>

Thickness: 155 cm

Contact: sharp, increase in grain size

Extent: laterally extensive

Sedimentary structures: good imbrication, cross bedding in sand lenses

Texture:

Grain size – Max: 23 cm Min: f. sand Average: 2-3 cm

Roundness – rounded to subangular

Sorting: poorly sorted with pockets of well sorted sand

Color: tannish light red

Composition:

Matrix: mostly quartz

Clasts: more red sandstones than unit 1

Cement: carbonate

General rock name: clast supported cobble pebble gravel

Secondary features: calcite cement

Final notes: finer at base, gets coarser towards middle, and then finer at top where sand lenses appear.

<u>Unit 6:</u>

Thickness: 295 cm

Covered slope – sand weathering unit

Same as unit 4

<u>Unit 7:</u>

Thickness: 145

Contact: fairly abrupt

Unit is rich in red sandstone cobbles (~15 cm)

Clast supported pebble cobble gravel

Crude imbrication

Pebble pockets are present (similar to other units below)

Matrix is cemented

<u>Unit 8:</u>

Thickness: 270 cm

Same as unit 5, although lacking the abundant red sandstones

Quartzites (rounded) appear to dominate and some sand pockets ore present

Not as well cemented, but still has carbonate cement

<u>Unit 9:</u>

Thickness: 170 cm

GC-05-LF-OSL2 collected from this unit

Medium scale bedding (5-10 cm) cross bedding observed in places

Planar beds also present

Fine to medium sand, moderately sorted, subrounded
Unit seems to pinch out to the west, away from the Paria River, although pockets can be seen in other units.

Unit 10
Thickness: 90 cm
Same as unit 5
Sandstone clasts not quite as large
Unit seems slightly more subangular throughout, with several local clasts present

Unit 11:
Thickness: 770 cm
Contact: abrupt, change in grain size and type
Extensive: laterally extensive, holding up highest terrace level with coarse grained exposure
Sedimentary structures: n/a
Texture:
Grain size – Max: >1 m Min: vf. sand Average: 9 cm
Roundness – subangular to angular
Sorting: very poorly sorted
Color: red sandstone
Composition:
Matrix: mostly quartz
Clasts: almost entirely red sandstone, with low amounts of other clast types
Cement: matrix hard to dislodge, compacted
General rock name: clast supported angular boulder cobble gravel
Secondary features: n/a
Final notes: deposit looks like it was a catastrophic event; side canyon or hillslope sediment; apparent almost open framework structure; boulders seem to be concentrated on top and bottom with more consistent cobbles making up the middle portion; walking up through the deposit, appears to maybe not be all one event – maybe multiple pockets that are distinctly separate.

Unit 12:
Thickness: 50 cm
Rounded fluvial gravels lay on surface, must have been above originally; some river gravel/sand lenses maybe present in the guts of unit 11, along the upper portion.

Appendix D. TOTAL-STATION SURVEY DATA

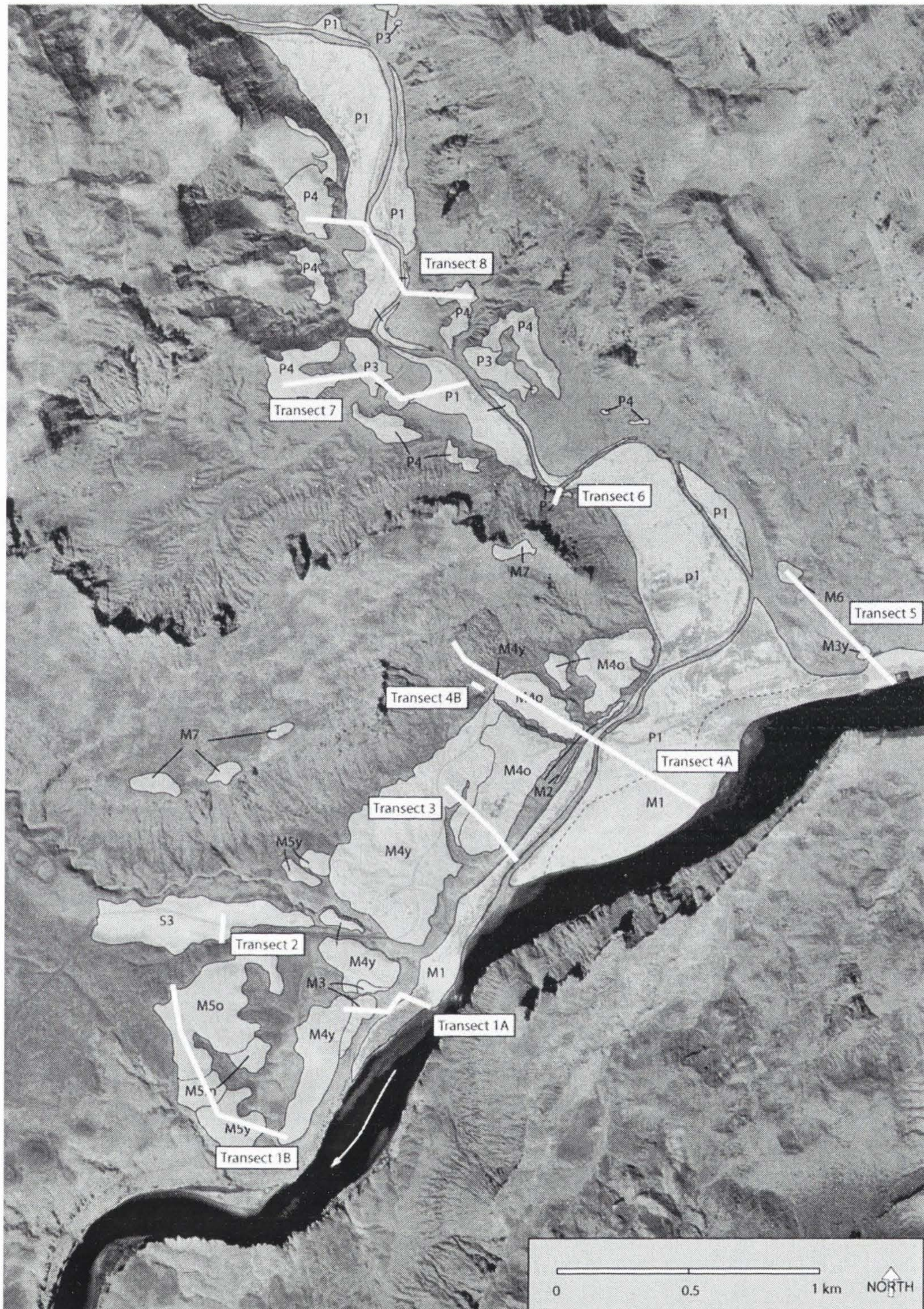

Figure D.1. Map of Quaternary deposits in the Lees Ferry area, showing approximate locations where survey transects were measured.

Table D.1. Raw survey data collected from the deposits along the Colorado and Paria rivers at Lees Ferry. Cross sections from each of nine transects were created using the raw easting, northing, and elevation survey data provided by the total station and were not projected in UTM coordinates due to the intercomparable nature of the study. Cross sections were generally measured perpendicular to the drainage axis; however, slight turns were sometimes introduced in order to capture terrace relations. In addition, two transects were started from one location and then completed after moving the total station. Multiple benchmark shots were included in order to connect the two survey lines. To correct for turns, all data were projected at right angles onto a line perpendicular to the drainage axis. The "distance along transect" column represents where data plotted along this line. In addition, the elevation of survey points within each transect was adjusted in relation to a high water datum (13,000 cfs).

Survey Transect #1 -- Location A				Southern-most Survey Transect -- Near Paria Riffle		
Instrument Height (m)	1.63					
GPS Location	N 4078920; E 446059					
Pt. Id	Easting	Northing	Elevation	Dist. Along Transect	Elevation Above River	Notes
2	252.939	18.084	-28.121	0.000	0.000	High water level (13,000 cfs)
3	230.105	21.701	-26.027	23.119	2.094	Holocene deposit
4	230.064	21.700	-26.007	23.160	2.114	Holocene deposit
5	150.015	-2.597	-21.730	106.815	6.391	Holocene deposit
6	98.688	-95.576	-21.737	213.020	6.384	Holocene deposit
7	94.966	-94.827	-21.983	216.817	6.138	Holocene deposit
8	92.458	-94.017	-21.725	219.452	6.396	Holocene deposit
9	91.883	-93.926	-20.714	220.034	7.407	Holocene deposit
10	90.330	-93.388	-20.488	221.678	7.633	Holocene deposit
11	81.748	-91.090	-20.271	230.562	7.850	Holocene deposit
12	75.335	-89.608	-19.875	237.144	8.246	Holocene deposit
13	69.228	-88.386	-19.414	243.372	8.707	Holocene deposit
14	63.261	-87.614	-18.666	249.389	9.455	End alluvium, start bedrock
15	59.505	-86.872	-17.558	253.218	10.563	Bedrock
16	56.363	-86.535	-16.102	256.378	12.019	Bedrock
17	52.922	-86.163	-15.021	259.839	13.100	Bedrock
18	48.421	-86.082	-14.161	264.341	13.960	Bedrock
19	46.209	-85.557	-13.778	266.614	14.343	Strath
20	42.527	-85.134	-12.705	270.320	15.416	M3 terrace riser
21	37.315	-85.437	-11.120	275.541	17.001	M3 terrace riser
22	33.586	-86.032	-9.817	279.317	18.304	M3 terrace riser
23	29.300	-86.776	-8.097	283.667	20.024	M3 terrace riser
24	25.337	-87.693	-6.632	287.735	21.489	M3 terrace riser
25	21.203	-89.183	-5.335	292.129	22.786	M3 terrace riser
26	17.685	-90.967	-4.416	296.074	23.705	M3 terrace riser
27	13.740	-93.742	-3.622	300.897	24.499	M3 terrace riser
28	9.621	-95.794	-3.042	305.499	25.079	M3 terrace tread
29	6.163	-98.666	-2.781	309.994	25.340	M3 terrace tread
30	1.420	-101.969	-2.637	315.774	25.484	M3 terrace tread

31	-3.409	-105.940	-2.538	322.026	25.583	M3 terrace tread
32	-9.417	-108.246	-2.307	328.461	25.814	M3 terrace tread
33	-15.437	-110.988	-1.901	335.076	26.220	M3 terrace tread
34	-19.657	-112.780	-1.450	339.661	26.671	M3 terrace tread
35	-23.638	-114.471	-0.901	343.986	27.220	M3 terrace tread
36	-27.575	-115.518	-0.305	348.060	27.816	Covered bedrock
37	-32.075	-117.831	0.625	353.120	28.746	Covered bedrock
38	-35.396	-118.000	1.114	356.445	29.235	Covered bedrock
39	-40.662	-118.763	2.696	361.766	30.817	Strath
40	-55.575	-95.835	3.213	n/a	29.240	M4 strath; around corner in gully
41	-42.756	-119.190	3.626	363.903	31.747	M4 terrace riser
42	-45.843	-119.475	4.927	367.003	33.048	M4 terrace riser
43	-49.030	-120.326	6.012	370.302	34.133	M4 terrace riser
44	-52.541	-121.702	6.633	374.073	34.754	M4 terrace riser
45	-56.529	-122.927	7.258	378.245	35.379	M4 terrace riser
46	-61.419	-124.861	7.866	383.503	35.987	M4 tread below soil pit
47	-64.905	-126.689	8.134	387.440	36.255	M4 terrace tread heading sw
48	-68.737	-133.194	8.482	394.989	36.603	M4 terrace tread heading sw
49	-72.416	-139.252	8.712	402.077	36.833	M4 terrace tread heading sw
50	-76.401	-148.971	9.072	412.581	37.193	M4 terrace tread heading sw
51	-80.833	-162.410	9.533	426.732	37.654	M4 terrace tread heading sw
52	-86.330	-175.065	10.089	440.529	38.210	M4 terrace tread heading sw
53	-91.100	-188.488	10.671	454.775	38.792	M4 terrace tread heading sw
54	-95.729	-197.150	10.986	464.596	39.107	M4 terrace tread heading sw
55	-105.021	-210.130	11.443	480.559	39.564	M4 terrace tread heading sw
56	-118.244	-227.546	12.044	502.426	40.165	M4 terrace tread heading sw
57	-130.932	-239.628	12.545	519.946	40.666	M4 terrace tread heading sw
58	-145.382	-250.225	13.126	537.866	41.247	M4 terrace tread heading sw
59	-155.997	-256.820	13.588	550.363	41.709	M4 terrace tread heading sw
60	-179.000	-268.025	14.740	575.950	42.861	M4 terrace tread heading sw
61	-184.151	-268.897	14.910	581.174	43.031	Lateral alluvial contact
62	-197.367	-267.882	15.797	594.429	43.918	Bedrock
63	-201.201	-268.671	17.158	598.343	45.279	Bedrock
64	-207.425	-273.703	18.869	606.347	46.990	Bedrock
65	-214.840	-279.723	19.915	615.898	48.036	Bedrock
66	-220.921	-284.669	20.751	623.736	48.872	Bedrock
67	-229.167	-290.211	21.652	633.672	49.773	Bedrock
68	-240.785	-296.664	24.156	646.961	52.277	Bedrock
69	-247.737	-299.324	26.316	654.405	54.437	Bedrock
70	-256.908	-302.545	28.337	664.125	56.458	Bedrock
71	-265.874	-305.963	30.575	673.721	58.696	Bedrock
72	-269.299	-308.713	31.393	678.113	59.514	Bedrock
73	-275.116	-310.701	32.366	684.260	60.487	Strath
74	-279.704	-312.792	33.330	689.302	61.451	M6 terrace riser
75	-286.478	-315.912	34.673	696.760	62.794	M6 terrace riser
76	-294.007	-319.703	35.425	705.190	63.546	M6 terrace riser
77	-299.714	-323.037	35.922	711.799	64.043	M6 terrace riser
78	-308.437	-326.643	36.722	721.238	64.843	M6 terrace riser
79	-316.352	-329.136	37.292	729.537	65.413	M6y terrace tread

80	-323.477	-328.860	37.522	736.667	65.643	M6y terrace tread
81	-331.668	-330.678	37.826	745.057	65.947	M6y terrace tread
82	-340.065	-329.065	38.085	753.608	66.206	M6y terrace tread
83	-349.309	-326.062	38.010	763.327	66.131	M6y terrace tread
84	-359.509	-322.955	37.856	773.990	65.977	M6y terrace tread
85	-365.237	-320.351	37.981	780.282	66.102	M6y terrace tread
86	-372.344	-315.767	38.579	788.739	66.700	M6y terrace tread (3 R.H.)
87	-378.618	-311.662	39.191	796.237	67.312	M6y terrace tread (3 R.H.)
88	-384.219	-307.776	39.972	803.054	68.093	M6y terrace tread (3 R.H.)
89	-390.052	-303.177	40.889	810.482	69.010	M6y terrace tread (3 R.H.)
90	-399.836	-297.057	42.202	822.022	70.323	M6y terrace tread (3 R.H.)
91	-408.467	-293.630	42.939	831.309	71.060	M6o terrace tread (3 R.H.)
92	-420.034	-289.816	43.739	843.488	71.860	M6o terrace tread (3 R.H.)
93	-431.092	-285.919	44.391	855.213	72.512	M6o terrace tread (3 R.H.)
94	-439.230	-280.875	44.779	864.787	72.900	M6o terrace tread (3 R.H.)
95	-449.919	-274.821	45.292	877.072	73.413	M6o terrace tread (3 R.H.)
96	-456.359	-264.016	45.797	889.650	73.918	M6o terrace tread (3 R.H.)
97	-462.278	-253.408	46.288	901.798	74.409	M6o terrace tread (3 R.H.)
100	22.230	-52.498	-12.345	n/a	13.682	M3 strath elevation
101	-12.907	-49.571	-8.893	n/a	17.134	OSL 10 elevation
102	-19.568	-41.677	-5.913	n/a	20.114	OSL 11 elevation

Survey Transect #1 -- Location B			Southern-most Survey Transect -- Near Paria Riffle			
Instrument Height (m)	1.65					
GPS Location	N 4078537; E 445852					
Pt. Id	Easting	Northing	Elevation	Dist. Along Transect	Elevation Above River	Notes
105	-68.535	-555.545	4.590	0.000	30.617	M4 strath
106	-72.981	-554.246	5.739	1.299	31.766	M4 terrace riser
107	-77.57	-553.209	7.123	2.336	33.150	M4 terrace riser
108	-82.057	-551.637	8.779	3.908	34.806	M4 terrace riser
109	-85.897	-551.394	10.188	4.151	36.215	M4 terrace riser
110	-89.165	-550.842	11.395	4.703	37.422	M4 terrace riser
111	-92.35	-549.734	12.569	5.811	38.596	M4 terrace riser
112	-95.183	-548.366	13.352	7.179	39.379	M4 terrace riser
113	-96.566	-548.079	13.546	7.466	39.573	M4 terrace tread
114	-98.335	-547.778	13.669	7.767	39.696	M4 terrace tread
115	-100.026	-547.640	13.659	7.905	39.686	M4 terrace tread
116	-101.854	-547.300	13.572	8.245	39.599	M4 terrace tread
117	-211.608	-648.090	14.334	0.000	40.361	M5 strath (after traverse downstream)
118	-217.184	-646.973	15.682	1.117	41.709	M5 terrace riser
119	-222.885	-645.580	17.074	2.510	43.101	M5 terrace riser
120	-228.819	-643.801	18.595	4.289	44.622	M5 terrace riser
121	-233.178	-642.691	19.714	5.399	45.741	M5 terrace riser
122	-238.278	-641.275	21.003	6.815	47.030	M5 terrace riser
123	-243.55	-639.354	22.392	8.736	48.419	M5 terrace riser
124	-248.038	-637.778	23.569	10.312	49.596	M5 terrace riser

125	-253.556	-635.590	24.969	12.500	50.996	M5 terrace riser
126	-258.356	-634.298	26.049	13.792	52.076	M5 terrace riser
127	-262.908	-632.145	27.006	15.945	53.033	M5 terrace riser
128	-269.261	-629.069	28.052	19.021	54.079	M5 terrace riser
129	-274.821	-627.029	28.847	21.061	54.874	M5 terrace riser
130	-279.328	-625.493	29.493	22.597	55.520	M5 terrace riser
131	-285.439	-623.116	30.164	24.974	56.191	M5 terrace riser
132	-290.536	-620.043	30.807	28.047	56.834	M5 terrace riser
133	-296.132	-615.412	31.711	32.678	57.738	M5 terrace riser
134	-300.864	-610.441	32.153	37.649	58.180	M5 terrace tread
135	-305.582	-604.291	32.500	43.799	58.527	M5 terrace tread
136	-313.263	-595.403	32.899	52.687	58.926	M5 terrace tread
137	-319.413	-587.955	33.171	60.135	59.198	M5 terrace tread
138	-326.966	-580.276	33.405	67.814	59.432	M5 terrace tread
139	-334.94	-571.393	33.707	76.697	59.734	M5 terrace tread
140	-344.8	-559.444	34.241	88.646	60.268	M5 terrace tread
141	-355.26	-550.652	34.727	97.438	60.754	M5 terrace tread
142	-369.378	-540.460	35.354	107.630	61.381	M5 terrace tread
143	-380.389	-534.137	36.173	113.953	62.200	M5 terrace tread
144	-392.327	-527.488	36.875	120.602	62.902	M5 terrace tread
145	-403.048	-521.207	37.513	126.883	63.540	M5 terrace tread (2 R.H.)
146	-409.762	-517.739	38.140	130.351	64.167	M5 terrace tread (2 R.H.)
147	-417.219	-514.505	39.101	133.585	65.128	M6 terrace riser obscrd (2rh)
148	-424.809	-511.957	40.039	136.133	66.066	M6 terrace riser obscrd (2rh)
149	-430.633	-510.217	40.854	137.873	66.881	M6 terrace riser obscrd (2rh)
150	-436.958	-508.573	41.765	139.517	67.792	M6 terrace riser obscrd (2rh)
151	-444.135	-505.384	42.693	142.706	68.720	M6 terrace riser obscrd (2rh)
152	-449.592	-503.220	43.291	144.870	69.318	M6 terrace riser obscrd (2rh)
153	-453.883	-501.466	43.651	146.624	69.678	M6 terrace riser obscrd (2rh)
154	-458.983	-500.620	44.034	147.470	70.061	M6 terrace riser obscrd (2rh)
155	-462.508	-499.066	44.281	149.024	70.308	M6y terrace tread (2 R.H.)
156	-465.987	-497.719	44.451	150.371	70.478	M6y terrace tread (2 R.H.)
157	-469.43	-496.126	44.572	151.964	70.599	M6y terrace tread (2 R.H.)
158	-472.604	-494.815	44.554	153.275	70.581	M6y terrace tread (2 R.H.)
159	-475.806	-492.815	44.554	155.275	70.581	M6y terrace tread (2 R.H.)
164	-472.144	-230.404	46.445	417.686	72.472	Resume M6 from Survey 1A
165	-475.857	-226.206	46.725	421.884	72.752	Resume M6 from Survey 1A
166	-481.156	-220.999	47.428	427.091	73.455	Resume M6 from Survey 1A
167	-485.91	-217.358	47.780	430.732	73.807	Resume M6 from Survey 1A
168	-491.557	-213.502	48.331	434.588	74.358	Resume M6 from Survey 1A
169	-498.055	-210.158	48.895	437.932	74.922	Resume M6 from Survey 1A
170	-505.044	-206.380	49.656	441.710	75.683	Resume M6 from Survey 1A
171	-511.732	-202.423	50.561	445.667	76.588	Resume M6 from Survey 1A
172	-518.619	-198.637	51.048	449.453	77.075	Resume M6 from Survey 1A
173	-525.065	-194.902	51.447	453.188	77.474	Resume M6 from Survey 1A
174	-531.771	-191.072	51.784	457.018	77.811	Resume M6 from Survey 1A
175	-539.173	-187.604	52.187	460.486	78.214	Resume M6 from Survey 1A
176	-544.509	-184.229	52.404	463.861	78.431	Resume M6 from Survey 1A
177	-549.551	-182.195	52.534	465.895	78.561	Resume M6 from Survey 1A

178	-554.072	-180.833	52.512	467.257	78.539	Resume M6 from Survey 1A
179	-557.595	-179.593	52.191	468.497	78.218	Resume M6 from Survey 1A
180	-560.851	-177.989	51.166	470.101	77.193	Resume M6 from Survey 1A
181	-564.229	-175.775	49.778	472.315	75.805	Resume M6 from Survey 1A
182	-567.047	-173.617	48.487	474.473	74.514	Resume M6 from Survey 1A
183	-570.255	-170.547	46.306	477.543	72.333	Resume M6 from Survey 1A
184	-572.451	-168.749	44.790	479.341	70.817	Resume M6 from Survey 1A
185	-576.702	-163.912	41.851	484.178	67.878	Resume M6 from Survey 1A
186	-621.368	-55.246	21.905	592.844	47.932	Backside M6 bedrock strath

Survey Transect #2	** No backsight due to small survey distance**					Survey Transect through Kaufman spring deposit
Inst. Height (m)	1.58					
GPS Location	N 4078998; E 445534					
				Dist. Along	Elevation	
Pt. Id	Easting	Northing	Elevation	Transect	Above River	Notes
192	-595.415	-87.196	22.268	0.000	48.295	Variable paludal contact
194	-549.545	-66.142	23.504	50.471	49.531	Moenkopi consistent strath
195	-551.168	-60.452	24.087	56.388	50.114	Spring deposit surface
196	-551.605	-55.682	25.095	61.178	51.122	Spring deposit surface
197	-552.272	-51.901	25.583	65.017	51.610	Spring deposit surface
198	-557.535	-27.360	25.597	90.116	51.624	Spring deposit surface
199	-558.713	-25.809	26.637	92.064	52.664	Spring deposit surface
200	-560.775	-24.169	27.448	94.699	53.475	Spring deposit surface
201	-565.388	-15.575	28.672	104.452	54.699	Spring deposit surface
202	-568.844	-12.207	29.843	109.278	55.870	Spring deposit surface
203	-574.611	-8.793	30.907	115.980	56.934	Spring deposit surface
204	-578.760	-6.765	31.738	120.598	57.765	Spring deposit surface
205	-587.303	2.830	32.394	133.445	58.421	Spring deposit surface
206	-589.894	7.812	33.228	139.061	59.255	Spring deposit surface
207	-612.602	-4.942	34.959	165.105	60.986	Elevation of highest point

Survey Transect 1 Adjustments

98	-179.361	-399.621	18.510	Benchmark 1 (1 R.H.)
104	-92.212	109.343	6.359	Benchmark #1
Adjustment 1	**-87.149**	**-508.964**	**12.151**	
160	-382.251	11.142	32.753	Benchmark #2 (back to 1 R.H.)
160	*-469.400*	*-497.822*	*44.904*	*Benchmark #2 Corrected*
163	79.666	-332.683	-5.487	Benchmark #2
Adjustment 2	**-549.066**	**-165.139**	**50.391**	
190	-98.626	36.365	-25.077	Emergency benchmark for next survey -- compare with shot 191
190	*-647.692*	*-128.774*	*25.314*	*Shot 190 Corrected*
191	-107.465	30.645	-24.411	Emergency Benchmark -- Same as shot 187
Adjustment 3	**-540.227**	**-159.419**	**49.725**	

Survey Transect 1 Errors

Survey 1 Location A	Easting	Northing	Elevation	
1	-18.252	4.910	1.737	Backsight #1
99	-18.251	4.913	1.737	Backsight #1
Survey Error	**0.001**	**0.003**	**0.000**	
Survey 1 Location B				
103	-1.459	18.524	-0.090	Backsight #2
161	-1.458	18.524	-0.090	Backsight #2
Survey Error	**0.001**	**0.000**	**0.000**	

Survey Transect #3 — Southern-Middle Survey Transect -- Housing Terrace and M4y Surafaces

Ins. Height (m): 1.73

GPS Location: N 4079229; E 446331

Pt. Id	Easting	Northing	Elevation	Dist. Along Transect	Elevation Above River	Notes
210	117.256	-31.849	-13.508	0.000	0.000	High water level (13,000 cfs)
211	114.572	-31.953	-12.942	2.686	0.566	Holocene alluvium
212	111.330	-31.028	-12.619	6.057	0.889	Holocene alluvium
213	105.367	-29.431	-12.612	12.231	0.896	Holocene alluvium
214	102.167	-26.847	-11.917	16.344	1.591	Holocene alluvium
215	98.754	-25.310	-12.366	20.087	1.142	Holocene alluvium
216	94.150	-24.131	-12.314	24.839	1.194	Holocene alluvium
217	81.176	-17.711	-10.906	39.315	2.602	Holocene alluvium
218	78.527	-15.828	-10.868	42.565	2.640	Holocene alluvium
219	77.016	-15.320	-10.176	44.159	3.332	Holocene alluvium
220	75.055	-14.608	-9.365	46.245	4.143	Holocene alluvium
221	72.726	-11.551	-8.540	50.088	4.968	Holocene alluvium
222	69.972	-8.782	-8.197	53.994	5.311	Holocene alluvium
223	67.372	-4.394	-8.114	59.094	5.394	Holocene alluvium
224	63.791	0.305	-7.923	65.002	5.585	Holocene alluvium
225	60.709	4.073	-8.034	69.870	5.474	Holocene alluvium
226	55.565	7.245	-7.862	75.913	5.646	Holocene alluvium (next shot upstream ~100 m)
227	90.796	155.656	5.699	228.449	19.207	Bedrock (on roadside cliff)
228	90.205	160.981	8.393	233.806	21.901	Bedrock (on roadside cliff)
229	91.700	164.328	9.465	237.472	22.973	Bedrock (on roadside cliff)
230	92.349	168.856	10.579	242.046	24.087	M4 strath
231	90.843	173.002	11.416	246.458	24.924	M4 terrace riser
232	89.646	178.405	13.090	251.992	26.598	M4 terrace riser
233	88.590	182.953	14.571	256.661	28.079	M4 terrace riser
234	87.683	187.003	15.664	260.811	29.172	M4 terrace riser
235	86.720	191.350	16.837	265.263	30.345	M4 terrace riser
236	85.603	195.483	17.851	269.545	31.359	M4 terrace riser
237	83.828	199.540	19.292	273.973	32.800	M4 terrace riser
238	82.774	203.130	20.766	277.714	34.274	M4 terrace riser

239	81.339	206.500	22.508	281.377	36.016	M4 terrace riser
240	79.633	210.348	24.354	285.586	37.862	M4 terrace riser
241	79.568	210.339	24.354	285.652	37.862	M4 riser (suspiciously bad shot)
242	78.384	214.748	26.001	290.217	39.509	M4 terrace riser
243	76.178	220.533	27.703	296.409	41.211	M4 terrace riser
244	75.456	225.369	28.949	301.298	42.457	M4 terrace riser
245	74.140	228.792	30.015	304.965	43.523	M4 terrace riser
246	74.417	235.055	30.788	311.235	44.296	M4 terrace riser
247	74.233	243.576	31.575	319.757	45.083	M4 terrace riser
248	74.741	252.721	31.987	328.917	45.495	M4o tread (housing terrace)
249	74.533	260.175	32.329	336.373	45.837	M4o (housing terrace) (2 R.H.)
250	70.173	261.972	32.419	341.089	45.927	M4o (housing terrace) (2 R.H.)
251	60.352	265.766	32.596	351.618	46.104	M4o (housing terrace) (2 R.H.)
252	50.835	269.436	32.703	361.818	46.211	M4o (housing terrace) (2 R.H.)
253	20.607	278.717	33.408	393.438	46.916	M4o (housing terrace) (3 R.H.)
254	8.108	280.728	33.033	406.098	46.541	M4o (housing terrace) (3 R.H.)
255	8.046	280.633	33.035	406.212	46.543	M4o (housing terrace) (3 R.H.)
256	-22.721	271.812	29.409	438.218	42.917	M4y tread (1 R.H.)
257	-24.445	272.627	29.930	440.125	43.438	M4y tread (1 R.H.)
258	-25.957	273.284	30.159	441.774	43.667	M4y tread (1 R.H.)
259	-27.504	273.961	30.091	443.462	43.599	M4y tread (1 R.H.)
260	-29.640	275.100	29.625	445.883	43.133	M4y tread (1 R.H.)
261	-94.326	317.629	29.725	523.297	43.233	M4y tread (1 R.H.)
262	-96.945	319.270	30.397	526.388	43.905	M4y tread (1 R.H.)
263	-99.175	321.350	30.746	529.438	44.254	M4y tread (1 R.H.)
264	-101.466	323.440	30.985	532.539	44.493	M4y tread (1 R.H.)
265	-104.332	325.480	31.101	536.057	44.609	M4y tread (1 R.H.)
266	-107.672	327.300	31.183	539.860	44.691	M4y tread (1 R.H.)
267	-111.567	327.305	31.162	543.755	44.670	M4y tread (1 R.H.)
268	-117.200	326.712	31.033	549.419	44.541	M4y tread (1 R.H.)
269	-120.635	326.318	30.678	552.877	44.186	M4y tread (1 R.H.)
270	-122.217	325.702	29.997	554.575	43.505	M4y tread (1 R.H.)
275	-112.745	127.213	21.376	n/a	33.995	OSL 13 elevation -- middle of M4
276	-157.405	65.892	19.762	n/a	32.381	OSL 12 elevation -- lower M4
277	-191.847	83.762	28.177	n/a	40.796	OSL 14 elevation -- upper-mid M4

Survey Transect #4 -- Location A — Northern-Middle Survey Transect -- Near Stop Sign

Inst. Height (m)	1.77					
GPS Location	N 4079712; E 446639					
				Dist. Along	Elevation	
Pt. Id	Easting	Northing	Elevation	Transect	Above River	Notes
280	240.066	221.256	-29.922	n/a	8.672	Bedrock (3 R.H.)
281	238.021	221.625	-29.253	n/a	9.341	Bedrock (3 R.H.)
282	237.783	221.437	-26.507	n/a	12.087	Bedrock strath of M1/flood deposit
283	236.647	224.696	-24.993	n/a	13.601	Top of M1/flood deposit
284	234.294	225.285	-24.722	n/a	13.872	Top of M1/flood deposit
285	231.756	225.740	-24.550	n/a	14.044	Top of M1/flood deposit
286	230.606	226.183	-24.669	n/a	13.925	Top of M1/flood deposit
287	167.972	146.879	-27.928	n/a	10.666	Elevation of OSL 8
288	143.567	170.710	-20.333	n/a	18.261	Basal bdrck contact below OSL 9

289	144.466	174.887	-18.402	n/a	20.192	OSL 9 elevation in M4 deposit
290	380.994	-257.363	-38.594	0.000	0.000	High water level (13,000 cfs)
291	368.992	-246.864	-37.011	15.946	1.583	Modern alluvium
292	358.410	-232.869	-36.156	33.491	2.438	Modern alluvium
293	351.043	-222.552	-36.096	46.169	2.498	Modern alluvium
294	344.365	-211.855	-35.605	58.779	2.989	Modern alluvium
295	342.222	-208.402	-34.991	62.843	3.603	Modern alluvium
296	338.870	-202.565	-34.973	69.574	3.621	Modern alluvium
297	326.417	-182.200	-35.727	93.445	2.867	Modern alluvium
298	320.959	-170.983	-35.854	105.919	2.740	Modern alluvium
299	309.582	-152.712	-36.278	127.443	2.316	Modern alluvium
300	291.719	-121.150	-36.337	163.709	2.257	Modern alluvium
301	277.606	-80.772	-36.498	206.482	2.096	Modern alluvium
302	261.094	-36.308	-36.604	253.913	1.990	Modern alluvium
303	252.744	-17.117	-36.552	274.842	2.042	Modern alluvium
304	251.755	-14.658	-35.569	277.493	3.025	Modern alluvium
305	250.666	-11.662	-34.309	280.680	4.285	Modern alluvium
306	249.561	-9.950	-33.786	282.718	4.808	Modern alluvium
307	247.501	-6.100	-33.672	287.085	4.922	Modern alluvium
308	244.386	-0.449	-33.273	293.537	5.321	Modern alluvium
309	240.317	8.271	-33.102	303.160	5.492	Modern alluvium
310	235.105	23.379	-33.463	319.142	5.131	Modern alluvium
311	218.381	34.862	-33.394	339.428	5.200	Modern alluvium
312	203.138	47.187	-33.894	359.031	4.700	Modern alluvium
313	188.142	61.915	-33.592	380.050	5.002	Modern alluvium
314	126.843	92.338	-29.422	448.483	9.172	Covered bedrock
315	122.180	93.707	-27.987	453.343	10.607	Covered bedrock
316	118.233	95.972	-26.527	457.894	12.067	Covered bedrock
317	113.925	98.684	-24.509	462.984	14.085	Covered bedrock
318	110.396	101.208	-22.775	467.323	15.819	M4 bedrcok strath
319	107.988	102.010	-21.677	469.861	16.917	M4 bedrcok riser
320	102.695	102.790	-19.991	475.211	18.603	M4 terrace riser
321	97.084	102.826	-17.913	480.822	20.681	M4 terrace riser
322	90.901	102.200	-15.652	487.037	22.942	M4 terrace riser
323	82.077	98.779	-13.133	496.501	25.461	M4 terrace riser
324	76.838	98.642	-11.795	501.741	26.799	M4 terrace riser
325	70.495	98.980	-9.617	508.093	28.977	M4 terrace riser
326	64.826	100.806	-7.620	514.049	30.974	M4 terrace riser
327	59.206	101.625	-6.718	519.729	31.876	M4 terrace riser
328	54.053	103.456	-4.732	525.197	33.862	M4 terrace riser
329	54.117	103.452	-4.700	525.261	33.894	M4 terrace riser
330	50.618	106.119	-3.782	529.661	34.812	M4 terrace riser
331	45.521	109.079	-2.970	535.555	35.624	M4 terrace riser
332	40.907	112.423	-1.541	541.253	37.053	M4 terrace riser
333	35.674	115.793	-0.596	547.478	37.998	M4 terrace riser
334	35.576	115.781	-0.612	547.576	37.982	M4 terrace riser
335	32.771	118.281	0.736	551.334	39.330	M4 terrace riser
336	29.217	121.684	2.480	556.254	41.074	M4 terrace riser
337	25.302	124.014	4.276	560.810	42.870	M4 terrace riser
338	21.253	125.036	6.076	564.986	44.670	M4 terrace riser
339	18.624	125.668	7.238	567.690	45.832	M4 terrace riser
340	17.301	126.221	7.519	569.124	46.113	M4o terrace tread
341	13.430	129.488	7.591	574.189	46.185	M4o terrace tread
342	3.761	133.537	7.623	584.672	46.217	M4o terrace tread
343	-6.281	137.465	7.596	595.455	46.190	M4o terrace tread
344	-17.640	141.180	7.287	607.406	45.881	M4o terrace tread

345	-33.114	145.883	7.220	623.579	45.814	M4o terrace tread
346	-51.876	148.785	7.297	642.564	45.891	M4o terrace tread
347	-68.964	152.278	7.270	660.005	45.864	M4o terrace tread
348	-83.329	155.869	7.355	674.812	45.949	M4o terrace tread
349	-97.095	160.240	7.163	689.256	45.757	M4o terrace tread
350	-111.482	165.427	7.115	704.549	45.709	M4o terrace tread
351	-161.209	176.278	6.545	755.446	45.139	M4o terrace tread
352	-161.273	176.254	6.454	755.515	45.048	M4o terrace tread
353	-204.772	211.405	4.320	n/a	42.914	OSL 1 elevation
354	-205.300	211.775	5.181	812.084	43.775	M4y terrace tread ??
355	-206.947	212.328	5.412	813.822	44.006	M4y terrace tread ??
356	-208.872	213.350	5.577	816.001	44.171	Extent of M4 --bdrck contact
357	-213.967	214.550	5.763	821.235	44.357	Bedrock slope -- walking up ridge
358	-221.082	215.988	6.569	828.494	45.163	Bedrock slope -- walking up ridge
359	-229.372	217.598	6.985	836.939	45.579	Bedrock slope -- walking up ridge
360	-238.831	219.337	7.375	846.557	45.969	Bedrock slope -- walking up ridge
361	-246.716	221.473	7.674	854.726	46.268	Bedrock slope -- walking up ridge
362	-255.688	223.548	7.998	863.935	46.592	Bedrock slope -- walking up ridge
363	-266.895	228.181	8.233	876.062	46.827	Bedrock slope -- walking up ridge
364	-271.860	228.313	9.369	881.028	47.963	Bedrock slope -- walking up ridge
365	-274.598	228.864	9.921	883.821	48.515	Bedrock slope -- walking up ridge
366	-279.646	233.212	10.412	890.484	49.006	Bedrock slope -- walking up ridge
367	-281.869	235.971	11.087	894.027	49.681	Base of bedrock boulder
368	-284.414	242.489	12.643	901.024	51.237	Hillslope profile
369	-285.564	244.295	13.588	903.165	52.182	Base of bedrock boulder
370	-287.383	246.704	14.658	906.184	53.252	Hillslope profile
371	-292.642	247.650	15.899	911.527	54.493	Base of bedrock boulder
372	-295.397	250.329	18.031	915.370	56.625	Hillslope profile
373	-297.660	251.337	19.389	917.847	57.983	Hillslope profile
374	-299.114	251.600	20.033	919.325	58.627	Base of bedrock boulder
375	-299.842	252.215	20.029	920.278	58.623	Hillslope profile
376	-301.541	254.061	19.569	922.787	58.163	Hillslope profile
377	-303.569	255.908	19.212	925.530	57.806	Hillslope profile
378	-306.442	258.331	19.512	929.288	58.106	Hillslope profile
379	-309.646	260.590	19.822	933.208	58.416	Hillslope profile
380	-312.585	262.530	20.544	936.730	59.138	Hillslope profile
381	-320.648	260.778	20.276	944.981	58.870	Base of bedrock boulder in gully
382	-321.563	262.940	21.582	947.329	60.176	Base of bedrock boulder in gully
383	-321.333	266.984	22.505	951.379	61.099	Base of bedrock boulder in gully
384	-320.587	270.756	23.729	955.224	62.323	Hillslope profile
385	-321.247	273.175	25.034	957.732	63.628	Hillslope profile
386	-322.067	274.801	25.872	959.553	64.466	Hillslope profile
387	-339.524	269.248	27.692	977.872	66.286	Base of boulder -- modern hillslope
388	-341.265	271.242	29.255	980.519	67.849	Base of boulder -- modern hillslope
389	-342.878	272.410	30.597	982.510	69.191	Base of boulder -- modern hillslope
390	-344.271	274.055	32.055	984.666	70.649	Modern hillslope
391	-347.376	275.944	33.815	988.300	72.409	Modern hillslope
392	-349.908	277.880	34.567	991.488	73.161	Modern hillslope
393	-351.740	279.861	35.757	994.186	74.351	Modern hillslope
394	-353.564	282.703	37.401	997.563	75.995	Modern hillslope
395	-356.280	285.917	39.757	1001.771	78.351	Modern hillslope
396	-357.402	289.155	41.711	1005.198	80.305	Bedrock at base of boulder
397	-360.051	291.641	42.973	1008.830	81.567	Bedrock at base of boulder
398	-360.422	292.649	44.107	1009.905	82.701	Modern hillslope
399	-362.234	295.746	46.743	1013.493	85.337	Modern hillslope
400	-364.236	300.299	49.548	1018.466	88.142	Modern hillslope

401	-365.628	302.544	51.689	1021.108	90.283	Modern hillslope
402	-367.757	305.440	54.446	1024.702	93.040	Modern hillslope
403	-369.627	309.164	57.195	1028.869	95.789	Modern hillslope
404	-372.290	312.199	60.051	1032.907	98.645	Modern hillslope
405	-374.845	315.800	63.294	1037.322	101.888	Modern hillslope
406	-377.089	319.133	66.444	1041.340	105.038	Modern hillslope
407	-379.345	322.408	69.368	1045.317	107.962	Modern hillslope
408	-380.137	323.473	70.329	1046.645	108.923	Modern hillslope
409	-380.268	324.627	71.604	1047.806	110.198	Modern hillslope
410	-381.007	327.202	73.862	1050.485	112.456	Modern hillslope
411	-382.131	329.184	75.625	1052.763	114.219	Modern hillslope
412	-382.118	329.188	75.900	1052.777	114.494	Cliff (no rod)
413	-382.098	329.048	77.006	1052.918	115.600	Cliff (no rod)

Survey Transect #4 -- Location B			Northern-Mid Survey Transect -- Near Stop Sign (cont…) / Hillslope Profile			
Inst. Height (m)		1.53				
GPS Location	N 4079950; E 446513					
Pt. Id	Easting	Northing	Elevation	Dist. Along Transect	Elevation Above River	Notes
417	-320.669	264.466	0.774	0.000	39.368	Modrn hllslp beneath boulders
418	-317.330	263.270	2.142	3.547	40.736	Modrn hllslp beneath boulders
419	-315.105	263.252	3.044	5.772	41.638	Modrn hllslp beneath boulders
420	-311.820	264.799	3.132	9.403	41.726	Modrn hllslp beneath boulders
421	-309.362	265.616	3.933	11.993	42.527	Modrn hllslp beneath boulders
422	-307.296	266.419	5.115	14.210	43.709	Modrn hllslp beneath boulders
423	-305.538	267.251	5.951	16.155	44.545	Modrn hllslp beneath boulders
424	-301.355	268.521	6.191	20.526	44.785	Modrn hllslp beneath boulders
425	-297.890	269.472	7.018	24.119	45.612	Modrn hllslp beneath boulders
426	-295.093	270.589	7.707	27.131	46.301	Modrn hllslp beneath boulders
427	-291.356	271.755	8.231	31.046	46.825	Modrn hllslp beneath boulders
428	-287.023	273.493	8.889	35.714	47.483	Modrn hllslp beneath boulders
429	-281.611	274.657	9.311	41.250	47.905	Modrn hllslp beneath boulders
430	-276.927	275.786	9.943	46.068	48.537	Modrn hllslp beneath boulders
431	-273.108	276.623	10.906	49.978	49.500	Modrn hllslp beneath boulders
432	-270.149	277.563	11.955	53.083	50.549	Base of large boulder
433	-314.395	278.902	2.397		40.991	Modrn hllslp below balanced rock
434	-314.148	279.456	3.813		42.407	Paleo-hillslope balanced rock (no Rod)
435	-318.705	269.701	3.720		42.314	Paleo-hillslope, monster boulder (no Rod)
436	-319.199	267.579	4.279		42.873	Paleo-hillslope, monster boulder (no Rod)
437	-320.663	264.677	4.560		43.154	Paleo-hillslope, monster boulder (no Rod)
438	-319.454	263.002	4.843		43.437	Paleo-hillslope, monster boulder (no Rod)
439	-318.243	262.981	5.110		43.704	Paleo-hillslope, monster boulder (no Rod)
440	-317.464	263.201	5.502		44.096	Paleo-hillslope, monster boulder (no Rod)
441	-308.782	267.329	7.089		45.683	Paleo-hillslope, monster boulder (no Rod)
442	-307.831	267.651	7.716		46.310	Paleo-hillslope, monster boulder (no Rod)
443	-306.841	267.715	8.206		46.800	P.H. Monster boulder (no Rod)
444	-343.735	234.751	4.936		43.530	Top elevation -- boulder in roadcut (1 R.H.)

445	-347.545	236.297	-0.280		38.314	Bottom elevation of boulder; underlying alluvium

Survey Transect 4 Adjustment

415	-274.758	228.681	10.146	Benchmark #5
416	112.007	20.947	10.572	Benchmark #5
Adjustment	**-386.765**	**207.734**	**-0.426**	

SurveyTransect 4Error

279	-18.589	-14.612	4.079	Backsight #6
414	-18.684	-14.537	4.079	Backsight #6 (wind blew it over, best guess as to where is was)
Survey Error	**-0.095**	**-0.075**	**0.000**	

Survey Transect #5 — Northernmost Survey Transect -- Near Lees Ferry Boat Ramp

Inst. Height (m): 1.74

GPS Location: N 4080072; E 447747

Pt. Id	Easting	Northing	Elevation	Dist. Along Transect	Elevation Above River	Notes
447	93.123	-103.564	-6.707	0.000	0.000	High water level (13,000 cfs)
448	-24.384	-37.966	-0.509	134.577	6.198	Modern stream-bed; strath obscured
449	-26.414	-38.320	1.010	136.638	7.717	M2 terrace riser
450	-30.716	-37.063	2.279	141.120	8.986	M2 terrace riser
451	-34.941	-35.683	3.766	145.564	10.473	M2 terrace riser
452	-38.843	-34.487	5.158	149.645	11.865	M2 terrace riser
453	-42.123	-32.866	6.334	153.304	13.041	M2 terrace riser
454	-45.182	-31.855	7.138	156.526	13.845	M2 terrace riser
455	-47.248	-30.337	7.426	159.090	14.133	M2 terrace tread
456	-49.971	-28.821	7.598	162.206	14.305	M2 terrace tread
457	-53.304	-27.101	7.688	165.957	14.395	M2 terrace tread
458	-57.585	-20.820	7.721	173.558	14.428	M2 terrace tread
459	-63.060	-15.546	8.039	181.160	14.746	M2 terrace tread
460	-67.732	-10.624	8.724	187.946	15.431	M2 terrace tread
461	-73.031	-4.417	9.356	196.108	16.063	M2 terrace tread
462	-79.154	1.033	9.894	204.305	16.601	M2 terrace tread
463	-87.213	4.779	10.689	213.192	17.396	M2 terrace tread
464	-95.327	7.934	11.936	221.898	18.643	End of alluvium, lat. bedrock contact
465	-105.238	8.983	14.041	231.864	20.748	Bedrock slope -- Shinarump
466	-119.121	10.191	18.879	245.799	25.586	Bedrock slope -- Shinarump
467	-135.514	13.543	22.897	262.532	29.604	Bedrock slope -- Shinarump
468	-160.078	20.142	25.667	287.967	32.374	Bedrock slope -- Shinarump
469	-182.483	26.634	30.932	311.293	37.639	Bedrock slope -- Shinarump
470	-202.306	31.146	34.902	331.623	41.609	Bedrock slope -- Shinarump
471	-225.506	40.010	39.296	356.459	46.003	Bedrock slope -- Shinarump
472	-252.680	41.696	44.811	383.685	51.518	Bedrock slope -- Shinarump
473	-277.849	46.423	47.378	409.294	54.085	Bedrock slope -- Shinarump
474	-295.551	52.835	49.642	428.122	56.349	Bedrock slope -- Shinarump
475	-306.310	60.586	52.534	441.382	59.241	Bedrock slope -- Shinarump
476	-327.619	59.510	56.614	462.718	63.321	Bedrock slope -- Shinarump
477	-340.018	67.629	61.100	477.539	67.807	Bedrock slope -- Shinarump
478	-346.390	74.531	65.254	486.932	71.961	Bedrock strath, covered
479	-349.191	77.698	68.004	491.160	74.711	M7 terrace riser
480	-353.630	81.433	70.557	496.962	77.264	M7 terrace riser

481	-358.579	85.232	73.148	503.201	79.855	M7 terrace riser
482	-362.990	88.109	74.759	508.467	81.466	M7 terrace riser
483	-368.207	90.547	76.065	514.225	82.772	M7 terrace riser
484	-372.639	91.871	76.876	518.851	83.583	M7 terrace riser
485	-375.896	93.064	77.411	522.320	84.118	M7 terrace riser
486	-377.967	93.417	77.537	524.420	84.244	M7 terrace tread
487	-380.262	93.726	77.608	526.736	84.315	M7 terrace tread
488	-383.830	94.823	77.729	530.469	84.436	M7 terrace tread

Survey Transect 5 error

446	-4.688	-16.315	-0.017	Backsight #6
489	-4.691	-16.314	-0.016	Backsight #6
Survey Error	**0.003**	**0.001**	**0.001**	

Survey Transect #6	Lower Paria River transect -- just upstream of Paria trail parking area					
Inst. Height (m)	--					
GPS Location	N 4081098; E 446300					
				Dist. Along	Elevation	
Pt. Id	Easting	Northing	Elevation	Transect	Above. River	Notes
482	-1380.737	-50.550	53.183			Benchmark
483	-1380.727	-50.636	53.126			Benchmark
484	-1380.716	-50.624	53.132			Benchmark
485	-601.884	162.454	-25.009	0.000	0.000	Paria River (high flow)
486	-602.675	163.917	-23.864	1.663	1.145	Up from river
487	-604.692	166.461	-21.739	4.910	3.270	Up from river
488	-606.565	166.590	-21.412	6.787	3.597	Hiking trail
489	-612.156	167.573	-20.877	12.464	4.132	Hiking trail
490	-626.081	156.233	-18.920	30.422	6.089	OSL 6
491	-628.110	160.324	-15.219	34.989	9.790	Further up deposit
492	-619.819	172.258	-10.702	49.520	14.307	OSL 7
493	-620.032	171.991	-10.368	49.862	14.641	Last fluvial deposit
494	-617.380	177.056	-8.080	55.579	16.929	Overlying hillslope deposit
495	-613.514	180.835	-4.134	60.985	20.875	Overlying hillslope deposit
496	-612.637	181.766	-3.507	62.264	21.502	Overlying hillslope deposit
497	-611.776	184.250	-2.478	64.893	22.531	Overlying hillslope deposit
498	-611.000	185.676	-1.802	66.517	23.207	Overlying hillslope deposit
499	-609.804	186.993	-0.210	68.296	24.799	Overlying hillslope deposit
500	-608.984	190.405	1.006	71.805	26.015	Overlying hillslope deposit
501	-608.571	192.498	1.670	73.938	26.679	Overlying hillslope deposit
502	-608.789	195.014	2.300	76.464	27.309	Overlying hillslope deposit
503	-609.455	196.951	2.995	78.512	28.004	Overlying hillslope deposit
504	-609.944	198.322	3.365	79.967	28.374	Overlying hillslope deposit
505	-609.940	198.974	3.559	80.619	28.568	Overlying hillslope deposit
506	-609.984	199.411	3.602	81.059	28.611	Overlying hillslope deposit
507	-610.206	199.694	3.559	81.418	28.568	Lateral bedrock contact
508	-611.326	201.807	3.406	83.810	28.415	Bedrock
509	-612.142	204.650	3.446	86.768	28.455	Bedrock
510	-611.074	206.513	3.844	88.915	28.853	Bedrock
511	-609.958	208.644	4.638	91.321	29.647	Bedrock
512	-609.189	210.597	5.408	93.420	30.417	Bedrock
513	-608.837	211.514	5.882	94.402	30.891	Bedrock
514	-608.435	212.005	6.581	95.036	31.590	Bedrock

515	-607.974	212.687	7.289	95.860	32.298	Bedrock
516	-607.182	215.350	7.683	98.638	32.692	Bedrock
517	-606.695	218.365	8.080	101.692	33.089	Bedrock
518	-606.472	220.618	8.939	103.956	33.948	Bedrock
519	-605.998	222.914	9.942	106.300	34.951	Bedrock

Survey Transect #7	Mid Paria River transect					
Inst. Height (m)	--					
GPS Location	N 4081098; E 446300					
Pt. Id	Easting	Northing	Elevation	Dist. Along Transect	Elevation Above River	Notes
520	143.826	138.151	-21.820	0.000	0.000	River level
521	143.937	141.178	-21.229	3.029	0.591	Hereford Holocene deposits
522	144.076	145.750	-20.900	7.603	0.920	Hereford Holocene deposits
523	144.416	148.878	-20.909	10.750	0.911	Hereford Holocene deposits
524	144.317	149.835	-20.071	11.712	1.749	Hereford Holocene deposits
525	144.291	150.639	-19.515	12.516	2.305	Hereford Holocene deposits
526	144.144	152.979	-19.289	14.861	2.531	Hereford Holocene deposits
527	145.244	155.534	-18.461	17.642	3.359	Hereford Holocene deposits
528	146.463	157.056	-18.233	19.592	3.587	Hereford Holocene deposits
529	149.380	159.093	-17.949	23.150	3.871	Hereford Holocene deposits
530	150.872	161.169	-17.428	25.707	4.392	Hereford Holocene deposits
531	151.350	162.516	-17.067	27.136	4.753	Hereford Holocene deposits
532	153.222	164.767	-16.835	30.064	4.985	Hereford Holocene deposits
533	154.092	166.210	-16.203	31.749	5.617	Hereford Holocene deposits
534	165.505	158.731	-16.088	45.394	5.732	Hereford Holocene deposits
535	169.037	158.847	-15.809	48.928	6.011	Bedrock
536	171.266	158.807	-15.293	51.157	6.527	Bedrock
537	174.091	157.834	-14.404	54.145	7.416	Bedrock
538	176.154	157.762	-13.398	56.209	8.422	Bedrock strath
539	177.347	158.414	-12.747	57.569	9.073	Deposit of 2??
540	179.102	158.905	-11.820	59.391	10.000	Deposit of 2??
541	180.505	159.740	-11.105	61.024	10.715	Deposit of 2??
542	182.174	160.747	-10.617	62.973	11.203	Deposit of 2??
543	183.664	161.927	-10.435	64.874	11.385	Deposit of 2??
544	185.480	163.119	-10.309	67.046	11.511	Deposit of 2??
545	187.783	164.299	-10.194	69.634	11.626	Deposit of 2??
546	190.291	164.620	-10.169	72.162	11.651	Deposit of 2??
547	192.952	165.917	-10.049	75.123	11.771	Deposit of 2??
548	195.660	166.490	-9.864	77.891	11.956	Deposit of 2??
549	198.411	167.381	-9.644	80.782	12.176	Deposit of 2??
550	201.124	167.451	-9.396	83.496	12.424	Deposit of 2??
551	205.403	166.814	-9.315	87.822	12.505	Deposit of 2??
552	209.541	165.499	-9.140	92.164	12.680	Deposit of 2??
553	213.227	165.142	-8.864	95.867	12.956	Deposit of 2??
554	217.961	162.814	-8.328	101.143	13.492	Deposit of 2??
555	221.631	162.190	-7.820	104.866	14.000	Deposit of 2??
556	224.732	162.075	-7.308	107.969	14.512	Deposit of 2??
557	227.258	162.899	-6.933	110.626	14.887	Deposit of 2??
558	229.967	163.811	-6.372	113.484	15.448	Deposit of 2??
559	232.173	165.502	-5.918	116.264	15.902	Deposit of 2??
560	235.919	166.641	-5.353	120.179	16.467	Deposit of 2??
561	238.211	168.814	-5.031	123.337	16.789	Deposit of 2??
562	240.095	171.176	-4.837	126.359	16.983	Deposit of 2??

563	242.686	172.936	-4.600	129.491	17.220	Deposit of 2??
564	245.187	174.799	-4.460	132.610	17.360	Deposit of 2??
565	247.648	176.737	-4.247	135.742	17.573	Deposit of 2??
566	250.118	178.997	-4.063	139.090	17.757	Deposit of 2??
567	252.877	180.601	-4.127	142.281	17.693	Deposit of 2??
568	256.103	182.361	-4.158	145.956	17.662	Deposit of 2??
569	260.144	183.764	-4.000	150.234	17.820	Deposit of 2??
570	263.170	184.673	-3.959	153.393	17.861	Deposit of 2??
571	266.717	185.857	-3.737	157.133	18.083	Deposit of 2??
572	269.803	187.445	-3.380	160.603	18.440	Deposit of 2??
573	273.514	189.676	-2.589	164.933	19.231	Deposit of 2??
574	276.660	192.380	-1.824	169.082	19.996	Deposit of 2??
575	280.380	195.090	-0.885	173.684	20.935	Deposit of 2??
576	282.736	197.007	-0.141	176.722	21.679	Deposit of 2??
577	285.957	199.767	0.846	180.963	22.666	Deposit of 2??
578	288.190	202.245	1.271	184.299	23.091	Deposit of 2??
579	290.505	204.069	1.796	187.246	23.616	Bedrock
580	292.326	205.492	2.306	189.557	24.126	Bedrock
581	294.556	207.213	3.047	192.374	24.867	Bedrock
582	297.724	208.791	4.005	195.913	25.825	Bedrock
583	301.143	211.765	5.587	200.445	27.407	Bedrock
584	303.263	213.081	6.826	202.940	28.646	Bedrock
585	305.223	214.257	7.954	205.226	29.774	Bedrock strath of 4??
586	306.180	215.493	8.745	206.789	30.565	Deposit of 4??
587	307.146	216.145	9.228	207.954	31.048	Deposit of 4??
588	308.718	217.262	9.515	209.883	31.335	Deposit of 4??
589	310.760	218.696	10.396	212.378	32.216	Deposit of 4??
590	311.472	221.061	11.428	214.848	33.248	Deposit of 4??
591	312.721	223.087	12.725	217.228	34.545	Deposit of 4??
592	313.533	224.694	13.876	219.029	35.696	Deposit of 4??
593	314.873	225.652	14.890	220.676	36.710	Deposit of 4??
594	316.227	227.156	16.023	222.699	37.843	Deposit of 4??
595	316.670	228.285	17.011	223.912	38.831	Deposit of 4??
596	317.891	230.758	18.749	226.670	40.569	Deposit of 4??
597	318.400	231.834	19.441	227.861	41.261	Deposit of 4??
598	319.102	233.336	20.321	229.519	42.141	Deposit of 4??
599	319.857	235.029	21.102	231.372	42.922	Deposit of 4??
600	320.327	237.426	21.726	233.815	43.546	Deposit of 4??
601	320.594	238.781	21.869	235.196	43.689	Deposit of 4??
602	320.869	241.012	21.930	237.444	43.750	Deposit of 4??
603	321.010	244.486	22.056	240.921	43.876	Deposit of 4??
604	321.248	249.573	22.199	246.013	44.019	Deposit of 4??
605	321.658	253.533	22.515	249.994	44.335	Deposit of 4??
606	322.793	256.833	23.161	253.484	44.981	Deposit of 4??
607	325.060	261.489	23.580	258.663	45.400	Deposit of 4??
608	326.425	264.483	23.783	261.953	45.603	Deposit of 4??
609	327.541	269.719	24.025	267.307	45.845	Local Landslide??
610	329.393	274.883	24.649	272.793	46.469	Local Landslide??
611	330.523	279.167	24.806	277.223	46.626	Local Landslide??
612	331.448	281.001	24.948	279.277	46.768	Local Landslide??
613	332.697	283.887	25.540	282.422	47.360	Local Landslide??
614	333.881	286.456	26.283	285.251	48.103	Local Landslide??
615	335.700	288.884	27.106	288.285	48.926	Local Landslide??
616	336.715	291.381	27.918	290.980	49.738	Local Landslide??
617	337.162	293.219	28.407	292.872	50.227	Local Landslide??
618	338.022	295.811	28.562	295.603	50.382	Local Landslide??

619	340.601	299.190	29.409	299.853	51.229	Local Landslide??
620	343.570	301.394	30.594	303.551	52.414	Local Landslide??
621	345.208	303.717	31.843	306.393	53.663	Local Landslide??
622	346.361	306.019	32.584	308.968	54.404	Deposit of 4??
623	348.447	307.935	33.077	311.800	54.897	Deposit of 4??
624	350.825	310.443	33.446	315.257	55.266	Deposit of 4??
625	352.672	312.485	34.048	318.010	55.868	Deposit of 4??
626	354.488	315.021	34.817	321.129	56.637	Deposit of 4??
627	357.457	319.270	35.433	326.313	57.253	Deposit of 4??
628	361.237	324.028	36.089	332.389	57.909	Deposit of 4??
629	368.676	330.936	37.185	342.541	59.005	Deposit of 4??
630	377.068	337.903	38.339	353.448	60.159	Deposit of 4??
631	385.817	346.489	40.518	365.707	62.338	Deposit of 4??
632	390.346	352.614	42.214	373.324	64.034	Deposit of 4??
633	391.933	357.395	43.898	378.362	65.718	Deposit of 4??
634	392.844	361.878	45.745	382.936	67.565	Deposit of 4??
635	393.307	365.674	47.749	386.760	69.569	Deposit of 4??
636	393.273	368.074	48.250	389.161	70.070	Deposit of 4??
637	394.351	369.724	48.408	391.132	70.228	Deposit of 4??
638	394.901	371.677	48.844	393.161	70.664	Deposit of 4??
639	238.195	333.903	19.558	554.355	41.378	Top of 4? Not well preserved
640	219.088	310.743	7.142	584.379	28.962	3?? Better preserved surface
641	214.569	307.427	6.718	589.984	28.538	3?? Better preserved surface
642	208.975	303.673	6.216	596.721	28.036	3?? Better preserved surface
643	204.276	302.367	6.183	601.598	28.003	3?? Better preserved surface
644	196.524	298.249	4.931	610.376	26.751	Strath of 3??
645	164.984	223.895	-12.100	691.143	9.720	Top of 1/2?? Well preserved
646	164.668	218.083	-12.120	696.964	9.700	Top of 1/2?? Well preserved
647	164.157	212.652	-12.195	702.419	9.625	Top of 1/2?? Well preserved
648	165.027	206.229	-12.398	708.900	9.422	Top of 1/2?? Well preserved
649	228.485	193.807	-9.657		12.163	OSL 5

Survey Transect #8	Upper Paria River -- thick deposit					
Inst. Height (m)	--					
GPS Location	N 4081098; E 446300					
				Dist. Along	Elevation	
Pt. Id	Easting	Northing	Elevation	Transect	Above River	Notes
650	-149.233	-194.468	20.039	0.000	41.562	5/4o?? Deposit
651	-146.153	-191.418	20.157	4.335	41.680	5/4o?? Deposit
652	-142.967	-187.846	20.237	9.121	41.760	5/4o?? Deposit
653	-140.573	-183.627	19.967	13.972	41.490	5/4o?? Deposit
654	-137.104	-178.412	19.614	20.235	41.137	5/4o?? Deposit
655	-136.503	-177.256	19.224	21.538	40.747	5/4o?? Deposit
656	-135.765	-175.624	18.608	23.329	40.131	5/4o?? Deposit
657	-134.280	-173.425	18.087	25.983	39.610	5/4o?? Deposit
658	-131.253	-168.881	17.467	31.443	38.990	5/4y surface -- sandy cap
659	-128.883	-166.548	17.033	34.768	38.556	5/4y surface -- sandy cap
660	-124.745	-163.577	16.992	39.862	38.515	5/4y surface -- sandy cap
661	-120.539	-161.944	17.333	44.374	38.856	5/4y surface -- sandy cap
662	-117.854	-160.769	17.478	47.305	39.001	5/4y surface -- sandy cap
663	-116.841	-160.288	17.352	48.427	38.875	5/4y surface -- sandy cap
664	-113.286	-159.962	17.007	51.996	38.530	5/4y surface -- sandy cap
665	-109.696	-159.240	17.081	55.658	38.604	5/4y surface -- sandy cap
666	-106.240	-159.591	17.061	59.132	38.584	5/4y surface -- sandy cap

667	-105.135	-158.745	16.705	60.524	38.228	5/4y surface -- sandy cap
668	-103.916	-158.175	16.298	61.869	37.821	5/4y surface -- sandy cap
669	-101.987	-157.327	16.095	63.977	37.618	5/4y surface -- sandy cap
670	-99.967	-156.421	15.984	66.191	37.507	5/4y surface -- sandy cap
671	-99.129	-155.959	15.594	67.147	37.117	5/4y surface -- sandy cap
672	-97.838	-155.165	14.746	68.663	36.269	5/4y surface -- sandy cap
673	-96.910	-154.667	14.082	69.716	35.605	5/4y surface -- sandy cap
674	-95.572	-154.641	13.217	71.054	34.740	5/4y surface -- sandy cap
675	-94.591	-153.915	12.438	72.275	33.961	5/4y surface -- sandy cap
676	-94.414	-152.987	11.949	73.220	33.472	Bedrock Strath
677	-86.198	-151.736	8.650	81.530	30.173	Bedrock (down in a gully)
678	-79.110	-143.110	3.793	92.695	25.316	Bedrock (down in a gully)
679	-74.806	-138.193	0.661	99.230	22.184	Bedrock (down in a gully)
680	-72.233	-135.193	-1.224	103.182	20.299	Bedrock (down in a gully)
681	-68.426	-129.903	-1.865	109.699	19.658	Bedrock (down in a gully)
682	-54.377	-108.038	-6.974	135.689	14.549	Bedrock (down in a gully)
683	-40.346	-95.343	-9.580	154.610	11.943	Bedrock (down in a gully)
684	-36.585	-91.576	-11.795	159.934	9.728	Bedrock (down in a gully)
685	-34.692	-88.893	-12.577	163.217	8.946	Bedrock (down in a gully)
686	-27.368	-83.362	-9.654	172.395	11.869	Bedrock (down in a gully)
687	-22.091	-81.820	-6.536	177.893	14.987	Bedrock (down in a gully)
688	-17.829	-80.524	-4.293	182.347	17.230	Bedrock (down in a gully)
689	-14.582	-80.142	-2.306	185.617	19.217	Bedrock strath on backside
690	-12.589	-80.045	-1.311	187.612	20.212	Deposit of 5??
691	-10.933	-79.949	-0.435	189.271	21.088	Deposit of 5??
692	-8.757	-79.692	0.374	191.462	21.897	Deposit of 5??
693	-6.656	-78.918	1.219	193.701	22.742	Deposit of 5??
694	-5.108	-78.314	1.579	195.363	23.102	Deposit of 5??
695	-3.289	-77.970	1.865	197.214	23.388	Deposit of 5??
696	-0.687	-77.365	2.023	199.885	23.546	Deposit of 5??
697	4.103	-75.536	2.135	205.013	23.658	Deposit of 5??
698	10.806	-73.157	2.415	212.125	23.938	Deposit of 5??
699	16.613	-69.673	2.780	218.897	24.303	Deposit of 5??
700	22.018	-67.070	2.945	224.896	24.468	Deposit of 5??
701	27.215	-63.986	2.986	230.940	24.509	Deposit of 5??
702	32.639	-62.240	2.949	236.638	24.472	Deposit of 5??
703	35.997	-61.474	2.848	240.082	24.371	Deposit of 5??
704	34.460	-40.620	2.801	260.993	24.324	Deposit of 5??
705	35.635	-38.102	2.406	263.771	23.929	Deposit of 5??
706	38.032	-35.472	1.247	267.330	22.770	Deposit of 5??
707	39.624	-33.509	0.498	269.857	22.021	Deposit of 5??
708	40.560	-32.259	-0.229	271.419	21.294	Deposit of 5??
709	40.964	-31.351	-0.856	272.412	20.667	Deposit of 5??
710	41.296	-31.101	-1.191	272.828	20.332	Bedrock strath
711	44.223	-26.420	-4.480	278.349	17.043	Bedrock
712	46.518	-21.799	-7.133	283.508	14.390	Bedrock
713	46.554	-21.425	-7.852	283.884	13.671	Bedrock
714	48.424	-17.895	-9.161	287.879	12.362	Bedrock
715	51.391	-13.733	-12.121	292.990	9.402	Bedrock
716	65.621	-0.592	-16.922	312.360	4.601	Hereford Holocence alluvium
717	94.223	30.617	-17.900	354.693	3.623	Hereford Holocence alluvium
718	132.635	70.945	-18.375	410.387	3.148	Hereford Holocence alluvium
719	166.093	105.335	-18.397	458.367	3.126	Hereford Holocence alluvium
720	180.609	116.795	-18.912	476.861	2.611	Hereford Holo. alluvium
721	179.383	118.155	-20.597	478.692	0.926	Hereford Holo. alluvium (2 rh)
722	179.798	119.846	-20.829	480.434	0.694	Hereford Holo. alluvium (2 rh)

723	179.795	120.065	-21.523	480.653	0.000	River level (2 rod heights)
724	477.461	-148.504	-18.926	881.570	0.000	River level (m0ved upstream)
725	479.032	-148.843	-17.928	883.177	0.998	Hereford Holocene Alluvium
726	482.795	-148.638	-16.047	886.945	2.879	Hereford Holocene Alluvium
727	493.411	-142.045	-15.237	899.442	3.689	Hereford Holocene Alluvium
728	518.905	-128.834	-14.404	928.156	4.522	Hereford Holocene Alluvium
729	551.744	-110.563	-13.590	965.735	5.336	Hereford Holocene Alluvium
730	555.786	-109.586	-13.178	969.894	5.748	Bedrock
731	558.970	-108.888	-12.000	973.153	6.926	Bedrock
732	559.053	-109.778	-9.459	974.047	9.467	Bedrock
733	561.511	-109.448	-8.416	976.527	10.510	Bedrock
734	563.948	-108.966	-7.385	979.011	11.541	Bedrock
735	566.644	-107.955	-5.769	981.891	13.157	Bedrock
736	568.954	-106.940	-4.271	984.414	14.655	Bedrock
737	570.946	-105.661	-3.172	986.781	15.754	Bedrock strath
738	572.094	-104.591	-2.180	988.351	16.746	4y/o?? Deposit
739	573.947	-104.558	-1.019	990.204	17.907	4y/o?? Deposit
740	575.379	-103.875	0.197	991.790	19.123	4y/o?? Deposit
741	577.464	-103.381	1.608	993.933	20.534	4y/o?? Deposit
742	579.048	-102.649	3.327	995.678	22.253	4y/o?? Deposit
743	580.915	-101.818	4.254	997.722	23.180	4y/o?? Deposit
744	582.246	-100.882	4.830	999.349	23.756	4y/o?? Deposit
745	584.039	-100.184	5.106	1001.273	24.032	4y/o?? Deposit
746	586.096	-99.612	5.443	1003.408	24.369	4y/o?? Deposit
747	588.758	-98.160	5.921	1006.440	24.847	4y/o?? Deposit
748	591.072	-97.517	6.400	1008.842	25.326	4y/o?? Deposit
749	594.172	-96.823	7.135	1012.019	26.061	4y/o?? Deposit
750	598.029	-94.696	7.998	1016.423	26.924	4y/o?? Deposit
751	600.260	-93.918	8.836	1018.786	27.762	4y/o?? Deposit
752	602.576	-93.041	9.874	1021.262	28.800	4y/o?? Deposit
753	605.373	-91.933	10.957	1024.271	29.883	4y/o?? Deposit
754	607.284	-91.063	12.516	1026.371	31.442	4y/o?? Deposit
755	609.686	-89.434	13.580	1029.273	32.506	4y/o?? Deposit
756	612.858	-88.254	14.929	1032.657	33.855	4y/o?? Deposit
757	615.256	-87.450	16.047	1035.186	34.973	4y/o?? Deposit
758	616.972	-86.506	17.077	1037.145	36.003	4y/o?? Deposit
759	620.120	-84.192	19.284	1041.052	38.210	4y/o?? Deposit
760	622.808	-83.195	20.687	1043.919	39.613	4y/o?? Deposit
761	626.016	-82.256	22.048	1047.261	40.974	4y/o?? Deposit
762	628.811	-80.952	22.903	1050.346	41.829	4y/o?? Deposit
763	632.252	-79.890	24.440	1053.947	43.366	4y/o?? Deposit
764	634.140	-79.093	25.291	1055.996	44.217	4y/o?? Deposit
765	636.074	-78.306	26.053	1058.084	44.979	4y/o?? Deposit
766	637.814	-77.477	26.441	1060.012	45.367	4y/o?? Deposit
767	639.589	-76.244	26.918	1062.173	45.844	4y/o?? Deposit
768	642.137	-74.825	27.357	1065.089	46.283	4y/o?? Deposit
769	645.407	-72.950	27.618	1068.859	46.544	4y/o?? Deposit
770	648.881	-71.787	27.689	1072.522	46.615	4y/o?? Deposit
771	656.645	-69.416	27.991	1080.640	46.917	4y/o?? Deposit
772	665.270	-69.571	28.259	1089.267	47.185	4y/o?? Deposit
773	677.468	-69.516	28.537	1101.465	47.463	4y/o?? Deposit
774	688.023	-71.080	29.288	1112.135	48.214	4y/o?? Deposit
775	692.622	-71.562	29.677	1116.759	48.603	4y/o?? Deposit
776	696.428	-72.324	29.695	1120.641	48.621	4y/o?? Deposit
777	701.870	-73.379	29.557	1126.184	48.483	4y/o?? Deposit

778	706.396	-74.228	29.360	1130.789	48.286	4y/o?? Deposit
779	709.648	-74.974	29.091	1134.125	48.017	4y/o?? Deposit
780	604.277	-27.195	14.402		33.328	OSL 2
781	589.591	-14.241	4.686		23.612	OSL 3
782	555.585	-29.130	-1.317		17.609	OSL 4

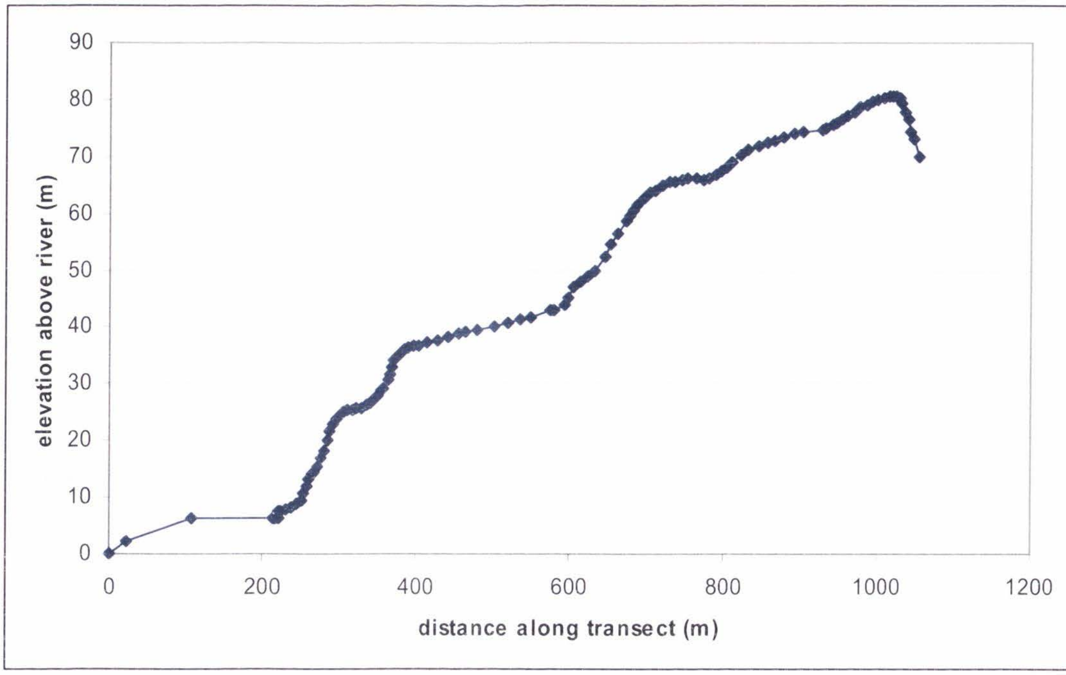

Figure D.2. Raw Survey points from Transects 1A and 1B.

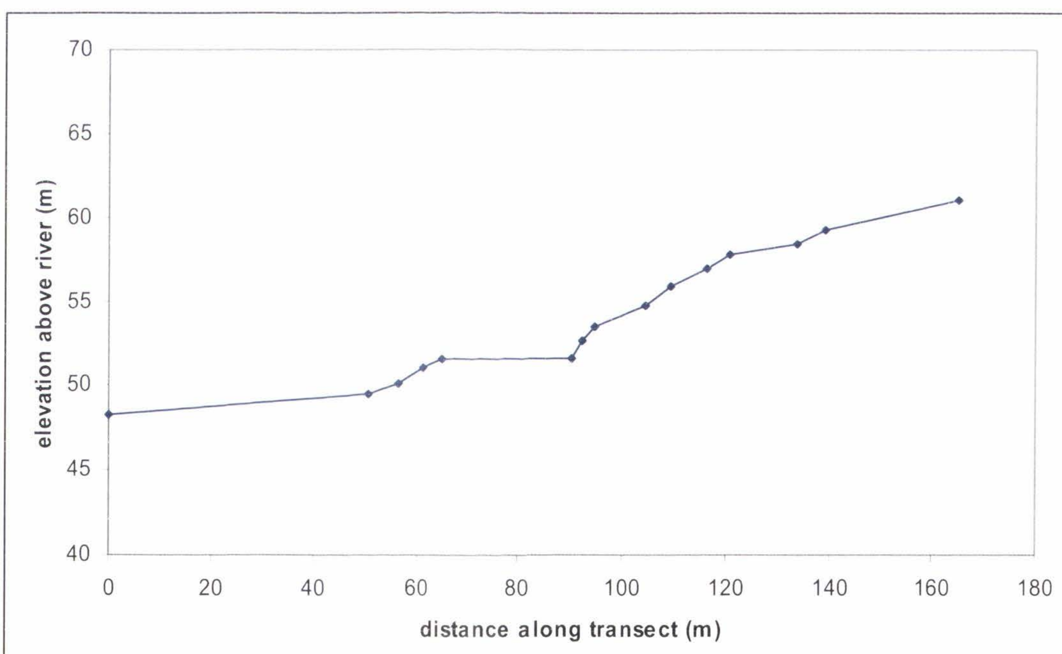

Figure D.3. Raw Survey points from Transect 2.

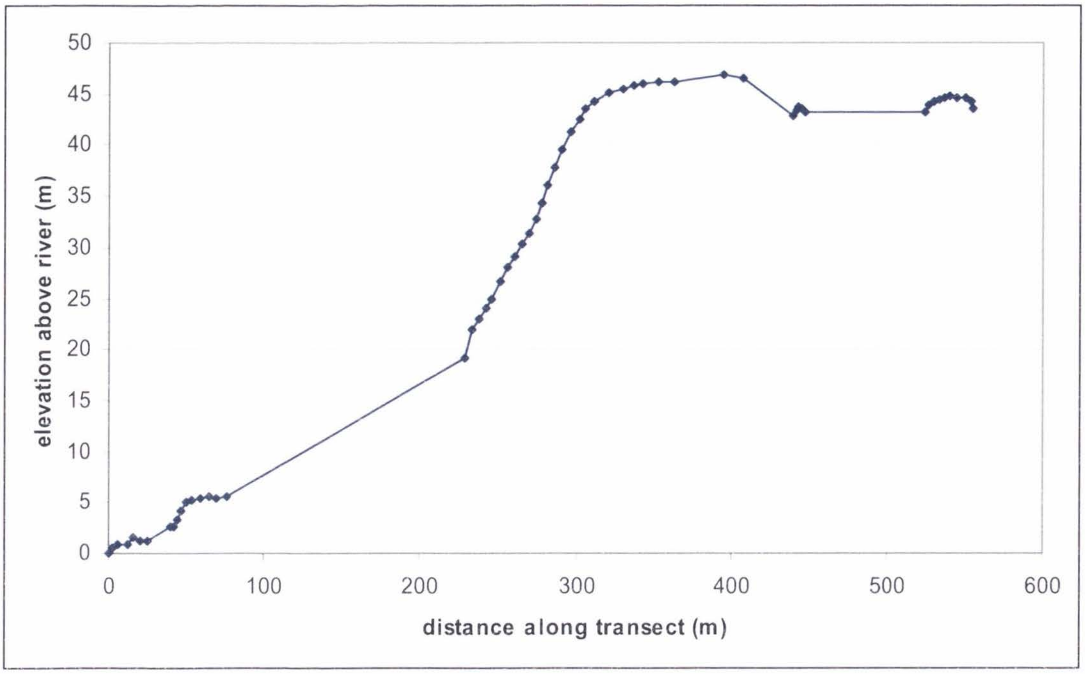

Figure D.4. Raw Survey points from Transect 3.

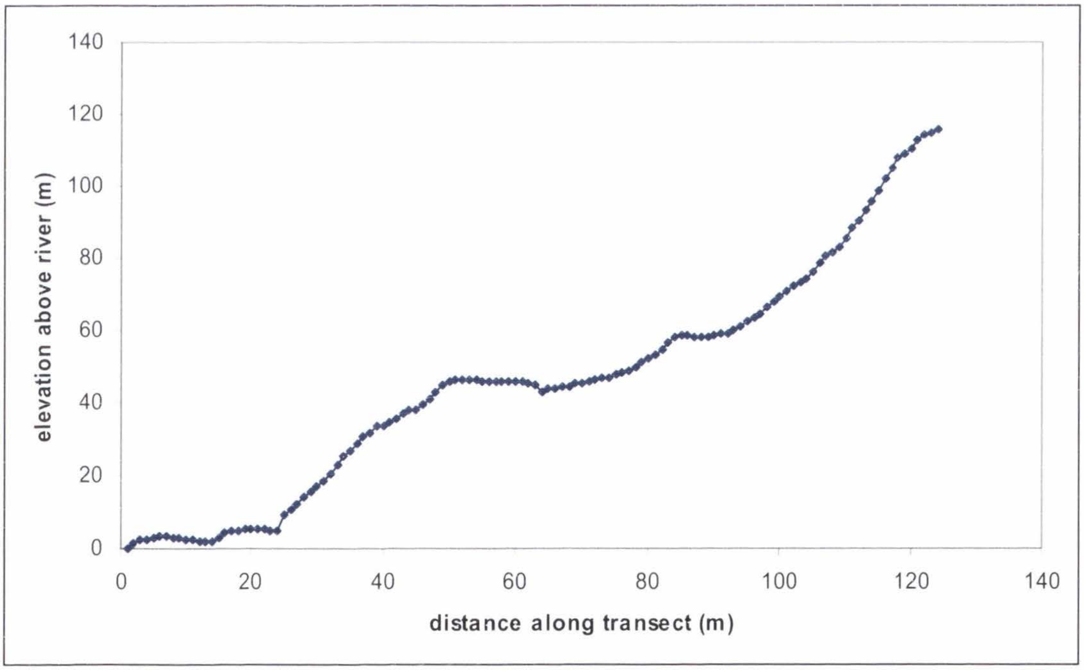

Figure D.5. Raw Survey points from Transect 4A.

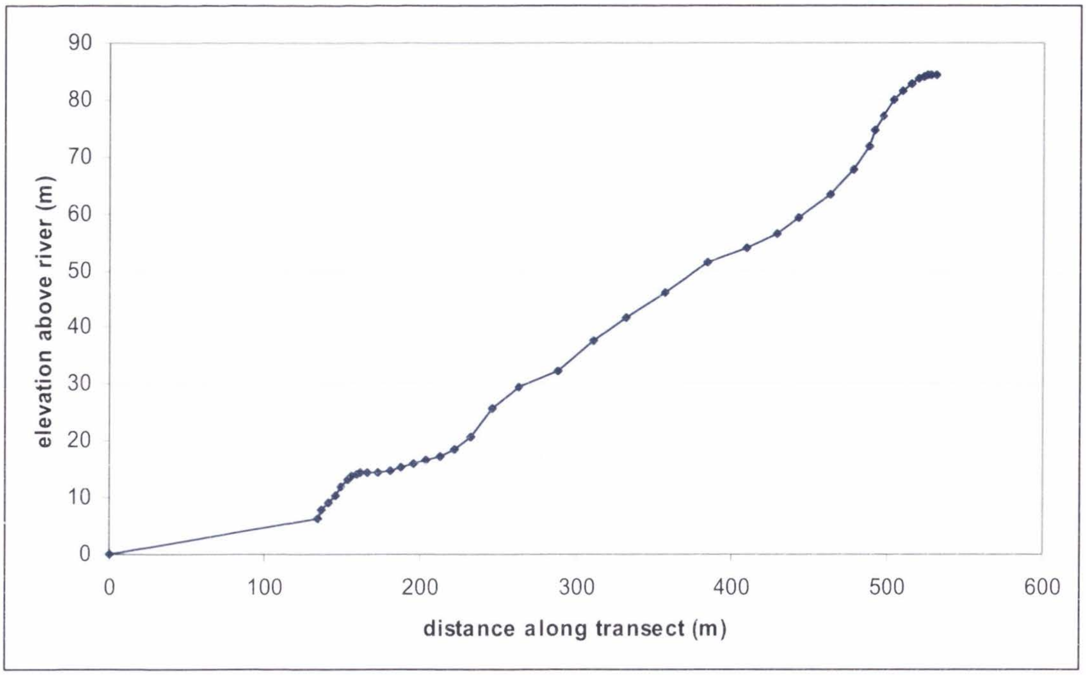

Figure D.6. Raw Survey points from Transect 5.

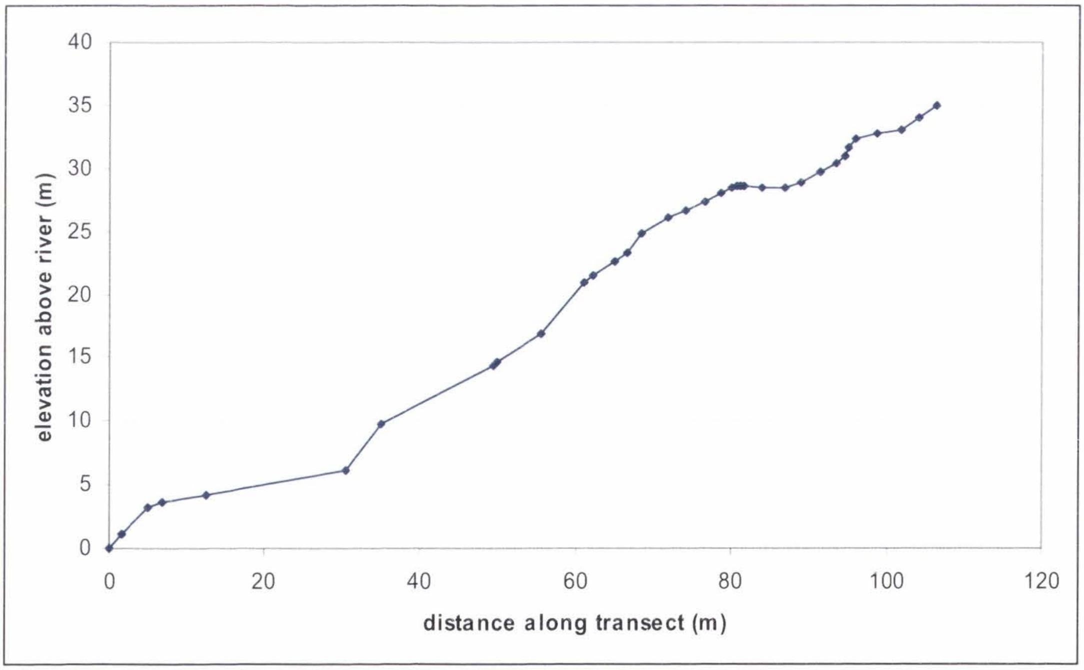

Figure D.7. Raw Survey points from Transect 6.

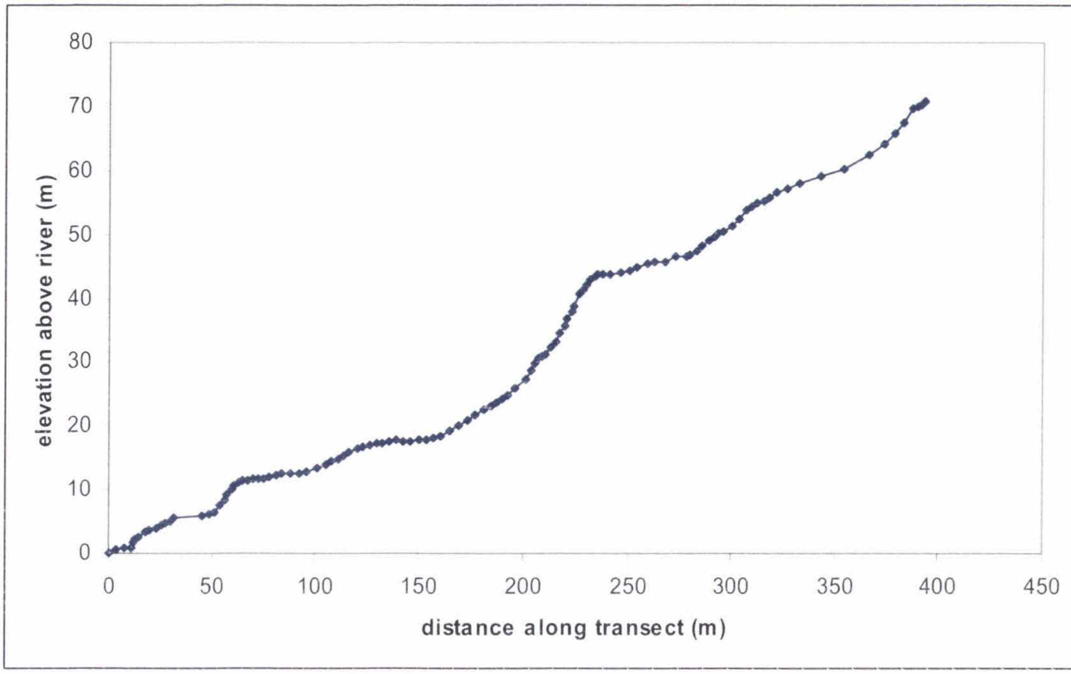

Figure D.8. Raw Survey points from Transect 7.

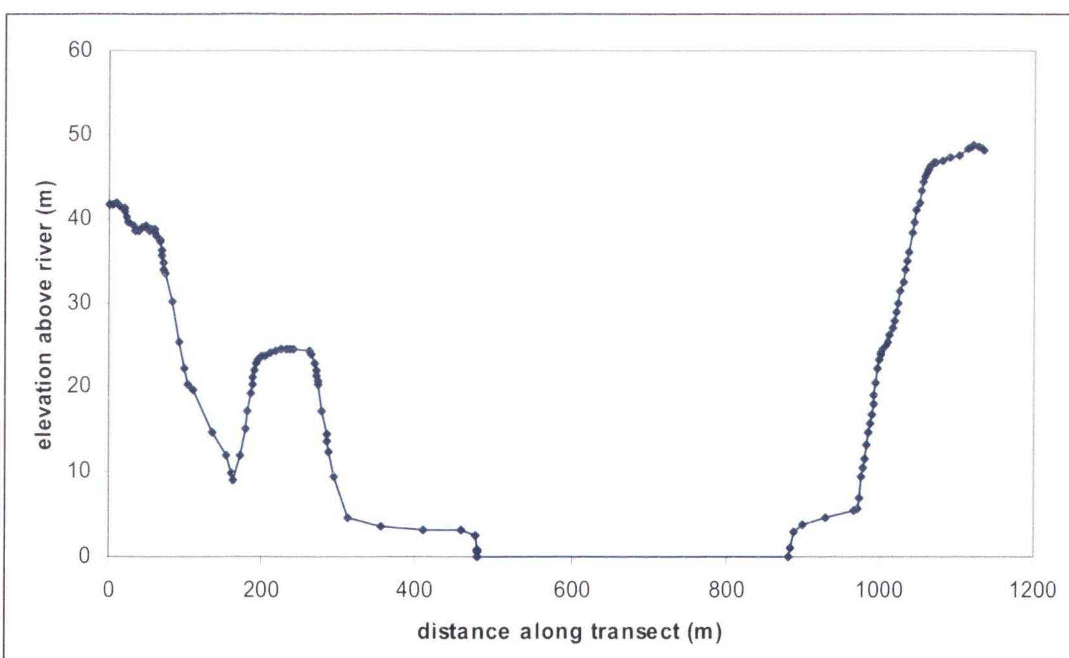

Figure D.9. Raw Survey points from Transect 8.

Appendix E. TERRESTRIAL COSMOGENIC ^{10}BE NUCLIDE DATA

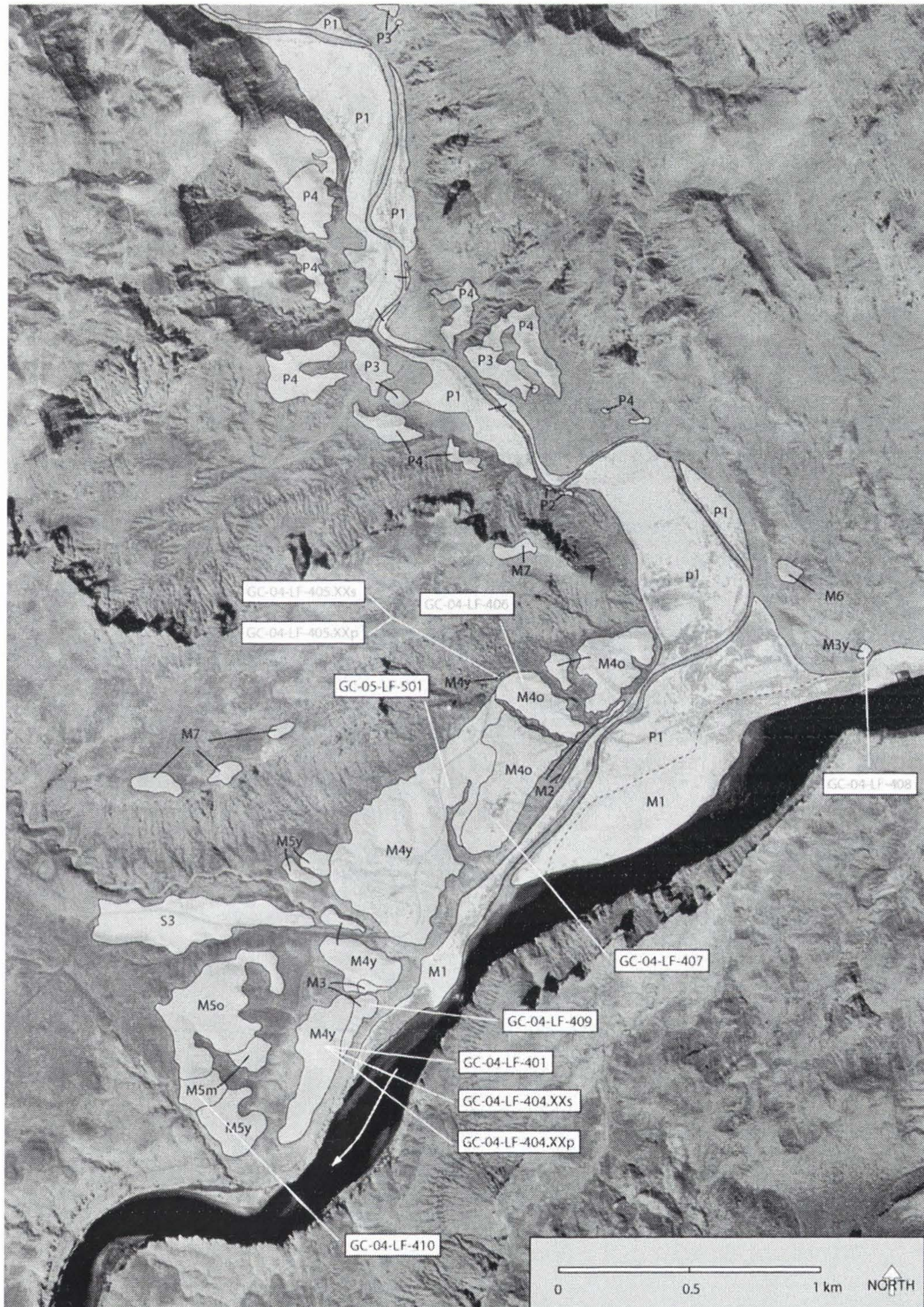

Figure E.1. Map of Quaternary deposits in the Lees Ferry area, showing approximate locations where TCN samples were collected. Gray text indicates samples that were collected but are no longer being processed.

Table E.1. Site, chemical, and calculated data for terrestrial cosmogenic ^{10}Be nuclide ages.

CNEF	Field	Location Data		Dpth	Prod. Rate	10Be/9Be		Cnc.	Inhert.	Age	2σ unc.		Deposit
ID	ID	Lat.	Alt.		Atoms/	Corrted	2σ unc	Ato m/g	Ato m/g		Pre	Acc	
		Deg.	km	m	Gy/Yr	x 10^{-5}	%	X 10^4	X 10^4	kyr	kyr	kyr	
Samples for exposure age calculation													
1590	GC-04-LF-401	36.852	0.985	--	9.89	382		94.6		**86**			M4y
1591	GC-04-LF-407	36.859	0.995	--	9.97	195		94.9		**97**			M4o
1592	GC-04-LF-408	36.865	0.960	--	9.71	218		106.2		**112**			M2 ?
1593	GC-04-LF-409	36.854	0.975	--	9.82	99		48.2		**50**			M3
1594	GC-04-LF-410	36.850	1.021	--	10.17	284		138.5		**141**			M5m
	GC-05-LF-501												
Samples for inheritance estimation													
1595	GC04-LF-404.30s	36.852	0.985	0.30	6.45	284		62.7		**82**			M4
1596	GC04-LF-404.60s	36.852	0.985	0.60	4.10	206		44.8		**84**			M4
1597	GC04-LF-404.10 0s	36.852	0.985	1.00	2.28	161		32.2		**96**			M4
1598	GC04-LF-404.14 0s	36.852	0.985	1.40	1.29	114		22.4		**91**			M4
1599	GC04-LF-404.18 0s	36.852	0.985	1.80	0.76	96		17.3		**87**			M4
1600	GC04-LF-404.22 0s	36.852	0.985	2.20	0.47	81		14.8		**86**			M4
1601	GC04-LF-404.30p	36.852	0.985	0.30	6.41	169		80.2		**111**			M4
1602	GC04-LF-404.60p	36.852	0.985	0.60	4.07	143		50.9		**101**			M4
1603	GC04-LF-404.100p	36.852	0.985	1.00	2.27	63		26.0		**68**			M4
1604	GC04-LF-404.140p	36.852	0.985	1.40	1.29	69		21.0		**80**			M4
1605	GC04-LF-404.180p	36.852	0.985	1.80	0.75	94		32.4		**306**			M4
1606	GC04-LF-404.220p	36.852	0.985	2.20	0.46	200		84.7		**2834**			M4

Table E.2. Lees Ferry cosmogenic samples: field notes and general descriptions.

GC-04-LF-401
June 12, 2004
Location:
UTM-- 445932 E 4078639 N, Zone 12.
~2 km south of Housing terrace, just above (west) of Paria gully ppt. gauge.
~Elevation: 3230 feet (taken off topo map).
Surface Characteristic:
Possible M4 terrace deposit, M4y terrace surface.
Dimensions: 1 km length, 100 m width (max), tilting slightly to southwest away from river.
No rubification of clasts.
Most clasts are not fractured on surface.
Av horizon ~1 cm thick.
Fragments of pedogenic carbonates on surface.
Max clast size: ~20 cm.
Majority of clasts are very well rounded.
20-30% clasts are sub-angular.
Less than 1 plant/ sq. meter (prickly pear and sage grass).
Lithology: quartzite and chert dominate.

1 surface sample of mostly 2 cm diameter clasts collected.
Greater than 100 pebbles collected within 100 m of road ending – Future site or soil profile.
Should give min. age of deposit.
Recent erosion, possibly indicated by poor pavement, but no apparent gullying.
Generally a flat surface.
Avoided sampling near plants.
Sample collected ~4 m from edge of terrace.

GC-04-LF-404…
October 17, 2004
Series of Depth-Profile Samples #1
Soil Pit dug at location of surface sample GC-04-LF-401.
3 bulk-density samples collected through the vertical sequence.

Location:
UTM-- 445932 E 4078639 N, Zone 12.
~2 km south of Housing terrace, just above (west) of Paria gully ppt. gauge.
~Elevation: 3230 feet (taken off topo map).
Site Characteristics:
Possible M4 terrace deposit, M4y terrace surface.
Bioturbation extended to ~10 cm depth, therefore sampling began at 30cm rather than 50 cm as outlined in Gosse sampling strategy… Out of zone of mixing.
Sampling for all depths performed around level line within ±2.5 cm due to the presence of large clasts and pebbles.
Sampling for all depths performed around all three walls in order to increase the sampling swath.
Samples from all depths were collected of all material in pit and then sieved in order to collect both the sand and pebble fraction.

GC-04-LF-404.30 S & P
Sample collected at 30 cm depth as specified above.

GC-04-LF-404.60 S & P

Sample collected at 60 cm depth as specified above.

GC-04-LF-404.100 S & P
Sample collected at 100 cm depth as specified above.

GC-04-LF-404.140 S & P
Sample collected at 140 cm depth as specified above.

GC-04-LF-404.180 S & P
Sample collected at 180 cm depth as specified above.

GC-04-LF-404.220 S & P
Sample collected at 220 cm depth as specified above.

GC-04-LF-405…
October 18, 2004
Series of Depth-Profile Samples #2
3 bulk-density samples collected through the vertical sequence.
Location:
UTM: 446458 E 4079938 N, Zone 12.
~300 m north of Lees Ferry Ranger Station.
Prominent sandy road cut on west side of road.
Possible M4 terrace deposit.
Elevation: ~3260 feet.
Outcrop Characteristics:
Deposit is tabular and lenticular bedded, with inter-fingering fine sands and silts (overbank) and lenses of pebble-cobble-gravels (side stem dominated).
Gravels display imbrication in a southward direction.
Outcrop exists due to ~4 m high road cut.
Sand lenses could represent overbank Colorado River (light-tan color of fine sands).
Sampling for all depths performed around level line within ±2.5 cm.
Samples from all depths were collected of all material in outcrop and then sieved in order to collect both the sand and pebble fraction.
Horizon shielding may need to be corrected for…

Compass Bearing = C.B. Horizon Angle = H.A.

C.B	H.A.	C.B.	H.A.	C.B.	H.A.	C.B	H.A.	C.B.	H.A.	C.B	H.A.
0°	22°	60°	13°	120°	7°	180°	2°	240°	20°	300°	28°
20°	15°	80°	10°	140°	12°	200°	4°	260°	19°	320°	26°
40°	13°	100°	9°	160°	5°	220°	7°	280°	24°	340°	24°

GC-04-LF-405.78 S & P
Sample collected at 78 cm depth as specified above.

GC-04-LF-405.148 S & P
Sample collected at 148 cm depth as specified above.

GC-04-LF-405.198 S & P
Sample collected at 198 cm depth as specified above.

GC-04-LF-405.300 S & P
Sample collected at 300 cm depth as specified above.

GC-04-LF-405.431 S & P

Sample collected at 431 cm depth as specified above.

GC-04-LF-405.563 S & P

Sample collected at 563 cm depth as specified above.

GC-04-LF-406

October 18, 2004

Location:

UTM-- 446456 E 4079811 N, Zone 12.
~4 m north of 1st power line east of the main road.
On the north-western flanks of the housing terrace.
~Elevation: 3260 feet.

Surface Characteristic:

Possible M4 terrace deposit, M4y terrace surface.
Surface is ~2 m lower than the highest Housing terrace surface.
Dimensions: 12 m in N/S direction, and 5-8 m in E/W direction.
Located on the flanks of the Housing terrace.
No rubification of clasts.
Av horizon ~4 cm thick (maybe thicker because of enhanced slopewash).
Good desert varnish, although many of the darkest clasts have likely been previously varnished in the Shinarump deposit.
Many clasts come from the Shinarump, good quartzites, many of them sampled in depth-profile #2.
Many clasts are fractured at the surface.
Mainstem (yellow) quartzites are not as abundant as at sample location for GC-04-LF-401.
Majority of clasts are not well-rounded, although many well rounded clasts are fractured.
Few pedogenic carbonates at the surface (1% of clasts).
Less than 1 plant / sq. meter.
Moderately-well to well-developed pavement on surface.
Max clast size: 20 cm.
Average clast size: 2 cm.

1 surface sample of mostly 2 cm diameter clasts collected.
Greater than 100 pebbles collected ~4 m from edge of terrace.
Should give min. age of deposit.
Generally a flat surface, although slopes slightly towards ravine to the north.
Avoided sampling near plants.
Inheritance will be calculated in depth-profile samples.

GC-04-LF-407

October 18, 2004

Location:

UTM-- 446485 E 4079472 N, Zone 12.
The Housing Terrace (south end).
~5 m south of the fence corner of the southern-most house.
~Elevation: 3265 feet.

Surface Characteristic:

Possible M4 terrace deposit, M4o terrace surface.
Bigger clasts than M4y sample GC-04-LF-406.
Dimensions: ~1 km (N/S) by 200-300 m (E/W).
This is THE Housing terrace.
Some volcanic clasts (not many) present at surface.

No rubification of clasts.
Very few pedogenic carbonates observed on the surface.
Av horizon ~4 cm thick.
Moderately developed desert varnish.
Well-developed desert pavement.
Most clasts are rounded, although some sub-angular and fractured clasts are present.
Mainstem (yellow) quartzites are more abundant than at GC-04-LF-406, and perhaps equal to GC-04-LF-401.
Less than 1 plant / sq. meter.
Max clast size: 20 cm.
Average clast size: 3-4 cm.

1 surface sample of mostly 2 cm diameter quartzite clasts collected.
Greater than 100 pebbles collected ~3 m from edge of terrace.
Should give min. age of deposit/terrace surface.
Generally a flat surface, although surface slopes slightly to the south (same direction as modern river).
Avoided sampling near plants.
Inheritance will be calculated in depth-profile sample #1.

GC-04-LF-408
October 19, 2004
Location:
UTM-- 447685 E 4080059 N, Zone 12.
Possible M2 terrace deposit.
Located ~70 m west of bathroom at the Lees Ferry boat ramp.
Sample collected ~3 m NW of telephone pole.
~Elevation: 3150 feet.
Surface Characteristic:
Dimensions: ~25 m (E/W) by 6-7 m (N/S).
More volcanic clasts than any other surface samples previously.
No rubification of clasts.
Very few pedogenic carbonates observed on the surface.
Av horizon ~3 cm thick.
Moderately well-developed pavement.
Desert varnish is moderately well-developed, although not as good as other sample surfaces.
Most clasts are rounded, very few fractured clasts are present.
Mainstem (yellow) quartzites and volcanics dominate the surface clasts composition.
Less than 1 plant / sq. meter.
Max clast size: 15 cm.
Average clast size: 1-2 cm.

1 surface sample of mostly 2 cm diameter quartzite clasts collected.
Greater than 100 pebbles collected ~3 m from edge of terrace.
Should give min. age of deposit/terrace surface.
Sample collected in NW portion of the terrace ~3-4 m from edge.
Generally a flat surface, although slopes gently to the east towards the Colorado River.
Avoided sampling near plants and telephone pole.
Inheritance will be calculated from depth-profile samples.

GC-04-LF-409
October 19, 2004
Location:

UTM-- 446031 E 4078859 N, Zone 12.
Possible M3 terrace deposit.
Located just above Paria beach parking lot to the SW.
Sample collected in center of deposit, ~3-4 m from edges.
~Elevation: 3200 feet.

Surface Characteristic:

Fewer volcanics than at GC-04-LF-408 sample site.
Dimensions: ~8 m (E/W) by 8 m (N/S).
No rubification of clasts.
Few pedogenic carbonates observed on the surface, although slightly more than at GC-04-LF-408.
Av horizon ~2.5 cm thick.
Well-developed pavement.
Well developed desert varnish, more than GC-04-LF-408.
Most clasts are rounded to sub-rounded.
Few fractured clasts.
Less than 1 plant / sq. meter.
Max clast size: 22 cm.
Average clast size: 1 cm.

1 surface sample of mostly 2 cm diameter quartzite clasts collected.
Greater than 100 pebbles collected ~3-4 m from edge of terrace.
Should give min. age of deposit/terrace surface.
Generally a flat surface, although slopes gently to the east towards the Colorado River.
Avoided sampling near plants.
Inheritance will be calculated from depth-profile samples.

GC-04-LF-410
October 19, 2004
Location:

UTM-- 445585 E 4078458 N, Zone 12.
Possible M6 terrace deposit, M6y terrace surface.
Located above M4y where soil pit dug, on the southern most finger of the bird-shaped mapped unit.
~1 km south and west of Paria beach parking lot.
~Elevation: 3350 feet.

Surface Characteristic:

Dimensions: ~500 m (E/W) by 400 m (N/S).
Clasts in pavement have algae rinds on them.
No rubification of clasts.
Well-developed pavement.
Moderately to well developed desert varnish.
Moderate amount of pedogenic carbonates observed on the surface.
Av horizon ~3.5-4 cm thick.
Most clasts are rounded to sub-rounded.
Some clasts are fractured.
Quartzites dominate the surface-clast composition.
More broken chert than other deposits.
More limestone (<5%) than other surfaces sampled.
Less than 1 plant / sq. meter.
Max clast size: 25 cm.
Average clast size: 3 cm.

1 surface sample of mostly 2 cm diameter quartzite clasts collected.
Greater than 100 pebbles collected ~6 m from edge of terrace.
Sample collected on the southern and eastern most portion of the terrace surface.

Should give min. age of deposit/terrace surface.
Avoided sampling near plants.
Inheritance will be calculated from depth-profile samples.

GC-05-LF-501
May 26, 2005
Location:
UTM--
Possible M4 deposit, M4y terrace surface.
Located southeast of ranger station ~100 m, just above main road.
Part of survey transect 3… surface is approximately 2 m lower than the main housing terrace, just to the west of staff houses.
~Elevation: 3350 feet.
Surface Characteristic:
Dimensions: ~50 x 30 m (N/S).
Well-developed pavement.
Moderately to well developed desert varnish.
Av horizon ~2-3 cm thick.
Most clasts are rounded to sub-rounded.
Quartzites dominate the surface-clast composition.
Less than 1 plant / sq. meter.
Max clast size: 25 cm.
Average clast size: 3 cm.

1 surface sample of mostly 2 cm diameter quartzite clasts collected.
Greater than 100 pebbles collected ~6 m from edge of terrace.
Should give min. age of deposit/terrace surface.
Avoided sampling near plants.
Inheritance will be calculated from depth-profile samples.

Appendix F. OPTICALLY STIMULATED LUMINSCENCE DATA
Ages and errors shown in this appendix reflect data completed as of December 31, 2006, and may differ slightly from those reported in the thesis body due to the completion of more recent work.

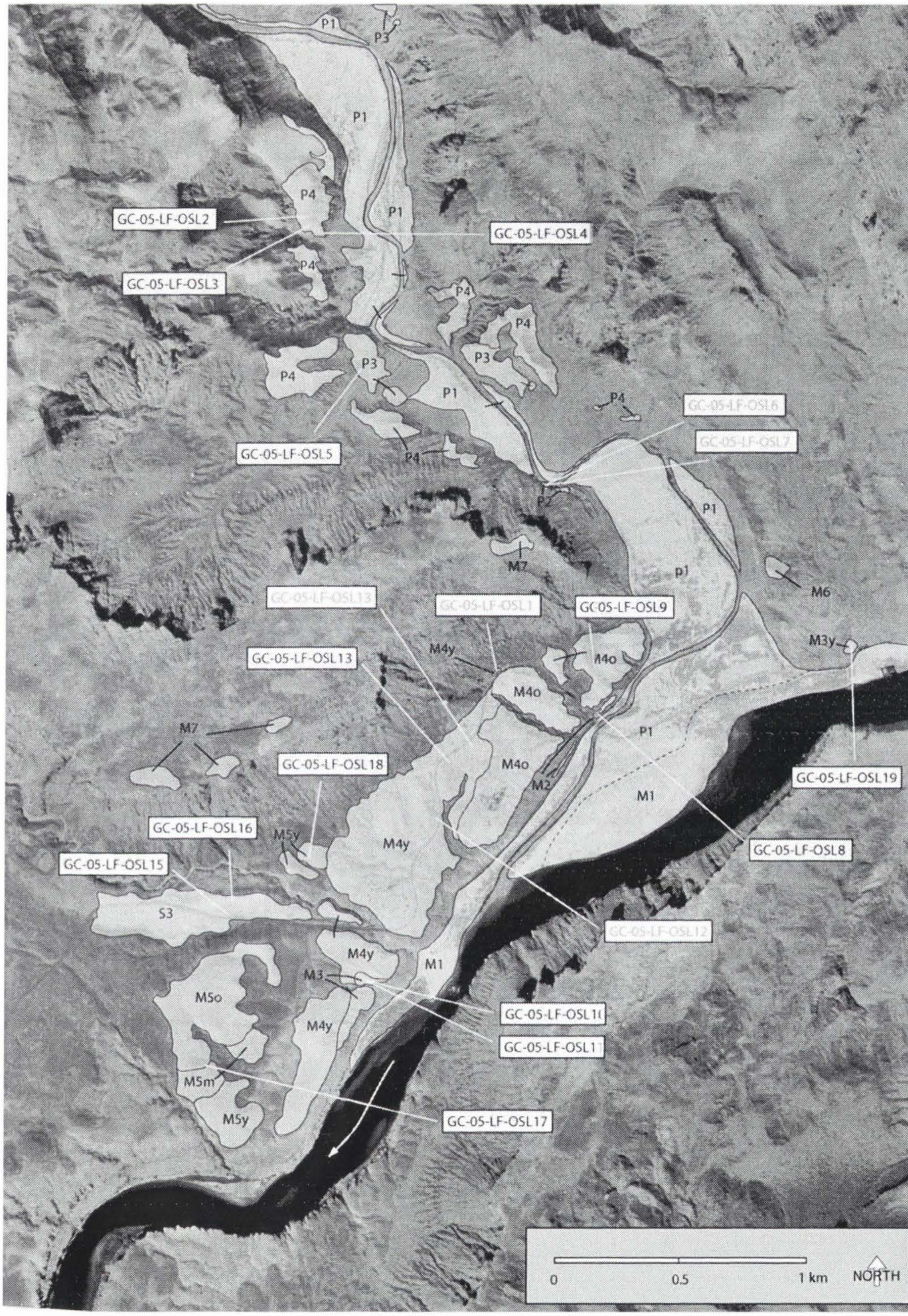

Figure F.1. Map of Quaternary deposits in the Lees Ferry area, showing approximate locations where OSL samples were collected. Gray text indicates samples that were collected but are no longer being processed.

Table F.1. OSL sample numbers and location descriptions for samples collected at Lees Ferry.

Sample #	UNL Sample #	Location Description	UTM Coordinates	Depth Below Surface (m)
GC-04-LF-OSL1	UNL-1127	M4 terrace deposit, roadcut near Ranger Station	446458 E, 4079938 N	1.2
GC-04-LF-OSL2	UNL-1139	P4(?) terrace on thick Paria River deposit - upper sample	445838 E, 4081493 N	13.5
GC-04-LF-OSL3	UNL-1145	P4(?) terrace on thick Paria River deposit - middle sample	445842 E, 4081450 N	10.0
GC-04-LF-OSL4	UNL-1138	P4(?) terrace on thick Paria River deposit - lower sample	445876 E, 4081459 N	30.0
GC-04-LF-OSL5	UNL-1141	P3 terrace downstream of thick Paria deposit	445996 E, 4081085 N	6.2
GC-04-LF-OSL6	UNL-1146	P2/flood deposit (?) closest to Lonely Dell Parking	446690 E, 4080594 N	8.0
GC-04-LF-OSL7	UNL-1147	P2/flood deposit (?) closest to Lonely Dell Parking	446690 E, 4080594 N	3.0
GC-04-LF-OSL8	UNL-1134	M2 near Paria stop sign, super sandy flood	446827 E, 4079827 N	3.2
GC-04-LF-OSL9	UNL-1128	M4 terrace deposit, up small drainage near stop sign - lower sample	446807 E, 4079863 N	22.0
GC-04-LF-OSL10	UNL-1133	M3 terrace deposit in culvert/gully cut near Paria beach - lower sample	446036 E, 4078918 N	6.5
GC-04-LF-OSL11	UNL-1142	M3 terrace deposit in culvert/gully cut near Paria beach - upper sample	446036 E, 4078918 N	3.8
GC-04-LF-OSL12	UNL-1149	M4 terrace deposit in separatede island of M4 on west side of road	446255 E, 4079606 N	14.0
GC-04-LF-OSL13	UNL-1140	M4 terrace deposit on east side of road up to ranger station - middle	446292 E, 4079546 N	9.7
GC-04-LF-OSL14	UNL-1148	M4 terrace deposit on east side of road up to ranger station - upper	446288 E, 4079636 N	3.0
GC-04-LF-OSL15	UNL-1143	Spring deposit of Kaufman - lower sample – S3.	445504 E, 4078111 N	9.2
GC-04-LF-OSL16	UNL-1144	Spring deposit of Kaufman - upper sample – S3.	445504 E, 4078111 N	1.2
GC-04-LF-OSL17	UNL-1353	M5 deposit taken near cosmo surface sample GC-04-LF-410	445585 E, 4078458 N	2.0
GC-04-LF-OSL18	UNL-1352	M5y deposit taken from terrace west of campground - middle of deposit	445797 E, 4079287 N	5.0
GC-04-LF-OSL19	UNL-1351	M2 deposit taken from terrace west of bathroom at ramp - top of deposit	447685 E, 4080059 N	1.5

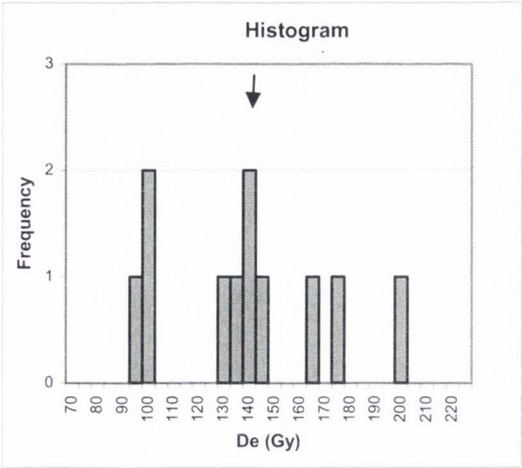

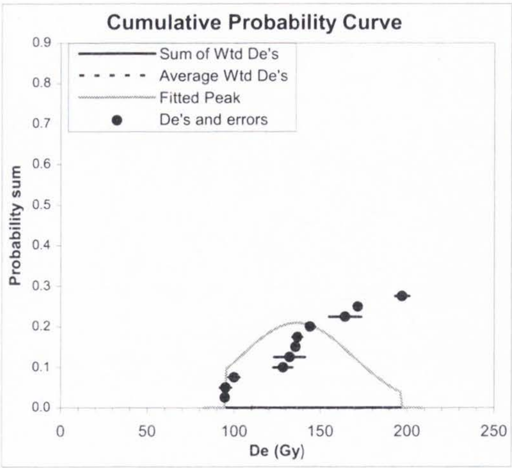

GC-05-LF-OSL2 **P4, Lees Ferry**
UNL-1139

	De (Gy)	±	Age (ka)	±
wt Mean =	**136.26**	**32.60**	**102.4**	**25.1**
Peak fit =	136.26	32.60	102.4	25.1
Median =	135.27		101.7	24.9
Min =	94.66		71.2	17.4
Max =	197.12		148.2	36.3
S.D. =	32.60	used here		
Standard error =	9.83			

De (Gy)	Error	Age (ka)	±
94.66	**0.63**	71.17	17.41
95.05	**3.29**	71.46	17.49
99.92	**3.11**	75.12	18.38
128.14	**5.54**	96.33	23.57
132.09	**9.14**	99.31	24.30
135.27	**1.43**	101.69	24.88
136.67	**3.16**	102.75	25.14
144.23	**2.60**	108.43	26.53
164.21	**9.35**	123.45	30.21
171.52	**0.84**	128.95	31.55
197.12	**4.14**	148.20	36.26

Random Errors=	24.06	%
Systematic Error=	4.43	%
Total Error=	24.47	%

Bin Width =	5	Gy	
n =	11	Disks	
		+/-	
dose rate=	1.33	0.06	Gy/ka
U =	1.20	0.1	ppm
Th =	3.10	0.3	ppm
K2O =	0.96	0.02	wt. %
Rb2O=	33.0	1.3	ppm
H2O=	2.0	2.0	wt. %

Cosmic=	0.05	Gy/ka
depth =	13.5	m
latitude=	36	degrees (north positive)
longitude=	-112	degrees (east positive)
elevation=	0.90	km asl

Sample descript: medium-scale cross bedding, planar lamina, f to m sand
Sample location: UTM 12 4081493 N, 445838

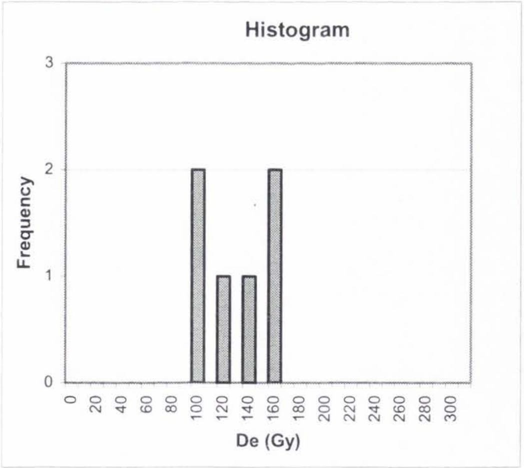

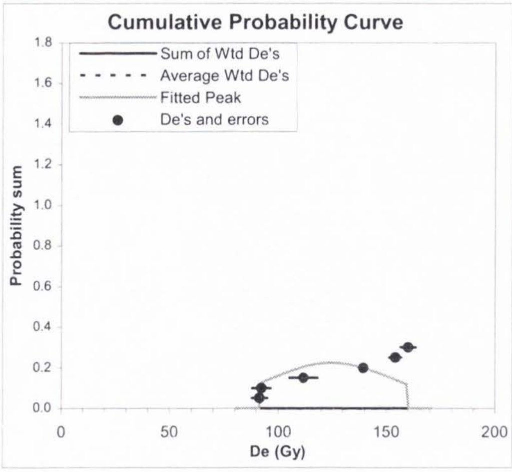

GC-05-LF-OSL3	P4, Lees Ferry				De (Gy)	Error	Age (ka)	±
UNL-1145					**91.46**	**3.56**	70.28	17.55
	De (Gy)	±	Age (ka)	±	**92.26**	**4.24**	70.90	17.70
wt Mean =	**124.86**	**30.50**	**95.9**	**24.0**	**111.84**	**6.59**	85.94	21.46
					139.52	**1.75**	107.21	26.77
Peak fit =	124.86	30.50	95.9	24.0	**154.12**	**2.75**	118.43	29.57
Median =	125.68		96.6	24.1	**159.95**	**3.50**	122.91	30.69
Min =	91.46		70.3	17.5				
Max =	159.95		122.9	30.7				

S.D. =	30.50	used here	
Standard error =	12.45		
Random Errors=	24.57	%	
Systematic Error=	4.43	%	
Total Error=	24.97	%	
Bin Width =	10	Gy	
n =	6	Disks	
		+/-	
dose rate=	1.30	0.06	Gy/ka
U =	0.90	0.1	ppm
Th =	3.00	0.3	ppm
K2O =	1.00	0.02	wt. %
Rb2O=	33.9	1.4	ppm
H2O=	2.0	2.0	wt. %
Cosmic=	0.07	Gy/ka	
depth =	10.0	m	
latitude=	36	degrees (north positive)	
longitude=	-112	degrees (east positive)	
elevation=	0.90	km asl	

Sample descript: f to m sand, small-scale cross strata, some pebbles present
Sample location: UTM 12 4081450 N, 445842 E

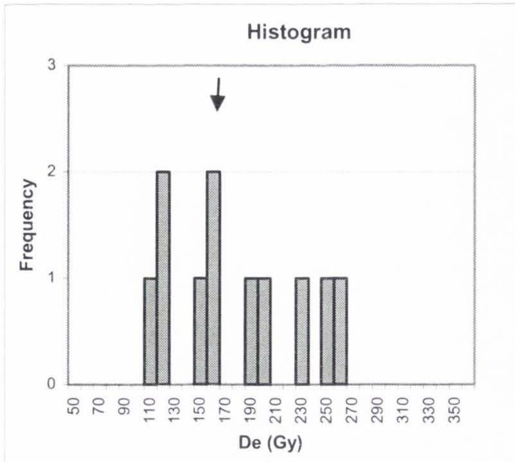

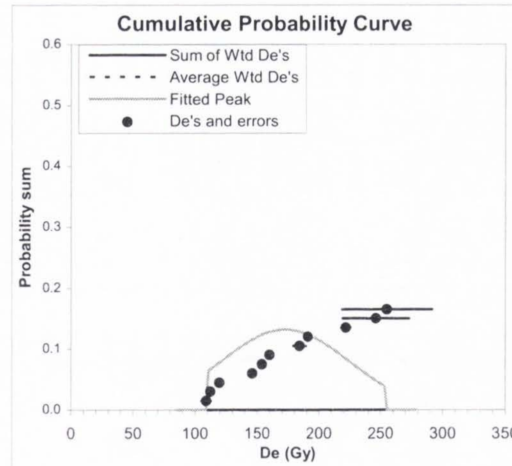

GC-05-LF-OSL4 P4, Lees Ferry
UNL-1138

	De (Gy)	±	Age (ka)	±
wt Mean =	**172.63**	**51.80**	**199.5**	**60.9**
Peak fit =	172.63	51.80	199.5	60.9
Median =	159.92		184.8	56.4
Min =	108.95		125.9	38.4
Max =	255.09		294.8	90.0
S.D. =	51.80	used here		
Standard error =	15.62			

De (Gy)	Error	Age (ka)	±
108.95	**3.89**	125.90	38.43
112.43	**3.00**	129.92	39.66
119.50	**0.52**	138.10	42.15
145.95	**2.35**	168.67	51.49
153.84	**1.09**	177.78	54.27
159.92	**3.27**	184.81	56.41
184.05	**5.07**	212.69	64.93
191.07	**0.14**	220.80	67.40
221.87	**3.89**	256.40	78.27
246.21	**26.94**	284.52	86.85
255.09	**36.40**	294.78	89.98

Random Errors=	30.20	%	
Systematic Error=	4.45	%	
Total Error=	30.53	%	
Bin Width =	10	**Gy**	
n =	11	**Disks**	
		+/-	
dose rate=	0.87	0.04	**Gy/ka**
U =	0.70	0.1	**ppm**
Th =	2.40	0.2	**ppm**
K2O =	0.64	0.02	**wt. %**
Rb2O=	22.4	0.9	**ppm**
H2O=	2.0	2.0	**wt. %**
Cosmic=	0.02	**Gy/ka**	
depth =	30.0	**m**	
latitude=	36	**degrees (north positive)**	
longitude=	-112	**degrees (east positive)**	
elevation=	0.90	**km asl**	

Sample descript: f to m sand, small-scale cross strata
Sample location: UTM 12 4081459 N, 445876 E

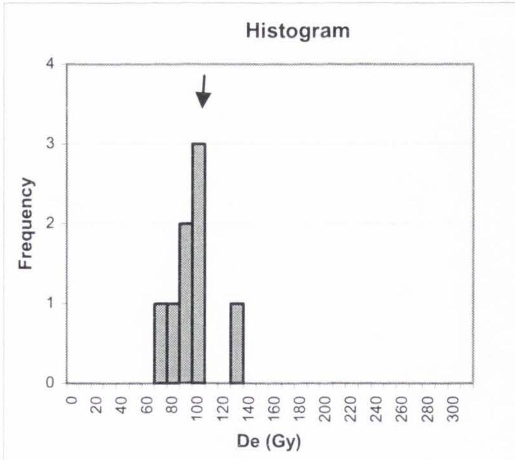

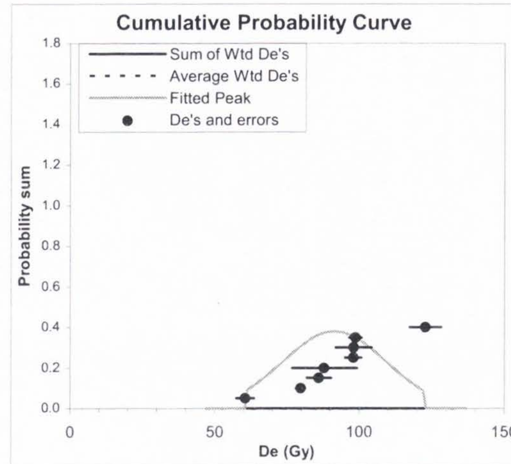

GC-05-LF-OSL5	**P3, Lees Ferry**				**De (Gy)**	**Error**	**Age (ka)**	**±**
UNL-1141					**60.57**	**3.04**	48.87	9.97
	De (Gy)	**±**	**Age (ka)**	**±**	**79.63**	**1.64**	64.24	13.11
wt Mean =	**91.48**	**17.98**	**73.8**	**15.1**	**86.03**	**4.33**	69.41	14.17
					87.94	**11.24**	70.95	14.48
Peak fit =	91.48	17.98	73.8	15.1	**97.97**	**2.80**	79.04	16.13
Median =	92.96		75.0	15.3	**98.12**	**6.22**	79.17	16.16
Min =	60.57		48.9	10.0	**98.75**	**2.10**	79.67	16.26
Max =	122.86		99.1	20.2	**122.86**	**5.43**	99.12	20.23

S.D. =	17.98	used here	
Standard error =	6.36		
Random Errors=	19.95	%	
Systematic Error=	4.32	%	
Total Error=	20.41	%	
Bin Width =	10	**Gy**	
n =	8	**Disks**	
		+/-	
dose rate=	1.24	0.06	**Gy/ka**
U =	1.20	0.1	**ppm**
Th =	5.20	0.5	**ppm**
K2O =	0.60	0.02	**wt. %**
Rb2O=	20.5	0.8	**ppm**
H2O=	2.0	2.0	**wt. %**
Cosmic=	0.11	**Gy/ka**	
depth =	6.2	**m**	
latitude=	36	**degrees (north positive)**	
longitude=	-112	**degrees (east positive)**	
elevation=	0.90	**km asl**	

Sample descript: low angle and planar cross strata, f to m sand
Sample location: UTM 12 4081085 N, 445996 E

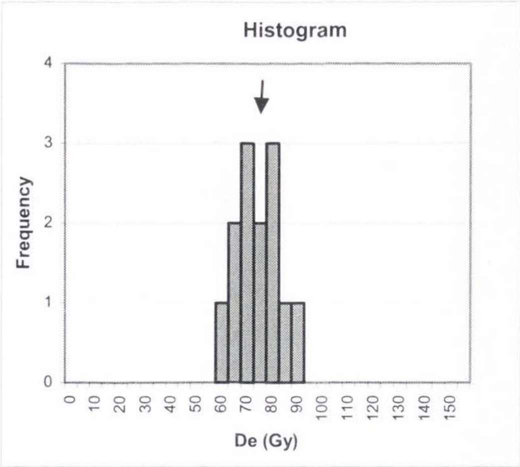

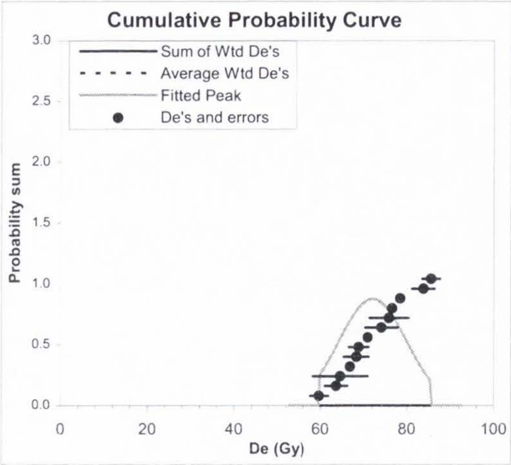

GC-05-LF-OSL8 M2, Lees Ferry
UNL-1134

	De (Gy)	±	Age (ka)	±
wt Mean =	**72.13**	**7.80**	**20.7**	**2.5**
Peak fit =	72.13	7.80	20.7	2.5
Median =	71.02		20.4	2.4
Min =	59.74		17.1	2.1
Max =	85.57		24.5	2.9

S.D. =	7.80	used here
Standard error =	2.16	
Random Errors=	11.16	%
Systematic Error=	4.39	%
Total Error=	11.99	%
Bin Width =	5	Gy
n =	13	Disks

		+/-	
dose rate=	3.49	0.15	Gy/ka
U =	3.10	0.2	ppm
Th =	11.40	1.0	ppm
K2O =	2.24	0.06	wt. %
Rb2O=	81.1	3.2	ppm
H2O=	2.0	2.0	wt. %

Cosmic=	0.16	Gy/ka
depth =	3.2	m
latitude=	36	degrees (north positive)
longitude=	-112	degrees (east positive)
elevation=	0.90	km asl

Sample descript: silt to f sand, no regular bedding
Sample location: UTM 12 4079827 N, 446827 E

De (Gy)	Error	Age (ka)	±
59.74	**2.09**	17.12	2.05
63.65	**2.65**	18.24	2.19
64.65	**6.33**	18.53	2.22
66.92	**0.03**	19.18	2.30
68.32	**2.90**	19.58	2.35
68.87	**2.31**	19.74	2.37
71.02	**0.57**	20.35	2.44
74.14	**3.76**	21.25	2.55
75.90	**4.50**	21.75	2.61
76.61	**0.85**	21.96	2.63
78.48	**0.03**	22.49	2.70
83.79	**2.62**	24.01	2.88
85.57	**2.05**	24.52	2.94

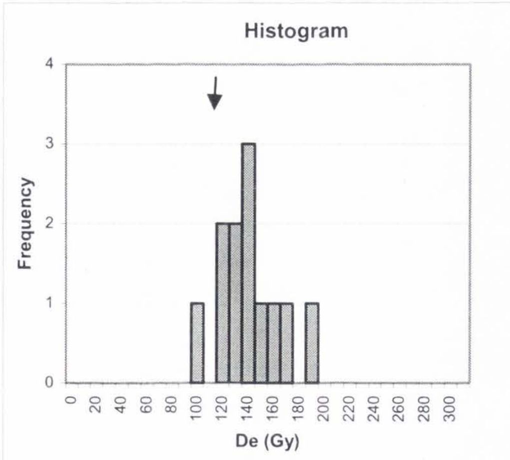

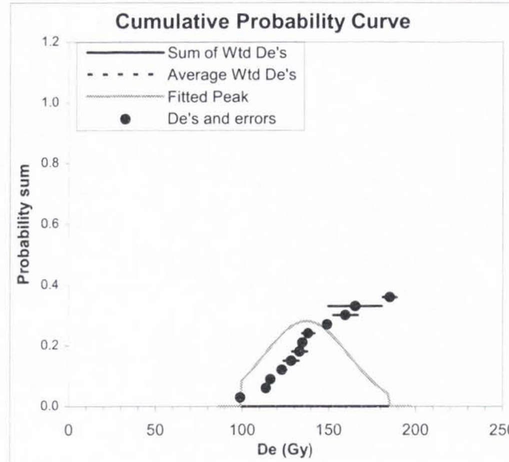

GC-05-LF-OSL9 **M4, Lees Ferry**
UNL-1128

	De (Gy)	±	Age (ka)	±
wt Mean =	**137.07**	**24.30**	**109.7**	**20.3**
Peak fit =	137.07	24.30	109.7	20.3
Median =	133.84		107.1	19.8
Min =	98.92		79.2	14.6
Max =	185.22		148.2	27.4

De (Gy)	Error	Age (ka)	±
98.92	**0.82**	79.16	14.63
113.69	**2.34**	90.98	16.82
116.25	**2.13**	93.03	17.19
122.92	**2.55**	98.37	18.18
128.18	**4.41**	102.58	18.96
132.98	**4.31**	106.42	19.67
134.70	**2.21**	107.80	19.92
138.16	**3.74**	110.56	20.44
149.03	**1.43**	119.26	22.04
159.59	**7.08**	127.71	23.61
165.14	**15.51**	132.15	24.43
185.22	**4.03**	148.22	27.40

S.D. =	24.30	used here	
Standard error =	7.01		
Random Errors=	17.93	%	
Systematic Error=	4.48	%	
Total Error=	18.48	%	
Bin Width =	10	Gy	
n =	12	Disks	
		+/-	
dose rate=	1.25	0.05	Gy/ka
U =	0.90	0.1	ppm
Th =	2.90	0.3	ppm
K2O =	1.00	0.02	wt. %
Rb2O=	33.7	1.3	ppm
H2O=	2.0	2.0	wt. %
Cosmic=	0.03	Gy/ka	
depth =	22.0	m	
latitude=	36	degrees (north positive)	
longitude=	-112	degrees (east positive)	
elevation=	0.90	km asl	

Sample descript: f to m sand, faint small-scale cross strata
Sample location: UTM 12 4079863 N, 446807 E

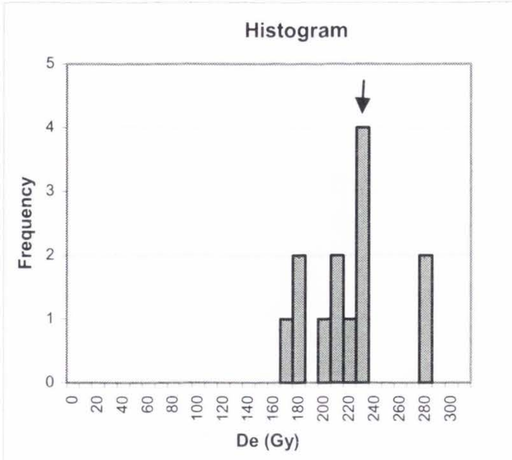

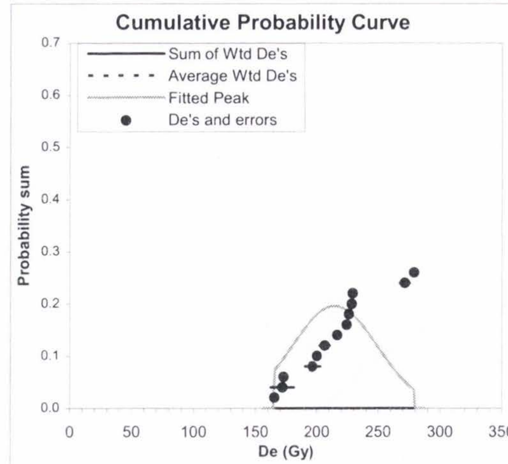

GC-05-LF-OSL10 M3, Lees Ferry
UNL-1133

	De (Gy)	±	Age (ka)	±
wt Mean =	**214.50**	**34.89**	**71.5**	**12.2**
Peak fit =	214.50	34.89	71.5	12.2
Median =	216.59		72.2	12.3
Min =	165.41		55.1	9.4
Max =	278.90		93.0	15.9

De (Gy)	Error	Age (ka)	±
165.41	**0.34**	55.14	9.40
171.79	**9.52**	57.26	9.76
172.79	**1.47**	57.60	9.82
196.49	**6.58**	65.50	11.17
200.38	**1.95**	66.80	11.39
206.58	**4.16**	68.86	11.74
216.59	**0.59**	72.20	12.31
224.26	**0.32**	74.76	12.75
226.20	**2.98**	75.40	12.86
228.35	**2.12**	76.12	12.98
229.33	**2.64**	76.45	13.03
271.50	**4.12**	90.50	15.43
278.90	**2.62**	92.97	15.85

S.D. =	34.89	used here	
Standard error =	9.68		
Random Errors=	16.47	%	
Systematic Error=	4.42	%	
Total Error=	17.05	%	
Bin Width =	10	Gy	
n =	13	Disks	
		+/-	
dose rate=	3.00	0.13	Gy/ka
U =	2.90	0.2	ppm
Th =	8.00	0.7	ppm
K2O =	2.05	0.05	wt. %
Rb2O=	77.1	3.1	ppm
H2O=	2.0	2.0	wt. %
Cosmic=	0.11	Gy/ka	
depth =	6.5	m	
latitude=	36	degrees (north positive)	
longitude=	-112	degrees (east positive)	
elevation=	0.90	km asl	

Sample descript: silt to f sand, planar and low angle cross strata (small-scale)
Sample location: UTM 12 4078918 N, 446036 E

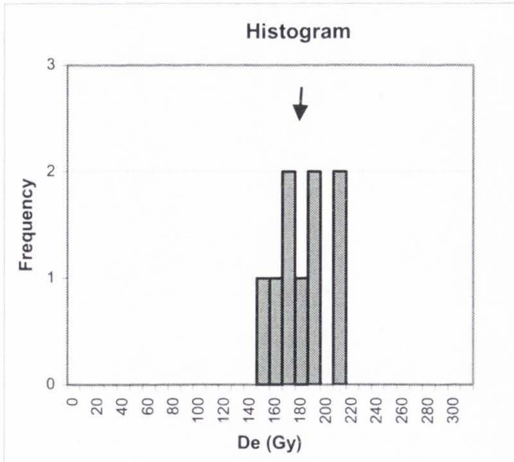

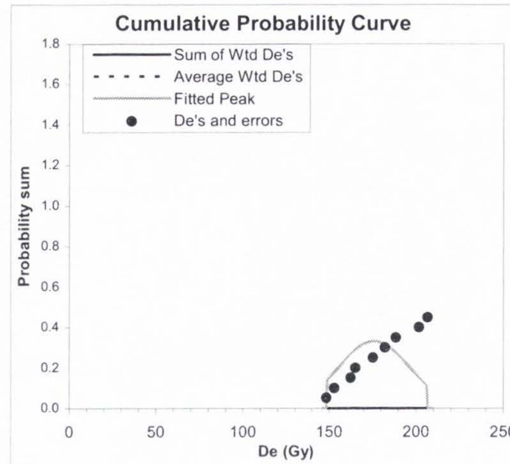

GC-05-LF-OSL11 S3, Lees Ferry
UNL-1142

	De (Gy)	±	Age (ka)	±
wt Mean =	**175.90**	**20.58**	**68.3**	**8.7**
Peak fit =	175.90	20.58	68.3	8.7
Median =	175.27		68.1	8.7
Min =	148.36		57.6	7.3
Max =	206.64		80.3	10.2

De (Gy)	Error	Age (ka)	±
148.36	**0.69**	57.64	7.33
152.97	**2.02**	59.43	7.56
162.37	**1.00**	63.08	8.03
165.21	**0.69**	64.19	8.17
175.27	**0.68**	68.10	8.66
182.14	**1.20**	70.77	9.00
188.47	**0.37**	73.23	9.32
201.64	**0.88**	78.34	9.97
206.64	**0.41**	80.29	10.21

S.D. =	20.58	used here	
Standard error =	6.86		
Random Errors=	11.93	%	
Systematic Error=	4.42	%	
Total Error=	12.72	%	
Bin Width =	10	Gy	
n =	9	Disks	
		+/-	
dose rate=	2.57	0.11	Gy/ka
U =	2.10	0.1	ppm
Th =	5.70	0.5	ppm
K2O =	1.90	0.05	wt. %
Rb2O=	67.8	2.7	ppm
H2O=	2.0	2.0	wt. %
Cosmic=	0.15	Gy/ka	
depth =	3.8	m	
latitude=	36	degrees (north positive)	
longitude=	-112	degrees (east positive)	
elevation=	0.90	km asl	

Sample descript: silt to f sand, massive
Sample location: UTM 4079606 N, 446255 E

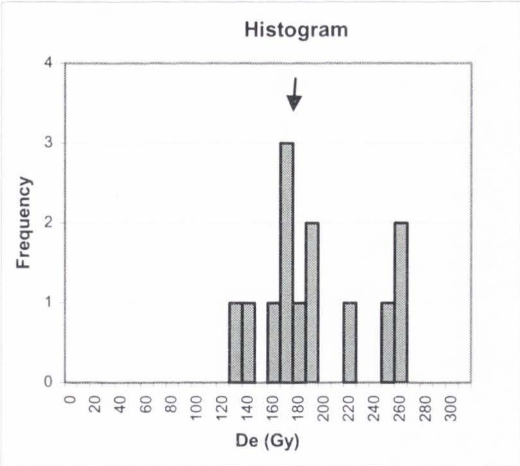

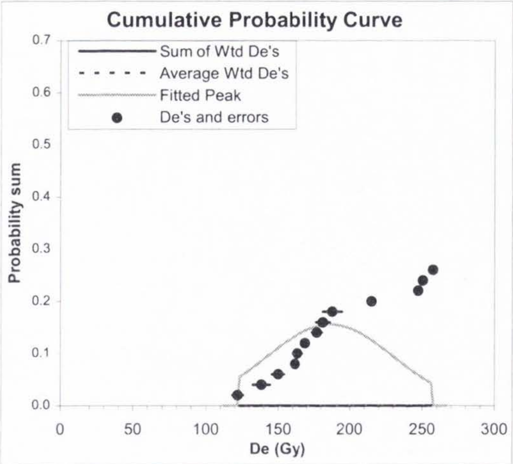

GC-05-LF-OSL13 M4, Lees Ferry
UNL-1140

	De (Gy)	±	Age (ka)	±
wt Mean =	**186.32**	**43.80**	**96.7**	**23.3**
Peak fit =	186.32	43.80	96.7	23.3
Median =	177.25		92.0	22.1
Min =	121.99		63.3	15.2
Max =	257.60		133.7	32.1

S.D. =	43.80	used here
Standard error =	12.15	
Random Errors=	23.61	%
Systematic Error=	4.51	%
Total Error=	24.04	%
Bin Width =	10	Gy
n =	13	Disks

		+/-	
dose rate=	1.93	0.08	Gy/ka
U =	1.10	0.1	ppm
Th =	3.30	0.3	ppm
K2O =	1.69	0.04	wt. %
Rb2O=	57.5	2.3	ppm
H2O=	2.0	2.0	wt. %

Cosmic=	0.08	Gy/ka
depth =	9.7	m
latitude=	36	degrees (north positive)
longitude=	-112	degrees (east positive)
elevation=	0.90	km asl

Sample descript: f sand, planar and low angle cross strata
Sample location: UTM 12 4079546 N, 446292 E

De (Gy)	Error	Age (ka)	±
121.99	**3.84**	63.34	15.22
138.42	**5.95**	71.86	17.27
150.02	**4.32**	77.89	18.72
161.93	**1.33**	84.07	20.21
163.60	**3.42**	84.94	20.42
168.91	**1.60**	87.70	21.08
177.25	**3.41**	92.03	22.12
181.40	**4.70**	94.18	22.64
188.00	**6.77**	97.61	23.46
215.26	**1.22**	111.76	26.86
247.29	**1.85**	128.39	30.86
250.46	**1.92**	130.04	31.26
257.60	**1.66**	133.75	32.15

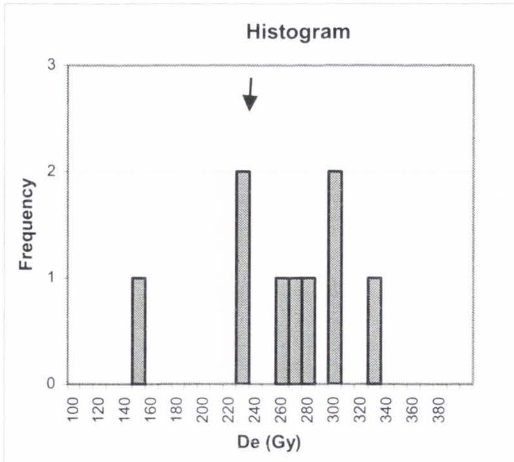

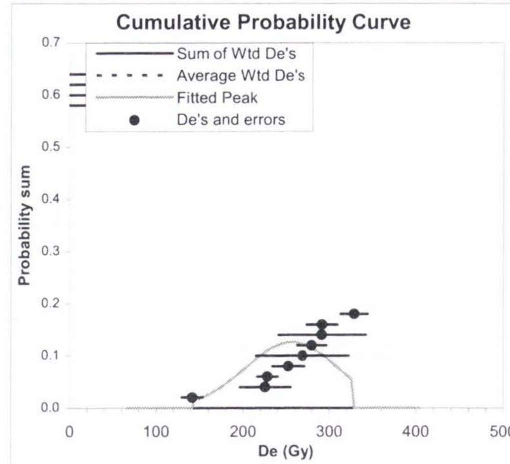

GC-05-LF-OSL15 S3, Lees Ferry
UNL-1143

	De (Gy)	±	Age (ka)	±
wt Mean =	**256.20**	**54.03**	**69.6**	**15.1**
Peak fit =	256.20	54.03	69.6	15.1
Median =	268.55		72.9	15.8
Min =	141.24		38.3	8.3
Max =	328.43		89.2	19.4

De (Gy)	Error	Age (ka)	±
141.24	**11.86**	38.35	8.33
225.46	**29.52**	61.21	13.30
227.93	**11.85**	61.88	13.45
252.15	**18.39**	68.46	14.88
268.55	**53.78**	72.91	15.84
279.40	**17.02**	75.86	16.48
291.22	**50.70**	79.07	17.18
291.39	**17.62**	79.11	17.19
328.43	**15.76**	89.17	19.38

S.D. =	54.03	used here	
Standard error =	18.01		
Random Errors=	21.27	%	
Systematic Error=	4.43	%	
Total Error=	21.73	%	
Bin Width =	10	**Gy**	
n =	9	**Disks**	
		+/-	
dose rate=	3.68	0.16	**Gy/ka**
U =	6.30	0.4	**ppm**
Th =	5.20	0.5	**ppm**
K2O =	2.13	0.05	**wt. %**
Rb2O=	75.1	3.0	**ppm**
H2O=	2.0	2.0	**wt. %**
Cosmic=	0.08	**Gy/ka**	
depth =	9.2	**m**	
latitude=	36	**degrees (north positive)**	
longitude=	-112	**degrees (east positive)**	
elevation=	0.90	**km asl**	

Sample descript: very fine sand and silt, carbonate and gypsum beds
Sample location: UTM 12 4078111 N, 445504 E

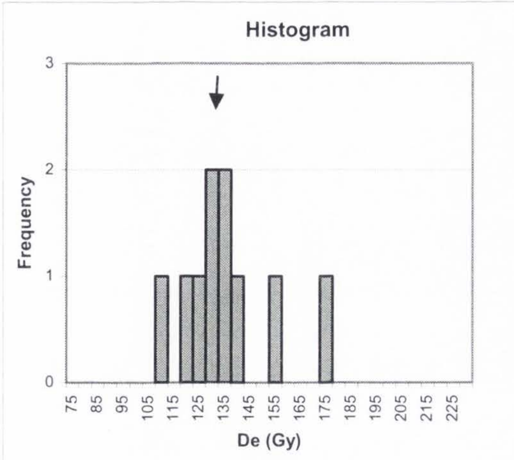

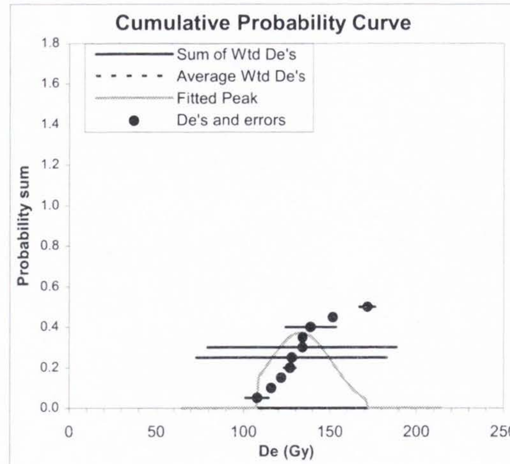

GC-05-LF-OSL16 S3, Lees Ferry
UNL-1144

	De (Gy)	±	Age (ka)	±
wt Mean =	**133.02**	**18.27**	**40.1**	**5.9**
Peak fit =	133.02	18.27	40.1	5.9
Median =	130.96		39.5	5.8
Min =	107.84		32.5	4.8
Max =	171.73		51.8	7.6
S.D. =	18.27	used here		
Standard error =	5.78			

De (Gy)	Error	Age (ka)	±
107.84	**6.71**	32.53	4.75
115.97	**0.83**	34.99	5.11
121.52	**0.73**	36.66	5.35
126.69	**3.41**	38.22	5.58
127.93	**55.12**	38.59	5.64
133.99	**54.62**	40.42	5.90
134.00	**0.22**	40.42	5.90
138.83	**14.67**	41.88	6.12
151.66	**2.07**	45.75	6.68
171.73	**4.65**	51.81	7.57

Random Errors=	13.91	%	
Systematic Error=	4.44	%	
Total Error=	14.61	%	
Bin Width =	5	Gy	
n =	10	Disks	
		+/-	
dose rate=	3.31	0.13	Gy/ka
U =	2.30	0.2	ppm
Th =	6.60	0.6	ppm
K2O =	2.58	0.06	wt. %
Rb2O=	87.8	3.5	ppm
H2O=	2.0	2.0	wt. %
Cosmic=	0.20	Gy/ka	
depth =	1.2	m	
latitude=	36	degrees (north positive)	
longitude=	-112	degrees (east positive)	
elevation=	0.90	km asl	

Sample descript: very fine sand and silt, carbonate and gypsum beds
Sample location: UTM 12 4078111 N, 445504 E

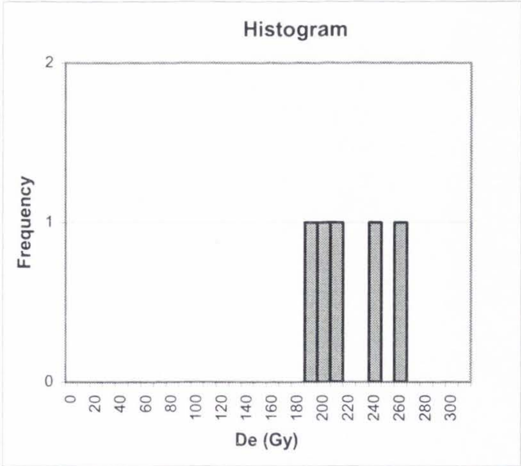

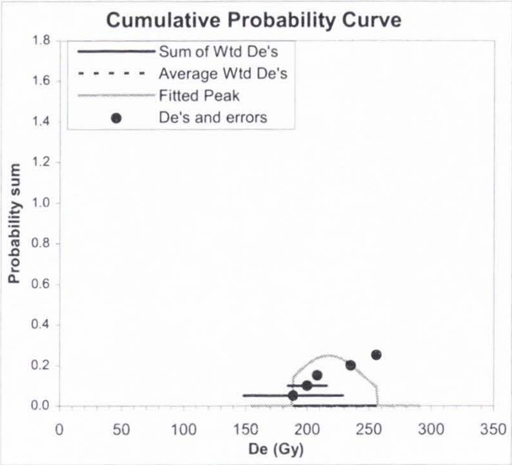

GC-06-LF-OSL17 M5, Lees Ferry
UNL-1353

	De (Gy)	±	Age (ka)	±
wt Mean =	**217.51**	**27.50**	**93.4**	**12.7**
Peak fit =	217.51	27.50	93.4	12.7
Median =	208.11		89.4	12.1
Min =	188.53		81.0	11.0
Max =	255.96		110.0	14.9

De (Gy)	Error	Age (ka)	±
188.53	**40.33**	80.98	11.00
199.91	**15.88**	85.88	11.66
208.11	**0.00**	89.40	12.14
235.05	**0.00**	100.97	13.71
255.96	**0.90**	109.95	14.93

S.D. =	27.50	used here
Standard error =	12.30	
Random Errors=	12.84	%
Systematic Error=	4.41	%
Total Error=	13.58	%
Bin Width =	10	Gy
n =	5	Disks

		+/-	
dose rate=	2.33	0.09	Gy/ka
U =	1.50	0.1	ppm
Th =	5.20	0.5	ppm
K2O =	1.77	0.04	wt. %
Rb2O=	58.5	2.3	ppm
H2O=	2.0	2.0	wt. %

Cosmic=	0.18	Gy/ka
depth =	2.0	m
latitude=	36	degrees (north positive)
longitude=	-112	degrees (east positive)
elevation=	0.90	km asl

Sample descript: cobbles and pebbles, small sandy pocket between clasts
Sample descript: UTM 12 4078458 N, 445585 E

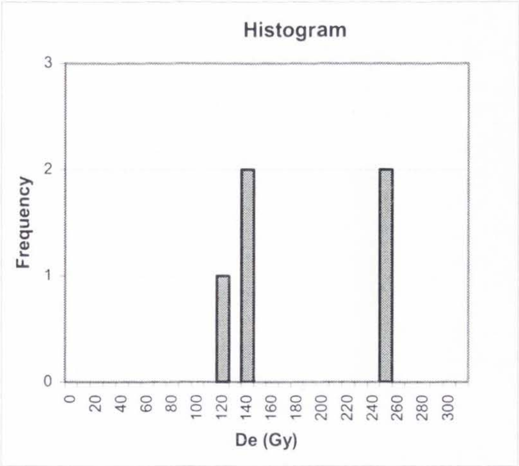

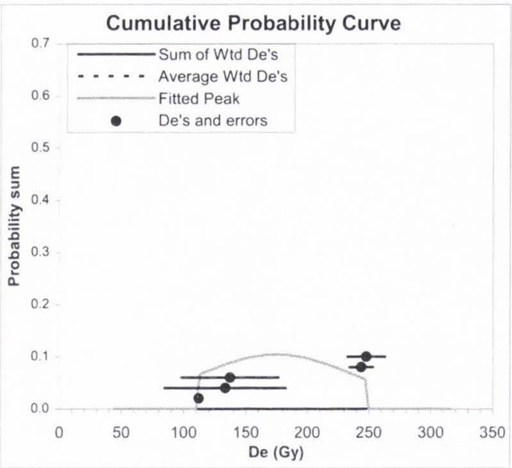

GC-06-LF-OSL18 M5, Lees Ferry
UNL-1352

	De (Gy)	±	Age (ka)	±
wt Mean =	**174.87**	**65.48**	**102.5**	**38.7**
Peak fit =	174.87	65.48	102.5	38.7
Median =	137.26		80.4	30.4
Min =	112.06		65.7	24.8
Max =	247.87		145.3	54.9

De (Gy)	Error	Age (ka)	±
112.06	**0.00**	65.68	24.81
133.44	**48.94**	78.21	29.54
137.26	**39.11**	80.45	30.39
243.74	**9.60**	142.86	53.97
247.87	**15.23**	145.28	54.88

S.D. =	65.48	used here
Standard error =	29.28	
Random Errors=	37.52	%
Systematic Error=	4.39	%
Total Error=	37.78	%
Bin Width =	10	Gy
n =	5	Disks

		+/-	
dose rate=	1.71	0.07	Gy/ka
U =	1.70	0.1	ppm
Th =	3.40	0.3	ppm
K2O =	1.17	0.03	wt. %
Rb2O=	38.7	1.5	ppm
H2O=	2.0	2.0	wt. %

Cosmic=	0.13	Gy/ka
depth =	5.0	m
latitude=	36	degrees (north positive)
longitude=	-112	degrees (east positive)
elevation=	0.90	km asl

Sample descript: f to m sand, beautiful sand...
Sample location: UTM 12 4079287 N, 445797 E

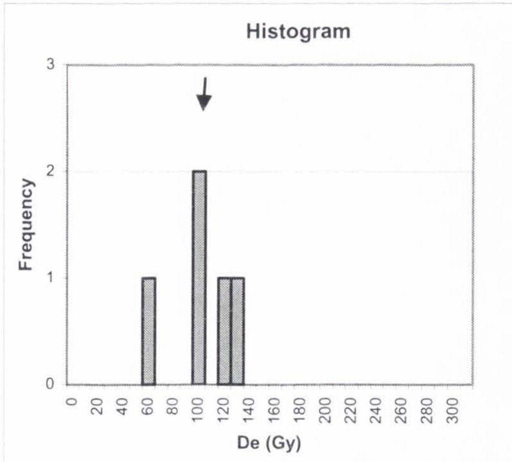

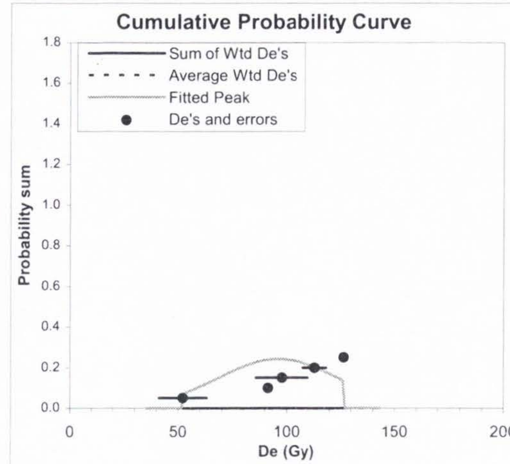

GC-06-LF-OSL19 M3y, Lees Ferry
UNL-1351

	De (Gy)	±	Age (ka)	±
wt Mean =	**96.24**	**28.15**	**35.6**	**10.6**
Peak fit =	96.24	28.15	35.6	10.6
Median =	97.87		36.2	10.7
Min =	52.18		19.3	5.7
Max =	126.55		46.8	13.9

De (Gy)	Error	Age (ka)	±
52.18	**10.96**	19.29	5.73
91.48	**0.19**	33.82	10.04
97.87	**12.04**	36.19	10.75
113.10	**5.36**	41.82	12.42
126.55	**0.00**	46.79	13.89

S.D. =	28.15	used here	
Standard error =	12.59		
Random Errors=	29.37	%	
Systematic Error=	4.37	%	
Total Error=	29.69	%	
Bin Width =	10	Gy	
n =	5	Disks	
		+/-	
dose rate=	2.70	0.11	Gy/ka
U =	2.30	0.2	ppm
Th =	8.00	0.7	ppm
K2O =	1.75	0.04	wt. %
Rb2O=	59.4	2.4	ppm
H2O=	2.0	2.0	wt. %
Cosmic=	0.20	Gy/ka	
depth =	1.5	m	
latitude=	36	degrees (north positive)	
longitude=	-112	degrees (east positive)	
elevation=	0.90	km asl	

Sample descript: vf to m sand, fairly well sorted, small pebble lens above sampled unit
Sample location: UTM 12 4080059 N, 447685 E